# Synthesis and Characterization of Metal-Bis(dithiolene) Complexes and *N*-heterocyclic Silver-Carbene Complexes

A Thesis
Submitted for the degree of
**DOCTOR OF PHILOSOPHY**

***By***

**Kishore Ravada**

**School of Chemistry**
**University of Hyderabad**
**Hyderabad 500 046**
**Andhra Pradesh**
**India**

**September, 2012**

*Dedicated to*

**The Lord Jesus Christ**

*Who died for me on the CROSS and gave me Eternal Life.*

**My Parents, Prasada Rao and Suseela**

*Who lead me in a principled manner and made my dreams come true.*

**All My Teachers**

*Who brought me to this stage.*

**Indian Soldiers**

*Who are working sacrificially for me to give the freedom and security.*

**Prof. Samar Kumar Das, F.A.Sc**
**School of chemistry**
**University of Hyderabad**
**Gachibowli, Hyderabad-500046, India**
**Work: +91-40-23011007**
**Residence: +91-40-23010536**
**Fax: +91-40-2301246**
**E-mail: skdsc@uohyd.ernet.in**

# CERTIFICATE

Certified that the work contained in the thesis entitled "**Synthesis and Characterization of Metal-Bis(dithiolene) Complexes and *N*-heterocyclic Silver-Carbene Complexes"** has been carried out by Mr. Kishore Ravada under my supervision and the same has not been submitted elsewhere for a degree.

**Prof. Samar K. Das**

**(Supervisor)**

**Dean**

**School of Chemistry**

## STATEMENT

I hereby declare that the matter embodied in the thesis is the result of investigation carried out by me in the School of Chemistry, University of Hyderabad, Hyderabad, India, under the supervision of **Prof. Samar K. Das**.

In keeping with the general practice of reporting scientific observations, due acknowledgements have been made wherever the work described is based on the findings of other investigators. Any omission, which might have occurred by oversight or error, is regretted.

**Kishore Ravada**

University of Hyderabad
September, 2012

# Acknowledgements

I express my deep sense of gratitude and profound thanks to my supervisor **Prof. Samar K. Das** for his valuable guidance, patience, encouragement, and for the freedom he gave me in carrying out research. His optimistic approach towards every aspect was admirable and inspiring. Throughout my Ph.D tenure, he is always approachable, helpful, friendly and extremely tolerant. I consider my association with him as a cherishable memory in my life.

I take this opportunity to thank Prof. M. V. Rajasekharan, Dean, School of Chemistry for providing us the facilities needed for our research. I extend my sincere thank to former Deans Prof. D. Basavaiah and Prof. M. Periasamy, and all the faculty members, School of Chemistry for their co-operation on various aspects.

I am deeply indebted to Prof. S. Pal for his suggestions and allowing me to perform studies using the electrochemical facilities for my doctoral work.

I feel fortunate to have friends Anand, Suresh (Physics), Ajay, GDP garu, Shiva (IICT), Indira, Satya Lakshmi who have been my close friends over the years, for keeping me sane, giving me perspective and who have made the time more enjoyable.

It is great pleasure to thank my lab seniors Dr. V. Shivaiah, Dr. S. Supriya, Dr. V. Madhu, Dr. Raghavaiah, Dr. C. H. Pradeep, Dr. Prabhakar, Dr. Arumuganathan, and Dr. Tanmay for their help, pleasant company, and cooperation during my Ph.D. tenure. From the bottom of my heart I thank to my friends and labmates Dr. GDP, Dr. Rambabu, Dr. Srinivas, Bharat, Mrs. Monima, for their support throughout the tenure. Without their help and encouragement it is not possible to complete the work. I wish to thank my juniors, Mrs. Sridevi garu, Mr. Veeranna, Chinnabbai, Ms. Paulami, Krishna, Praveen, Ms. Olivia for their cooperation, help and creating cheerful work atmosphere. I thank to M.Sc and UGC networking project students Ms. Arti, Jagadessh, Shivaiah, Ashok, Sreenivas (ugc), Moses, Lavanya, Dr. Pratap, Sunitha, Pal, Raju and Y. Mahesh to work with me and helping to complete my thesis work.

I also thank all the non-teaching staff of the School of Chemistry for their assistance on various occasions. I thank DST funded National Single Crystal X-ray Diffraction Facility, UGC / UPE for providing the basic requirements and CSIR for the financial support.

I would like to acknowledge Prof. A.V. Prasada Rao, Prof. GNR, Prof. Sivarao, Prof. Vani and N. Murty sir during my post graduation at Andhra University, Visakhapatnam.

My special thanks to Jagruti-coaching center teacher Prof. Jaya Prakash. I take this opportunity to thank all my school and college teachers, Babu rao (Telugu teacher), Srinu (Social Science), Surya Narayana Murthy, Appala Naidu, Jogendernadh, Kameshwari, Rama Rao (Social Science), Venu sir and Krishna Kishore, Kalyan, Sattibabu.

I am lucky enough to have the support of many School of Chemistry friends and colleagues Dr. DK, Prabhu, Nagaraju, Rama Krishna, Dr. M. Ramu, Satish Anna, Dr. Saikath (GM), Dr. Phani Pavan, Dr. Ramesh, Dr. Vikram, Vijji, Santhosh, Balu, Narayana, Chandrsekhar, Bashak, Pramithi, Nagarjuna, Gupta, Hari, Karunakar, Srinu (LGP), Mallesh, Ramu yadav, Bhanu, Srinivas, Seshu, Sudharani, Venu, Dr. Suresh, Madhu, Ramaraju, Ramkumar, Prakash, Ramesh, S. Naidu (sunny), Sekhar Reddy, Haneesh, Ganesh, Vigensh, Praveen, Malakappa, Swamy, Krishna chary, Dr. Naba, Suryanarayana, Rajesh, Maddy, Ashok, Chandu, Dr. Ravi, Dr. Raji, Dr. Anindita, Tulika, Tirupathi Reddy, Pavan, Yaseen, Sasi, Anjaneyalu, Ramesh, Gangadhar, Srinu, Nagarjuna reddy, Sekhar Reddy, Katta, Raghavaiah, Satpal, Guru Braham, Laxaman, Dr. Sivaranjan Reddy, Rajgopal Sr., Rajgopal Jr., N. P. Reddy, Sarita akka, Dr. Kishore, Dr. Ramkumar, Dr. Vijendhra Reddy, Chary, Bharani, Shivaprasad, Srinivas Reddy, Ganesh, Srinivas (RB lab), Raveendra Babu, Vanaja, Naveen, Ramana, Sandeep, Tridib, Obaiah, Satish (PKP), Vikranth, exceptionally generous in helping me at various occasions.

*A friend is someone who knows all about you and still loves you*, I am indeed fortunate to have friends like Anand, Raja (Kalyan), P. Kishore, Bharat who have been good friends over the years, and make my moments with them as a bunch of joyful memories throughout my life. I specially thanks to my M.Sc. classmates Rajgopal, Ganesh, DP, Sarita, Pandu (Ramana Murthy), Syamala, Appa Rao, Anil, Raghupati, Poliraju, Kiran, Murthy (BARC), Vijaya Rao, Vijay vardan, J.P, Vijay (Phy), Seshagiri, Ammi Reddy, Kalyan (FDW), Goutam, Surya, Lavanya, AU Srs & Jrs Dr. Indraneel garu, Dr. Suresh, Dr. John Pal, Dr. Gopala Rao, Dr. Asheer Naidu, Brahmaji, Appa Rao anna and P. Sudarshan Rao, Valli, Phani, for offering memorable moments to share with them.

. I would like to thank my school friends (DVM) Kishore, Laxman, Gopi, Ch. Sreenu, Shankar, Rajesh, Satti babu, Bondapalli, Raju, Ganta Sreenivas, Ranjit, P. Rama, Sudha, Rajani, Sujatha, Rama, Devi, Devulamma.

My village (GPNagaram) friends Chiranjeevi, Soma Sekhar, Bheema, Chakri, Ratanakar, Gopi, Anil, P. Ramu, Kishore, Sreenivas, Bhaskar, Goutam, Dhanu, Ravi Kanth, Parveen, M. Satyanarayana, Shivaji, Jagadeesh, Suresh, B. Kiran, Reddy Srinivas, Umakanth, Ravi, Appaji.

My special thank to my friends Sreenu (Bapatla), Balu, Teja, Vidyavati, Ganapathi, Bogesh, N. Venkateswara Rao (bava), Ch. Seshu, Ch. Varma, Pratap, Surya (Cadila Pha.), Venky (DRDO), Ali, Venki (NMR), Ravi (GPM).

I would like to acknowledge the NRS hostel mates Chairman (phalgun), Sanjeev, G.K., Durgarao (baaa), Srinu, for making the hostel life more memorable.

I also thank my Church members, Pastor Peter Samuel, Nirupama akka, Bro. Sham Kishore, and my UESI members, Kodanda Ram, Baby, Ashray, Dr. N. Sreenivasa Rao, Rajani, Ramesh Anna, Vijaya, Vedananda anna (NPA), Anil Kumar, Kishore (KP), Dr. Daniel Reddy, Rambabu, Bheem, Venkaiah, Prabhu, Babu Rao, Manoj, Varma, Mani, Rajesh, Nagarjuna, Kiran (Agra), Ratnakar, Andrew Anna, Vijay, L. Kanth, Ravi Kiran, Vijay Prasad Anna, Johnson, Benhur, Eswar, Neelima, Prathyusha, Ancy, Adam Anna, Grace, Anil (battu) and Divakar Pastor, Prabhakar pastor for their kind loving nature and spiritual support during my stay in the campus. My heartful thank to my Br. Suneeth Kumar (Save A Child Founder) and sisters Ruth, Salomi, Swaroopa, Pragathi and Samuel.

I thank to family friends, Jogarao Master, Parvati Amma garu, Raja, Lata, Geeta and Gaddibabu, Eswari akka, Kotipalli, Kanaka Ratanam, Srinu Mayya, Roja akka, Dhana Pinni, Rajulamma, Suresh.

It is great pleasure to thank my family members Amma, Nanna, Sisters (Shobha, Swarna), Ammamma, Naga Mamma, my lovable cute nieces Samhita (Sweety), Nava Supriya (Honey), Sruthi (Babbu) and my brother-in-laws Thomas Vidyadhar, Abhishak for their support and affection throughout my life. All my achievements are the outcome of my parent's encouragements and blessings.

***Ravada Kishore.....***

University of Hyderabad
September, 2012

# CONTENTS

# Introduction and Motivation of the Present Work: A Broad Outline of Metal 1,2-Dithiolene Chemistry and *N*-Heterocyclic Carbene Complexes

1 Chapter

## 1.1. Dithiolene Ligands and its Electronic Structure

The term dithiolene refers to a ligand of the formula $R_2C_2S_2$, which can exist in three different forms (depending upon their oxidation states). They are the dianionic "alkene-1,2-dithiolate", the neutral "1,2-dithione" and a monoanionic radical intermediate "1,2-ene-dithiete" between the dianionic and neutral forms as shown in Scheme 1.1. When the later two are complexed to a metal centre, the oxidation state of the ligand (and therefore the metal centre) cannot be easily defined. Hence, dithiolene ligands are referred to as non-innocent ligands. According to Jorgensen definition,[1] "ligands are innocent when they allow oxidation states of the central atoms to be defined". Ward and McCleverty[2] have pointed out that the term non-innocent is applied properly when it is referred to a particular combination of the metal and the ligand rather than redox-active ligands alone. When, metal-centered and ligand-centered orbitals lie at different energies, their redox potentials are well separated and the related redox processes can be assigned to the metal or the ligand without ambiguity; on the contrary, ambiguity is found where a significant mixing between the metal-centered and ligand-centered orbitals occurs. Thus the same ligand can behave as innocent or non-innocent depending on the metal involved in the complexes.

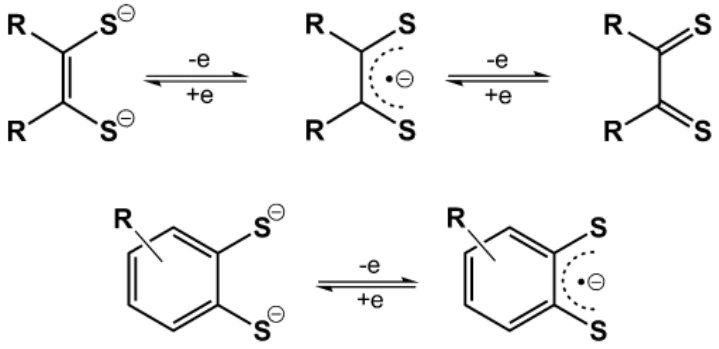


**Scheme 1.1.** Olefinic (top) and aromatic (bottom) dithiolene ligand redox levels.

## 1.2. Nomenclature

In the description of "dithiolene", there is considerable irregularity, within the literature, which is generally decided by the substituent(s) on dithiolene and the oxidation state of the concerned metal.[3] The term dithiolene was initially introduced by McCleverty and co-workers[4] and Balch *et al.*[5] to give a general name for the ligand that does not specify a particular oxidation state. After that, this suggestion was generally accepted, and "dithiolene" is now universally accepted term. The general formula of 1,2-dithiolate dianion is $R_2C_2S_2^{2-}$. Nomenclature, such as, 1,2-ethenedithiolate or 1,2-benzenedithiolate as base terminology is useful as a reliable naming practice for the free ligands. However, the term dithiolate does not specify that dithiolenes are different from saturated 1,2-dithiolate ligands and does not group structures that have related electronic configurations and bonding tendencies. This 1,2-dithiolene can also be described by different nomenclatures such as 1,2-alkenedithiol or 1,2-dithiete or 1,2-dithione depending on the oxidation states. This concept can be expressed by the Scheme 1.1.

## 1.3. Types of Dithiolene ligands

The unsaturated dithiolato ligands have been divided into groups of having odd and even numbers of π–orbitals, respectively.

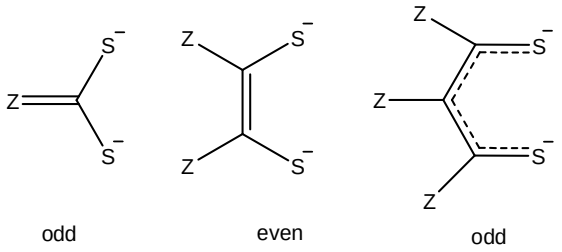


Above mentioned 1,1-dithiolene (odd), 1,2–dithiolene (even), and 1,3–dithiolene (odd), ligands form complexes with four-membered rings, five-membered rings, and six-membered rings, respectively, which have been shown in Scheme 1.2.

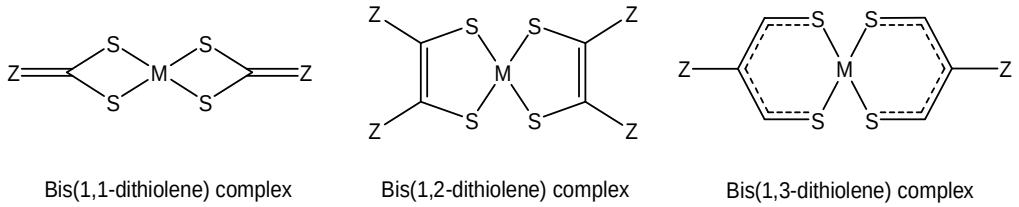


**Scheme 1.2.** Formation of metal complexes with different dithiolene ligands.

**1,1'–dithiolates**

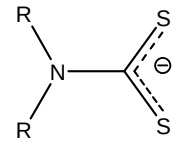

Alkyl dithiocarbamate

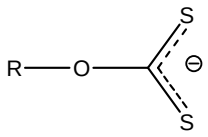

Alkyl Xanthate

**1,3–dithiolates**

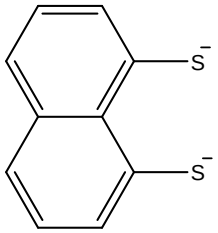

1,8-Napthalene-dithiolate

**1,2-dithiolates**

There is a considerable interest in 1,2-dithiolate ligands and more number of 1,2-dithiolate ligands are reported in the literature.[3a] Due to the broad range of 1,2-dithiolenes in the literature, these can be further classified into following categories.

**Arene-1,2-dithiolates**

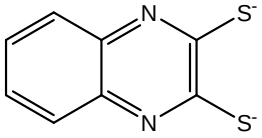

$\{qdt\}^{2-}$

Quinoxaline-2,3-dithiolate

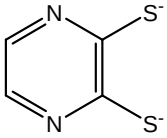

$\{pydt\}^{2-}$

Pyrazine-2,3-dithiolate

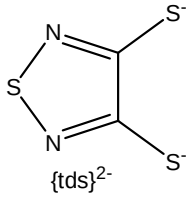

$\{tds\}^{2-}$

2,1,3-Thiadiazole-4,5-dithiolate

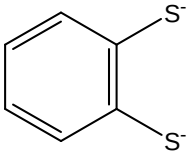

$\{bdt\}^{2-}$

Benzene-1,2-dithiolate

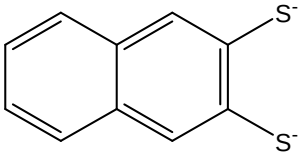

Napthalene-2,3-dithiolate

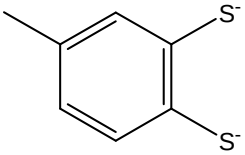

$\{tdt\}^{2-}$

Toluene-3,4-dithiolate

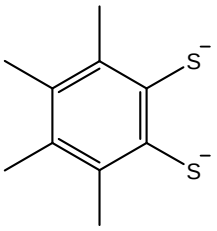

Toluene-3,4-dithiolate

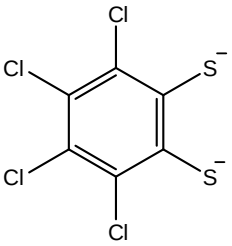

Toluene-3,4-dithiolate

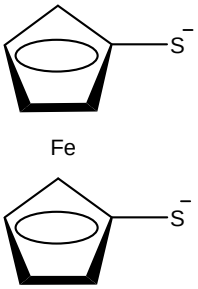

1,1'-dithiolatoferrocene $[FcS_2]^{2-}$

## Alkene-1,2-dithiolates

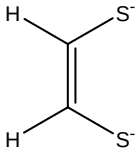

$\{edt\}^{2-}$

Ethene-1,2-dithiolate

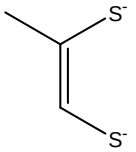

Propene-1,2-dithiolate

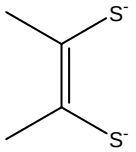

But-2-ene-2,3-dithiolate

## Inorganic-1,2-dithiolates

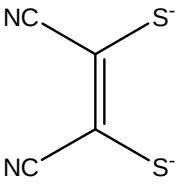

$\{mnt\}^{2-}$

1,2-Malonitrile-1,2-dithiolate

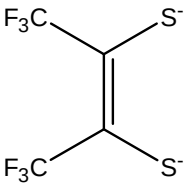

$\{tfd\}^{2-}$

1,2-Bis(trifluormethyl)ethylenedithiolate

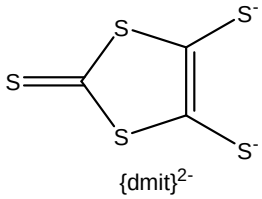

$\{dmit\}^{2-}$

1,3-Dithiole-2-thione-4,5-dithiolate

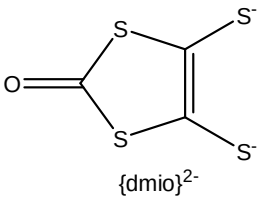

$\{dmio\}^{2-}$

1,3-Dithiole-2-one-4,5-dithiolate

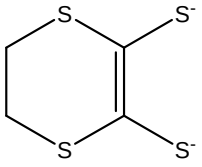

$\{dddt\}^{2-}$

5,6-Dihydro-1,4-dithiine-2,3-dithiolate

## 1.4. Classification of Metal 1,2–Dithiolene Complexes

Metal dithiolene complexes can be classified in terms of the structure and bonding of the bidentate sulfur chelate of the dithiolene ligand. Unlike free saturated 1,2-dithiolene ligands, dithiolene ligands in complexes form relatively rigid and roughly planar five-membered ring with considerable electronic flexibility. This flexibility allows the redox state of the complex to be varied without significant alternation of the basic geometry of the structure. The use of dithiols and dithiolates for analytical purpose was known as early as the 1930s; the field did not become active and expand rapidly until the 1960s when three groups (Schrauzer at Munich, Gray at Columbia, and Davison/Holm at Harvard) independently came to realize the unique nature of dithiolene ligands.[6-8] First they established that the square–planar nature, redox activity, and broad scope of the highly colored bis(dithiolene) complexes of late transition metals, such as Fe, Co, Rh, Ir, Ni, Pd, Pt, Cu, Au and Zn. Later on, this area has further been explored in terms of synthesis and structural characterization of tris and tetrakis(dithiolene) complexes, whereby, their geometries were established by Wieghardt and Wiyhermuller.[9] In the last three decades, remarkable progress in this research arose because of their immense contributions in the areas of materials science, enzymology, analytical science and reactivity, which broadened the impact and importance of dithiolene chemistry.[10] Metal dithiolene complexes often exist in numerous oxidation states. This is due to the more delocalized nature of dithiolene ligands. However, differences in C–C and C–S bond distances have been used to understand electronic configuration of a dithiolene complex.

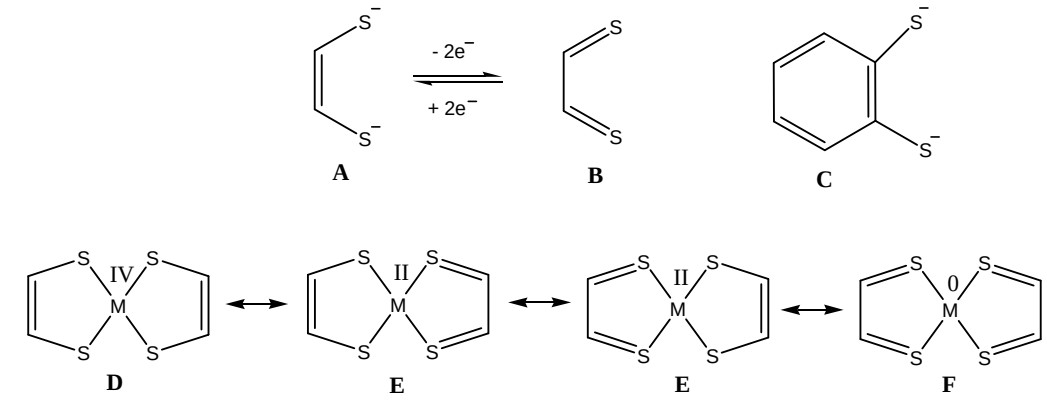

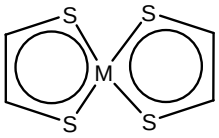


**G**

**Scheme 1.3.** Various bonding description of M(dithiolene)$_2$ complexes.

The Scheme 1.3 represents the oxidation state of the five-membered ring, that is often better described as a combination of dithiolate and dithiolene forms (D, E, and F), whereas in G, the electron density is distributed over the five-membered ring atoms. Despite the uncertainty in dithiolene ligand and metal oxidation state, a metal oxidation state formalism will occasionally be used in the dithiolene chapter. This formalism considers the ligands as "dithiolates" (A / C) that form complexes as in "D". A discussion of this formalism is presented by Alavarez *et al.*[11] Dithiolene ligands are coordinated to the metal, and it may allows for the possibility of interligand S–S bonding interactions, which helps to stabilize the particular structures and/or affect specific molecular distortions. The dithiolene ligand π orbitals interact with the metal dπ orbitals to give frontier orbitals of mixed-ligand and of metal character. In both the bis- and tris(dithiolene) complexes, electrons are not localized at the ligands, but are delocalized throughout the metal-dithiolene five-membered rings and exhibit a certain degree of aromaticity.

**Classification**

Various dithiolene complexes, that have been developed so far, are mainly classified into three main categories:

**(a) Homoleptic dithiolene complexes:** These type of complexes have the $ML_n$ formulae, in which L = dithiolene ligand (1,1-, 1,2-, or 1,3-), and $n$ = 2 [bis(dithiolene)] or 3 [tris(dithiolene)]. Some of the homoleptic dithiolene complexes are recently prepared by Fourmigue's and Boucekkine groups.[12] Some of these homoleptic fashion type complexes are represented below.

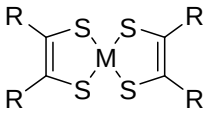

R family

Cyclic and non cyclic SR family

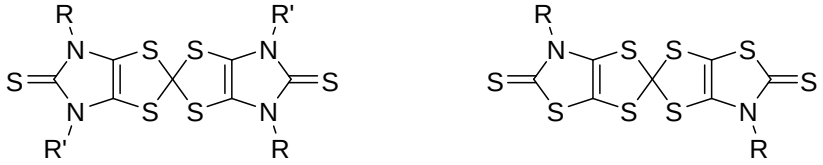

*N*-R family

(**b**) **Heteroleptic dithiolene complexes**: These type of complexes have the $X_mML_n$ formulae, where $m$ = 1, 2 or 3; $n$ = 1, 2 and X is a non-dithiolene ligand (*i.e*. heteroleptic dithiolene complexes contain at least one dithiolene and one other ligand). It has several classes (**I**) Carbonyl complexes:[13] $[M(CO)_4(S_2C_2Z_2)]$, $[M(CO)_2(S_2C_2Z_2)_2]$; in these complexes carbonyl groups are labile and can be displaced by a variety of other ligands, such as chalcogenide, phosphine, and halogen ligands. (**II**) Nitrosyl complexes:[14] $[Fe(NO)(S–S)_2]^–$; these species are stable toward aerial oxidation but are often attacked by two-electron donor ligands (L), such as pyridine (py), DMF, or $PPh_3$, resulting in expulsion of NO and formation of the corresponding adduct $[Fe(L)(S–S)_2]^–$. (**III**) Complexes with metal-ligand multiple bonds:[15] generally it has two type of complexes metal-oxo, and metal-nitrido complexes, with the formulae $[M(L)(S–S)_2]^{z–}$ (L = N, O; Z = 1, 2). (**IV**) Organometallic complexes:[16] cyclopentadienyl moiety with another dithiolene ligand complexes.

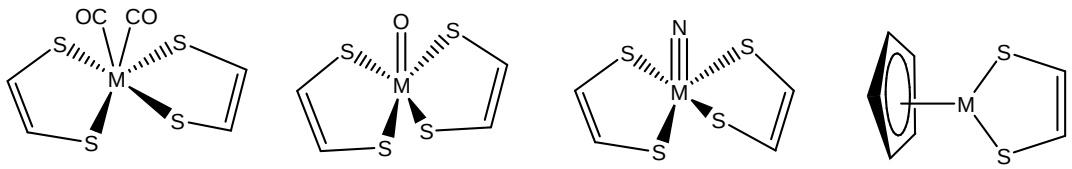

## 1.5. Properties and Applications of Metal 1,2–Dithiolene Complexes

### 1.5.1. Solid-State Properties

Fascinating properties are demonstrated in metal dithiolenes, based on molecular coordination compounds. These exhibit unusual solid-state properties, such as magnetic,[17] conducting and nonlinear optics (NLO) properties.[18] Indeed, the existence of these many properties are due to the high degree of π–electron delocalization throughout ligand-metal center, depending on the substitutents on the ligand. This class oc compounds also have ability to carry a molecular charge that depends upon the nature of the central metal ion and of the ligand.

### 1.5.2. Conducting Properties

Since the discovery of the first organic semiconductor perylene-bromine complex in 1954,[19] a large number of molecular conductors, including more than 100 moleuclar superconductors have been prepared. Conducting molecular materials are characterized by the following features:

– Clear and simple electronic structure which can be well described by the tight-binding band picture based on the extended Huckel molecular orbital caluculation.[20]

– A variety of physical properties that originate from low-dimensionality strongly correlated electron-electron interaction, frustration effect, and so on.

– Softness of the crystal lattice and sensitivity to external stimuli.

– Plenty of possibilities for chemical design.

In general, π-conjugated system associated molecular conductors are divided into two categories: electron donor and electron acceptor. In order to obtain the metallic state, the formation of at least one partially filled energy band is required. A straight forward access to the molecular metal can be achieved by arranging open-shell molecules (radicals) to facilitate intermolecular electron transfer. In most cases, cation radicals or anion radicals, generated from the donor or the acceptor, have been used for the formation of metallic molecular crystals and the conduction band originates from HOMO of the donor or LUMO of the acceptor. It should be added that electron transfer between HOMO and LUMO bands in a single-component molecular crystal can also generate partially filled energy bands, which is observed in the first single-component molecular metal $Ni(tmdt)_2$.

Since planar π-conjugated molecules tend to stack to form the column structure, molecular metals, developed in the early stage, have the one-dimensional electronic structure which is characterized by a pair of planar Fermi surfaces and is associated with a metal-insulator transition at low temperatures. An organic donor BEDT-TTF (Figure 1.1), where sulfur containing six-membered rings are attached to the TTF moiety, effectively enhance the 2-D intermolecular interaction and provides various types of metallic and superconducting cation radical salts.[21]

In the early stage of the development of molecular conductors based on metal complexes, partially oxidized tetracyanoplatinate salts (for example, KCP; $K_2[Pt(CN)_4]Br_{0.30}\cdot 3H_2O$) and related materials were intensively studied.[22] In this system, the square-planar platinum complexes are stacked to form a linear Pt-atom chain. The conduction band originates from the overlap of $5dz^2$ orbitals of the central platinum atom and exhibits the 1-D character. Metal dithiolene complexes posses a delocalized electron system as a planar central core $M(C_2S_2)_2$. The conduction band is formed by the ligand π orbitals or mixed-metal-ligand orbitals where the sulfur atoms play an important role.[23] Depending on the choice of substituent groups attached to the central core, metal dithiolene complexes behave as both the donor and the acceptor. Development of molecular conductors based on the dithiolene complexes was triggered by the discovery of the metallic behavior in an anion radical salt $(H_3O)_{0.33}Li_{0.8}[Pt(mnt)_2]\cdot 1.67H_2O$ (Figure 1.2).[24] Among metal dithiolene complexes, the metal-dmit complexes $M(dmit)_2$ (M = Ni, Pd) have been the most studied system. In the $M(dmit)_2$ molecule, HOMO and LUMO have the $b_{1u}$ and $b_{2g}$ symmetry orbitals. The metal d orbitals can mix into the LUMO, but cannot contribute to the HOMO due to the symmetry constraints which destabilize the HOMO and leads to a small energy splitting between HOMO and LUMO. The side-by-side intermolecular interaction, which leads to the formation of the 2-D electronic structure, is strong for the HOMO and weak for the LUMO. This is because some of overlap integrals for the intermolecular S···S pairs are canceled out due to the $b_{2g}$ symmetry of the LUMO. Although the $M(dmit)_2$ molecule is belonged to the acceptor, the nature of the conduction band in their anion radical salts strongly depends on the central metal. In general, the conduction band of the Pd system originates from the HOMO, while the conduction band of the Ni system originates from the LUMO. This unusual feature of the Pd system is the HOMO-LUMO band inversion. This is due to the strong dimerization and the small energy splitting between HOMO and LUMO.[25] In a series of anion radical

salts with closed-shell cations (cation)$[Pd(mnt)_2]_2$ (Cation = $Et_xMe_{4-x}Z^+$; Z = N, P, As, Sb and $x$ = 0,1,2), the dimer units $[Pd(mnt)_2]_2^-$ form a strongly correlated 2-D system with a quasi triangular lattice and exotic properties derived from frustration and strong correlation are reported.[23]

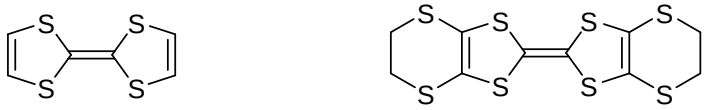

TTF



BEDT-TTF

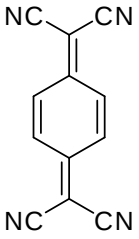

TCNQ

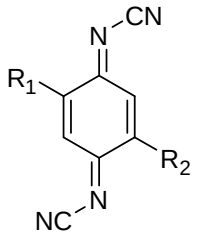

$R_1$,$R_2$-DCNQ1

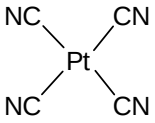

$Pt(CN)_4$

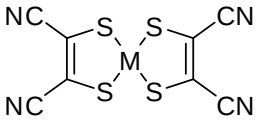

$M(mnt)_2$

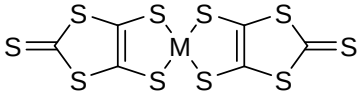

$M(dmit)_2$

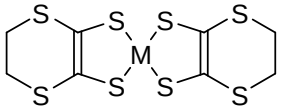

$M(dddt)_2$

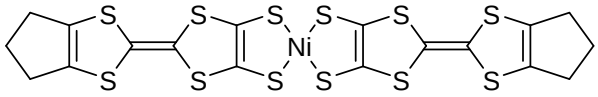

$Ni(tmdt)_2$

**Figure 1.1.** Examples of component molecules for molecular conductors

In these Pd salts, the choice of the counter cation tunes the degrees of frustration and correlation which are associated with the molecular arrangement. On the other hand, in the Ni salts, the choice of the counter cation provides a variety of molecular arrangements. Apart from these dithiolene complexes, the organic−inorganic hybrid materials of

dithiolene-polyoxometalate complexes have also been reported in 1989.[26,27] These complexes exhibited singular, non-centrosymmetric character which originates in a set of "interfacial" C−H···O hydrogen bonds with the top and bottom closed-packed oxygen atom surface layers of the polyoxometalate anions.

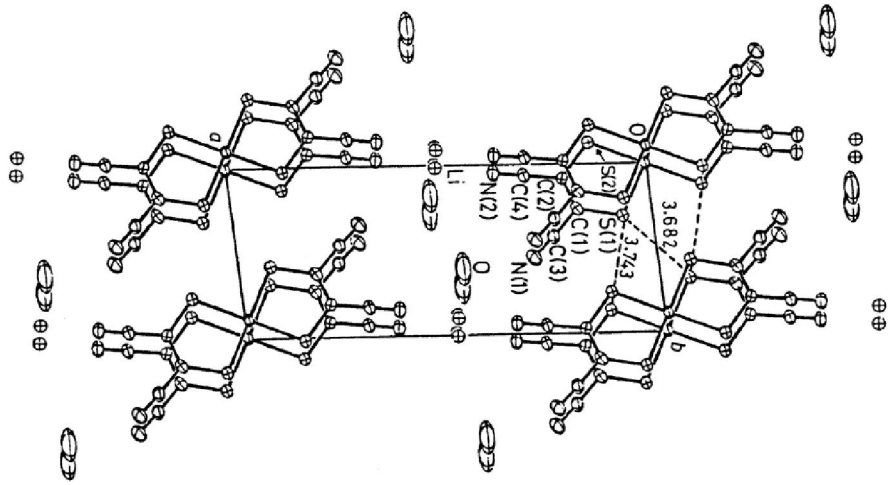


**Figure 1.2.** Crystal structure of $(H_3O)_{0.33}Li_{0.8}[Pt(mnt)_2]\cdot 1.67H_2O$.

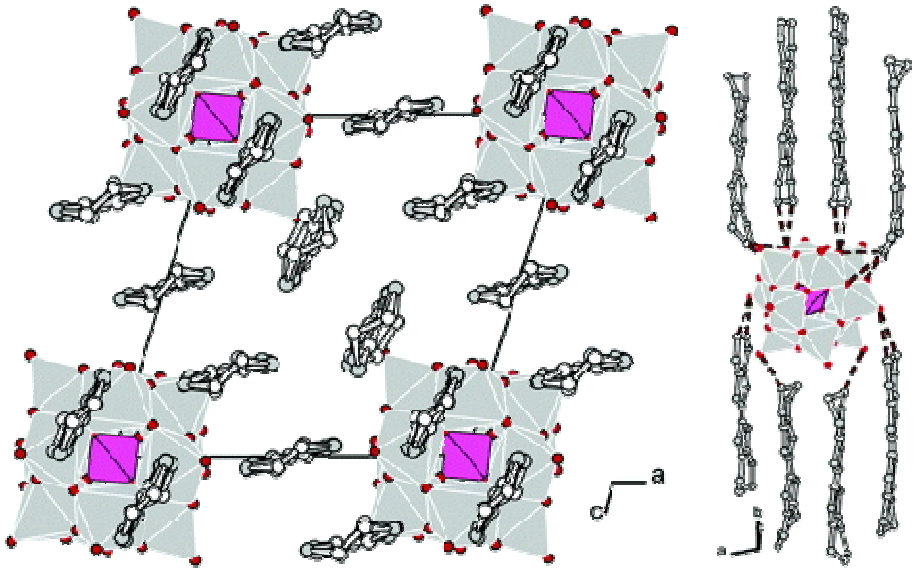


**Figure 1.3.** Polyoxometalate and BEDT-TTF based molecules in monoclinic, space group. *I2* $\alpha$-$(BEDT\text{-}TTF)_4(SiW_{12}O_{40})$.

### 1.5.3. Near-IR Dithiolene Complexes:

**Back ground:** The near-infrared (NIR) region of the electromagnetic spectrum, usually defined between 750 and about 2500 nm, was discovered by the German and British scientists Friedrich-Wilhelm (Sir Frederick William) and Herschel (1738-1822) in 1800. Its association with heat (calorific rays) gave rise to one of the contemporary uses of this kind of radiation. However, in recent years the near infrared has become of additional interest in quiet diverse areas, which are mentioned below:

–In atmospheric chemistry, the NIR absorption of "greenhouse gases" is responsible for the global heat balance and temperature, and the increasing anthropogenic release of such substances is causing worldwide concern over their climatic consequences.

– In astronomy, near-infrared spectroscopy can be used for searching potentially life-sustaining molecules on planets and for studying the origin of galaxies.

– Since much of the solar radiation reaching the surface of the earth lies in the NIR region there is a continuing interest in developing NIR dyes as sensitizers for solar cells.[28]

– Glass fibre efficiency in communications technology as recently honored through the Nobel Prize in Physcis (Charles K. Kao, 2009) is possible mainly due to the attenuation minimum of pure silica in certain NIR bands, such as, the 1300-1350 and 1500-1600 nm regions. The low cost of NIR irradiation sources has also contributed to their use in liquid crystal devices and other systems designed for optical signal proceesing (e.g. switching, wavelength conversion, memory).[29]

– NIR spectroscopic analysis of food and related biological materials has become an indispensable and efficient technique in process monitoring and quality control.[30]

– Medical applications of NIR radiation make use of the partial transparency of tissue at such wavelengths and include diagnostics aspects (e.g. non-invasive thermal or biological imaging as well as therapy).[31]

From the above-described facts, it follows that NIR dyes are sought among right materials, and coordination compounds, such as, the well established dithiolene complexes, that offer absorption and emission activity in the near-IR spectral region.

**Favorable conditions for near-IR absorbing dyes:**

Dyes for applications in the NIR region require small differences in the energy between HOMO and LUMO. The donor–acceptor concept was established by König[32] and Ismailsky.[33] It was further developed by Dilthey and Wizinger[34] and incorporated into the perturbation molecular orbital theory (PMO) model by Dewar.[35] According to this

concept; long–wavelength absorption is expected if π–systems are substituted with donor (D) and acceptor (A) groups. Very strong donor and acceptor groups can be applied in a double arrangement according to building principle (**D — π — A — π — D**) and can cause long–wavelength absorption.

The literature provides extremely limited data about the near-IR dyes. The first near–infrared (NIR) absorbing organic compounds (some of phenylenediamine derivatives) were synthesized at the beginning of this century. The usage of NIR dyes has an prominent feature, because they serve as excellent indicators of the progress of novel technologies, especially the development of NIR semiconductor lasers, optical data storage field DRAW (Direct Reading After Writing) or WORM (Write Once Read Many). Metal bis(dithiolene) complexes have been used as good candidates for near-IR dyes, because (1) metal bis(dithiolene) complexes show intense electronic absorption in the NIR region, especially Ni-dithiolene complexes. (2) Metal dithiolene complexes have ability to exist in several clearly defined oxidation states which are fully connected through reversible redox steps. (3) Another characteristic property of dithiolene coordination complexes is their high thermal and photochemical stability. Based on this research, it leads to conclusion that the dithiolene complexes should contain following reqirements (Scheme 1.4 & 1.5):

(1) Coplanarity of ligand π-system and dithiolene;

(2) Presence of an extended π-system;

(3) Presence of electron donating substituents;

(4) Fixing of the substituents into rigid coplanarity with the ligand;

(5) Attachment of sterically bulky substituents to increase solubility;

(6) Variation of the central metal to obtain different shifts and to tune the relaxation time.

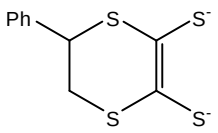


$\{phdt\}^{2-}$ 1028 nm

(43,000) $C_6H_6$

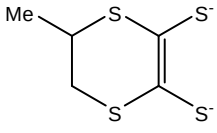


$\{medt\}^{2-}$ 1029 nm

(36,000) $C_6H_6$

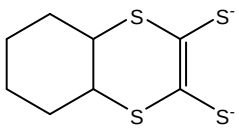


$\{bddt\}^{2-}$ 1035 nm

(63,000) $C_6H_6$

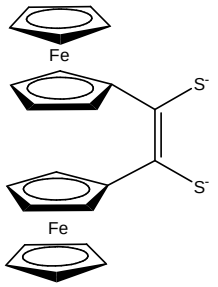


1310 nm

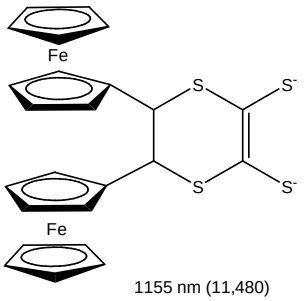


1155 nm (11,480)

**Scheme 1.4**

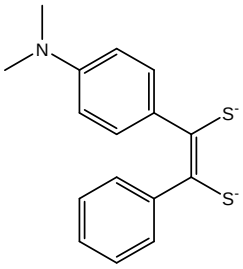


1060 nm (28,000)

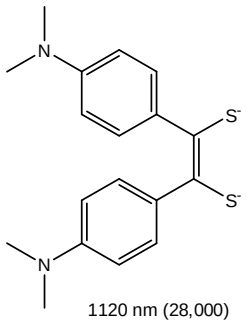


1120 nm (28,000)

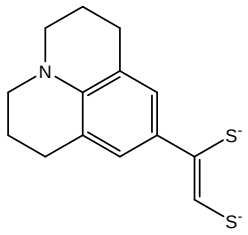


1180 nm (35,000)

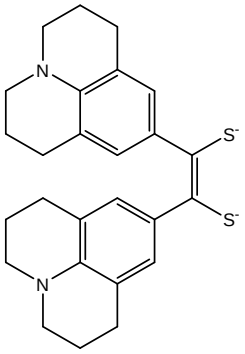


1270 nm (45,000)

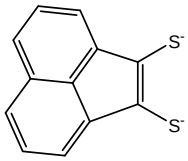


1140 nm (30,000)

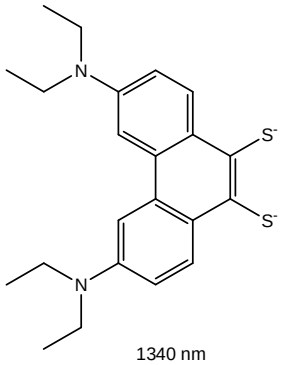


1340 nm

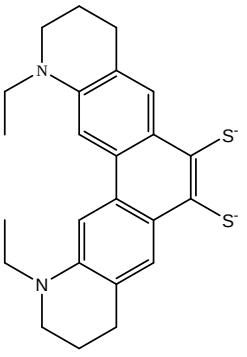


1380 nm

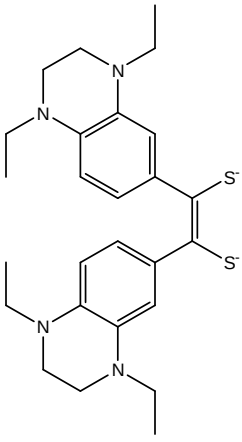


1370 nm (42,000)

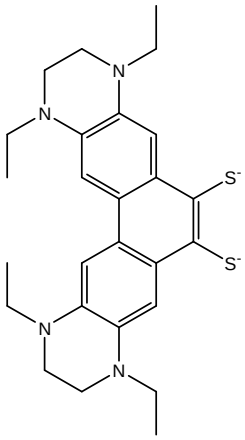


1440nm

**Scheme 1.5**

Although the dithiolene metal complexes show an absorption band in the NIR region, they are not useful as colorants in the recording layer of the optical DRAW disk,[36] due to their low reflectivity of the GaAlAs diode lasers. But the nickel based dithiolene complexes has been applied to the optical DRAW disk as an inhibitor of laser induced fading.[37] The metal dithiolene complexes have also attracted much interest as Q–switching NIR dyes applications.

### 1.5.3.1. $\{M[(mnt)_2]\}^{n-}$ (n = 1,2 and 3) Based Dithiolene Complexes:

The transition metal ion in a bis(1,2-dithiolato)metal complex favors a planar coordination environment. However, the distorted square planar coordination geometry around a metal centre has also been observed.[38] For example, in the cases of the metal center being $Mn^{2+}$, $Fe^{3+}$ or $Co^{2+}$ ions in the complexes $[RBzPy]_2[Fe_2(mnt)_4]$, $[Bu_4N]_2[Fe_2(mnt)_4]$, $[Bu_4N]_2[Fe_2(edt)_4]$, $[Et_4N]_2[Mn_2(edt)_4]$, $Co_2[S_2C_2(CF_3)_2]$ and $[Bu_4N]_2[Co_2(S_2C_6Cl_4)_4]$,[39] the deviation from planarity is mainly caused by dimerization *via* M···S interactions. For bis(1,2-dithiolato)cuprate(II) complexes, notably, there are few cases of a significantly non-planar environment around a tetra-coordinate $Cu^{2+}$ centre resulting from the weakly intermolecular interactions between the cation and anion.[40] Theoretical investigation for the $[Cu(mnt)_2]^{2-}$ complex further disclosed that the energy gap between distorted and perfect square-planar coordination geometry is not much higher than the values of the crystal packing forces.[41] As a result, the configuration preference for the $[Cu(mnt)_2]^{2-}$ complexes will be controlled by the combination of a variety of intermolecular interactions.[41] For the bis(1,2-dithiolato)nickelate(II) species, reports of significant non-planar environment around a tetra-coordinate $Ni^{2+}$ ion are very rare, based on CCDC literature (until August 2007); only eight complexes having dihedral angle more than 10° between the mean planes of two S–Ni–S chelate rings have been reported.[42] According to DFT calculations of $[Ni(mnt)_2]^{2-}$ anion moiety, the square-planar geometry is more stable configuration for the nickel atom.[43]

**Cation role:**

It is well known that the donor–acceptor type salt could give rise to a charge transfer (CT) transition band in its electronic absorption spectrum, with band position depending on the energy gap between acceptor LUMO and donor HOMO. Consequently, the spectral property for such a charge transfer transition band is tunable via systematic modification of the acceptor/donor molecular structure.[44] The bis(1,2-dithiolato)metal

complexes show intense near-IR absorbance,[45,46] and the origin of this transition may be discussed under two headings: (1) the HOMO and LUMO are delocalized over two dithiolate ligands, and electronic transition between these orbitals gives rise to a strong absorption in the near-IR region. Donor substituents in the parent dithiolate raise the energy level of HOMO more than that of LUMO, resulting in a shift of the near-IR absorbance to lower frequencies; (2) the electronic transition from the HOMO of the bis(1,2-dithiolato)metal anion to the LUMO of the cation gives rise to an intense ion-pair charge transfer (IPCT) band in the near-IR region.[40a] Therefore, modifying the molecular structure of the cation provides a useful strategy for the fine-tuning of IPCT band.

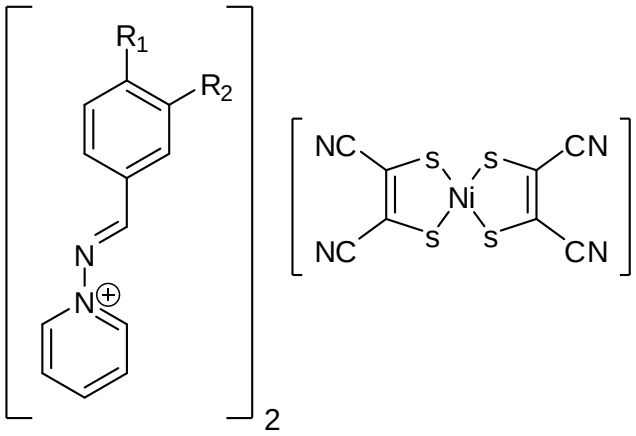


| $R_1$ | $R_2$ | Compound code |
|---|---|---|
| $NO_2$ | H | (**1**) |
| $CH_3$ | H | (**2**) |
| Br | H | (**3**) |
| Cl | H | (**4**) |
| H | $NO_2$ | (**5**) |

**Scheme 1.6.** Nickel based dithiolene complexes **1**–**5**.

In the nickel based dithiolene complexes (R-benzylidene-1-aminopyridinium derivatives and $[Ni(mnt)_2]^{2-}$), cation is different from one compound to another compound (Scheme 1.6). Based on cationic moiety, properties of dithiolene complex has been modified. For example, from the above mentioned compounds, compound **1** exhibit only

distorted square-planar geometry (Figure 1.4) around nickel metal atom and remaining all four compounds exhibit perfect square-planar geometry around nickel atom. Apart from this, in the solid state complexes **2**–**5** show the intense absorption in the UV-vis region (200-700 nm) with a moderately intense absorption band. The spectral shape of compound **1** is strikingly different from the other four, in which a very strong absorption is obsereved from the UV-vis to near-IR region and its low energy absorption tail extends up to 1200 nm (Figure 1.5). The UV-vis-NIR spectra of **1**–**5** were recorded in acetonitrile solution. In this spectra, there are two bands centered at 473 nm ($\pi \rightarrow \pi^*$ transition within the cation and anion) and ~862 nm (IPCT transition). The first band (473 nm) is independent on the concentration of cation, whereas the intensity of second band is dependent on concentration of cation (Figure 1.6).

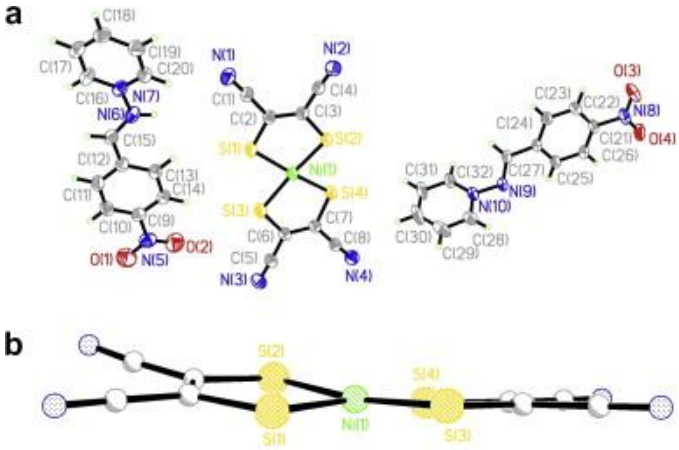


**Figure 1.4.** (a) ORTEP view of **1** with thermal ellipsoids at the 30% probability level; (b) the molecular configuration shows a distorted anionic geometry.

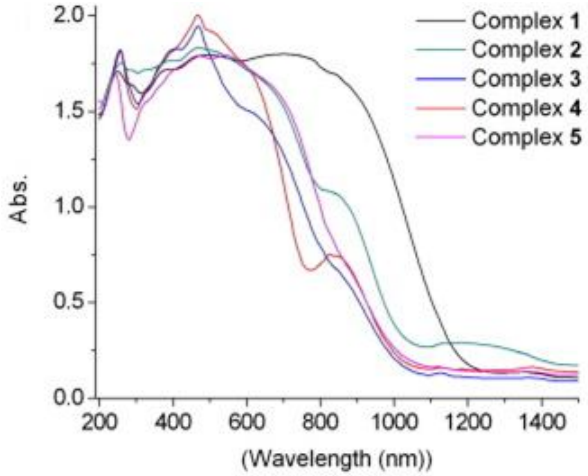


**Figure 1.5.** Diffuse reflactance spectra of compounds **1**–**5**.

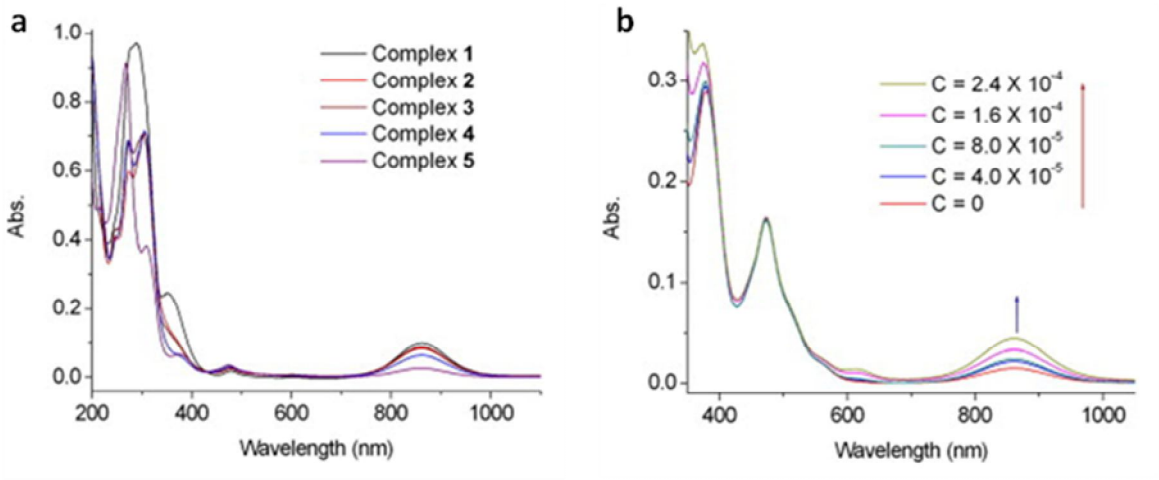


**Figure 1.6.** (a) UV-vis-NIR absorption spectra for the compounds **1**–**5**, (b) $[TBA]_2[Ni(mnt)_2]$ (c = 5.0 X $10^{-5}$ mol $L^{-1}$) with different concerntration of [*p*-$NO_2$Bz-1-Apy]I.

### 1.5.3.2. Substituent Effect on Dithiolene Complexes:

**(I)**

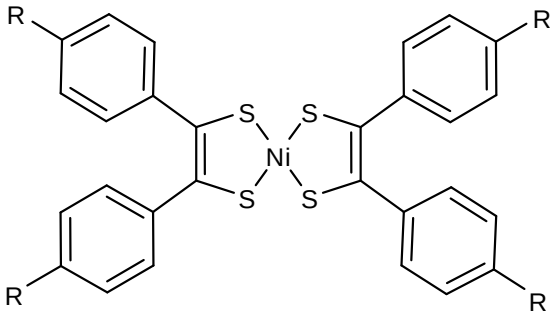


R = H (**A**)
= Me (**B**)
= COOMe (**C**)
= COOH (**D**)

**Scheme 1.7.**

Dithiolene complexes are much influenced by the substituent groups which are present in dithioelene core moiety; due to the delocalization in chelate ring system, this factor plays key role to exhibit absorption in NIR region in the concered electronic spectra. For example: based on Scheme 1.7, there are four types of nickel based dithiolene complexes, in which **A**, **B**, and **C** exhibit intense absorption bands below 400 nm and broad absorption bands with high molar extinction coefficients in the NIR region (700–1100 nm).[47] The bands below 400 nm originate from the ligand-to-metal charge-transfer (LMCT) transsition and intra ligand transitions. The intense feature absorption bands in

the NIR region are generally assigned to the $\pi \rightarrow \pi^*$ transition between HOMO and LUMO. The $\lambda_{max}$ values of **A**, **B** and **C** are 857, 884 and 868 nm respectively. The maximum absorption data of **A**, **B**, and **C** in different solvents are shown in Table 1.1. The positive solvatochromism is confirmed with increase in polarity of the solvent. From this, one can interpret that the polar excited molecules of the complex are more susceptible to the solvation effect than ground state molecules when combined with the polar solvent, resulting in the lower energy of the excited molecules. Correspondingly, the decreased energy difference is achieved and the red-shifted $\lambda_{max}$ can be observed. Furthermore, **C** suffers a larger effect when DMF and DMSO were used causing the peak to fall upto 944 nm in DMF and 957 nm in DMSO.

The functional group, attached to benzene ring, influences the absorption maximum of dithioelene complexes. The methyl-substituted phenyl derivative **B** exhibits the maximum absorption band at 884 nm in $CH_2Cl_2$. It is red-shifted by 27 and 16 nm compared with H-substituted complex **A** and methoxy carbonyl- substituted phenyl derivative **C**, respectively. This can be explained by the fact that the methyl group, being the electron donating substituent, increases the electron density of the dithiolene moiety and decreases the gap of HOMO and LUMO, which then results in the red-shift of the NIR absorption maximum of **B**. This result is consistent with the conclusion of the recent review. For **C**, it is blue-shifted by 16 nm compared with **B** and red shifted by 11 nm compared with **A**. This can be explained as follows: the methoxy carbonyl group, being the electron withdrawing substituent, decreases the electron density of the dithiolene moiety as compared with **B**. When compared with **A**, the methoxycarbonyl group of **C** increases the conjugation of the whole molecular plane and extends p delocalization. The results show that the $\lambda_{max}$ of nickel bis (dithiolene) complexes are affected by the substitution.

**Table 1.1.** Absortion data of compounds **A**–**C** in different solvents.

| Sample | Ether | DCM | THF | $CHCl_3$ | DIOXANE | DMF | DMSO |
|---|---|---|---|---|---|---|---|
| **A** | 844 | 857 | 856 | 858 | 856 | 871 | 871 |
| **B** | 869 | 884 | 880 | 883 | 880 | 895 | 896 |
| **C** | 861 | 868 | 867 | 871 | 869 | 944 | 957 |

**(II)**

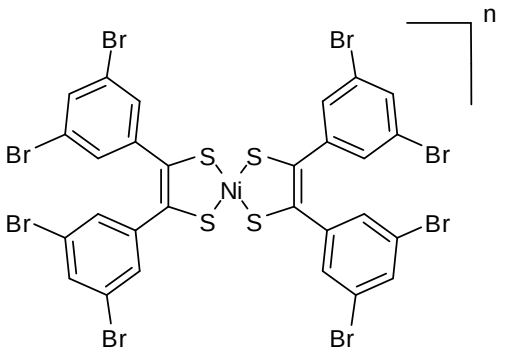


n = 0 (**1a**)
n = -1 (**1b**)

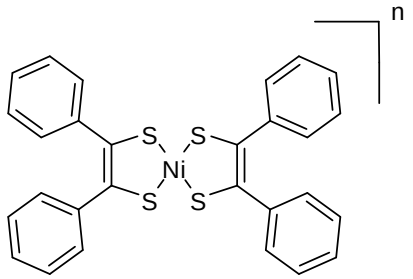


n = 0 (**2a**)
n = -1 (**2b**)

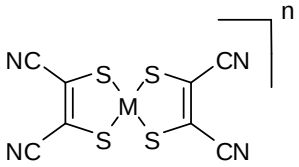


n = -1 (**3b**)
n = -2 (**3c**)

**Scheme 1.8.**

A nickel dithiolene complex system containing 3,5-$C_6H_3Br_2$ substituted phenyl groups,[48] is shown in Scheme 1.8. The electronic spectroscopy is an excellent tool to define the neutral or anionic nature of the Ni-dithiolene complexes. A strong absorption band at the low energy region is a distinctive of neutral complex, which shifts to a lower energy with less intensity in the monoanionic complex and this band is not present in the electronic spectrum of dianionic complex. Electronic spectra of **1a** and **1b** were recorded in DCM. Compounds **3b** and **3c** were insoluble in DCM and hence spectra were recorded in acetonitrile. Based on DFT calculations on $Ni(S_2C_2Me_2)_2$,[49] the HOMO for this neutral species is the $b_{1u}$ orbital (it was fully occupied which is primarily ligand based with minor contribution from the metal). The intense charge transfer absorption is due to the $b_{1u} \rightarrow b_{2g}$ transition. The $b_{2g}$ orbital in the one-electron reduced monoanionic species is singly occupied (Figure 1.7). The contribution of electrons from nickel to these b2g orbital increases with reduction, and the band positions also shift. Because of the involvement of the dithiolene orbitals, the position of the low energy transition is dependent on the substituent on the dithiolene ligand itself. For example, in monoanionic complexes, the

low energy band shifts to low energy with increasing electron-releasing character of the substituent.

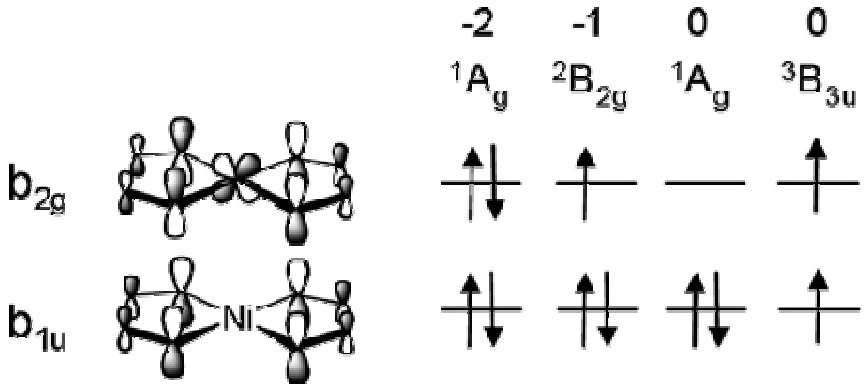


**Figure 1.7.** Frontier orbitals of $[Ni(S_2C_2R_2)]^{n-}$ ($n$ = 2, 1, 0) relevant to their redox and low-energy electronic absorption properties. The ground state electronic configurations of the dianion, anion, and neutral are shown, as well as the lowest-energy triplet state of the neutral.

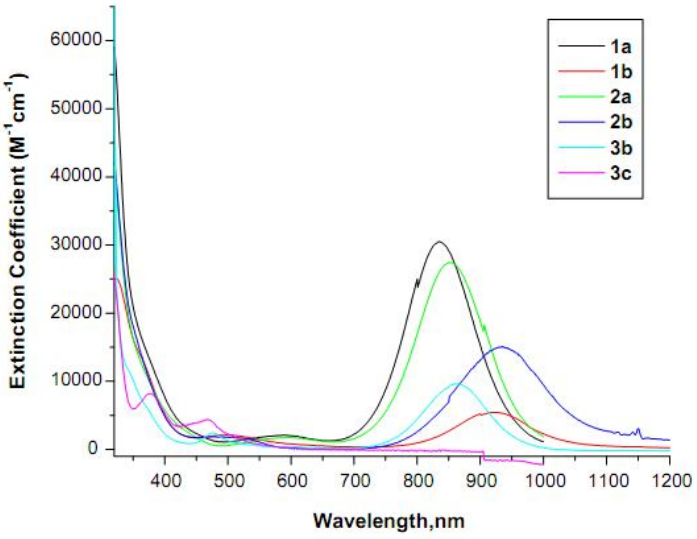


**Figure 1.8.** Electronic spectra of Ni-complexes recorded at room tempertature. **1a**, **1b**, **2a** and **2b** were recorded in $CH_2Cl_2$. **3b** and **3c** were recorded in $CH_3CN$.

From the electronic absorption spectra (Figure 1.8), the first band near 852 nm for the compound **2a** shifts to 834 nm in **1a** – a shift of 18 nm, while 935 nm band in **2b** moves to 927 nm in **1b**, which is only an 8 nm shift. However, this band shifts to 863 nm in the case of **3b**. Thus the low energy band maxima follow the order: **1b** ~ **2b** > **3b**. The intensities of these bands in three compounds are different; the band in **3b** is the least

intense. Because the intensity comes from the mixing of the orbital coefficients involved in the optical transition, it is suggestive that the orbitals of ground and the excited states are not mixed as effectively in these three compounds. Some of the results on neutral complexes with general formula,[50] $Ni[S_2C_2(p\text{-}C_6H_4X)_2]_2$ have also been related to the above discussion part.

**(III)**

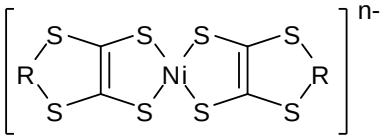


R = -CH(Ph)$CH_2$- n = 1 (**6**) R = -CH(Ph)$CH_2$- n = 0 (**7**)

R = -CH(Me)$CH_2$- n = 1 (**8**) R = -CH(Me)$CH_2$- n = 0 (**9**)

R = -$CH_2CH_2$- n = 1 (**10**) R = -$CH_2CH_2$- n = 1 (**11**)

R = -$CH_2CH_2CH_2$- n = 1 (**12**)

**Scheme 1.9**

Metal complexes with sulfur-rich dithiolene ligands are ineresting in the field of conductive materials, because intermolecular sulfur-sulfur interactions of the ligands.[51] Based on this aspect, Boon-Chuan *et.al*.[52] prepared multi-sulfur dithiolene ligand metal complexes (Scheme 1.9). In complex **7**, the closest Ni···Ni distance is 6.977 Å, which is the length of the *b* axis. The shortest interstack S···S contact is 3.687 Å, which is about the sum of the van der Waals radii (3.70 Å).[53] The large separation between stacks is due to the phenyl substitution on the external part of the ligand. Figure 1.9 shows the NIR spectra of complexes **6** and **7**. Complex **6** in acetonitrile solution shows a strong broad absorption at 1172 nm , while complex **7** in benzene solution exhibits this absorption at 1028 nm. Table 1.2, lists the near-IR absorption maxima and absorbances of these complexes. The EHMO calculations assigned to this strong electronic absorption band is due to a $\pi\rightarrow\pi^*$ transition ($2A_u$, $2B_u$, $3B_{3u}$, 2B3u $\rightarrow$ $3B_{2g}$) of the delocalized ligand.[54] The electron delocalization in the coordination ring and the central metal is made possible by the stronger overlap involving d-orbitals of sulfur and this leads to bathochromic shifts of the multi-sulfur 1,2-dithiolene complexes. Based on data in Table 1.2, it can be noted that complexes **6**, **8** and **10** exhibit NIR absorption bands at 1172, 1177 and 1175 nm, respectively. This indicates the electron-donating ability of the substituents is in the order

Me > H > Ph. But this effect is not significant in [Ni(medt)$_2$] (**9**) and [Ni(phdt)$_2$] (**7**). Attachment of bulky substituents, such as phenyl and methyl groups, would increase solubility, which is favorable for the use of Q-switching dyes.[55]

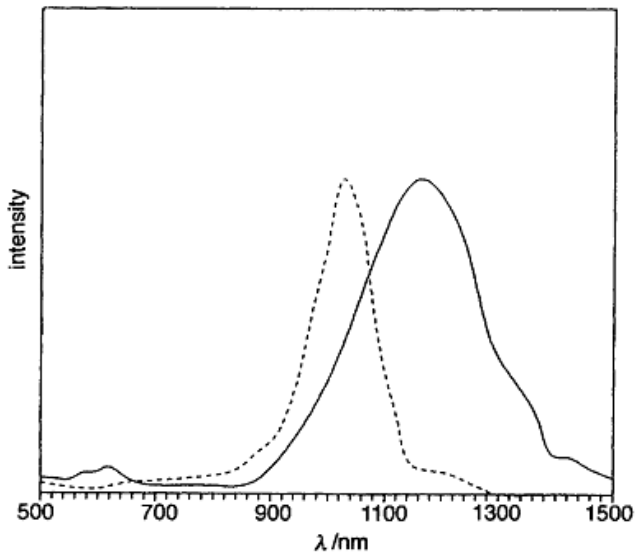


**Figure 1.9.** Absorption spectra of **6** in acetonitrile (–) and **7** in benzene (----).

**Table 1.2** Absorbance bands of the complexes of dithiolenes (at 25 °c).

| Comlex Name | Complex | Solvent | $\lambda_{max}$ (nm) |
|---|---|---|---|
| **6** | [TBA][Ni(Phdt)$_2$] | Acetonitrile | 1172 |
| **7** | [Ni(Phdt)$_2$] | Benzene | 1028 |
| **8** | [TBA][Ni(Medt)$_2$] | Acetonitrile | 1177 |
| **9** | [Ni(Medt)$_2$] | Benzene | 1029 |
| **10** | [TBA][Ni(dddt)$_2$] | Acetonitrile | 1175 |
| **11** | [TBA][Ni(pddt)$_2$] | Acetonitrile | 938 |

### 1.5.4. Nonlinear Optical Materials

#### Second-Order NLO

Optical properties, in particular, nonlinear optical properties are of interest for a number of photonic applications, including high speed optical switching, telecommunication, optical data processing and storage.[56] Nonlinear optical properties arise when the interaction of radiation with the matter occurs, which at small field induces an instantaneous

displacement (polarization: $P_0 = \mu = \alpha E$ where $\alpha$ is the linear polarizability) of the electronic density away from the nucleus (linear optics), involving high fields (laser light).

The basic requirements for NLO active molecules, that possess large β values, include an electron donor group (D) connected with an electron acceptor group (A) by a π–conjugated polarizable bridge.[57,58] The nonlinear optical properties of such dipolar, polarizable (D–π–A) molecules are characterized by low energy, D→A intermolecular charge transfer (ICT) excitations.

In this context, metal dithiolene complexes have attracted interest in terms of NLO properties owing to their highly delocalized electron configuration and the possibility of the transfer of electron density between metal and ligand which induces an intense near-IR absorption transition.[59] Among these, symmetric and asymmetric square-planar $d^8$ metal–dithiolene complexes can be suitable to generate third order NLO properties,[60] but only asymmetric complexes at the molecular level, such as mixed-ligand complexes with push/pull ligands, and a non-centrosymmetric crystal packing for a bulk material, are required to generate second order NLO properties.[61,62]

Interestingly, some of the unsymmetrical bis(dithiolene) complexes (**12**–**15**) and heteroleptic dithiolene complexes (**16**–**19**), which exhibit second order NLO properties are shown in Schemes 1.11 and 1.12, respectively. In those, most promising and extensively studied compounds are heteroleptic Ni(diimine)(dithiolate) complexes as shown Scheme 1.12.[18,63] In order to increase hyperpolarizability of the complexes, the best candidate system should be Pt, with electron donating substituents on the dithiolate ligands (to increase the donor strength), whereas electron withdrawing substituents should be placed on diimine as for as Pt atom is concerned. These compounds exhibit $\beta_0$ values within the range from 0 to $-16 \times 10^{-30}$ esu, depending upon the substituents.

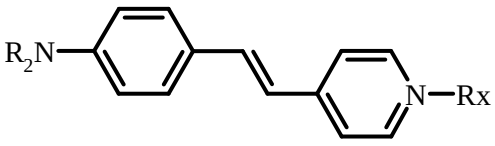


R = Me, Et, Bu, etc.

**Scheme 1.10.**

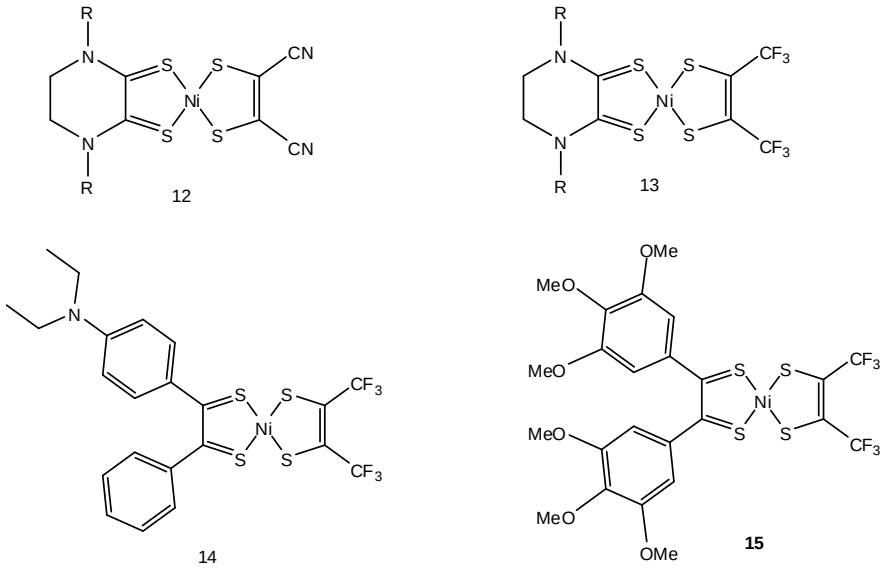


**Scheme 1.11.**

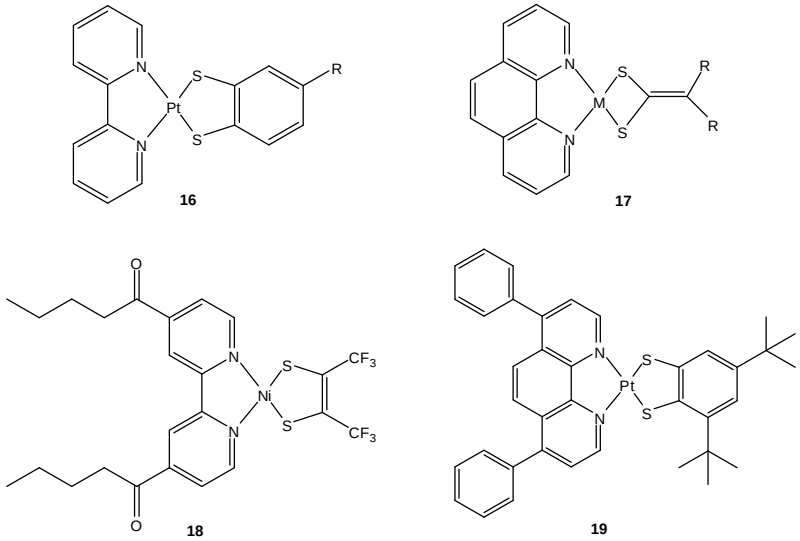


**Scheme 1.12.**

## Third Order NLO

Recently, more and more symmetrical bis(dithiolene) complexes with third-order optical nonlinearity or optical limiting effects have been explored because third order NLO effects do not require any symmetry restriction.[64] Some of the metal bis(dithiolene) complexes exhibiting third order NLO are shown in Scheme 1.13. Third order NLO properties of dmit-based and mnt-based metal complexes with sandwiched organometallic cations $[CpFe(\eta\text{-}C_6H_6)]^+$ have also been reported.[65]

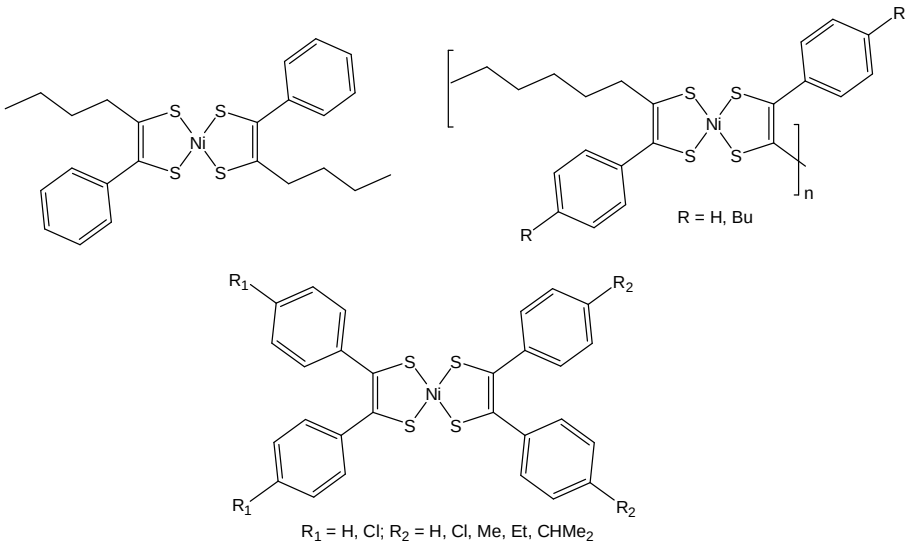


**Scheme 1.13.**

Heteroleptic dithiolene complexes have also been studied for their third-order NLO properties that involve the dmit and mnt ligands as shown in Scheme 1.14,[66] in which, only the dmit based compounds exhibit a large third-order optical nonlinearity, due to their large planar conjugated system compared to the mnt analogues.

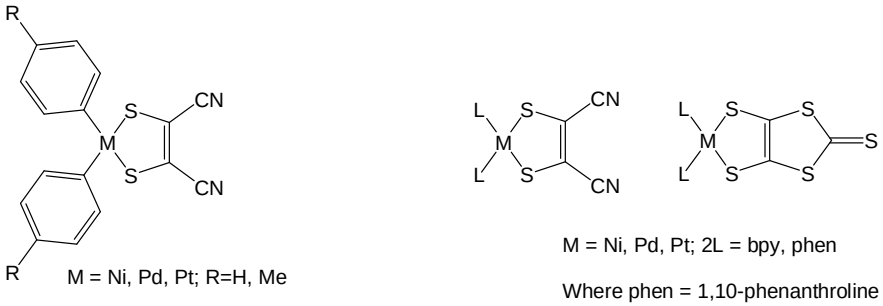


**Scheme 1.14.**

### 1.5.5. Metal Dithiolene Complexes in Catalysis

The recent research on studying metal dithiolene complexes is a growing field in the sense of catalysis also. The metal dithiolene complexes are useful catalyst for organic transformations. However, there are very few reports on organic transformations that use a metal bis(dithiolene) complex as a catalyst. Yokoyama and co-workers[67] described that, the cobaltadithiolene is effective catalyst for synthesis of γ,δ–unsaturated cyanofluoroamide and the reaction is shown in Scheme 1.15. This synthetic reaction proceeded smoothly under mild reaction conditions and only the cyanofluoroamide

product was obtained. Interestingly, without cobaltadithiolene complex, no target product was obtained. Another compound tin-bis(1,2-benzenedithiolene) (Scheme 1.16) has been used as an effective catalyst for the reduction of azides to amines, which was reported by Bosch *et al.*[68] They observed that a series of primary, secondary, tertiary aromatic, and heteroaromatic azides can be reduced in excellent yields under very mild conditions in the presence of $NaBH_4$. Thus, borohydride ion was a reasonable choice for the reduction of azides to amines, but it is not sufficiently active against azides and favorably the use of tin-bis(1,2-benzenedithiolene) as a catalyst has solved the problem.

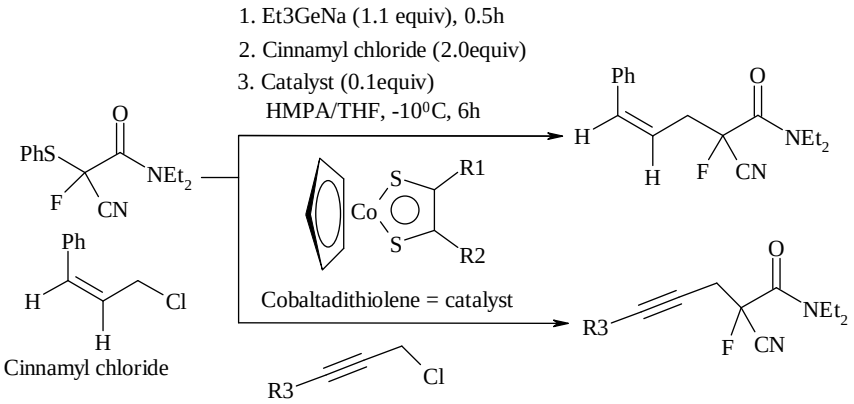


**Scheme 1.15.** Synthesis of γ,δ–unsaturated cyanofluoroamide with cobaltadithiolene complex as catalyst.

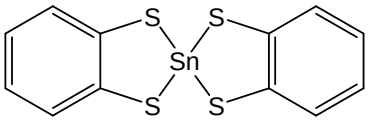

Tin-bis(1,2-benzenedithiolene)

**Scheme 1.16.**

### 1.5.6. Metal Dithiolenes in Biology

In contrast to their long history of dithiolene complexes and the studies of their properties towards material science with respect to photonics and electronic conductors, only since last three decades, biological aspects of metal dithiolene systems have been explored. It is now established that dithiolene-chelate is involved / present in the active site of certain metalloenzymes, especially Mo- and W- containing enzymes. Depending upon the active-site of the structure dithiolene-containing molybdenum and tungsten enzymes, these are classified into four families as shown in Scheme 1.17.[69]

Dithiolenes play an important role in natural systems. Thus, a dithiolene group is present as an integral component of molybdopterin (MPT), the moiety that binds the molybdenum (or tungsten) at the catalytic center of enzymes that transfer an oxygen atom to or from the substrate. A wide range of reactions are present in virtually all living systems catalyzed by these enzymes, and many of these enzymes are structurally characterized. Each catalytic centre is shown to involve a single metal atom bound to one or two MPT groups, plus other donor atoms. Spectroscopic information indicates that the oxygen atom transfer reaction takes place at the metal centre, the oxidation state of which changes from M(VI) to M(IV) (or vice-versa). This chemistry has been replicated by low molecular weight analogues of these centers. However, challenges remain in understanding the coordination chemistry of these centers; the role of the pterin and pyran ring that together with the dithiolene to form MPT is not very clear. Whether other roles for dithiolene complexes will be found in Nature remains to be seen. However, the present knowledge should encourage further investigations of dithiolene complexes as catalysts, especially when the process involves a redox change.

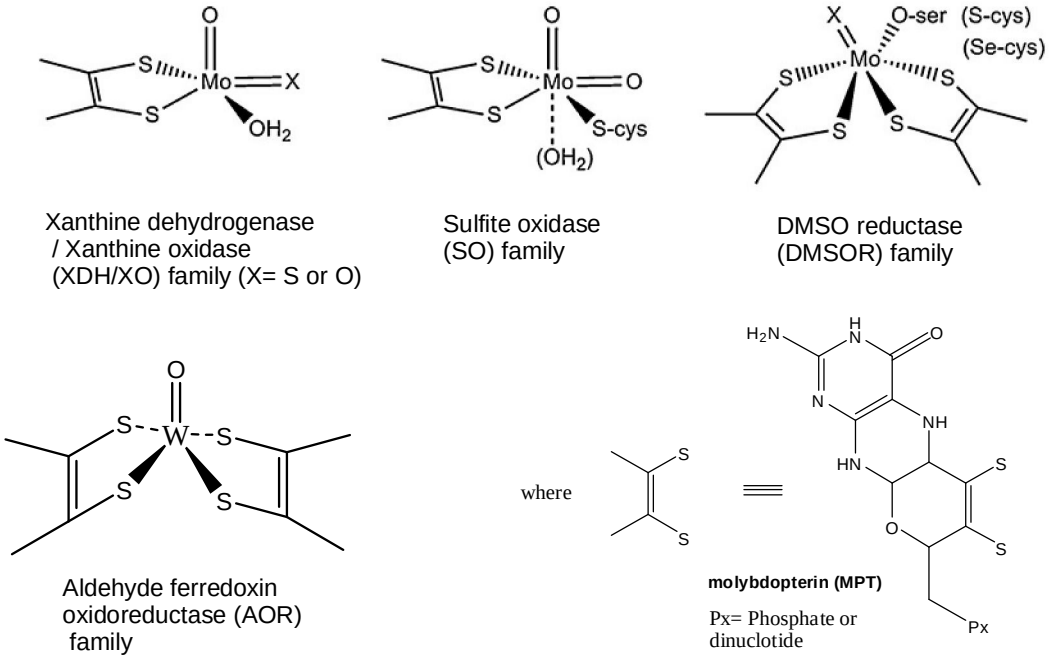


**Scheme 1.17.** The four families of dithiolene-containing molybdenum and tungsten enzymes based on structure of the catalytic reaction centers.

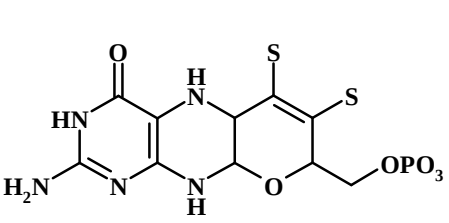

Molybdopterin (MPT)

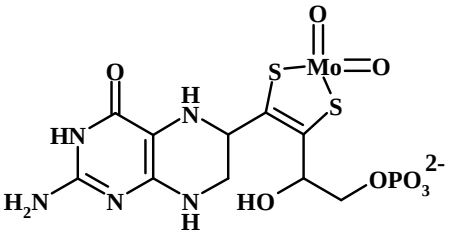

Molybdenum cofactor

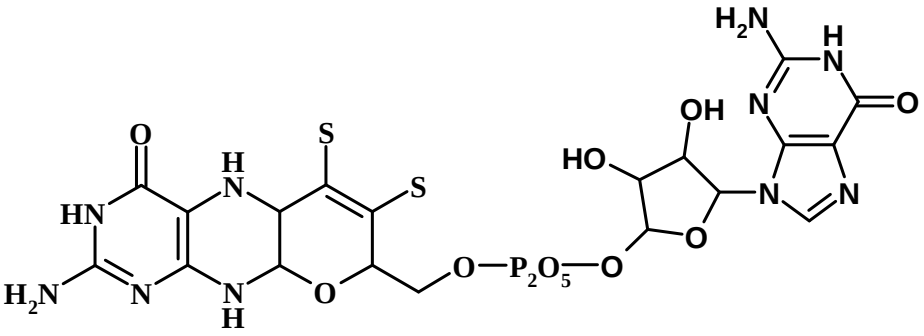

Molybdopterin guanine dinucleotide (MGD)

**Scheme 1.18.** Schematic representation of the 1,2-dithiolene containing molybdenum and tungsten cofactors in relevant metalloenzymes.

More significantly, the complexes $[MO_2(bdt)_2]^{2-}$and $[MO_2(mnt)_2]^{2-}$ (M = Mo or W) constitute reasonable structural models for the active site of this class of enzymes.[70] The Mo containing enzyme is called molybdopterin and the crystal structure of one molybdenum-pterin cofactor enzyme, shows coordination of two pterin units to one molybdenum center.[71] Some schematic representations of the 1,2-dithiolene containing molybdenum and tungsten enzymes are depicted in Scheme 1.18.

Rajagopalan and his co-workers[72] have proposed a structure for the molybdenum cofactor from the various spectroscopic measurements.The proposed structure for the molybdenum cofactor depicts it as a complex of molybdopterin and Mo, with the metal linked to the dithiolene sulfurs. They have suggested that, the molybdopterin is not a unique molecule, since it is found in several forms that differ in the phosphate terminus of the side chain.

## 1.6. *N*-Heterocyclic Carbene Complexes

### 1.6.1. Classification of Carbenes

Metal carbene complexes are frequently classified in to two types: (1) Fischer carbenes, named after Ernst Otto Fischer which are characteristics strong π-acceptors at the metal and being electrophilic at the carbene carbon atom. (2) Schrock carbenes, named after Richard R. Schrock, are characterized by more nucleophilic carbene carbon centers; these species classically attribute higher valent metals. *N*-Heterocyclic carbenes (NHCs) were popularized, when Arduengo's group isolated the first stable carbene in 1991. Often it is not possible to classify a carbene complex with regards to its electrophilicity or nucleophilicity.

**Fischer carbenes:**

These type of carbenes are typically found with: low oxidation state metals, and middle and late transition metals (Fe(0), Mo(0), Cr(0)) with π-electron acceptor ligands, π-donor substituents on methylene group such as alkoxy and alkylated amino groups. According to Scheme 1.19, the chemical bonding is based on σ-type electron donation of the filled methylene lone pair orbital to an empty metal d-orbital, and π-electron back bonding from a filled metal d-orbital to the empty p-orbital on carbon. An example for this type of carbene complex is $(CO)_5Cr=C(NR_2)Ph$.

**Schrock carbenes:**

Schrock carbenes are classically found with: high oxidation states with early transition metals (Ti(IV), Ta(V)), and with π-donor ligands. Bonding in such type of complexes can be considered as coupling of triplet state metal and triplet carbene. These bonds are polarized towards carbon and consequently, the methylene group act as a nucleophile, which has been shown in Scheme 1.19. An example for this Schrock crabene complex is $Ta(=C(H)Bu^t)(CH_2Bu^t)_3$.

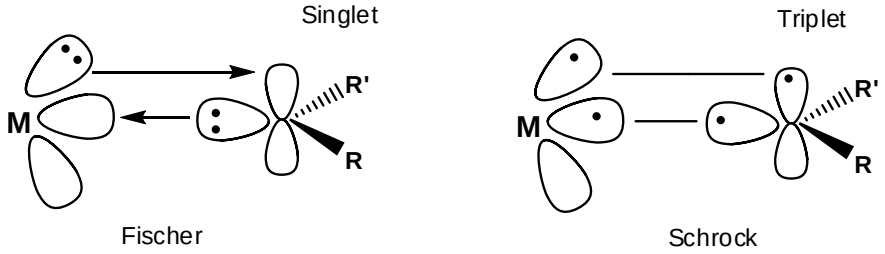


**Scheme 1.19.** General representation of Fischer and Schrock carbene complexes.

### 1.6.2. *N*-heterocyclic Carbenes:

*N*-heterocyclic carbenes (NHCs), are cyclic carbenes (Figure 1.10) that are usually derived from the deprotonation of imidazolium/benzimidazolium salts. NHC chemistry was first investigated by Wanzlick *et al.*[73] in the early 1960s leading to the synthesis of first NHC transition metal complexes of chromium and mercury (**20** and **21**) by Ofele[74] and Wanzlick and Schonherr[75] in 1968. In the following decades, Lappert and co-workers synthesized several NHC-metal complexes from electron-rich olefins (**22**).[76] The isolation of the first persistent carbene (also known as stable carbene / Arduengocarbene) 1,3-diadamantylimidazol-2-ylidene was isolated in 1991 by Arduengo *et al.*[77]

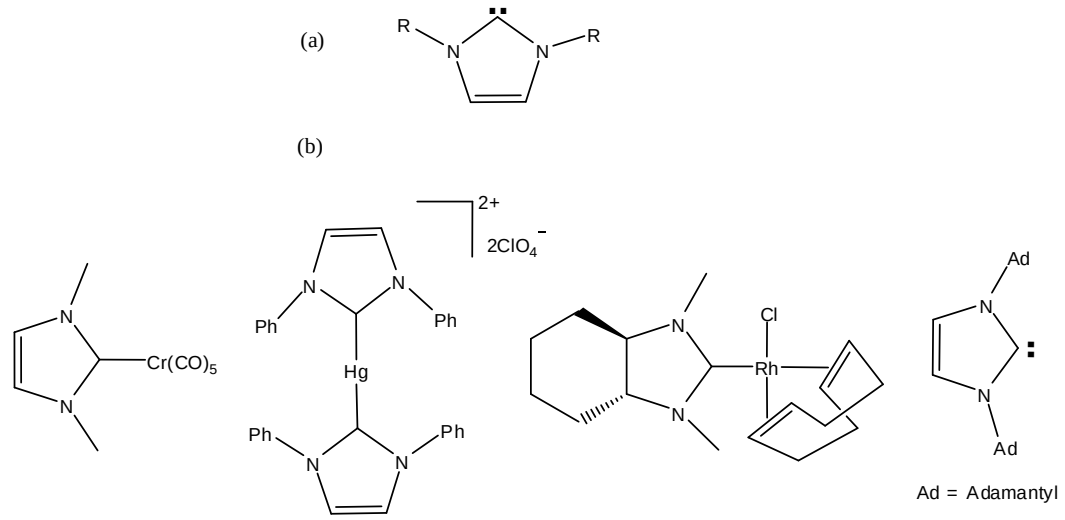


**Figure 1.10** (a) General representation of NHCs, (b) Early examples of NHC-complexes and Arduengo's isolated free carbene.

When bound to metals, *N*-heterocyclic carbenes are significantly less reactive than two major classes of carbene ligands, Schrock carbenes and Fischer carbenes. Among these two types of ligands, NHC's can be considered to be spectator ligands, because they do not undergo metathesis reactions, cyclopropanations, or many of the other reactions typically attributed to metal carbene.[78] NHCs are strong necleophiles and bind to both main group and transition metals often with greater stability than phosphines.[79] The carbene carbon atom of NHCs is stabilized by the pπ–pπ electron donation of the two adjacent nitrogen atoms, and which are good σ-donors. Recent theoretical and structural studies suggest the existence of some π-backbonding for certain metal centers[80,81] as shown in Scheme 1.20. Hence, the bond between the carbon and the metal center is

commonly represented by a single dative bond, whereas Fishcer and Schrock carbenes are usually depicted with double bonds to metal.

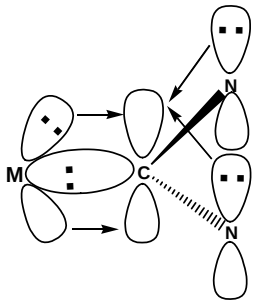


**Scheme 1.20.** Bonding of NHCs to metal centers

Because of the usefulness of the metal-NHC complexes, many synthetic methods have been explored. Based on the literature on metal-NHCs, the most widely used preparation methods can be divided broadly into five types:(a) reaction of free NHCs with metal precursors,[82a] (b) rection of electron-rich olefin dimers with organometallic fragments,[82b] (c) reaction of imidazolium salts with suitable basic transiton metal salts,[82c] (d) reaction of azolium salts with metal precursors under basic phase transfer catalysis (PTC) conditions,[82d] and (e) transmetallation with Ag(I)-NHCs.[82e] The last method is now well established for the preparation of various transition metal-NHCs including Au(I), Pd(II), Rh(I), Pt(II) etc.[83] Out of these five methods, two methods have been discussed in below section.

(a) **Reaction of free NHCs with metal precursors**:

In 1991, unexpectedly Arduengo *et al*. discovered stable carbenes. That time onwards, this area is well established for the preparation of NHC complexes. For this type of complexes, it requires a straight forward and high-yielding synthetic route. Imidazolium salts are heteroaromatic, ionic compounds, which can be deprotonated by strong bases such as potassium *tert*-butylate, NaH, or *n*-butyllithium to give *N*-heterocyclic carbenes. Generally, free *N*-heterocyclic carbenes in mixtures containing liq. ammonia has many advantages. According to Scheme 1.21, deprotonation of dissolved imidazolium salts in $NH_3$/THF or $NH_3$/acetonitrile (5:1) using stoichiometric amounts of base, yields the free carbenes. We can also prepare 1,3-dialkylimidazole-2-thiones from imidazolium salts and sulfur in the presence of a base, but in this case, the imidazolium salt should not be interacted with the base in the absence of sulfur.[84] There are several reports, which show 1,3-disubstituted imidazoline-2-ylidenes coordinated to transition metals in low and high oxidation states (e.g., $Cr^0$, $Mo^0$, $W^0$, $Fe^0$, $Re^I$, $Mn^I$, $Hf^{IV}$, $Nb^{IV}$, $Re^{VII}$).[85]

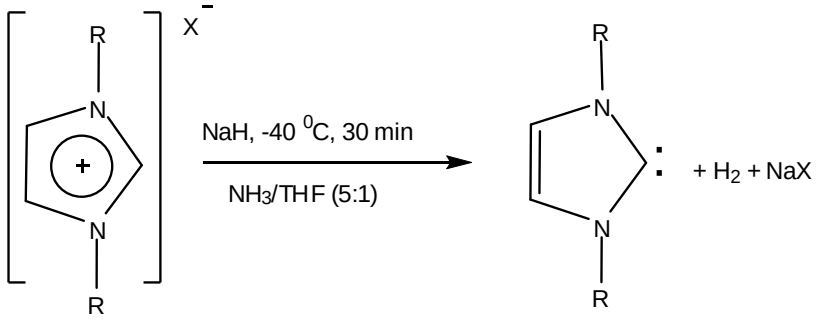


**Scheme 1.21.** Rapid deprotonation of imidazolium salts in liquid ammonia.

(c) **Reaction of azolium salts with metal precursors under basic phase transfer catalysis (PTC) conditions**:

Phase transfer catalysis is a special form of heterogeneous catalysis. Ionic reactants are often soluble in an aqueous phase but insoluble in an organic phase in the absence of the phase transfer catalyst. Hence, for the migration of a reactant from one phase to another phase "Phase Transfer Catalyst or PTC" can be used as catalyst in the reactions.[86] Initially, for the preparation of gold-carbene complexes, 1,3-disubstituted imidazolium cation was treated with AgOAc, NaH or BuLi in dry THF. In this type of methods, yields are very low, and care had to be taken to avoid extensive decomposition. For this reason, Ivan J. B. Lin *et al.* group used phase-transfer catalysis (PTC) techniques in the synthesis of metal ylides.[87] By this new method, $Au(SMe_2)Cl$ was treated with 1,3-disubstitutedimidazolium/benzimidazolium cation under the PTC (Cetyltrimethylammonium bromide, Tetrabutylammonium bromide, Triethylbenzylammonium chloride, Tetrabutlammonium bisulfate, Hexadecyltrimethylammonium bromide) in basic conditions leading to the formation gold-carbene complexes with greater than 80% yield.[88,89]

### 1.6.3. Silver-carbene Complexes:

Herrmann and Bertrand published excellent reviews in the year of 2000 concerning the synthesis of metal-NHCs; at that time very few Ag(I)-NHCs were reported.[90] Later on synthesis of Ag(I)-NHCs and their application in transmetallation reactions have greatly been increased in recent years. Lin, Garrison and Youngs *et.al.* published a review on Ag(I)-NHCs.[91] Based on literature,[91a] the silver-NHCs comprise of various NHC systems ranging from five membered to seven membered rings, including imidazolium, benzimidazolium, triazolium, pyrazolium, qunioxaline and naphtha anellated imidazolium, imidazo[1,5-*a*]pyridine, bipiperidine and biisoqunioline derived imidazolium,

bisimidazoliums with arene backbone, six-membered ring pyrimidinium, seven membered ring amidinium moieties, etc. Bertrand in 1997, reported that the reaction between triazolium triflate salt and a silver base such as Ag(OAc), yielded a polymeric Ag(I)-NHC.[92] Lin and co-workers published first example of Ag(I)-NHC by using $Ag_2O$ as a base.[82e]

Recently Rourke and co-workers published new type of Ag(I)–NHC complexes. They reported crystal structures with NHC ligands with the 2:1:1 (ligand: silver: halide) stoichiometry.[93] According to Scheme 1.22, there are three types of silver carbene complexes. In the crystal structure of **24**, the direct silver to chloride bond is 2.369 Å, the Ag–Ag distance is 3.994 Å and the Ag1–Cl–Ag1A angle is 94.5°. In the structure of **25**, the Ag–Ag distance is 3.486 Å. In the structure of **26**, the planar arrangement of the two coordinating carbons is found, with the C–Ag–C angle being 157°. The Ag–Br distance is really quite long 2.893 Å, which is shorter than the average Ag–Br distance (2.91 Å) from the literature. Ag-NHC complexes have also several applications in the field of catalysis, biological activity and transmetallation. [94]

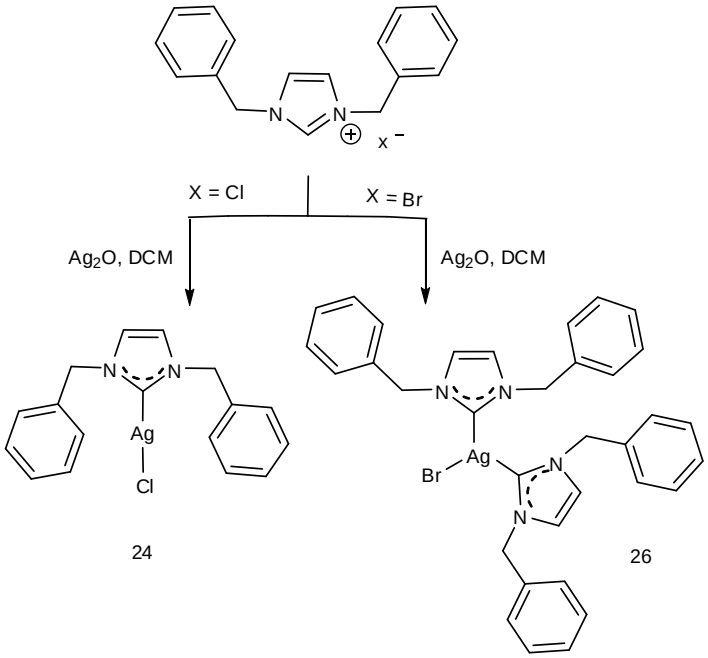

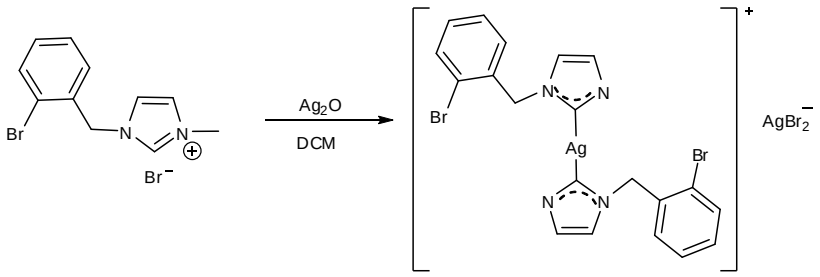


25

**Scheme 1.22.** Synthesis of Ag(I)-NHC complexes.

## 1.7. Motivation of the work

A great deal of coordination chemistry has emerged because inorganic chemists are curious to find out what happens when metals are coordinated by new ligands. Ion pair dithiolene complexes comprise of a special class of compounds in metal-dithiolne chemistry. New chemistry has been generated by the choice of versatile counter cations and substituents on the dithiolene ligands in ion pair dithiolene complexes, where nature of counter cations and substituents play an important role. In order to develop such new chemistry, there is a need to design and synthesize new ligands with various substituents. Modeling the active sites of metallo-enzymes with respect to their electronic properties, structure and reactivity represents another motive for new ligand synthesis. Since last five decades, metal-dithiolene complexes have proved to be an interesting subclass of inorganic coordination compounds that have generated continued interest in structure, bonding and reactivity. The findings show that the dithiolene complexes have useful reactivity and sensing properties and they display remarkable solid state properties, such as, super conductivity, magnetic, and optical properties. Because of their rich properties, the literature on metal-dithiolene complexes is so vast.

The geometry around the metal ion, in dithiolene complexes, mainly depends on the interactions of dithiolene ligands with the surrounding cations.[41] Based on literature,[95] catalytic activity of enzyme, porous networks of metal organic frameworks (MOFs), porous coordination polymers (PCPs) architectures depend mainly on the selection of the flexible ligand. Ruiz-Perez and co-workers systemically studied the flexible nature of malonate ligand for the self assembly of different structures. The flexibility of ligands is essential in achieving some particular properties, such as breathing ability in the solid state, adaptive recognition for coexisting counterions etc. This has inspired us to choose various counter cations in ion-pair dithiolene complexes as a structural determination of

the metal ion, which mainly, depends on the balanced/un-balanced supramolecular interactions around the anion. Apart from this, we choose another type of cations to study the geometry of the counter cations with the respective spherical $BF_4$ and metal-bis(dithiolato) complex anions.

Also *N*-containing based meta-dithiolene complexes are present in active sites of many metallo-enzymes. In this context, particularly qdt (quinoxaline-2,3-dithiolate) ligand and its molybdenum-oxo complexes have been investigated for modeling the active sites of molybdenum hydroxylase enzymes.[96] These studies have explored the changes in the redox properties and the electronic absorption spectra of relevant metal dithiolene complexes upon reversible protonation of the coordinated qdt ligand.[97] The electronic spectral studies and redox properties would be of greater interest in this area of heterocyclic based dithiolene chemistry. The photo-physical (luminescence) properties of platinum complexes of qdt-type ligand have been studied extensively by Eisenberg's group.[98] Furthermore, H. B. Gray *et al.* studied the effect of different substituents on the electronic structure of the $\{MS_4\}$ group in a systematic manner.[7a] These facts prompted us to design and synthesize new type of qdt-based ligands and to synthesize its metal bis(dithiolene) complexes followed by the physical properties. Currently, the generation of field-effect transistors (FET) is of further interest in charger carrying semiconductor materials. Recently, qdt-based systems have been used in the development of field-effect transistors by introducing the fused qdt-based systems to the TTF-skeleton.[99] Based on this, only limited reports have been observed in the literature. This would be a good area of synthesizing new TTF-fused derivatives with new hetrocyclic based ligands in greater extent.

*N*-heterocyclic carbenes (NHCs) are a novel class of electron-donating ligands, which have the advantage of forming strong metal-ligand bonds and have become universal ligands in organometallic and coordination chemistry. NHCs have found tremendous application in the field of catalysis; for example, C–H activation, C–C, C–O and C–N bond formation. It is not always convenient to employ the free NHCs as they are air and moisture sensitive. It is also not that easy to selectively deprotonate the imidazolium salts with strong bases; to avoid these difficulties in 1998 Au–NHCs complexes had been prepared from Ag–NHCs by carbene transfer.[100] In this regard, Ag–NHCs are used as transmetalation to produce Au, Pd, Cu–NHCs etc. This area stimulated us to prepare the silver based NHCs as a part of this thesis work.

## 1.8. References


1. Jorgensen, K. *Coord. Chem. Rev*. **1966**, *1*, 164.
2. Ward, M. D.; McCleverty, J. A. *J. Chem. Soc.; Dalton Trans.* **2002**, 275.
3. (a) Karlin, K. D.; Stiefel, E. I. *Prog. Inorg. Chem.* John Wiely, New York, **2004**, Volume *52*. (b) Locke, J.; McCleverty, J. A.; Wharton, E. J.; Winscom, C. J. *Chem. Commun*. **1966**, 677.
4. (a) McCleverty, J. A. *Prog. Inorg. Chem*. **1968**, *10*, 49. (b) Müller–Westerhoff, U. T.; Vance, B. in *Comprehensive Coordination Chemistry*, Vol. *2*, Wilkinson, G.; Gillard, R. D.; McCleverty, J. A. Eds. Pergamon Press, Oxford, **1987**, p 595. (c) Farrugia, L. J. *J. Appl. Crystallogr*. **1997**, *32*, 565. (d) Cowie, M.; Bennett, M. J. *Inorg. Chem.* **1976**, *15*, 1595; (e) Alvarez, S.; Vicente, R.; Hoffmann, R. *J. Am. Chem. Soc.* **1985**, *107*, 6253. (f) Burns R. P.; Mcauliffe, *Adv. Inorg. Chem. Radiochem.* **1979**, *22*, 303.
5. Balch, A. L.; Dance, I. G.; Holm, R. H. *J. Am. Chem. Soc.* **1968**, *90*, 1139.
6. (a) Schrauzer, G. N.; Mayweg, V. P. *J. Am Chem. Soc.* **1962**, *84*, 3221. (b) Smith, A. E.; Schrauzer, G. N.; Mayweg, V. P.; Heinrich, W. *J. Am Chem. Soc.* **1965**, *87*, 5798.
7. (a) Baker-Hawkes, M. J.; Billig, E.; Gray, H. B. *J. Am. Chem. Soc.* **1966,** *88*, 4870. (b) Shupack, S. I.; Billig, E.; Clark, R. J. H.; Williams, R.; Gray, H. B. *J. Am. Chem. Soc.* **1964,** *86*, 4594.
8. (a) Davison, A.; Edelstein, N.; Holm, R. H.; Maki, A. H. *J. Am Chem. Soc.* **1963**, *85*, 2029. (b) Davison, A.; Holm, R. H. *Inorg. Synth*. **1967**, *10*, 8.
9. (a) Sproules, S.; Banerjee, P.; Weyhermuller, T.; Yan, Y.; Donahue, J. P.; Wieghardt, K. *Inorg. Chem*. **2011**, *50*, 7106. (b) Sproules, S. P.; Weyhermuller, T.; Goddard, R.; Wieghardt, K. *Inorg. Chem.* **2011**, *50*, 12623. (c) Sproules, S.; Weyhermuller, T.; DeBeer, S.; Wieghardt, K. *Inorg. Chem*. **2010**, *49*, 5241.
10. (a) Jacobsen, H.; Donahue, J. P. *Inorg. Chem.* **2008**, *47*, 10037. (b) Matz, K. G.; Mtei, R. P.; Leung, B.; Burgmayer, S. J. N.; Kirk, M. L. *J. Am. Chem. Soc*. **2010**, *132*, 7830.
11. Alvarez, S.; Vicente, R.; Hoffmann, R. *J. Am. Chem. Soc*. **1985**, *107*, 6253.

12. (a) Meskaldji, S.; Belkhiri, L.; Arliguie, T.; Fourmigue, M.; Ephritikhine, M.; Boucekkine, A. *Inorg. Chem.* **2010**, *49*, 3192. (b) Roger, M.; Arliguie, T.; Thuery, P.; Fourmigue, M.; Ephritikhine, M. *Inorg. Chem.* **2005**, *44*, 594. (c) Roger, M.; Arliguie, T.; Thuery, P.; Fourmigue, M.; Ephritikhine, M. *Inorg. Chem.* **2005**, *44*, 584.

13. (a) Schrauzer, G. N.; Mayweg, V.; Heinrich, W. *J. Am. Chem. Soc.* **1966**, *88*, 5174. (b) Sung, K.-M.; Holm, R. H. *Inorg. Chem.* **2000**, *39*, 1275. (c) Goddard, C. A.; Holm, R. H. *Inorg. Chem.* **1999**, *38*, 5389.

14. McCleverty, J. A.; Ratcliff, B. *J. Chem. Soc. A.* **1970**, 1627.

15. (a) Lim, B. S.; Sung, K.-M.; Holm, R. H. *J. Am. Chem. Soc.* **2000**, *122*, 7410. (b) Sugimoto, H.; Hrihara, M.; Shiro, M.; Sugimoto, K.; Tanaka, K.; Miyake, H.; Tsukube, H. *Inorg. Chem.* **2005**, *44*, 6386. (c) Sellmann, D.; Wemple, M. W.; Donaubauer, W.; Heinemann, F. W. *Inorg. Chem.* **1997**, *36*, 1397.

16. (a) Nomura, M.; Okuyama, R.; Fujita-Takayama, C.; Kajitani, M. *Organometallics* **2005**, *24*, 5110. (b) Adams, H.; Bancroft, M. N.; Morris, M. J.; Riddiough, A. E. *Inorg. Chem.* **2009**, *48*, 9557. (c) Fourmigue, M. *Coord. Chem. Rev.* **1998**, *178-180*, 823.

17. (a) Coomber, A. T.; Beljonne, D.; Friend, R. H.; Brédas, J. L.; Charlton, A.; Robertson, N.; Underhill, A. E.; Kurmoo, M.; Day, P. *Nature* **1996**, *380*, 144. (b) Ren, X. M.; Nishihara, S.; Akutagawa, T.; Noro, S.; Nakamura, T. *Inorg. Chem.* **2006**, *45*, 2229. (c) Robertson, N.; Cronin, L. *Coord. Chem. Rev.* **2002**, *227*, 93.

18. (a) Kato, R. *Chem. Rev.* **2004**, *104*, 5319. (b) Chen, C.–T.; Liao, S. –Y.; Lin, K. –J.; Lai, L. –L. *Adv. Mater.* **1998**, *3*, 334.

19. Akamatu, H.; Inokuchi, H.; Matsunaga, Y. *Nature* **1954**, *173*, 168.

20. Mori, T.; Kobayashi, A.; Sasaki, Y.; Kobayashi, H.; Saito, G.; Inokuchi, H. *Bull Chem. Soc. Jpn.* **1984**, *57*, 627.

21. (a) Kagoshima, S.; Kato, R.; Fukuyama, H.; Seo, H.; Kino, H.; Bernier, P.; Lefrant, S.; Bidan, G. (eds) *Advances in synthetic metals* – twenty years of progress in science and tech. Elsevier Science, Amsterdam, p 262. (b) R. Kato, *Bull Chem. Soc. Jpn* **2000**, *73*, 515.

22. Miller, J. S.; Epstein, A. J. *Prog. Inorg. Chem.* **1976**, *20*, 1.

23. Kato, R. *Chem. Rev*. **2004**, *104*, 5319.

24. Underhill, A. E.; Ahmad, M. M. *J. Chem. Soc., Chem. Commun*. **1981**, 67.

25. Canadell, E.; Ravy, S.; Pouget, J. P.; Brossard, L. *Solid State Commun*. **1990**, *75*, 633.

26. (a) Batail, P.; Ouahab, L. CNRS French patent 2565978, **1984**. (b) Ouahab, L.; Batail, P.; Perrin, A.; Garrigou-Lagrange, C. *Mater. Res. Bull.* **1986**, *21*, 1223. (c) Batail P.; Ouahab, L.; Pénicaud, A.; Lenoir, C.; Perrin, A. *C. R. Acad. Sci., Ser. II* **1987**, *304*, 1111. (d) Batail, P.; Boubekeur, K.; Fourmigué, M.; Dolbecq, A.; Gabriel, J.-C.; Guirauden, A.; Livage, K.; Uriel, S. *New J. Chem*. **1994**, *18*, 999.

27. (a) Davidson, A.; Boubekeur, K.; Pénicaud, A.; Auban, P.; Lenoir, C.; Batail, P.; Hervé, G. *J. Chem. Soc., Chem. Commun.* **1989**, 1373. (b) Coronado, E.; Gomez-Garcia, C. J. *Chem. Rev*. **1998**, *98*, 273.

28. Gratzel, M. J. *Photochem. Photobiol C: Photochem. Rev*. **2003**, *4*, 145.

29. (a) Qian, G.; Wang, Z. Y. *Chem. Asian. J*. **2010**, *5*, 1006. (b) Marshall, K. L.; Painter, G.; Lotito, K.; Noto, A. G.; Chang, P. *Mol. Cryst. Liq. Cryst*. **2006**, *454*, 47. (c) Thorley, K. J.; Hales, J. M.; Anderson, H. L.; Perry, J. W. *Angew. Chem. Int. Ed*. **2008**, *47*, 7095.

30. (a) Ozaki, Y.; McClure, W. F.; Christy, A. A. (Eds.), Near-Infrared Spectroscopy in Food Science and Technology, Wiley-VCH, Weinheim, 2006. (b) Blanco, M.; Villarroya, I. *Trends Anal. Chem*. **2002**, *21*, 240.

31. (a) Zhao, W.; Carreira, E. M. *Angew. Chem. Int. Ed*. **2005**, *44*, 1677. (b) Detty, M. R.; Gibson, S. L.; Wagner, S. J. *J. Med. Chem.* **2004**, *47*, 3897.

32. König, W. *J. Prakt. Chem.* **1925**, *112*, 1.

33. Ismailsky, W.; Dissertation, Univessität Dresden, **1913.**

34. (a) Dilthey, W.; Wizinger, R. *J. Prakt. Chem.* **1928**, *118*, 321. (b) Wizinger, R. *Chimia* **1961**, *15*, 89. (c) Griffiths, J. *Colors and Constitution of Organic Molecules*, Academic press, London, **1976**, ISBN, 0–12–303550–3, LCCC 76–016971.

35. Dewar, M. J. S.; Dougherty, R. C. *The PMO Theory of Organic Compounds*, Akademie Verlag, Berlin, **1977** (Abh. Akad. Wiss. DDR Nr.8).

36. (a) Nakazumi, H. *J. Soc. Dyes Color*. **1988**, *104*, 121. (b) Shiozaki, H.; Nakazumi, H.; Kitao, T. *J. Soc. Dyers Color*. **1988**, *104*, 173. (c) Kuramoto, N. J. *J. Soc. Dyers Color*. **1990**, *106*, 181.

37. Namba, K. Jpn. Kokai Tokkyo Koho JP 60 73891, **1985**, *Eur. Pat. Appl. EP* 147083.

38. (a) M. Melnik, Kabesova, M. J. *Coordin. Chem.* **2000**, *50*, 323. (b) Beswick, C. L.; Schulman, J. M. Stiefel, E. I. *Prog. Inorg. Chem*. **2004**, *52*, 55.

39. (a) Ren, X. M.; Wu, P. H.; Zhang, W. W.; Meng, Q. J.; Chen, X. Y. *Trans. Met. Chem*. **2007**, *27*, 394. (b) Hamilton, W. C.; Bernal, I. *Inorg. Chem*. **1967**, *6*, 2003. (c) Snow, M. R.; Ibers, J. A. *Inorg. Chem*. **1973**, *12*, 249. (d) Christou, G.; Huffman, J. C. *J. Chem. Soc., Chem. Commun*. **1983**, 558. (e) Enemark, J. H.; Lipscomb, W. N. *Inorg. Chem.* **1965**, *4*, 1729. (f) Baker-Hawkes, M. J.; Dori, Z.; Eisenberg, R.; Gray, H. B. *J. Am. Chem. Soc*. **1968**, *90*, 4253.

40. (a) Madhu, V.; Das, S. K. *Polyhedron* **2004**, *23*, 1235. (b) Serr, B. R.; Headford, C. E. L.; Anderson, O. P.; Elliot, C. M.; Schauer, C. K. Akabori, K.; Spartalian, K.; Hatfield, W. E.; Rohrs, B. R. *Inorg. Chem.* **1990**, *29*, 2663.

41. Ren, X. M.; Ni, Z. P.; Noro, S.; Akutagawa, T.; Nishihara, S.; Nakamura, T.; Sui, Y. X.; Song, Y. *Cryst. Growth Des*. **2006**, *6*, 2530.

42. (a) Jeannin, O.; Delaunay, J.; Barriere, F.; Fourmigue, M. *Inorg. Chem*. **2005**, *44*, 9763. (b) Baudron, S. A.; Avarvari, N.; Batail, P. *Inorg. Chem.* **2005**, *44*, 3380. (c) Lim, B. S.; Fomitchev, D. V.; Holm, R. H. *Inorg. Chem.* **2001**, *40*, 4257. (d) Bryce, M. R.; Moore, A. J.; Batsanov, A. S.; Howard, J. A. K.; Goldenberg, L. M.; Pearson, C.; Petty, M. C.; Tanner, B. K. *Synth. Met*. **1997**, *86*, 1839. (e) Zhang, C.; Reddy, H. K.; Chadha, R. K.; Schrauzer, G. N. *J. Coord. Chem*. **1992**, *26*, 117. (f) Youm, K. T.; Kim, Y.; Do, Y.; Jun, M. J. *Inorg. Chim. Acta* **2000**, *310*, 203. (g) The CSD 3D Graphics Search System: Allen, F. H. *Acta Crystallogr., Sec. B.* **2002**, *58*, 380.

43. Yao, B.-Q.; Sun, J.-S.; Tian, Z.-F.; Ren, X.-M.; Gu, D.-W.; Shen, L.-J.; Xie, J. *Polyhedron* **2008**, *27*, 2833.

44. (a) Geiger Jr, W. E.; Maki, A. H. *J. Phys. Chem*. **1971**, *76*, 2387. (b) Kosower, E. M. *J. Am. Chem. Soc*. **1958**, *80*, 3253.

45. Bigoli, F.; Deplano, P.; Mercuri, M. L.; Pellinghelli, M. A.; Pilia, L.; Pintus, G.; Serpe, A.; Trogu, E. F. *Inorg. Chem.* **2002**, *41*, 5241.

46. Handrosch, C.; Dinnebier, R.; Bondarenko, G.; Bothe, E.; Heinemann, F.; Kisch, H. *Eur. J. Inorg. Chem.* **1999**, 1259.

47. Chen, C.-T.; Liao, S. Y.; Lin, K. J.; Chen, C. H.; Lin, T. Y. J. *Inorg. Chem.* **1999**, *38*, 2734

48. Basu, P.; Niga, A.; Mogesa, B.; Denti, S.; Nemykin, V. N. *Inorg. Chim. Acta* **2010**, *363*, 2857.

49. Huyett, J. E.; Choudhury, S. B.; Eichhorn, D. M.; Bryngelson, P. A.; Maroney, M. J.; Hoffman, B. M. *Inorg. Chem.* **1998**, *37*, 1361.

50. Sung, K.-M.; Holm, R. H.; *J. Am. Chem. Soc.* **2002**, *124*, 4312.

51. Valade, L.; Legros, P. P.; Bosseau, M.; Cassoux, P.; Garbauskas, M.; Interrante, L. V. J. *Chem. Soc., Dalton Trans.* **1985**, 783.

52. Zuo, J.-L.; Yao, T.-M.; You, F.; You, X.-Z.; Fun, H.-K.; Yip, B.-C. *J. Mater. Chem.* **1996**, *6*, 1633.

53. Bondi, A. *J. Phys. Chem.* **1964**, *68*, 441.

54. Fang, Q.; Sun, Y.-M.; You, X.-Z. *Chin. J. Chem. Phys.* **1992**, *1*, 129.

55. Muller-Westerhoff, U. T.; Yoon, D. I.; Plourde, K. *Mol. Cryst Liq. Cryst.* **1990**, *183*, 291.

56. Long, N. J. *Angew. Chem. Int. Ed. Engl.* **1995**, *34*, 21.

57. Lehn, J.-M. *Supramolecular Chemistry: Concepts and Perspectives*, VCH: Weinheim, **1995**.

58. Steed, J. W.; Atwood, J. L. *Supramolecular Chemistry*, John Wiley: Chichester, **2000**.

59. Nalwa, N. S. *Appl. Organomet. Chem.* **1991**, *5*, 349.

60. (a) Zhan, c.; Xu, W.; Zhang, D.; Li, D.; Lu, Z.; Nie, Y.; Zhu, D. *J. Mater. Chem.* **2002**, *12*, 2945. (b) Winter, C. S.; Oliver, S. N.; Rush, J. D.; Hill, C. A. S.; Underhill, A. E. *J. Appl. Phys.* **1992**, *71*, 512.

61. Coe, B. J. in: McCleverty, J. A.; Meyer, T. J. (Eds), Comprehensive Coordination Chemistry II, vol. 9, Elsevier- Pergamon, Oxford, 2004, p. 621.

62. Deplano, P.; Mercuri, M. L.; Serpe, A.; Pilia, L. in: Zabicky, J. (Ed.), Structure and Properties of d8-Metal Dithiolene Complexes: Chapter 16 in The Chemistry of Metal Enolates, Wiley & Sons, Ltd, 2009, p. 879.

63. (a) Cummings, S. D.; Eisenberg, R. *J. Am. Chem. Soc.* **1996**, *118*, 1949. (b) Chen, C.-T.; Liao, S. Y.; Lin, K. J.; Lin, T. Y. J.; Lia, L. L.; Chen, C. H.; *Nonlinear Optics*, **1999**, *22*, 35. (c) Chen, C.-T.; Liao, S. Y.; Lin, K. J.; Chen, C. H.; Lin, T. Y. J. *Inorg. Chem.* **1999**, *38*, 2734. (d) Cummings, S. D.; L.-T. Cheng Eisenberg, R. *Chem. Mater.* **1997**, *9*, 440. (e) Base, K.; Tiernry, M. T.; Fort, A.; Muller, J.; Grinstaff, M. W. *Inorg. Chem.* **1999**, *38*, 287. (f) Wenseleers, W.; Goovaerts, E.; Dhindsa, A. S.; Underhill, *Chem. Phys. Lett.* **1996**, *254*, 410.

64. (a) Winter, C. S.; Hill, C. A. S.; Underhill, A. E. *Appl. Phys. Lett.* **1991**, *58*, 107. (b) Zuo, J.-L.; Yao, T.-M.; You, F.; You, X.-Z.; Fun, H. K.; Yip, B. C. *J. Mater. Chem.* **1996**, *6*, 1633. (c) Bai, J.-F.; Zuo, J.-L.; Tan, W.-L.; Ji, W.; Shen, Z.; Fun, H.-K.; Chinnakali, K.; Razak, I. A.; You, X.-Z.; Che, C.-M. *J. Mater. Chem.* **1999**, *9*, 2419. (d) Ushijima, H.; Kawasaki, T.; Kamata, T.; Kodzasa, T.; Matsuda, H.; Fukaya, T.; Fujii, Y.; Mizukami, F.; *Mol. Cryst. Liq. Cryst.* **1996**, *286*, 597.

65. Yang, C. L.; Qin, J. G.; Si, J. H.; Wang, Y. G.; Ye, P. X.; Li, Y. L. *Synth. Met.* **1999**, *102*, 1578.

66. (a) Si, J.; Yang, Q.; Wang, Y.; Ye, P.; Wang, S.; Qin, J.; Liu, D. *Opt. Commun.* **1996**, *132*, 311. (b) Yang, C.; Yang, Q.; Si, J.; Wang, S.; Ye, P.; Qin, J. *Poc. SPIE-Int. Soc. Opt. Eng.* **1998**, *3556*, 102.

67. Yokoyama, Y.; Suzuki, S.; Furihata, H.; Takahi, S.; Nomura, M.; Kajitani, M. *Synthesis* **2004**, 701.

68. Bosch, I.; Costa, A. M.; Martin, M.; Urpi, F.; Vilarrasa, J. *Org. Lett.* **2000**, *2*, 397

69. (a) Hille, R. *Chem. Rev.* **1996**, *96*, 2757. (b) Johnson, M. K.; Rees, D. C.; Adams, M. W. W. *Chem. Rev.* **1996**, *96*, 2817. (c) Kisker, C.; Schindelin, H.; Rees, D. C. *Annu. Rev. Biochem.* **1997**, *66*, 233.

70. Ueyama, N.; Oku, H.; Kondo, M.; Okamura, T.; Yoshinaya, N.; Nakamura, A. *Inorg. Chem.* **1996**, *35*, 643.

71. Boyington, J. C.; Gladyshev, V. N.; Khangulov, S. V.; Stadtman, T. C.; Sun, P. D. *Science* **1997**, *275*, 1305.

72. (a) Kramer, S. P.; Johnson, J. L.; Ribeiro, A. A.; Millington, D. S.; Rajagopalan, K. V. *J. Biol. Chem.* **1987**, *262*, 16357. (b) Pilato, R. S.; Stiefel, E. I. in *Bioinorganic catalysis*, Reedijk, J., Bouwman, E., Eds.; Marcel Dekker, New York, **1999**. (c)

Rajagopalan, K. V. *Adv. Enzymol. Relat. Areas Mol. Biol.* **1991**, *64*, 215–290. (d) Johnson, J. L.; Rajagopalan, K. V. *Proc. Natl. Acad. Sci. U. S. A.* **1982**, *79*, 6856.

73. (a) Wanzlick, H. W.; Kleiner, H.-J. *Angew.Chem*. **1961**, *73*, 493. (b) Wanzlick, H.-W. *Angew.Chem. Int. Ed. Engl*. **1962**, *1*, 75. (c) Wanzlick, H.-W.; Esser, F.; Kleiner, H.-J. *Chem. Ber*. **1963**, *96*, 1208.
74. Ofele, K. J. *Organomet. Chem*. **1968**, *12*, 42.
75. Wanzlick, H.-W.; Schonherr, H.-J, *Angew. Chem. Int. Ed*. *Engl*. **1968**, *7*, 141.
76. (a) Lappert, M. F. *J. Organomet. Chem*. **1975**, *100*, 139. (b) Hitchcock, P. B. L; Lappert, M. F. *J. Organomet. Chem.* **1982**, *239*, C26. (c) Lppert, M. F. *J. Organomet. Chem*. **1988**, *358*, 185.
77. Arduengo III, A. J.; Harlow, R. L.; Kline, M. *J. Am. Chem. Soc.* **1991**, *113*, 361.
78. Collman, J. P.; Hegedus, L. S.; Norton, J. R.; Finke, R. G. *Principles and Applications of Organotransition Metal Chemistry, University Science Books, California*, **1987**, (Chapter 16).
79. (a) Herrmann, W. A. *Angew. Chem. Int. Ed*. *Engl.* **2002**, *41*, 1290. (b) Bourissou, D.; Guerret, O.; Gabbai, F. P.; Bertrand, G. *Chem. Rev*. **2000**, *100*, 39. (c) Crudden, C. M.; Allen, D. P. *Coord. Chem. Rev*. **2004**, *248*, 2247.
80. (a) Lai, C.-L.; Guo, W.-H.; Lee, M-T.; Hu, C.-H. *J. Organomet. Chem*. **2005**, *690*, 5867. (b) Green, J. C.; Herbert, B. J. *J. Chem. Soc., Dalton Trans*. **2005**, *7*, 1214. (c) Deubel, D. V. *Organometallics* **2002**, *21*, 4303. (d) Nemcsok, D.; Wichmann, K.; Frenking, G. *Organometallics* **2004**, *23*, 3640.
81. (a) Clarke, M. J.; Taube, H. *J. Am. Chem. Soc*. **1975**, *97*, 1397. (b) Cavallo, L.; Correa, A.; Costabile, C.; Jacobsen, H. *J. Organomet. Chem*. **2005**, *690*, 5407.
82. (a) Herrmann, W. A.; Koher, C.; Goodern, L. J.; Artus, G. R. J. *Chem.-Eur. J*. **1996**, *2*, 1627. (b) Lappert, M. F. *J. Organomet. Chem*. **1988**, *358*, 185. (c) Wanzlick, H.-W.; Schonherr, H.-J. *Angew. Chem*. **1968**, *80*, 154. (d) Lee, K. M.; Lee, C. K.; Lin, I. J. B. *Angew. Chem. Int. Ed*. **1997**, *36*, 1850. (e) Wang, H. M. J.; Lin, I. J. B. *Organometallics* **1998**, *17*, 972.
83. (a) Wang, H. M.; Vasam, C. S. Tsai, T. Y. R.; Chrn. S.-H.; Chang, A. H. H.; Lin, I. J. B. *Organometallics* **2005**, *24*, 486. (b) Lee, C. K.; Lee, K. M.; Lin, I. J. B. *Organometallics* **2002**, *21*, 10. (c) Baker, M. V.; Barnard, P. J.; Brayshaw, S. K.; Hickey, J. L.; Skelton, B. W.; White, A. H. *Dalton Trans.* **2005**, 37. (d) Douthwaite, R. S.; Houghton, J.; Kariuki, M. *Chem. Commun*. **2004**, *32*, 698. (e)

Saravanakumr, S.; Oprea, A. I.; Kindermann, M. K.; Jones, P. G.; Heinicke, J. *Chem.-Eur. J.* **2006**, *12*, 3143. (f) Xu, G.; Gilbertson, S. R. *Org. Lett.* **2005**, *7*, 4605. (g) Poyatos, M.; Maisse-Francois, A.; Bellemin-Laponnaz, S.; Gade, L. H. *Organometallics* **2006**, *25*, 2634.

84. Arduengo-III, A. J. U. S. Patent 5104993 (Du Pont)

85. Herrmann, W. A.; Ofele, K.; Elison, M.; Kuhn, F. E.; Roesky, P. W. *J. Organomet. Chem.* **1994**, *480*, C7.

86. Bogdal, D.; Galica, M.; Bartus, G.; Wolinski, J.; Wronski, S. *Org. Process Res. Dev.* **2010**, *14*, 669.

87. Lin, I. J. B.; Shen, H. I.; Feng, D. F. *J. Chin.Chem. Soc*. **1995**, 783.

88. Lee, K. M.; Lee, C. K.; Lin, I. J. B. *Angew Chem. Int. Ed. Engl.* **1997**, *36*, 1850.

89. (a) Wang, H. M. J.; Lin, I. J. B. *Organometallics* **1998**, *17*, 972. (b) Kaufhold, O.; Flores-Figueroa, A.; Pape, T.; Hahn, F. E. *Organometallics* **2009**, *28*, 896.

90. (a) Bourissou, D.; Guerret, O.; Gabbai, F. P.; Bertrand, G. *Chem. Rev.* **2000**, *100*, 39. (b) Weskamp, T.; Bohm, V. P. W.; Herrmann, W. A. *J. Organomet. Chem.* **2000**, *600*, 12.

91. (a) Lin, I. J. B.; Vasam, C. S. *Coord. Chem. Rev.* **2007**, *251*, 642. (b) Grrison, J. C.; Youngs, W. J. *Chem. Rev.* **2005**, *105*, 3978.

92. Guerret, O.; Sole, S.; Gornitzka, H.; Trinquier, G.; Bertrand, G. *J. Organomet. Chem.* **2000**, *600*, 112.

93. Newman, C. P.; Clarkson, G. J.; Rourke, J. P. *J. Organomet. Chem.* **2007**, *692*, 2962.

94. (a) Van Veldhuizen, J. J.; Campbell, J. E.; Giudici, R. E.; Hoveyda, A. H. J. Am. Chem. Soc. 2005, 127, 6877. (b) Larsen, A. O.; Leu, W.; Oberhuber, C. N.; Campbell, J. E.; Hoveyda, A. H. *J. Am. Chem. Soc*. **2004**, *126*, 11130. (c) Patil, S.; Claffey, J.; Deally, A.; Hogan, M.; Gleeson, B.; Mendez, L. M. M.; Bunz, H. M.; Paradisi, F.; Tacke, M. *Eur. J. Inorg. Chem.* **2010**, 1020. (d) Liu, Q.-X.; Yin, L.-N.; Wu, X.-M.; Feng, J.-C.; Guo, J.-H.; Song, H.-B. *Polyhedron* **2008**, *27*, 87.

95. (a) Kumar, D. K.; Das, A.; Dastidar, P. *Cryst. Growth Des.* **2007**, 7, 205. (b) Yamada, K.; Tanaka, H.; Yagishita, S.; Adachi, K.; Uemura, T.; Kitagawa, S.; Kawata, S. *Inorg. Chem*. **2006**, 45, 4322.

96. (a) Boyde, S.; Garner, C. D.; Enemark, J. H.; Bruck, M. A.; Kristofzski, J. G. *J. Chem. Soc., Dalton. Trans.* **1987**, 2267. (b) Boyde, S.; Garner, C. D.; Enemark, J. H.; Ortega, R. B. *J. Chem. Soc., Dalton. Trans.* **1987**, 297. (c) Boyde, S.; Garner, C. D.; Enemark, J. H.; Ortega, R. B. Polyhedron **1986**, *5*, 377.

97. Rignedoli, A.; Peyronel, G.; Malavasi, W. *J. Inorg. Nucl. Chem.* **1976**, *38*, 1963.\

98. (a) Cummings, S. D.; Eisenberg, R. *Inorg. Chem.* **1995**, *34*, 2007. (b) Cummings, S. D.; Eisenberg, R. *Inorg. Chem*. **1995**, *34*, 3396.

99. (a) Naraso, J. Nishida, D. Kumaki, S. Tokito, Y. Yamashita, *J. Am. Chem. Soc.* **2006**, *128*, 9598. (b) Naraso, J. Nishida, S. Ando, J. Yamaguchi, K. Itaka, H. Koinuma, H. Tada, S. Tokito, Y. Yamashita, *J. Am. Chem. Soc.* **2005**, *127*, 10142.

100. I. J. B. Lin, Vasam, C. S. *Comments Inorg. Chem*. **2004**, *25*, 75.

# Diversities of Coordination Geometry Around $M^{2+}$ (M = Cu, Ni) Centre in the Bis(maleonitriledithiolato)metalate Complex Anions: Geometry Controlled by Varying Alkyl Chain Length of Imidazolium Cations

2 Chapter

**Abstract:–** Twelve new ion-pair metal-bis(dithiolene) complexes with the formulae, $[C_9H_{14}N_4][Cu(mnt)_2]$ **(1a)**, $[C_{10}H_{16}N_4][Cu(mnt)_2]$ **(1b)**, $[C_{11}H_{18}N_4][Cu(mnt)_2]$ **(1c)**, $[C_{12}H_{20}N_4][Cu(mnt)_2]$ **(1d)**, $[C_{13}H_{22}N_4][Cu(mnt)_2]$ **(1e)**, $[C_{14}H_{24}N_4][Cu(mnt)_2]$ **(1f)** and similar type of nickel(II) complexes (**2a**–**2f**) have been synthesized starting from M(II) salt (M = Cu, Ni), $Na_2mnt$ (disodium maleonitriledithiolate) and bromide salts of alkyl-bis(imidazolium) cations $[C_8H_{12}(CH_2)_nN_4Br_2]$ (n = 1–6, **a–f**). In this series of ion-pair compounds **1a**–**1f** and **2a**–**2f**, a common $[M(mnt)_2]^{2-}$ complex anion is associated with alkyl imidazolium cations of varied alkyl chain lengths. We have described a systematic study of deviation from square planar geometries (in terms of distortion) around the metal ion in customary square planar metal-dithiolene complexes. The distortion in the geometry around the metal ion can be explained on the basis of centre of symmetry along C–H···M (M = Cu, Ni) supramolecular interaction and un-balanced supramolecular interactions, such as, S···H, N···H and M···S type weak contacts. Dianionic copper(II) complexes **1a**–**1f** show an electronic absorption in the near infrared (NIR) region, which has been attributed to the charge transfer transition from the HOMO level of copper dithiolate anion $[Cu(mnt)_2]^{2-}$ to the LUMO level of alkyl imidazolium cation $[C_8H_{12}(CH_2)_nN_4]^{2+}$. All these compounds are unambiguously characterized by single crystal X-ray crystallography, and further characterized by IR-, $^1H$ NMR-, ESR-, LCMS-spectroscopic techniques, and electrochemical-studies.

## 2.1. Introduction

Transition metal bis(dithiolene) complexes have attracted considerable research attention for more than three decades,[1-3] because of their brilliant redox behavior and favorable solid state interactions in their corresponding metal coordination complexes. Metal bis(1,2-dithiolene) complexes have been studied extensively in terms of their conducting, super conducting, nonlinear optical and magnetic behavior.[4] Ion-pair dithiolene complexes have also been used as near-IR dyes and in Q-switching lasers studies.[4f] Planarity / non-planarity of the metal-dithiolene complex moiety is one of the important factors to exhibit absorption in the near-IR region.[1f,5] Generally dithiolene ligands form square-planar transition-metal bis(dithiolato) complexes;[6,7] some metal-dithiolene complexes show deviation from this planarity.[8,9] This deviation is usually caused by the constraints of the metal-chelate rings.[10] This sort of distortion is also found in metal-thiolato complex, for example, the asymmetric unit in the crystal structure of the complex $[Ni\{^{i}Pr_2P(S)NP(S)Ph_2\}_2]$, consists of two independent molecules: one of them is square planar and the other one is distorted square planar.[11] This was explained by the orientation of methyl groups and the supramolecular interactions that involve Ni···H–C hydrogen bond. The relevant square planar complex exhibits centre of symmetry along Ni···H–C hydrogen bond with a bond distance of 2.607 Å, and in the distorted molecule, two different Ni···H–C (2.722, 2.734 Å) supramolecular interactions are present, that indicates lack of centre of symmetry along Ni···H, resulting in distortion around meal ion. This study suggests that the geometry around the metal ion is influenced by intra-molecular hydrogen bonding interactions. Besides these asymmetric hydrogen bonding interactions, there are other factors that can influence the geometry around the metal ion, for example, varying alkyl chain length of the associated ligand can cause distortion of a square planar geometry around a metal ion by varying metal-ligand bond lengths.[12] The presence of bulky group can also influence the geometry around the metal ion, because packing of these bulky groups plays an important role.[13] In an iron-porphyrin system $FeTPP(N\text{-}MeIm)_2$ (TPP = tetrakis(*o*-pivalamidophenyl)porphyrins), when the bis-*N*-MeIm (*N*-methylimidazole) ligands, coordinated to iron, are replaced by bulky ligands DCHIm (1,5-dicyclohexylimidazole), the visible absorption bands are significantly red-shifted for the αααββ and αβαβ atropisomers of the relevant complex.[14] This shift has been explained on the basis of a change in porphyrin

structure from a planar to a nonplanar conformation.[15] The blue copper sites of copper blue protein exhibit a number of characteristics that arise from distorted coordination geometries at the metal centre.[16]

Thus the deviation of a square planar geometry around a metal ion can be caused by a number of factors that include centre of symmetry along M····H bond, increasing the chain of alkyl groups of the associated cation, presence of bulky groups and the supramolecular interactions of the types N····H, S····H, M····H and M····S weak contacts. The theme of the present work is, how increasing length of alkyl chain of imidazolium cation affect the geometry of a square planar copper bis(dithiolato) complex anion in solid state. We report here twelve new ion pair metal-bis(dithiolato) complexes $[C_8H_{12}(CH_2)_nN_4][M(mnt)_2]$ [n = 1 to 6, **1a-1f** and **2a-2f**] (M = Cu, Ni) in which the counter cations are varied by increasing chain length of the cation retaining the same complex anion $[Cu(mnt)_2]^{2-}$ and $[Ni(mnt)_2]^{2-}$ in all compounds **1a-1f** and **2a-2f** respectively. The geometry around the metal ion can be tuned by supramolecular interactions of the complex anion with the surrounding organic cations in respective ion-pair complexes. The non classical M····H bonding interactions are observed in organometallic compounds,[17] and in ion-pair dithiolene complexes.[18] In their diffuse reflectance spectra, there is a trend (the shift of the absorption maxima) among these complexes **1a-1f**. More specifically, if the distortion angle between two SCuS planes[1f] (of the complex anion) is more, the band in near-IR region shifts towards more low energy region. Thus, more is the distortion around the metal ion, the relevant absorption maximum shifts to more red region. All compounds **1a-1f**, **2a-2f** have been characterized by routine elemental analysis, $^1$H NMR, LC-MS, EPR spectroscopy and cyclic voltammetry and finally characterized (except **2f**) by single crystal X-ray diffraction.

## 2.2. Experimental Section

### 2.2.1. Materials and Methods

All chemicals were purchased from commercial sources and used without further purification. Micro analytical (C, H, N) data were obtained with a FLASH EA 1112 Series CHNS Analyzer. The IR spectra (with KBr pellets) were recorded in the range of 400-4000 $cm^{-1}$ on a JASCO FT/ IR-5300, and NICOLET 380 FT-IR spectrometer. UV-Vis spectra were recorded on a Cary

100 Bio UV-Vis spectrophotometer. Diffuse reflectance and near-IR absorption spectra were recorded on a UV-3600 Shimadzu UV-Vis-NIR spectrophotometer. The electron spin resonance (ESR) spectra were recorded on a (JEOL) JESFA200 ESR spectrometer. $^1$H NMR spectra was recorded on Bruker DRX- 400 and 500 spectrometer using $Si(CH_3)_4$ (TMS) as an internal standard. Solution mass spectra (LCMS) were obtained on a LCMS-2010A Shimadzu spectrometer. Powder X-ray diffraction patterns were recorded on a Bruker D8-Advance diffractometer using graphite monochromated $CuK_{\alpha 1}$ (1.5406Å) and $K_{\alpha 2}$ (1.54439Å) radiations. A Cypress model CS-1090/CS-1087 electroanalytical system was used for cyclic voltammetric experiments. The electrochemical experiments were measured in acetonitrile solvent containing $[Bu_4N][ClO_4]$ as a supporting electrolyte, using a conventional cell consisting of two platinum wires as working and counter electrodes and a Ag/AgCl electrode as a reference.

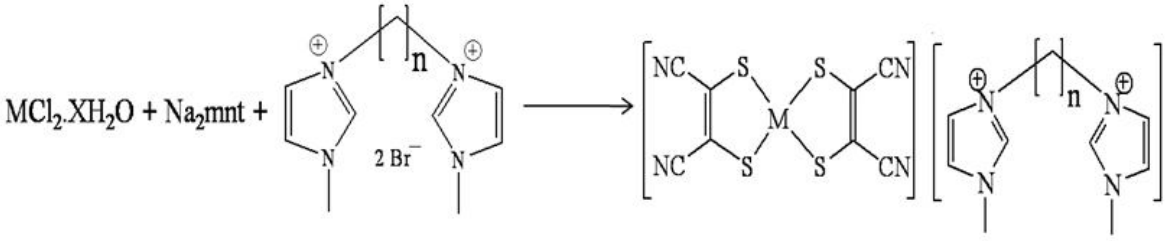


| M | X |
|---|---|
| Cu | 2 |
| Ni | 6 |

| n | |
|---|---|
| 1 | a |
| 2 | b |
| 3 | c |
| 4 | d |
| 5 | e |
| 6 | f |

| M | n | |
|---|---|---|
| Cu/Ni | 1 | 1a/2a |
| | 2 | 1b/2b |
| | 3 | 1c/2c |
| | 4 | 1d/2d |
| | 5 | 1e/2e |
| | 6 | 1f/2f |

**Scheme 2.1.** Synthetic procedure of the complexes

### 2.2.2. Synthesis

**General procedures for alkyl imidazolium derivatives (a-f)** (see also Scheme 2.1)**.** Preparation of imidazolium derivates are modified from literature procedure.[19] To the 1-methyl imidazole (2 mmol) solution of toluene (30 mL), 1,n-dibromo alkane (1 mmol) (n = 1 to 6) was added. This reaction mixture was refluxed for overnight and toluene was removed by rotary evaporator and the crude product was washed with n-hexane and air-dried and finally stored in freeze for solidification.

**3,3'-Methylenebis(1-methyl-1H-imidazol-3-ium) (a).** Yield: 79% (based on *N*-Me). Anal. Calc. for $C_9H_{14}Br_2N_4$: C, 31.97; H, 4.17; N, 16.57. Found: C, 32.24; H, 4.26; N: 16.88. IR spectrum (KBr pellet, $\nu/cm^{-1}$): 3458, 3049, 1788, 1641, 1548, 1460, 1331, 1172, 866. LCMS (*m/z)*: 178, 180 M, (M+2). $^1$H NMR (400 MHz, $\delta$ ppm) (DMSO-$d_6$): 9.57 (s, 2H, Ar-H), 8.10 (s, 2H, Ar-H), 7.81 (s, 2H, Ar-H), 6.77 (s, 2H, aliphatic-H), 3.89 (s, 6H, *N*-Me).

**3,3'-(Ethane-1,2-diyl)bis(1-methyl-1H-imidazol-3-ium) (b).** Yield: 73% (based on *N*-Me). Anal. Calc. for $C_{10}H_{16}Br_2N_4$: C, 34.11; H, 4.58; N, 15.91. Found: C, 34.38; H, 4.68; N: 16.27. IR spectrum (KBr pellet, $\nu/cm^{-1}$): 3435, 3145, 3079, 2854, 2071, 1638, 1556, 1364, 1019, 827. LCMS (*m/z)*: 192, 194 M, (M+2). $^1$H NMR (500 MHz, $\delta$ ppm) (DMSO-$d_6$): 9.22 (s, 2H, Ar-H), 7.80-7.82 (d, 2H, Ar-H), 7.74 (s, 2H, Ar-H), 4.24 (s, 4H, aliphatic), 3.86 (s, 6H, *N*-Me).

**3,3'-(Propane-1,3-diyl)bis(1-methyl-1H-imidazol-3-ium) (c).** Yield: 82% (based on *N*-Me). Anal. Calc. for $C_{11}H_{18}Br_2N_4$: C, 36.08; H, 4.95; N, 15.30. Found: C, 36.43; H, 4.84; N: 15.79. IR spectrum (KBr pellet, $\nu/cm^{-1}$): 3427, 3148, 3092, 2864, 2069, 1574, 1460, 1340, 1093, 1022, 841. LCMS (*m/z)*: 206, 208 M, (M+2). $^1$H NMR (500 MHz, $\delta$ ppm) (DMSO-$d_6$): 9.32 (s, 2H, Ar-H), 7.86 (s, 2H, Ar-H), 7.77 (s, 2H, Ar-H), 4.27 (s, 2H, aliphatic-H), 3.87 (s, 6H, *N*-Me).

**3,3'-(Butane-1,4-diyl)bis(1-methyl-1H-imidazol-3-ium) (d).** Yield: 71% (based on *N*-Me). Anal. Calc. for $C_{12}H_{20}Br_2N_4$: C, 37.91; H, 5.30; N, 14.73. Found: C, 37.58; H, 5.36; N: 15.11. IR spectrum (KBr pellet, $\nu/cm^{-1}$): 3430, 3150, 3073, 2958, 2854, 2235, 2054, 1627, 1578, 1326, 1167, 865. LCMS (*m/z)*: 220, 222 M, (M+2). $^1$H NMR (500 MHz, $\delta$ ppm) (DMSO-$d_6$): 9.19 (s, 2H, Ar-H), 7.79 (s, 2H, Ar-H), 7.73 (s, 2H, Ar-H), 4.22 (s, 4H, aliphatic), 3.86 (s, 6H, *N*-Me), 1.78 (s, 4H, aliphatic-H).

**3,3'-(Pentane-1,5-diyl)bis(1-methyl-1H-imidazol-3-ium) (e).** Yield: 76% (based on *N*-Me). Anal. Calc. for $C_{13}H_{22}Br_2N_4$: C, 39.61; H, 5.62; N, 14.21. Found: C, 39.89; H, 5.50; N: 14.59. IR spectrum (KBr pellet, $\nu/cm^{-1}$): 3424, 3150, 3095, 3947, 2865, 2476, 1632, 1457, 1167, 838. LCMS (*m/z)*: 234, 236 M, (M+2). $^1$H NMR (500 MHz, $\delta$ ppm)) (DMSO-$d_6$): 9.14 (s, 2H, Ar-H), 7.77 (m, 4H, Ar-H), 4.17 (s, 4H, aliphatic-H), 3.84 (s, 6H, *N*-Me), 1.82 (m, 4H, aliphatic-H), 1.22 (m, 2H, aliphatic-H).

**3,3'-(Hexane-1,6-diyl)bis(1-methyl-1H-imidazol-3-ium) (f).** Yield: 81% (based on *N*-Me). Anal. Calc. for $C_{14}H_{24}Br_2N_4$: C, 41.19; H, 5.92; N, 13.72. Found: C, 40.94; H, 6.01; N: 14.26. IR spectrum (KBr pellet, ν/cm$^{-1}$): 3435, 3148, 3078, 2934, 2085, 1616, 1460, 1338, 1167, 856, 785. LCMS (*m/z)*: 248, 250 M, (M+2). $^1$H NMR (400 MHz, $\delta$ ppm) (DMSO-$d_6$): 9.21 (s, 2H, Ar-H), 7.81 (s, 2H, Ar-H), 7.73 (s, 2H, Ar-H), 4.17 (t, 4H, aliphatic-H), 3.86 (s, 6H, *N*-Me), 1.78 (m, 4H, aliphatic-H), 1.27 (m, 4H, aliphatic-H).

**General synthetic procedure for ion-pair compounds 1a-1f and 2a-2f** (see also Scheme 2.1)**.** To a 10 mL MeOH solution of $Na_2mnt$[20] (2.0 mmol), 5 mL MeOH solution of $MCl_2$ (1.0 mmol, M = Cu, Ni) was added, stirred for 30 min. at room temperature and filtered. To this solution, 15 mL MeOH solution containing $[C_8H_{12}(CH_2)_nN_4]$ (n = 1 to 6, 1.0 mmol) was added, stirred at room temperature for 2 h and it was filtered off. The crude (black colored precipitate) product was crystallized from $CH_3CN$/ether by diffusion method to give dark-brown crystals for compounds **1a-1f** and **2a-2e**. Single crystals from each compound, suitable for X-ray diffraction study, was selected and characterized structurally. The elemental analyses and routine spectral data for **1a**–**1f** and **2a-2f** are described below.

**$[C_9H_{14}N_4][Cu(mnt)_2]$ (1a)**. Yield: 62% (based on copper). Anal. Calc. for $C_{17}H_{14}N_8S_4Cu$: C, 39.10; H, 2.70; N, 21.46. Found: C, 39.38; H, 2.68; N: 21.87. IR spectrum (KBr pellet, ν/cm$^{-1}$): 3101, 3073, 2263, 2197, 1578, 1545, 1452, 1161, 1117, 793. LCMS (*m/z)*: 179 $(M+H)^+$. $^1$H NMR (400 MHz, $\delta$ ppm) (DMSO-$d_6$): 9.34 (s, 2H, Ar-H), 7.94 (s, 2H, Ar-H), 7.80 (s, 2H, Ar-H), 6.62 (s, 2H, aliphatic-H), 3.91 (s, 6H, *N*-Me).

**$[C_{10}H_{16}N_4][Cu(mnt)_2]$ (1b)**. Yield: 58% (based on Cu). Anal. Calc. for $C_{18}H_{16}N_8S_4Cu$: C, 40.32; H, 3.00; N, 20.89. Found: C, 39.98; H, 3.08; N, 20.45. IR spectrum (KBr, ν/cm$^{-1}$): 3090, 2262, 2191, 1552, 1460, 1147, 1103, 837, 748. LCMS (*m/z*): 193 $(M+H)^+$. $^1$H NMR (400 MHz, $\delta$ ppm) (DMSO-$d_6$): 9.00 (s, 2H, Ar-H), 7.72 (s, 2H, Ar-H), 7.58 (s, 2H, Ar-H), 4.67 (s, 4H, aliphatic-H), 3.86 (s, 6H, *N*-Me).

**$[C_{11}H_{18}N_4][Cu(mnt)_2]$ (1c)**. Yield: 60% (based on Cu). Anal. Calc. for $C_{19}H_{18}N_8S_4Cu$: C, 41.18; H, 3.29; N, 20.36. Found: C, 41.56; H, 3.23; N, 20.69. IR spectrum (KBr, ν/cm$^{-1}$): 3144, 3105, 2359, 2193, 1620, 1572, 1464, 1147, 1049, 862, 760. LCMS (*m/z*): 207 $(M+H)^+$. $^1$H NMR (400 MHz, $\delta$ ppm) (DMSO-$d_6$): 9.11 (s, 2H, Ar-H), 7.75 (s, 4H, Ar-H), 4.23 (s, 4H, aliphatic-H), 3.88 (s, 6H, *N*-Me), 2.40 (s, 2H, aliphatic-H).

**$[C_{12}H_{20}N_4][Cu(mnt)_2]$ (1d)**. Yield: 57% (based on Cu). Anal. Calc. for $C_{20}H_{20}N_8S_4Cu$: C, 42.57; H, 3.57; N, 19.85. Found: C, 42.89; H, 3.51; N, 19.47. IR spectrum (KBr, ν/$cm^{-1}$): 3146, 3088, 2197, 1595, 1562, 1464, 1149, 839, 744. LCMS (*m/z*): 221 $(M+H)^+$. $^1H$ NMR (400 MHz, $\delta$ ppm) (DMSO-$d_6$): 9.10 (s, 2H, Ar-H), 7.72-7.74 (m, 4H, Ar-H), 4.21 (s, 4H, aliphatic), 3.86 (s, 6H, *N*-Me), 1.79 (s, 4H, aliphatic-H).

**$[C_{13}H_{22}N_4][Cu(mnt)_2]$ (1e)**. Yield: 61% (based on Cu). Anal. Calc. for $C_{21}H_{22}N_8S_4Cu$: C, 43.62; H, 3.83; N, 19.37. Found: C, 43.30; H, 3.88; N, 18.91. IR spectrum (KBr, $cm^{-1}$): 3144, 2932, 2355, 2262, 2193, 1556, 1454, 1147, 831, 748. LCMS (*m/z*): 235 $(M+H)^+$. $^1H$ NMR (400 MHz, $\delta$ ppm) (DMSO-$d_6$): 9.11 (s, 2H, Ar-H), 7.24 (d, 4H, Ar-H), 4.18 (s, 4H, aliphatic-H), 3.87 (s, 6H, *N*-Me), 1.86 (s, 4H, aliphatic-H), 1.26 (s, 2H, aliphatic-H).

**$[C_{14}H_{24}N_4][Cu(mnt)_2]$ (1f)**. Yield: 59% (based on Cu). Anal. Calc. for $C_{22}H_{24}N_8S_4Cu$: C, 44.61; H, 4.08; N, 18.91. Found: C, 44.89; H, 4.12; N, 18.59. IR spectrum (KBr pellet, ν/$cm^{-1}$): 3092, 2361, 2195, 1572, 1462, 1168, 1147, 862, 761. LCMS (*m/z*): 249 $(M+H)^+$. $^1H$ NMR (400 MHz, $\delta$ ppm) (DMSO-$d_6$): 9.11 (s, 2H, Ar-H), 7.73 (d, 4H, Ar-H), 4.16 (s, 4H, aliphatic-H), 3.86 (s, 6H, *N*-Me), 1.86 (s, 4H, aliphatic-H), 1.30 (s, 4H, aliphatic-H).

**$[(C_9H_{14}N_4)(CH_3CN)][Ni(mnt)_2]$ (2a)**. Yield: 67% (based on Ni). Anal. Calc. for $C_{19}H_{17}N_9NiS_4$: C, 40.87; H, 3.06; N, 22.57. Found: C, 40.48; H, 2.99; N: 22.17. IR spectrum (KBr pellet, ν/$cm^{-1}$): 3101, 3073, 2262, 2193, 1556, 1464, 1149, 839, 793. LCMS (*m/z)*: 179 $(M+H)^+$. $^1H$ NMR (400 MHz, $\delta$ ppm) (DMSO-$d_6$): 9.32 (s, 2H, Ar-H), 7.92 (s, 2H, Ar-H), 7.82 (s, 2H, Ar-H), 6.64 (s, 2H, aliphatic-H), 3.93 (s, 6H, *N*-Me), 1.91 (s, 3H).

**$[C_{10}H_{16}N_4][Ni(mnt)_2]$ (2b)**. Yield: 56% (based on Ni). Anal. Calc. for $C_{18}H_{16}N_8S_4Ni$: C, 40.69; H, 3.03; N, 21.08. Found: C, 40.25; H, 3.08; N, 20.48. IR spectrum (KBr, ν/$cm^{-1}$): 3144, 2359, 2193, 1552, 1464, 1147, 1049, 837, 748. LCMS (*m/z*): 193 $(M+H)^+$. $^1H$ NMR (400 MHz, $\delta$ ppm) (DMSO-$d_6$): 9.02 (s, 2H, Ar-H), 7.70 (s, 2H, Ar-H), 7.56 (s, 2H, Ar-H), 4.64 (s, 4H, aliphatic-H), 3.88 (s, 6H, *N*-Me).

**$[C_{11}H_{18}N_4][Ni(mnt)_2]$ (2c)**. Yield: 64% (based on Ni). Anal. Calc. for $C_{19}H_{18}N_8S_4Ni$: C, 41.85; H, 3.32; N, 20.54. Found: C, 41.56; H, 3.28; N, 20.89. IR spectrum (KBr, ν/$cm^{-1}$): 3090, 2262, 2191, 1578, 1545, 1452, 1049, 858, 762. LCMS (*m/z*): 207 $(M+H)^+$. $^1H$ NMR (400 MHz, $\delta$ ppm) (DMSO-$d_6$): 9.08 (s, 2H, Ar-H), 7.72 (s, 4H, Ar-H), 4.20 (s, 4H, aliphatic-H), 3.85 (s, 6H, *N*-Me), 2.37 (s, 2H, aliphatic-H).

**$[C_{12}H_{20}N_4][Ni(mnt)_2]$ (2d)**. Yield: 63% (based on Ni). Anal. Calc. for $C_{20}H_{20}N_8S_4Ni$: C, 42.94; H, 3.60; N, 20.03. Found: C, 42.59; H, 3.53; N, 19.47. IR spectrum (KBr, ν/cm$^{-1}$): 3144, 2932, 2262, 2193,1595, 1562, 1454, 1147, 831, 740. LCMS (*m/z*): 221 $(M+H)^+$. $^1$H NMR (400 MHz, $\delta$ ppm) (DMSO-$d_6$): 9.12 (s, 2H, Ar-H), 7.70-7.74 (m, 4H, Ar-H), 4.19 (s, 4H, aliphatic), 3.88 (s, 6H, *N*-Me), 1.76 (s, 4H, aliphatic-H).

**$[C_{13}H_{22}N_4][Ni(mnt)_2]$ (2e)**. Yield: 68% (based on Ni). Anal. Calc. for $C_{21}H_{22}N_8S_4Ni$: C, 43.99; H, 3.86; N, 19.54. Found: C, 43.30; H, 3.90; N, 18.91. IR spectrum (KBr, cm$^{-1}$): 3092, 2361, 2195, 1572, 1450, 1168, 1147, 862, 748. LCMS (*m/z*): 235 $(M+H)^+$. $^1$H NMR (400 MHz, $\delta$ ppm) (DMSO-$d_6$): 9.10 (s, 2H, Ar-H), 7.22 (d, 4H, Ar-H), 4.20 (s, 4H, aliphatic-H), 3.86 (s, 6H, *N*-Me), 1.88 (s, 4H, aliphatic-H), 1.24 (s, 2H, aliphatic-H).

**$[C_{14}H_{24}N_4][Ni(mnt)_2]$ (2f)**. Yield: 56% (based on Ni). Anal. Calc. for $C_{22}H_{24}N_8S_4Ni$: C, 44.98; H, 4.11; N, 19.07. Found: C, 44.59; H, 4.16; N, 18.69. IR spectrum (KBr pellet, ν/cm$^{-1}$): 3092, 2358, 2189, 1568, 1460, 1160, 1142, 862, 761. LCMS (*m/z*): 249 $(M+H)^+$. $^1$H NMR (400 MHz, $\delta$ ppm) (DMSO-$d_6$): 9.10 (s, 2H, Ar-H), 7.72 (d, 4H, Ar-H), 4.14 (s, 4H, aliphatic-H), 3.84 (s, 6H, *N*-Me), 1.86 (s, 4H, aliphatic-H), 1.32 (s, 4H, aliphatic-H).

### 2.2.3. Crystal structure determination

Data were measured at room temperature for compounds **1a-1f** and **2a-2e** on a Bruker SMART APEX CCD, area detector system [λ (Mo Kα) = 0.7103 Å], graphite monochromator, 2400 frames were recorded with an ω scan width of 0.3°, each for 10 s, crystal-detector distance 60 mm, collimator 0.5 mm.[21] Data reduction was performed with the SAINTPLUS software,[21a] absorption correction using an empirical method SADABS,[21b] structure solution using SHELXS-97 program,[21c] and refined using SHELXL-97 program.[21d] Hydrogen atoms on the aromatic rings were introduced on calculated positions and included in the refinement riding on their respective parent atoms.

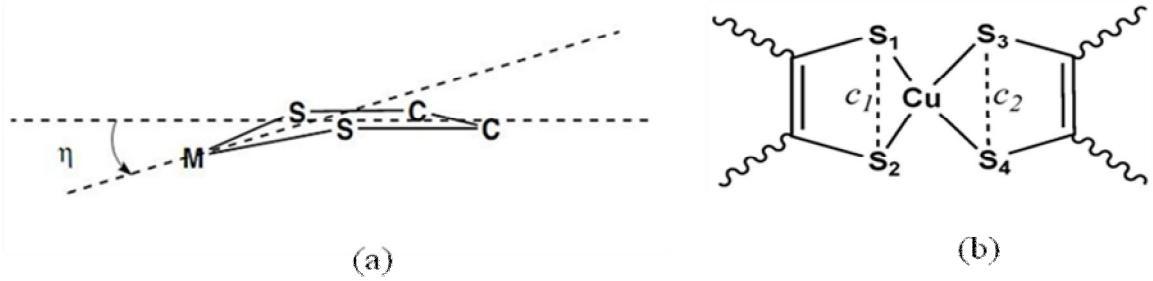


**Scheme 2.2.** (a) The bending anlge (η) in bent ligand, (b) the $c_1$–M–$c_2$ angle.

## 2.3. Results and Discussion

### 2.3.1. Synthesis

We have succeeded in preparing a new series of ion pair compounds with a range of imidazolium cations of varied alkyl chain length (n = 1 to 6) leading to compounds **1a-1f** and **2a-2f** (see Scheme 2.1). Compounds **1a-1f** and **2a-2f** are characterized by routine elemental analyses, IR, NMR, UV-Visible-NIR spectroscopic techniques, cyclic voltammetry and unambiguously characterized by single crystal X-ray structure determinations (except **2f**). Geometry around the metal ion in complexes **1a-1e** and **2a**, **2c** is distorted square planar whereas geometry of the metal ion in complexes **1f** and **2b**, **2d**, **2e** is perfectly square planar. Distortion of these complexes (**1a-1e** and **2a**, **2c**) can be explained on the basis of angle between MSS and SCCS planes,[1f] angle *c1*-M-*c2* (c1, c2 are the mid points between two sulfur atoms from two chelate rings in the anion $[M(mnt)_2]^{2-}$), and the angle between two SMS planes (S1MS2 and S3MS4) as shown in Scheme 2.2.

### 2.3.2. Description of Crystal Structure

**Compound $[C_9H_{14}N_4][Cu(mnt)_2]$ (1a)**. Crystals of this compound, suitable for X-ray analysis, have been grown from $CH_3CN$/ether by diffusion method. Compound **1a** crystallizes in triclinic system with *P-1* space group. The asymmetric unit contains a full molecule; an ORTEP diagram with labeled atoms has been shown in Figure 2.1(a). The basic crystallographic data are presented in Table 2.1. Here, the overall charge of this Cu(II) complex anion $[Cu(mnt)_2]^{2-}$ as expected is –2, and this anionic charge is compensated by a one $[C_9H_{14}N_4]^{2+}$ cation as observed in the crystal structure. In $[Cu(mnt)_2]^{2-}$ anion, the bond lengths of Cu–S are in the range of 2.254(1) to 2.269(1) Å and the bond angles in a chelate ring of SCuS are 92.01°(2) and 92.32°(2). The dihedral angle (λ), which can be defined by the angle between two five membered rings *i.e* S1–Cu–S2 and S3–Cu–S4 is 38.13°, indicates that the copper center in this complex **1a** is deviated from the square-planar coordination geometry. The $c_1$–Cu–$c_2$ angle is 176.89°; $c_1$ and $c_2$ are the mid points of the two sulfur atoms in the five membered chelate rings (usually for a perfect square planar complex, the $c_1$–M–$c_2$ is 180°). The bending angle (η) between the S3CuS4 and S3C5C6S4 plane is 4.21°, and in the other chelate ring the angle between S1CuS2 and S1C1C2S2 plane is 0.50°.

**(a)**

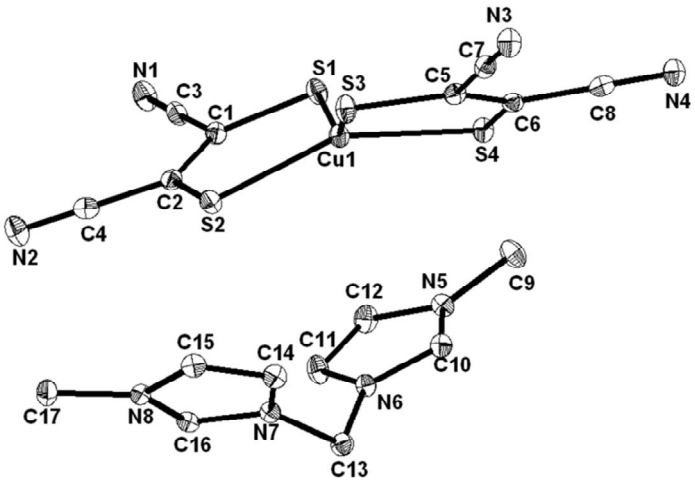
N3
C7
N1
S1
C3
S3
C5
C1
C6
C8
N4
Cu1
S4
C2
S2
C4
N2
C12
N5
C9
C15
C14
C11
C10
N6
C17
N8
N7
C16
C13

**(b)**

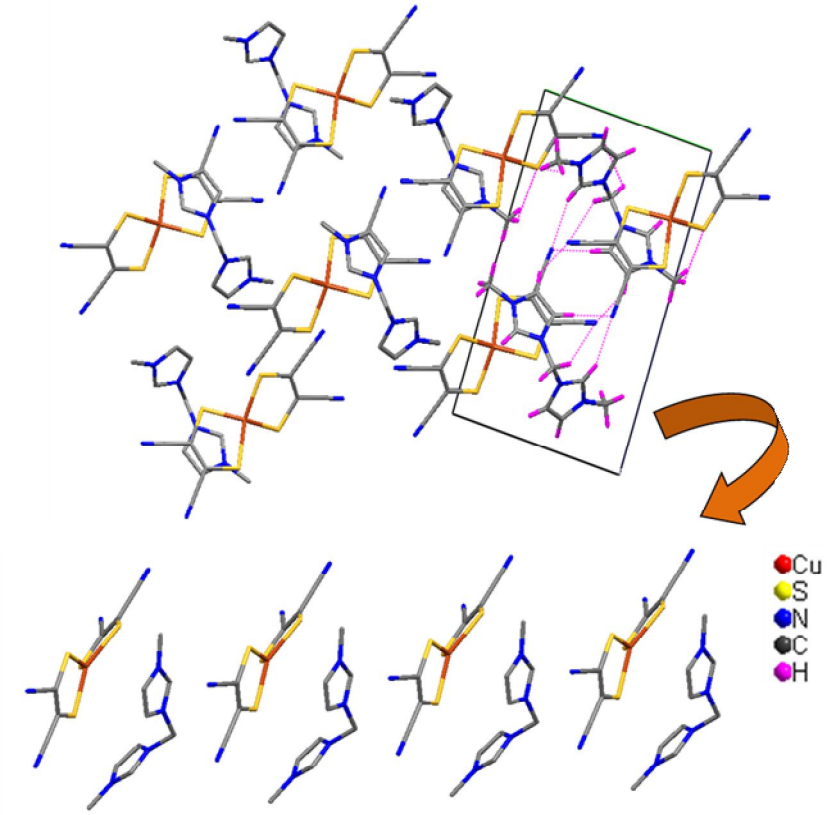
Cu
S
N
C
H

**(c)**

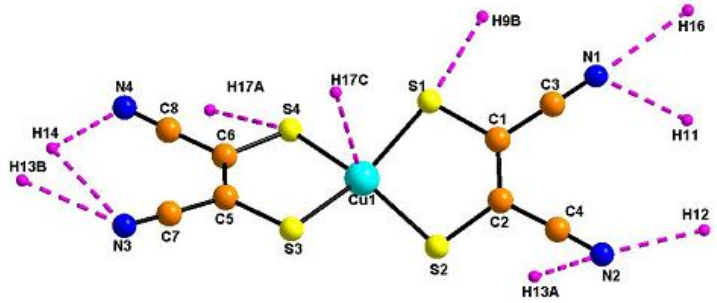


**Figure 2. 1.** (a) Thermal ellipsoidal diagram of the complex **1a** (with 40% pobability), (b) packing diagram of complex **1a**, and (c) hydrogen bonding interactions around the anion $[Cu(mnt)_2]^{2-}$ **(**Hydrogen bonding interaction are present in unit cell, remaining are for omitted for clarity).

This indicates that one chelate ring is comparatively more planar than the other chelate ring in the complex anion $[Cu(mnt)_2]^{2-}$. In the solid state, the $[Cu(mnt)_2]^{2-}$ anions (A) and $[C_9H_{14}N_4]^{2+}$ cations (C) are alternately stacked along crystallographic *c*-axis with a repeating order of ACACAC,[22] and form one dimensional columns through the π···π interactions (centroid-centroid) with an range of 3.841 to 3.966 Å separation between the imidazole moiety from cation and the chelate ring from the anion, which has been shown in Figure 2.1(b). In this complex **1a**, the d(H···A) distance of C–H···Cu hydrogen bond is 3.14 Å (which is more than the reported value 3.01Å)[23]; the d(D···A) separation of C–H···Cu hydrogen bond is 3.943 Å, and the C–H···Cu angle (θ) is 140.7° (see Table 2.2). In compound **1a**, there is only one cation which is situated towards the anion through metal-hydrogen bond (C–H···Cu) with a distance of 3.14 Å, and within the same distance and along that axis no other cation is available on other side of the anion. This implies that there is no centre of symmetry along the metal-hydrogen bond through the anion. Around the anion $[Cu(mnt)_2]^{2-}$, there are seven C–H···N and two C–H···S un-balanced interactions, present within the range of 2.34–2.70 Å, and 2.89–2.95 Å, respectively which has been shown in Figure 2.1(c). In its crystal packing, each anion is surrounded by five cations with an un-balanced C–H···S, C–H···N supramolecular interactions. Based on this data, there is a lack of centre of symmetry (*Ci*) along Cu···H hydrogen bond and unbalanced interactions around the anion. As a result, the geometry of metal is deviated from square planar coordination. The closest Cu···Cu and Cu···S interactions are 7.688(1) Å and 6.217(3) Å, respectively.

**Compound $[C_{10}H_{16}N_4][Cu(mnt)_2]$ (1b)**. Suitable sized-single crystals of compound **1b** were obtained from $CH_3CN$/ether diffusion method. Compound **1b** crystallizes in monoclinic system with *C2/c* space group. In its crystal structure, the asymmetric unit contains half of the molecule indicated with labeled atoms. The relevant ORTEP diagram is shown in Figure 2.2(a). The bond lengths of Cu–S are in the range of 2.252(8) Å to 2.265(17) Å and the S–Cu–S angle is 91.63(3)°; this angle is relatively smaller than the corresponding angle in complex **1a.** The dihedral angle (λ) between two SMS planes in $[Cu(mnt)_2]^{2-}$ anion is 32.0°, which is smaller than the corresponding angle in complex **1a**. Thus complex anion $[Cu(mnt)_2]^{2-}$ in **1b** is also not planar. The $c_1$–Cu–$c_2$ angle in $[Cu(mnt)_2]^{2-}$ anion of **1b** is 176.66°, indicating that there is a deviation from square-planar geometry at copper center. The bending angle (η) between S1CuS2 and S1C1C2S2 is 4.28°; it indicates that the chelate ring is near-planar (η<6° indicates highly planar nature of a dithiolene-ligand chelate).[1f] The supramolecular interactions between cation and anion through S···H and N···H hydrogen bonds lead to the formation of a 2-D network. In this network, the cations and anions are arranged in a slippage fashion;[3a,5a] as a consequence there is no significant π···π interactions between cation and anion (Figure 2.2(b)). This slippage fashion interactions in complex **1b**, between cation and anion through S···H and N···H hydrogen bonds (2.84 to 2.87 Å and 2.52 to 2.75 Å respectively) leads to shorter intermolecular contacts, 3.614(4) Å for C(7)···S(1) and 3.340(5) Å for C(6)···N(1); rest of the hydrogen bonding interactions are described in a Table 2.3.

**(a)**

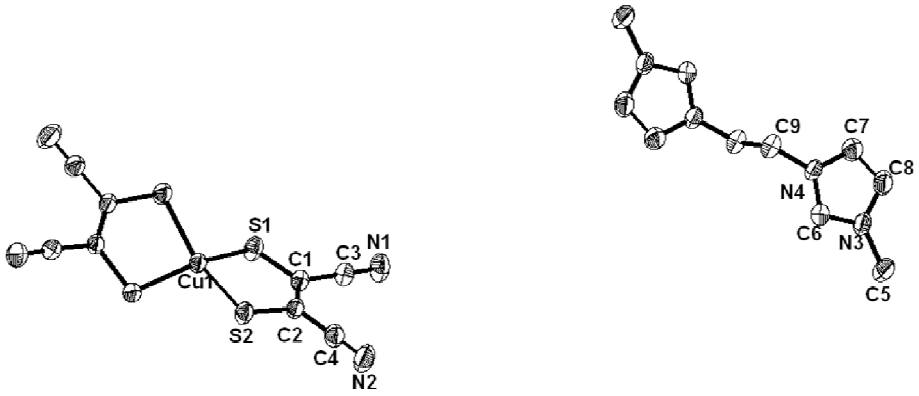

**(b)**

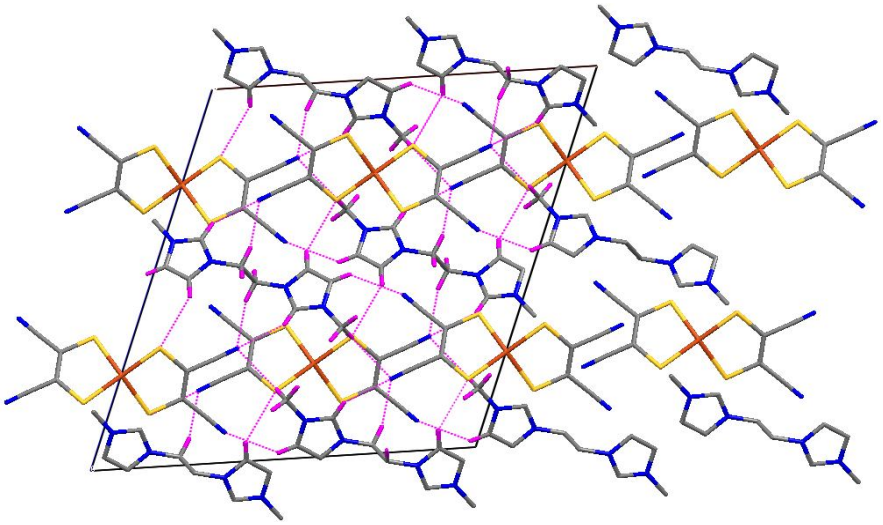

**(c)**

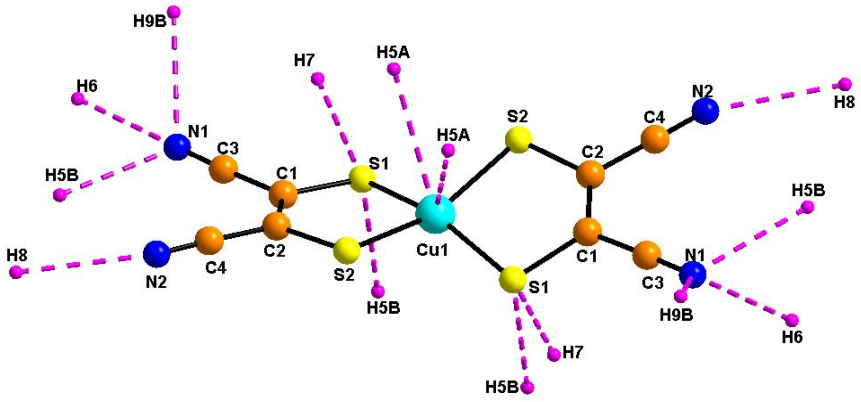


**Figure 2.2.** (a) Thermal ellipsoidal diagram of the complex **1b** (with 40% pobability), (b) packing diagram of complex **1b**, and (c) hydrogen bonding interactions around the anion $[Cu(mnt)_2]^{2-}$.

The C–H···Cu hydrogen bond in compound **1b** is characterized by H···Cu separation (d) 3.05 Å, C–H···Cu distance (D) 3.920 Å and the C–H···Cu (θ) angle 150.9°, which are closed to the relevant literature values.[23] In this compound, there are two cations are present at the same side of the anion with a distance of 3.05 Å through metal-hydrogen interactions, which clearly indicates that there is no centre of symmetry (*Ci*) along metal-hydrogen bond. Around the complex anion, there are balanced S···H and N···H interactions (Figure 2.2(c), each chelate ring is interacted with identical distances); but in case of Cu···S contacts, these are un-

balanced interactions. In complex **1b**, the Cu1···S1 separation is 7.18 Å and Cu1···S2 separation is 7.09 Å, which indicates sulfur atoms (S1 and S2) from two chelate rings in the anion interact with copper differently. Based on the lack of centre or symmetry and unbalanced supramolecular interactions, structure of the anion in complex **1b**, is deviated to distorted square planar.

**Compounds $[C_{11}H_{18}N_4][Cu(mnt)_2]$ (1c) and $[C_{12}H_{20}N_4][Cu(mnt)_2]$ (1d).** Dark brown crystals of these two complexes suitable for X-ray structure analysis have been grown from $CH_3CN$/ether by diffusion method. Both compounds **1c** and **1d** crystallize in *P*2(1)*/c* space group in monoclinic system. In their crystal structures, the asymmetric unit contains full molecule as represented with labeled atoms in Figures 2.3(a) and 2.4(a) respectively. The Cu–S bond lengths in compounds **1c** and **1d** are in the range of 2.246 to 2.266 Å and 2.258 to 2.273 Å, respectively. Notably, there is a short Cu–S bond length (Cu(1)–S(4) = 2.246(18) Å) in compound **1c**, which is shorter than Cu–S bonds in the crystal structures of compounds **1a** and **1b**. On the other hand, the Cu(1)–S(1) bond length of 2.273(1) Å in compound **1d** is longer than Cu–S bonds in the crystal structures of compounds **1a** and **1b**. The S–Cu–S bond angles in the anion $[Cu(mnt)_2]^{2-}$ of compounds **1c** and **1d** are in the range of 91.39(6)° to 91.81(7)° and 91.37(3)° to 91.56(3)° respectively.

**(a)** **(b)**

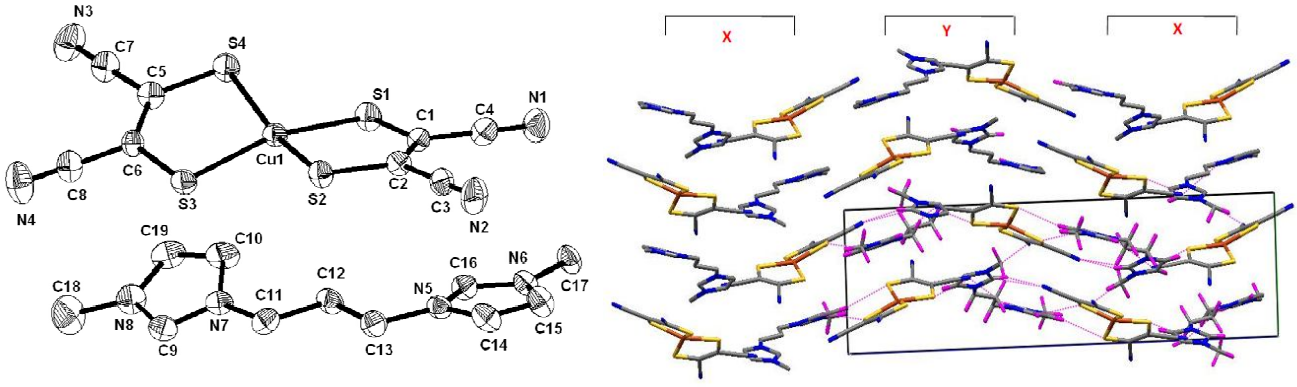

**(c)**

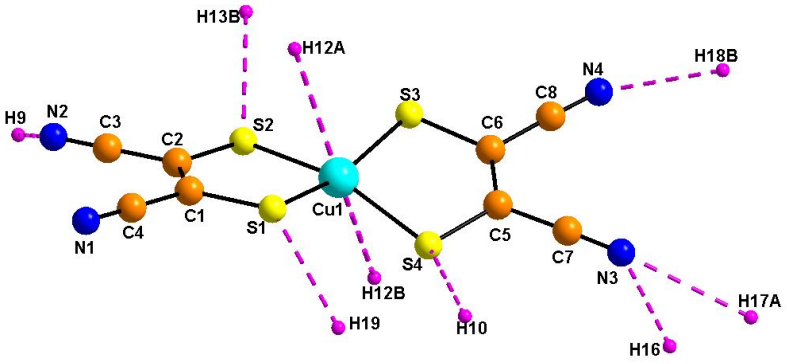


**Figure 2.3.** (a) Thermal ellipsoidal diagram of the complex **1c** (with 30% pobability), (b) packing diagram of complex **1c**, and (c) hydrogen bonding interactions around the anion $[Cu(mnt)_2]^{2-}$.

The deviation angles (λ) with respect to perfect square-planar geometry, that can be measured as the angle between two S–Cu–S planes in two chelate rings present in $[Cu(mnt)_2]^{2-}$ anions of the compounds **1c** and **1d**, are found to be 26.73° and 19.91° respectively. These angles are relatively smaller as compared to those in above discussed compounds **1a** and **1b**. The $c_1$–Cu–$c_2$ angles in compounds **1c** and **1d** are 179.22° and 178.48° respectively. The related bending angles (η) in the anion $[Cu(mnt)_2]^{2-}$ of **1c** and **1d** are 6.45°, 3.28° and 2.49°, 3.59° respectively. Thus each chelate ring deviates from the planar arrangement. The supramolecular interactions between cation and anion through S···H and N···H contacts lead to 2-D network structures (Figures 2.3(b) and 2.4(b) for compounds **1c** and **1d** respectively). As shown in Figure 2.3(b) for the crystal structure of compound **1c**, there are two different arrangement (named as X and Y) of cations and anions. In both arrangements X and Y, there is a stacking of cation-anion (C-A). The C-A in the X column is mirror image to the C-A of Y column. The packing arrangement of crystal structure of compound **1c** can be described as X Y X Y X Y and so on (Figure 2.3(b)). In the crystal structure of **1d**, there is a slippage arrangement of the cations and anions, which is similar to that in the crystal structure of compound **1b** (vide supra), except there is a small change in alignment of cations compared to that in compound **1b**. The Cu···H separation (d), C–H···Cu distance (D) and C–H···Cu angle (θ) are 2.98 Å, 3.86 Å and 151.6° respectively for compound **1c**, and 3.067 Å (d) 3.828 Å (D) and 137.2° (θ), respectively for compound **1d**. The intermolecular separations of Cu···Cu and Cu···S are 6.774 Å, 5.376 Å and 7.357 Å, 6.975 Å, for the compounds **1c** and **1d** respectively.

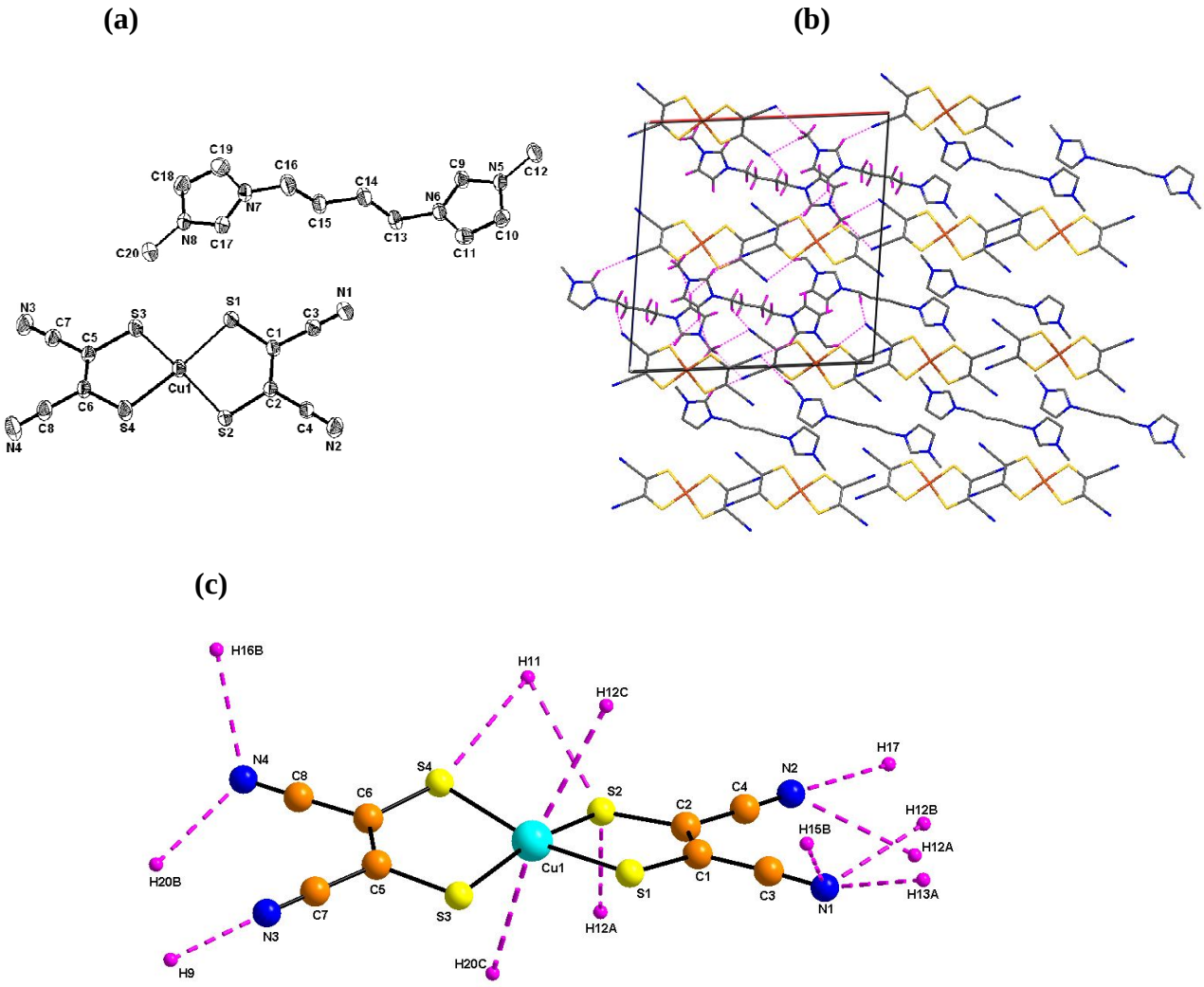


**Figure 2.4.** (a) Thermal ellipsoidal diagram of the complex **1d** (with 30% pobability), (b) packing diagram of complex **1d**, and (c) hydrogen bonding interactions around the anion $[Cu(mnt)_2]^{2-}$.

In compound **1c**, two cations are present at top and bottom of the complex anion $[Cu(mnt)_2]^{2-}$ with a different distances (2.98 Å and 3.06 Å) of C–H···Cu interactions. This clearly indicates that there is no centre of symmetry along metal-hydrogen bond interaction. Sulfur atoms (S1, S2 and S4) from the chelate rings interact with two different surrounding cations with symmetry code (#10, #11) operations. From the complex anion $[Cu(mnt)_2]^{2-}$, S1 and S4 interact with a common cation $[C_{11}H_{18}N_4]^{2+}$ through C–H(19)···S1, C–H(10)···S4 hydrogen bonds with distances of 2.93 and 2.98 Å respectively. A seven membered ring consisting of Cu1S1H19C19C10H10S4 with C–H···S interactions is observed and around the anion there are totally seven different S···H and N···H interactions that are present with three

surrounding cations, as shown in Figure 2.3(c). In compound **1c**, the structure of the anion is deviated from planarity due to lack of centre of symmetry (*Ci*) along the interaction of metal-hydrogen bond and unbalanced supramolecular interactions around the anion. In compound **1d**, there are two metal hydrogen bonding interactions of the complex anion with surrounding huge cations $[C_{12}H_{20}N_4]^{2+}$, that are situated at top and bottom of the anion with 3.07 Å and 3.11 Å of distances. Thus, there is no centre of symmetry along metal-hydrogen bond in the complex **1d**. Seven cations interact with the anion through eight C–H···N and three C–H···S supramolecular interactions. A four membered ring (Cu1S2H11S4) is observed in which two sulfur atoms (S2 and S4) from the two chelate rings are connected to the cation through common hydrogen bonds (C–H(11)···S2, C–H(11)···S4) with distances of 2.95 Å and 3.00 Å respectively as shown in Figure 2.4(c). Because of this interaction, movement of two chelate rings is restricted (S2 and S4 atoms are interacted to the cation with a common hydrogen bond). This indicates, there is no centre of symmetry along metal-hydrogen bond in compound **1d**, and due to un-balanced supramolecular interactions, coordination geometry of metal ion is deviated to the distorted square planar.

**Compound $[C_{13}H_{22}N_4][Cu(mnt)_2]$ (1e)**. Compound **1e** crystallizes in *P-1* space symmetry (triclinic) with half of the molecule present in its asymmetric unit (Figure 2.5(a)). The average Cu–S bond length and S–Cu–S bond angle in $[Cu(mnt)_2]^{2-}$ anion are 2.261 Å and 92.19° respectively. The dihedral angle (λ) in the $[Cu(mnt)_2]^{2-}$ anion is 37.06°, which is larger than those in compounds **1b**–**1d**, but this angle is comparable to that in compound **1a**.

**(a)**

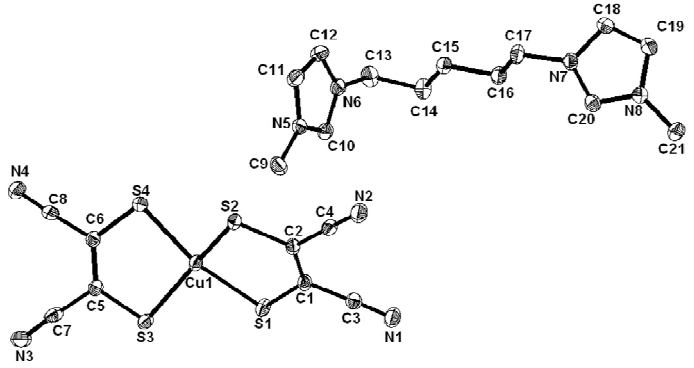

**(b)**

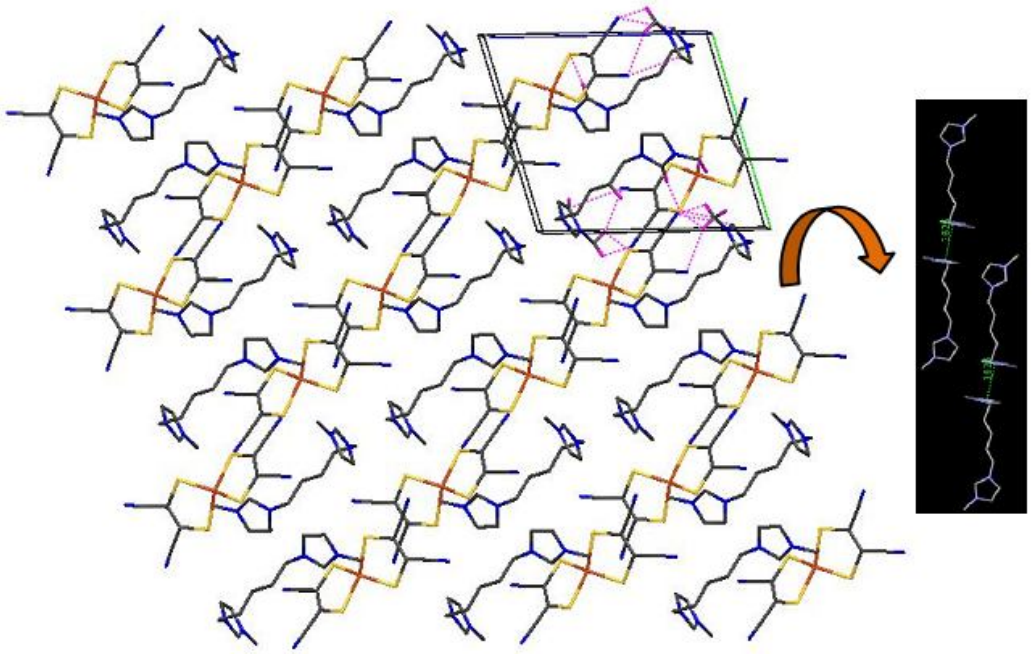

**(c)**

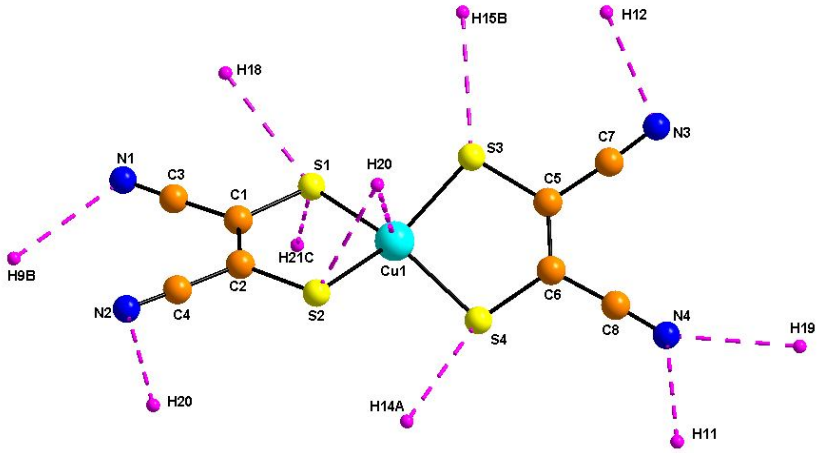


**Figure 2.5.** (a) Thermal ellipsoidal diagram of the complex **1e** (with 50% pobability), (b) packing diagram of complex **1e**, and (c) hydrogen bonding interactions around the anion $[Cu(mnt)_2]^{2-}$.

In compound **1e**, $[Cu(mnt)_2]^{2-}$ anion is a non-planar structure and all the nitrogen atoms are deviated from mean plane of {S1S2S3S4} ( N1: 0.878 Å, N2: 0.408 Å, N3: 0.990 Å and N4: 0.565 Å). The bending angle (η) in one chelate ring (Cu1S1C1C2S2) is 4.21°, and in the other chelate ring (Cu1S3C5C6S4) it is 0.56°, which indicates that one of the chelate ring in the $[Cu(mnt)_2]^{2-}$ anion is more deviated from the planarity than the other chelate ring. The

bending angles in compound **1e** are similar to those in compound **1a** (η = 4.21°, 0.50°). In the cationic part of its molecular structure, the angle between planes of two imidazole moieties is 67.07°, which is 55.11° in compound **1a**. The supramolecular S···H and N···H interactions lead the formation of a 2-D network, in which cations and anions are arranged in slippage fashion as shown in the case of compound **1b** (vide supra). There are π····π (Cg1–Cg2) stacking interactions between imidazole moieties (Cg1 = {C9C10C11N5N6}, and Cg2 is symmetry related equivalent of Cg1) from individual cations, in which each cation is positioned in between two $[Cu(mnt)_2]^{2-}$ anion moieties as shown in Figure 2.5(b). Intermolecular Cu···Cu and Cu···S separations are 6.940 Å and 6.025 Å, respectively. The d(H···A) distance of C–H···Cu hydrogen bond in compound **1e** is 2.91 Å, with an angle (θ) of 112.6°. The cationic moiety laying above the plane of the $[Cu(mnt)_2]^{2-}$ anion interacts with the complex anion $[Cu(mnt)_2]^{2-}$ via C–H···Cu distance of 2.91 Å. The non-appearance of any cationic moiety just below the plane of the complex anion $[Cu(mnt)_2]^{2-}$ (i.e., other side of the plane of the complex anion) indicates the lack of centre of symmetry along metal hydrogen interaction. In the crystal structure of compound **1e**, each anion interacts with five cationic units through C–H···S and C–H···N type of hydrogen bonding interactions as shown in Figure 2.5(c). The unbalanced supramolecular interactions around complex anion $[Cu(mnt)_2]^{2-}$ results in the distorted square planar geometry of the complex anion $[Cu(mnt)_2]^{2-}$.

**Compound $[C_{14}H_{24}N_4][Cu(mnt)_2]$ (1f).** Compound **1f** crystallizes in triclinic space group *P–1*. Figure 2.6(a) shows the asymmetric unit with half of the molecule. The angle between two SMS planes is zero *i.e.* the $c_1$–Cu–$c_2$ angle is 180º, which indicates that the dihedral angle between two SCuS planes is 0°; therefore in compound **1f**, the complex anion $[Cu(mnt)_2]^{2-}$ is perfectly square planar. This is in contrast to the situation in compounds **1a**–**1e**. In **1f**, the bending angles (η) between two chelate rings in the $[Cu(mnt)_2]^{2-}$ anion is 0° which supports the non deviation from planarity in the complex anion. The molecular structure shows π···π interactions between Cg1 and Cg2 chelated rings (Cg1= Cu1S1S2C1C2 from coordination complex anion moiety and Cg2 = N3C5C6C7N4 from imidazole cation moiety) with a distance of 3.785 Å (Figure 2.6(b)). The supramolecular interactions (S···H, N···H and Cu···S) around each chelate ring in the complex anion are identical resulting in balanced interactions around the complex anion. The d(H···A) separation and the d(D···A) distance of C–H···Cu

hydrogen bond and C–H···Cu angle (θ) are 2.72 Å, 3.614 Å and 156.2° respectively. These supramolecular interactions lead to the formation of a 1-D chain. The geometrical parameters for the above-mentioned metal hydrogen supramolecular interactions for all the compounds **1a**-**1f** are described in Table 2.2.

**(a)**

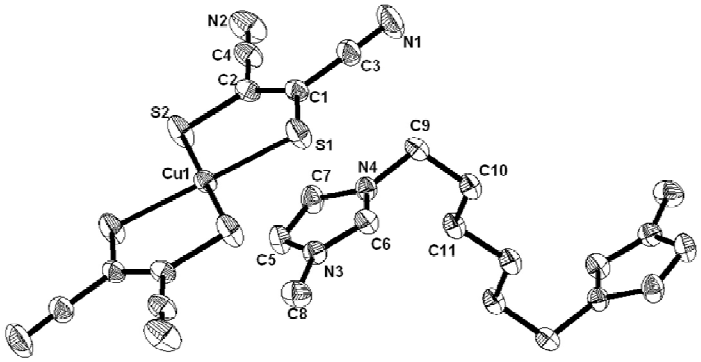


**(b)**

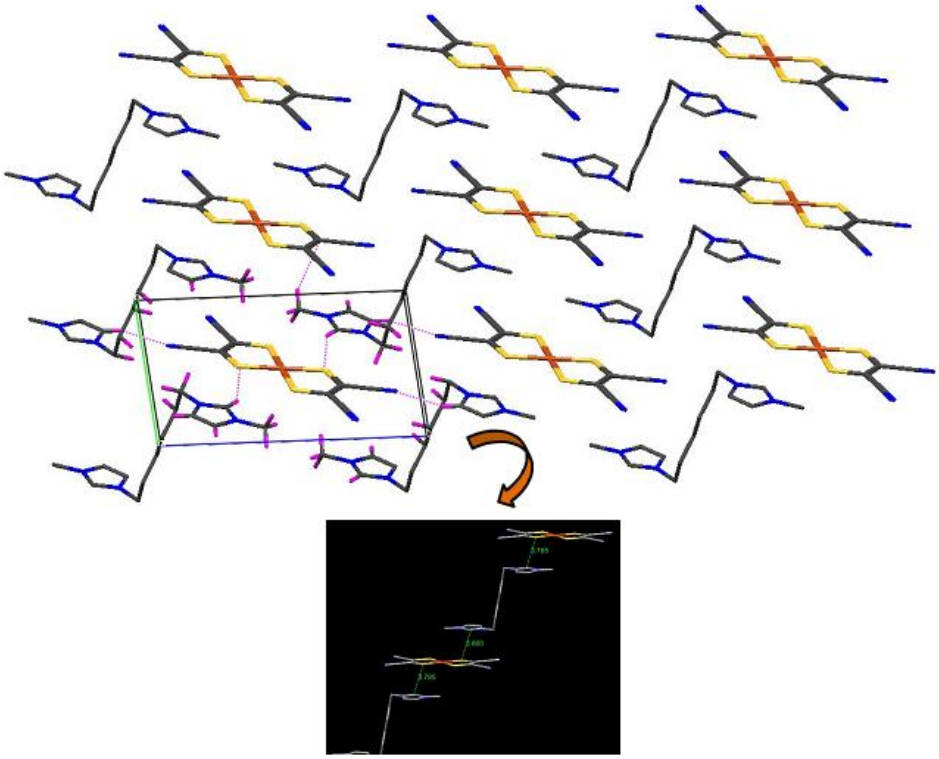

**(c)**

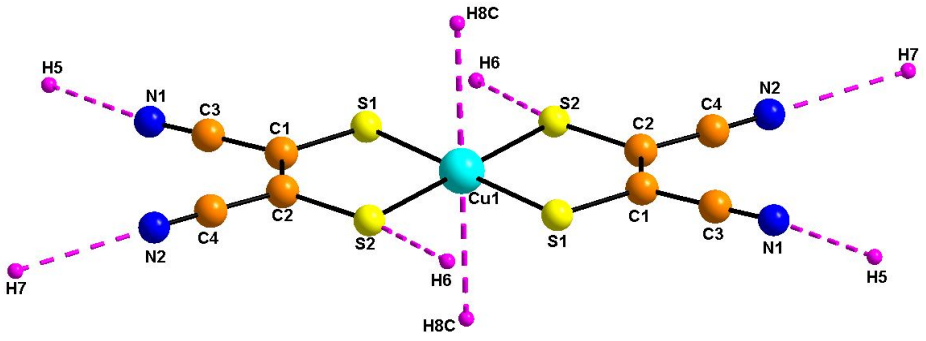


**Figure 2.6.** (a) Thermal ellipsoidal diagram of the complex **1f** (with 30% pobability), (b) packing diagram of complex **1f**, and (c) hydrogen bonding interactions around the anion $[Cu(mnt)_2]^{2-}$.

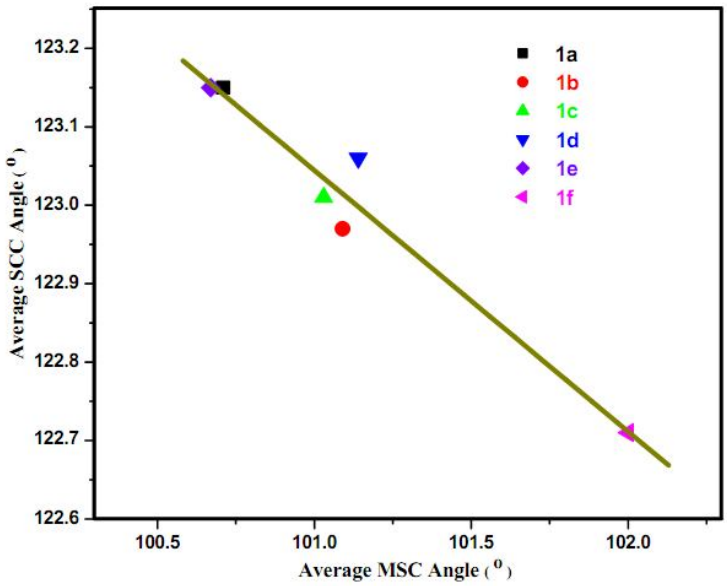


**Figure 2.7.** Plot between angles (Å) of MSC and SCC in the anion $[Cu(mnt)_2]^{2-}$ of the complexes **1a**-**1f**.

In **1f**, around the complex anion there are two cations are present: one cation is situated at the top of the complex anion and the other cation at the bottom of the complex anion with a same distance of 2.72 Å for C–H···Cu interactions. This clearly indicates there is a centre of symmetry (*Ci*) along the interaction of metal hydrogen bond through the anion. In this compound, six cations interact to the anion through equivalent distances of two C–H···S and four C–H···N hydrogen bonds as shown in Figure 2.6(c). In addition to these, we observe equivalent distances out of metal and sulfur interactions. All these indicate that there are

balanced equivalent interactions, present around the complex anion. Hence, the geometry around the central metal ion of the complex anion is perfectly square planar. Following Scheme 2.2, the MSC and SCC angles in complex anion $[Cu(mnt)_2]^{2-}$ of compound **1f** are 102.0° and 122.71 respectively. The same parameters in the complex anion $[Cu(mnt)_2]^{2-}$ of compound **1a** are 100.71° and 123.15° respectively. As shown in Figure 2.7, the larger MSC angles are offset by smaller SCC angles.[1f]

**Compounds $[(C_9H_{14}N_4(CH_3CN)][Ni(mnt)_2]$ (2a), $[C_{10}H_{16}N_4][Ni(mnt)_2]$ (2b), $[C_{11}H_{18}N_4][Ni(mnt)_2]$ (2c), $[C_{12}H_{20}N_4][Ni(mnt)_2]$ (2d), $[C_{14}H_{22}N_4][Ni(mnt)_2]$ (2e).**

Crystals of these compounds **2a**–**2e** are grown from $CH_3CN$/ether by diffusion method. Compounds **2a**, **2c** and **2e** are crystallized in monoclinic with *P*2(1)/*c* and *C*2/*c* space group; compounds **2b**, **2d** are crystallized in triclinic *P*-1. In the ion-pair dithiolene compounds **2a** and **2c** there are un-balanced supramolecular interactions are present around $[Ni(mnt)_2]^{2-}$ anion, due to these interactions the geometry around nickel metal is distorted square planar (4.89° and 3.21° for **2a** and **2c** respectively), which are resembles to the copper complexes **1a**–**1e**. In the case of other compounds **2b**, **2d** and **2e** the balanced supramolecular interactions are present around $[Ni(mnt)_2]^{2-}$ anion, hence the sulfur atoms in the two chelated rings of the anion moiety are not affected by these interactions, which leads to an perfect square-planar around nickel metal, these complexes are similar nature of the copper complex **1f**. Explanation of all these nickel complexes is similar to the copper complexes, the diagrammatic representation of nickel complexes **2a**–**2e** is shown in Figure 2.8. Crystallographic and hydrogen bonding tables for these compounds **2a**–**2e** are represented in Table 2.4 and 2.5.

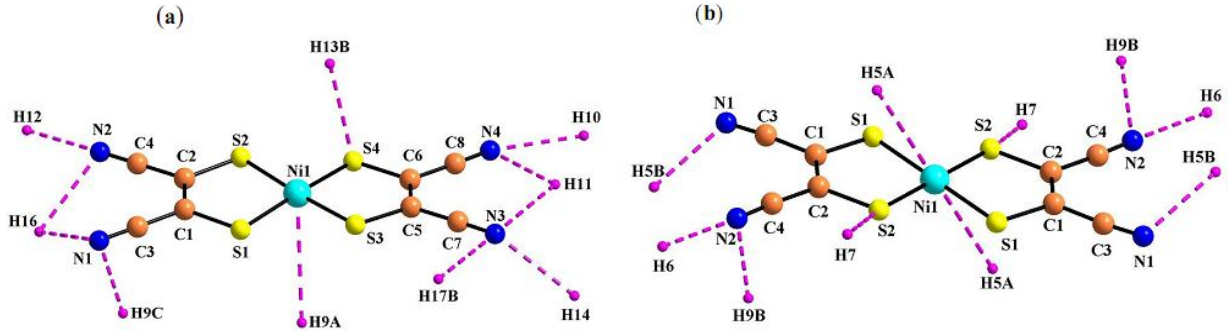

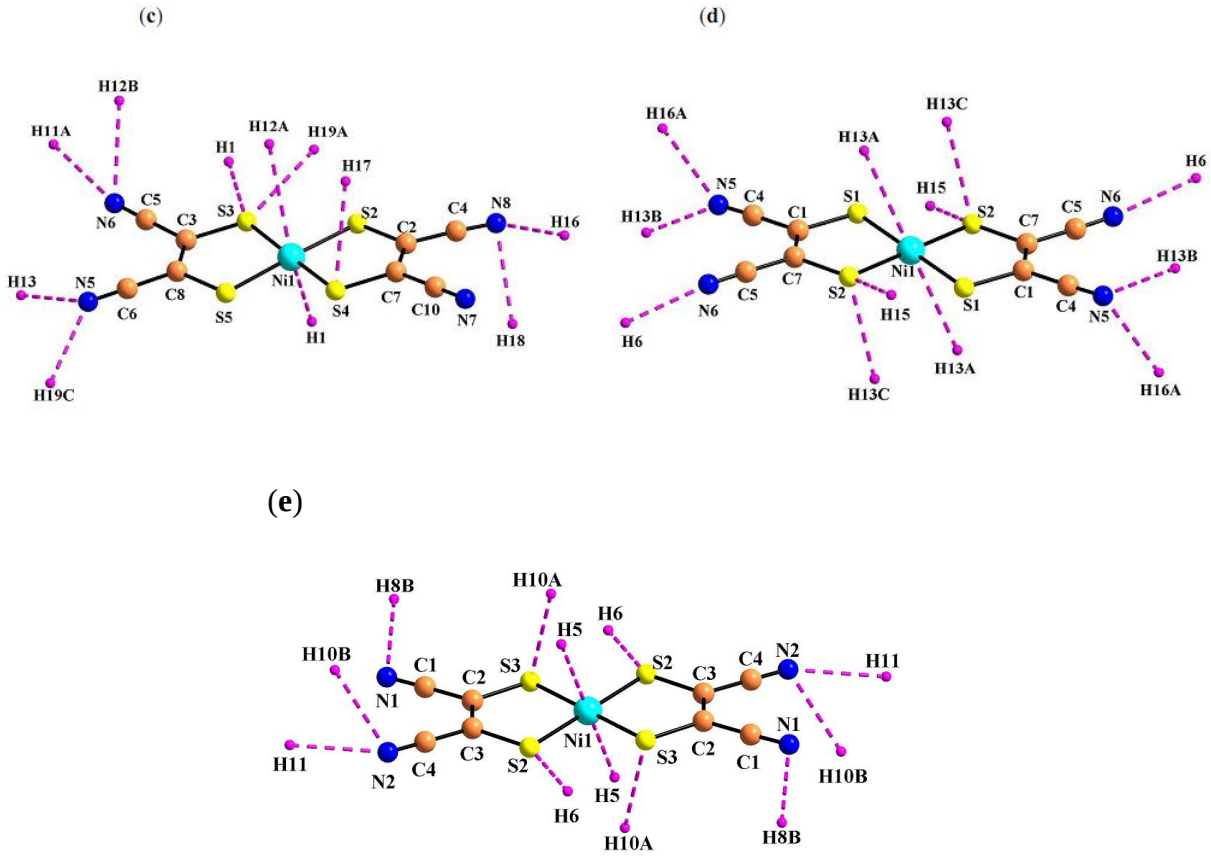


**Figure 2.8.** Balanced and un-balanced supramolecular interactions around $[Ni(mnt)_2]^{2-}$ anion: (a) to (e) indicates the compounds **2a** to **2e** respectively.

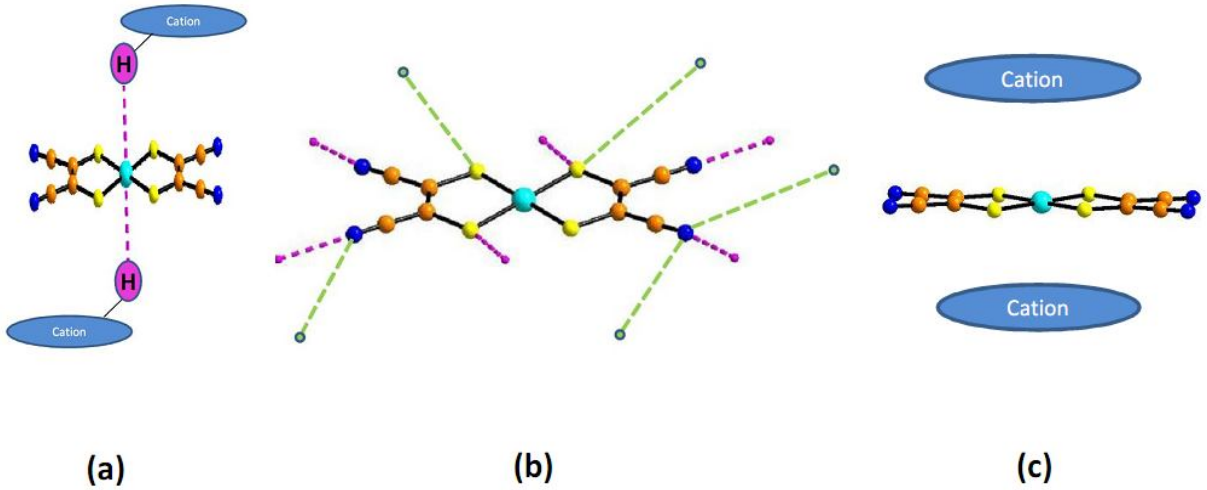


**Scheme 2.3.** (a) Centre of symmetry along metal-hydrogen interaction, (b) Equivalent and un-equivalent hydrogen bonding interactions, (c) Bulkiness around the anion $[Cu(mnt)_2]^{2-}$.

### 2.3.3. Discussion about the Distortion in Square-Planar Complexes

The deviation from the planarity in the series of above described square planar complexes can be explained by considering the following factors: lack of centre of symmetry (*Ci*) along metal hydrogen bond, unbalanced supramolecular interactions and crowdedness around the complex anion $[Cu(mnt)_2]^{2-}$. If a line is drawn through a point in the molecule in one direction and extended to equal distance in opposite direction meeting another similar group or atom, then the point (generally the central metal ion) is called as centre of symmetry (*Ci*). As shown in scheme 2.3(a), there is a centre of symmetry along the interaction of metal hydrogen bond in which the metal is $Cu^{2+}$ ion of the complex anion $[Cu(mnt)_2]^{2-}$, showing an identical hydrogen bonds from both sides of the anion with an identical distance. There are symmetrical or balanced interactions around the anion that are shown in purple color in scheme 2.3(b). The same scheme 2.3(b) also shows un-balanced supramolecular interactions involving different groups with dissimilar distances as indicated in green color. This leads to a change in spatial orientation of the chelate rings of the anion. Scheme 2.3(c) presents the possibility that in the crystals of the above mentioned compounds (**1a-1f**), the required cations are present closed to the complex anion and interact from top / bottom of molecular plane of the complex anion with a metal hydrogen bond. The geometry around the metal ion of the coordination complex anion $[Cu(mnt)_2]^{2-}$, naturally, depends on the crowdies or bulkiness of the cations in the relevant ion pair compound. Now we discuss the deviation of the molecular plane of the complex $[Cu(mnt)_2]^{2-}$ in compounds **1a**-**1f** with respect to the geometry around copper ion based on the above described factors, namely center of symmetry, unbalanced / unsymmetrical interactions and crowdedmess / bulkiness of the interacting groups.

In compound **1a**, there is one non-covalent metal hydrogen bond (C–H···Cu) with a distance of 3.14 Å; this indicates within this distance, there is a cation $[C_9H_{14}N_4]^{2+}$ hydrogen bonded to $[Cu(mnt)_2]^{2-}$ anion from one side. Moreover, there are un-balanced supramolecular S···H, N···H interactions around the complex anion $[Cu(mnt)_2]^{2-}$ (Figure 2.1c). The combination of these two factors leads to considerable amount of distortion around copper ion with a dihedral angle of 38.13°. In the case of compound **1b**, there are two non-covalent metal hydrogen bonds (C–H···Cu) with a distance of 3.05 Å; however, both cation moieties $[C_{10}H_{16}N_4]^{2+}$ are hydrogen bonded from same side of the $[Cu(mnt)_2]^{2-}$ anion (Figure 2.2c).

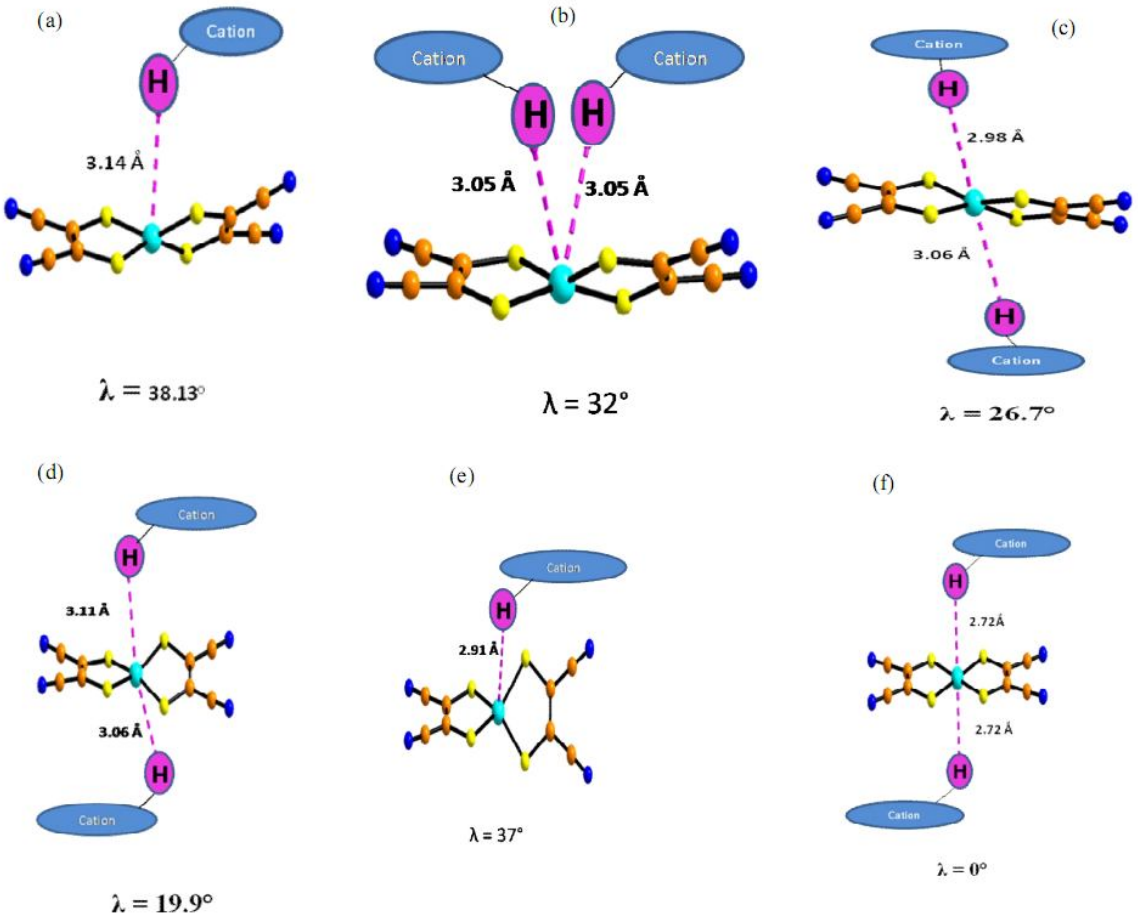


**Figure 2.9**. (a)–(e) indicates, cationic groups are attached through metal-hydrogen bond interaction in compounds **1a**–**1f**.

Thus the occurrence of a center of symmetry along the metal-hydrogen bond is not possible in this case. Unbalanced supramolecular interactions are relatively lesser than those in compound **1a**. So the dihedral angle (λ) for the complex anion in **1b** is decreased to 32.0°. In the case of compound **1c**, two cation moieties $[C_{11}H_{18}N_4]^{2+}$ are attached to the $[Cu(mnt)_2]^{2-}$ anion by C–H···Cu hydrogen bond from opposite sides (e.g., from top and bottom) of the molecular plane (Figure 2.3c). Similarly two cationic moieties of $[C_{12}H_{20}N_4]^{2+}$ are glued to $[Cu(mnt)_2]^{2-}$ by two C–H···Cu hydrogen bonds from top and bottom of the molecular plane in compound **1d** (Figure 2.4c). Thus the potential of unbalanced supramolecular interactions is considerably reduced and thereby the deviation of the chelate rings in $[Cu(mnt)_2]^{2-}$ is accordingly reduced. This leads to further decrease in deviation angle (26.73°) in complex **1c** in comparison to that in **1a** and **1b**. In the case of compound **1d**, two chelate rings of

$[Cu(mnt)_2]^{2-}$ anion are linked by a common C–H···S interaction (bifurcated hydrogen bonds), thereby restricting the chelate rings considerably from deviation. Therefore the relevant deviation angle is drastically reduced to 19.91° in compound **1d**. For the compound **1e**, the non-covalent C–H···Cu hydrogen bond separation is 2.91 Å, which is too short distance for a huge cation $[C_{13}H_{22}N_4]^{2+}$ to interact with the complex anion $[Cu(mnt)_2]^{2-}$; thus it affects the distortion of the chelate rings to a larger extent resulting in the deviation angle of 37.06° (Figure 2.5c). Finally in compound **1f**, two cationic moieties of $[C_{14}H_{24}N_4]^{2+}$ are hydrogen bonded to $[Cu(mnt)_2]^{2-}$ with C–H···Cu hydrogen bond separation is 2.72 Å. Even though this distance is too short for a huge cation, these two cation moieties $[C_{14}H_{24}N_4]^{2+}$ are glued from opposite sides of the molecular plane maintaining same distance of 2.72 Å leading to the center of symmetry along metal hydrogen bond. In addition, there are balanced C–H···S, C–H···N and Cu···S supramolecular interactions around $[Cu(mnt)_2]^{2-}$ anion. The combination of center of symmetry and balanced supramolecular interactions lead to the perfect square planar arrangement of $[Cu(mnt)_2]^{2-}$ with zero deviation angle.

Based on the above discussion, it can be concluded that un-balanced supramolecular S···H, N···H and Cu···S interactions are observed in compounds **1a-1e**. Bulkiness or occupancy nature of cations increase from compound **1a** to compound **1f**. The flexibility of chelate rings of the $[Cu(mnt)_2]^{2-}$ anion is restricted through surrounding supramolecular interactions. Movement of the chelate ring depends on the number of interactions with surrounding cations in ion-pair compounds. In case of compound **1f**, we observe that there is a centre of symmetry along metal-hydrogen bond and there are equivalent or balanced C–H···S, C–H···N, and Cu···S supramolecular interactions around $[Cu(mnt)_2]^{2-}$ resulting in perfect square planar arrangement of $[Cu(mnt)_2]^{2-}$ in compound **1f**. There is an equivalent force along all the sides of anion $[Cu(mnt)_2]^{2-}$, which implies that there is no more distortion from square planar nature. Diagrammatic representation of the cations which are linked to the anion through the interaction of metal hydrogen bond has been shown in Figure 2.9.

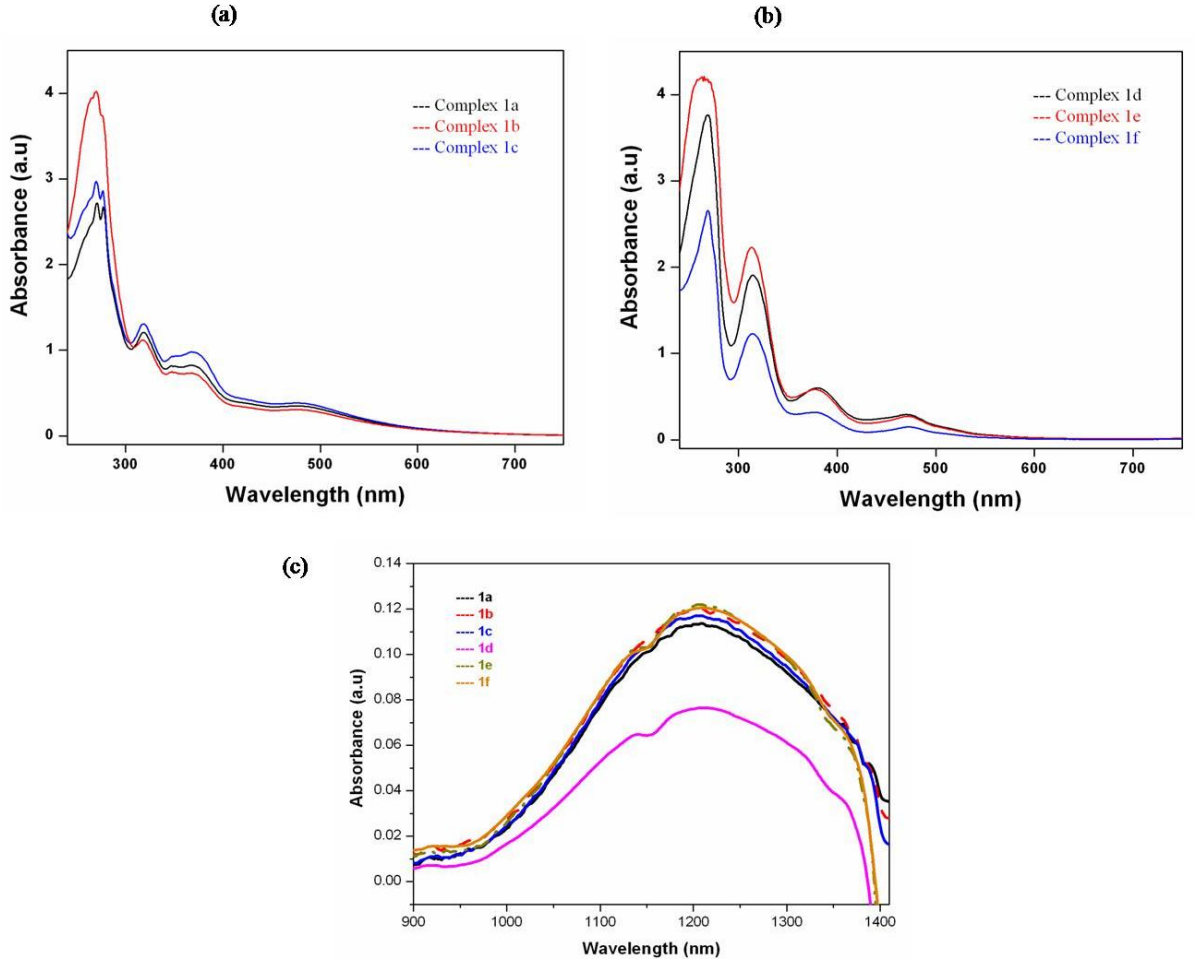


**Figure 2.10**. (a) & (b) are the UV-vis absorption spectra of the compounds **1a**–**1f**, (c) near-IR absorption spectra of the compounds **1a**–**1f**.

## 2.3.4. Spectroscopic and Electronic Characterization

### Electronic Absorption Spectra

Absorption spectra of the title compounds are measured in acetonitrile. For the entire ion-pair compounds **1a-1f**, we have observed five absorption bands in the range of 200-1300 nm, in which there are four intense bands due to allowed transitions. Bands at 270, 370 nm are assigned due to the L → M charge transfer transitions of $[M(mnt)_2]^{2-}$ (M = Cu(1), Ni(2)). Bands at 320 nm and 470 nm can be attributed as L → L* and M → L charge transfer transition respectively, as shown in Figure 2.10 (a) & (b).[24]

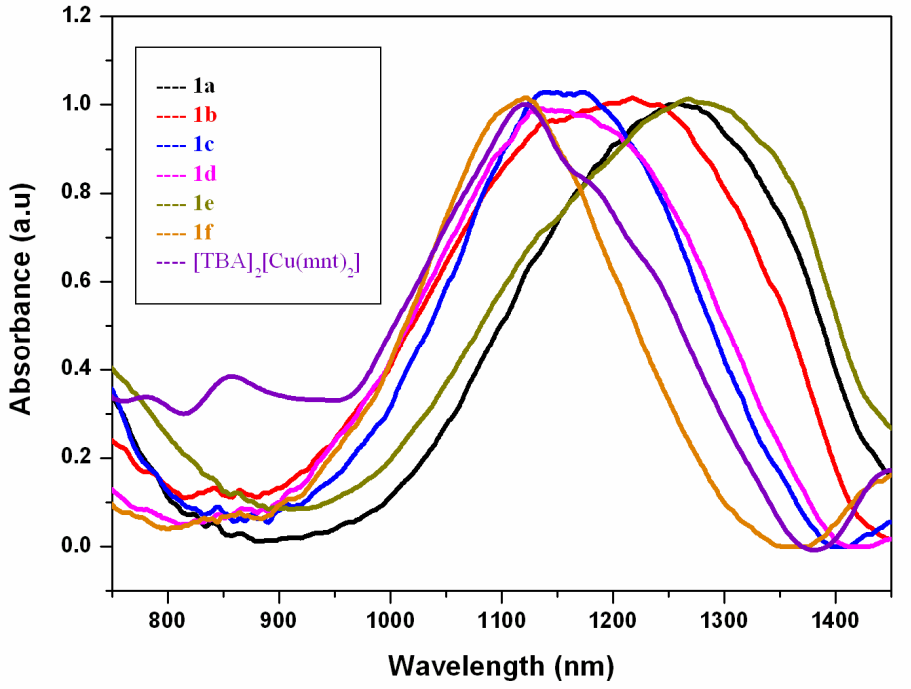


**Figure 2.11.** Diffuse reflectance spectra of complexes **1a-1f** and $[TBA]_2[Cu(mnt)_2]$.

Based on literature[25] copper based dithiolene complex, $[TBA]_2[Cu(mnt)_2]$ shows an absorption band in the near-IR region at 1205 nm ($\varepsilon$ = 70 $M^{-1}$ $cm^{-1}$). In the present study, copper based ion-pair dithiolene compounds **1a-1f** show a moderate absorbance at near-IR region (1210 nm) with a slight variation of molar extinction coefficient ($\varepsilon$ = 76 to 122 $M^{-1}$ $cm^{-1}$), which has been shown in Figure 2.10(c). Absorption spectra, that are characteristic of metal-bis(dithiolene) ion-pair complexes, are generally assigned to $\pi \rightarrow \pi^*$ transition between the highest occupied molecular orbital (HOMO) of the $[Cu(mnt)_2]^{2-}$ anion and lowest unoccupied molecular orbital (LUMO) of the alkyl chain imidazolium cation. In the solution absorption spectra, there is no shifting of the peak position for the complexes **1a-1f**.

In the diffuse reflectance spectra (Figure 2.11), we observe the band in the near-IR region for the all compounds **1a-1f**. Usually square-planar copper complexes show a peak at 1150 nm in the near-IR region. But, from the Figure 2.11, we observe that the peak positions for the complexes **1a-1f** vary within the range 1121 to 1268 nm. This indicates that the copper complexes with more deviation angle exhibit a strong bathochromic shift of the near-IR band compared to the copper complexes with less deviation angle. This shift amounts to 147 nm in the case of dithiolato-complexes from **1a** to **1f**. The deviation angle for the complex **1a** is

more ($\lambda$ = 38.13º) than those for the remaining complexes; thus the peak position for **1a** is 1268 nm. For the remaining complexes **1b** to **1d**, the decrease in deviation angle order is **1b** > **1c** > **1d**, hence the peak position also decreases in the similar manner 1218 > 1163 > 1137 nm, respectively. In the case of complex **1e,** the deviation angle is 37.06º, which is almost identical to that of complex **1a**, so that peak position is shifted accordingly to longer wavelength 1258 nm region. Finally compound **1f** having deviation angle of 0° shows the peak position at 1121 nm, which is comparable to that of the square planar complex $[TBA]_2[Cu(mnt)_2]$ showing peak position at 1120 nm. From this solid state absorption studies, it can be concluded that the energy gap between HOMO of the anion and LUMO of the cation is decreased in the case of complexes with more deviated angles.[5a] The deviation angles in the nickel complexes is very smaller (<5°) when compared to the copper complexes (~38°), hence effect of the distortion angle on the diffuse reflectance spectra of the nickel complexes **2a**–**2f** is very negligible, due to this all the nickel complexes exhibit band at nearly 850 nm, as shown in Figure 2.12.

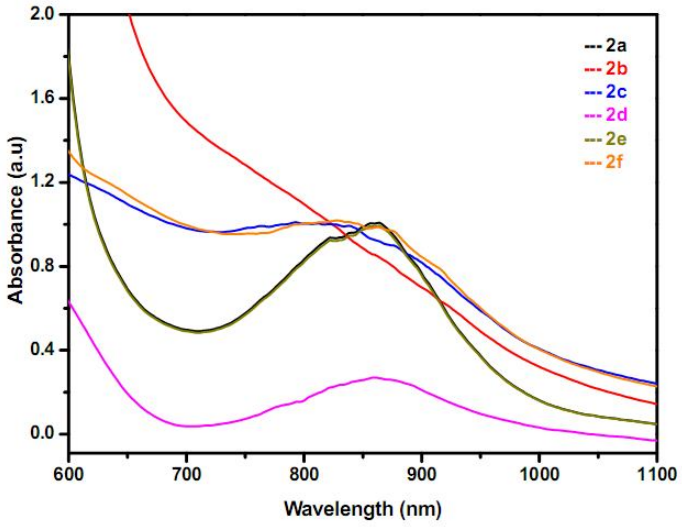


**Figure 2.12**. Diffuse reflectance spectra of complexes **2a-2f**.

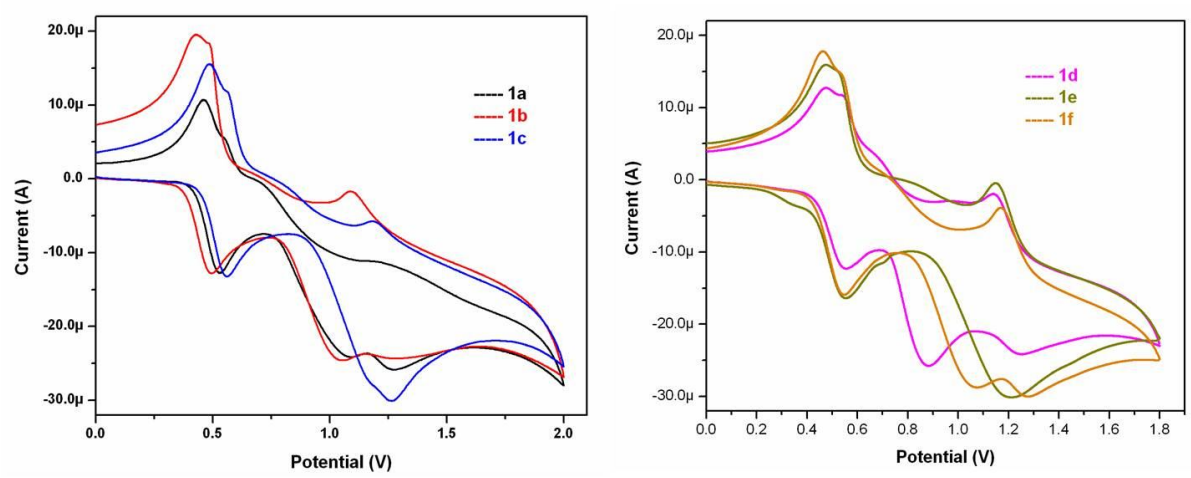


**Figure 2.13.** Cyclic voltammogram of the compounds **1a–1f** in TBAP/Acetonitrile at a scan rate 50 mV $s^{-1}$.

### 2.3.5. Electrochemistry

The electrochemical behavior of the complexes **1a-1f** in acetonitrile solutions have been studied, each containing 0.10 M $[Bu_4N][ClO_4]$ (TBAP) as supporting electrolyte at a platinum working electrode. The cyclic voltammograms of complexes **1a–1f** are shown in Figure 2.13. The cyclic voltammograms of copper compounds **1a–1f**, exhibit an oxidative response. The present electrochemical data can be explained on the basis of Scheme 2.4, proposed by McCleverty, Hoyer, and others.[26] According to this scheme, the first oxidative response for compounds **1a–1f** are ascribed due to the couple $[Cu^{III}(mnt)_2]^{1-}/[Cu^{II}(mnt)_2]^{2-}$. Oxidative responses at $E_{1/2}$ = +0.494, +0.461, +0.522, +0.511, +0.510, +0.504 V *vs* Ag/AgCl are for compounds **1a-1f** respectively. We did not attempt to assign the second oxidative responses for these compounds. We undertook the electrochemical studies of title compounds **1a-1f** to investigate the influence of alkyl imidazolium cation on the red-ox potential of complex anion $[Cu^{II}(mnt)_2]^{2-}$ by comparing present electrochemical data (compound **1a-1f**) with those of $[TBA]_2[Cu(mnt)_2]$. We found that first oxidative responses of compounds **1a-1f** (present study) agrees quite well with that reported for the $[TBA]_2[Cu(mnt)_2]$ complex.[25] This suggests that there is not much effect of alkyl imidazolium cation on the red-ox potential of complex anion $[Cu^{II}(mnt)_2]^{2-}$ in solution state. All the nickel complexes **2a–2f** also shows oxidative response due to the couple $[Ni^{III}(mnt)_2]^{1-}/[Ni^{II}(mnt)_2]^{2-}$. The $E_{1/2}$ of nickel complexes **2a–2f** is 0.50, 0.54, 0.56, 0.56, 0.48, 0.55 V vs Ag/AgCl respectively, as shown in Figure 2.14.

$$\left[ML_2\right] \overset{1^- \ e}{\underset{-e}{\rightleftharpoons}} \left[ML_2\right]^{2-} \overset{e}{\underset{-e}{\rightleftharpoons}} \left[ML_2\right]^{3-}$$

**Scheme 2.4.**

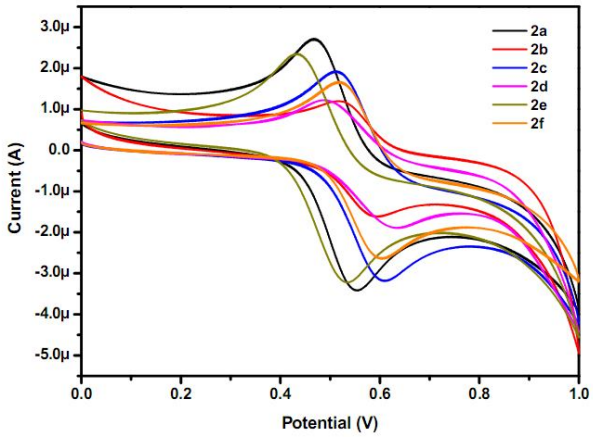


**Figure 2.14.** Cyclic voltammogram of the compounds **2a–2f** in TBAP/Acetonitrile at a scan rate 50 mV $s^{-1}$.

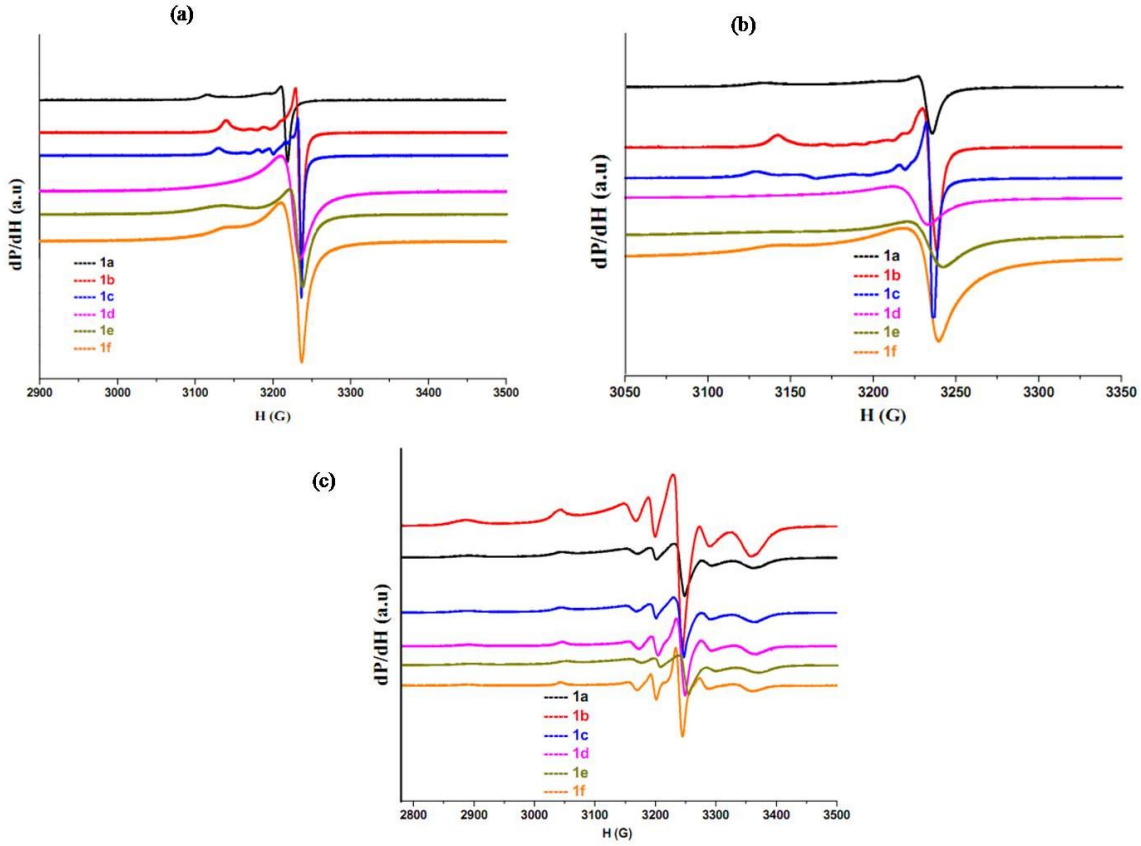


**Figure 2.15**. The EPR spectra of compounds **1a–1f**: (a) solid state at room temperature, (b) solid state at liquid nitrogen temperature, and (c) in DMF (frozen state at liquid nitrogen temperature).

### 2.3.6. ESR Spectroscopy

Figure 2.15 illustrates the representative EPR spectra of complexes **1a–1f** in the solid state both at room temperature (Freq. range is: 9155.559 to 9161.153 MHz, Field range is: 324.00 to 400.00 mT) and liquid nitrogen temperature (Freq. range: 9155.819 to 9162.786 MHz, Field: 324 mT), and frozen state at liquid nitrogen temperature (Freq. range: 9135.349 to 3151.168 MHz, Field: 336 mT). The EPR features are almost identical at both ambient and liquid nitrogen temperature for the solid. The ligand hyperfine structure provides direct information about the nature of the electronic ground state of the complex and the extent to electron spin delocalization over ligand orbitals.[27] We have observed hyperfine splitting in the EPR spectra of compounds **1a-1f** in frozen state at liquid nitrogen temperature as shown in Figure 2.15(c). HOMO level of the $[Cu(mnt)_2]^{2-}$ consists of the $3d_{xy}$ orbital of copper and hybrids of 3s, $3p_x$, and $3p_y$ orbitals of sulfur atoms. These atomic orbitals are mixed with the $p_z$ orbitals of copper and sulfur, and such mixing has a direct effect on the copper hyperfine splitting.[7a,9a,28] The g values ($g_\parallel > g_\perp$) of all these complexes are shown in Table 2.6, that are closed to those ($g_\parallel = 2.090$, $g_\perp = 2.024$ ; and $g_1 = 2.089$, $g_2 = 2.024$, $g_3 = 2.017$) of the non-planar Cu(II)-dithiolene complexes, $[mb]_2[Cu(mnt)_2].Me_2CO$ (mb = methylene blue)[9a] and $[(Ph)_4As]_2[Cu(mnt)_2]$[7a] respectively . These g values are also consistent ($g_\parallel = 2.08$, $g_\perp = 2.02$; $g_\parallel = 2.210$, $g_\perp = 2.018$; $g_\parallel = 2.21$, $g_\perp = 2.04$ and $g_\parallel = 2.095$, $g_\perp = 2.033$) of the planar copper complexes, $[Bu_4N]_2[Cu(mnt)_2]$, $[TBA]_2[Cu(bcd)_2]$ ($bcd^{2-}$ = 1-benzoyl-1-cyanoethylene-2,2-dithiolate), $[Cu(gua)_2].2DMF$ and $[Co(phen)_3][Cu(mnt)_2]$.[29,6g] From these data it can be concluded that there is an unpaired electron in the $d_{x2-y2}$ orbital of copper (II) in the ground state.[30]

### 2.3.7. XRPD

To ensure the phase purity of the products, X-ray powder diffraction data for all the compounds have been recorded. Similar diffraction patterns for the simulated data (calculated from single crystal data) and observed data prove the bulk homogeneity of the crystalline solids, as shown in Figure 2.16. Although the experimental patterns have few unindexed diffraction peaks and some are slightly broadened and shifted in comparison to those simulated from the single-crystal data, it can still be regarded that the bulk as-synthesized materials represent compounds **1a–1f**.

## 2.4. Conclusion

In summary, we have reported twelve new ion-pair compounds **1a**–**1f** and **2a**–**2f** in which the complex anion $[M(mnt)_2]^{2-}$ (M= Cu, Ni) is common but the length of the alkyl chain in cationic moiety is varied. The geometry around the central metal ion mainly depends on the supramolecular interactions with the respective cations in the ion-pair compounds. Distorted square planar and perfect square planar geometries of the metal centers depend on centre of symmetry (*Ci*) along metal-hydrogen bond through anion $[M(mnt)_2]^{2-}$, and balanced/unbalanced S···H, N···H and M···S supramolecular interactions with the cations. The compounds **1a**–**1f**, reported in this article, represent classic examples of ion pair compounds, in which the geometry of the metal ion in the complex anion / distortion from the planarity of the complex anion can be regulated by increasing / decreasing the alkyl chain length in between two imidazolium moieties in the cation. The complexes **1a-1f** show diffuse reflectance spectra, in which, we observe bathochromic shift (total span 147 nm) depending on angle between two SMS planes in the chelate rings of the anion $[Cu(mnt)_2]^{2-}$. We have demonstrated that this shift range depends on geometry around the metal ion of the complex anion in each ion pair compound. More is the dihedral angle in $[Cu(mnt)_2]^{2-}$ (or more is the distortion), more is the red shift in band maxima in their diffuse reflectance spectra (in the solid state). The significance of hydrogen bonding interactions in the solid state can be realized when we perform the solution electronic absorption studies for all compounds **1a-1f**, when we do not observe any shift (red shift) of band maxima. In the case of nickel complexes **2a-2f** there is no much affect of the distortion angle (deviation angles are < 5°) on the diffuse reflectance spectra, hence we observe a peak at ~850 nm. The present study opens a new dimension in solid state coordination chemistry of metal-dithiolene complexes, in which the energy of the solid state electronic absorption of a series of ion pair compounds can be tuned / varied by choosing an appropriate imidazolium cation in the concerned synthesis.

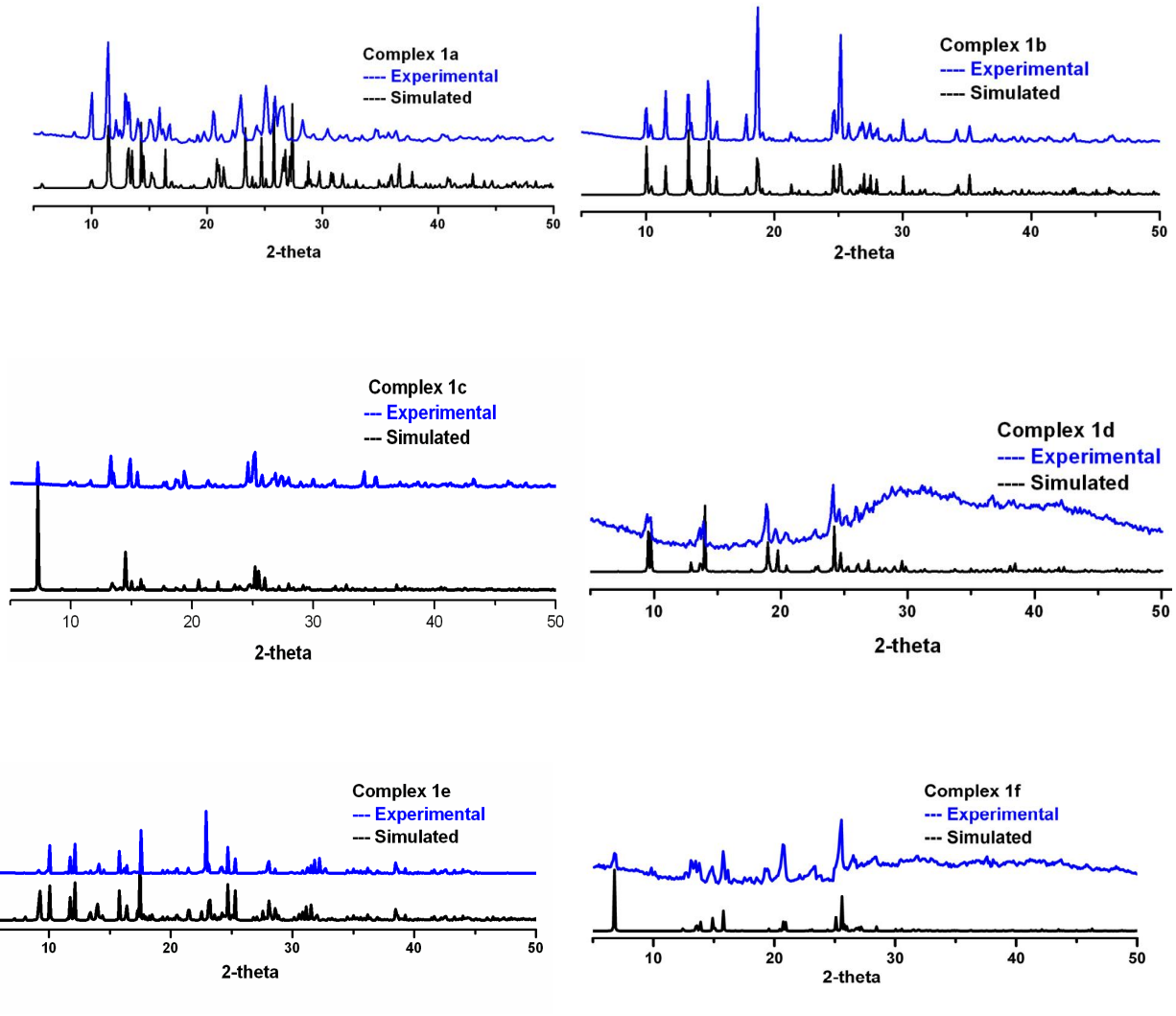


**Figure 2.16.** Powder X-ray patterns of the complexes **1a**-**1f**.

**Table 2.1.** Crystal data and structural refinement parameters for compounds **1a–1f**.

| | **1a** | **1b** | **1c** |
|---|---|---|---|
| Empirical formula | $C_{17}H_{14}N_8S_4Cu$ | $C_{18}H_{16}N_8S_4Cu$ | $C_{19}H_{18}N_8S_4Cu$ |
| Formula weight | 522.14 | 536.17 | 550.19 |
| *T*(K) / $\lambda$(Å) | 298(2), 0.71073 | 298(2), 0.71073 | 298(2), 0.71073 |
| Crystal system | triclinic | monoclinic | monoclinic |
| Space group | *P*–1 | *C2/c* | *P*2(1)*/c* |
| a (Å) | 7.683(7) | 18.232(13) | 12.2099(15) |
| b (Å) | 9.239(8) | 7.228(5) | 7.5015(9) |
| c (Å) | 15.405(14) | 18.838(14) | 26.639(3) |
| α (°) | 90.170(10) | 90.00 | 90.000 |
| β (°) | 91.718(10) | 111.267(11) | 96.688(2) |
| γ (°) | 106.935(10) | 90.00 | 90.000 |
| Volume (Å$^3$) | 1046.29(16) | 2313(3) | 2423.3(5) |
| Z, $\rho_{calcd}$ (g cm$^{-3}$) | 2, 1.637 | 4, 1.539 | 4, 1.508 |
| μ (mm$^{-1}$), *F*(000) | 1.466/530 | 1.328/1092 | 1.270/1124 |
| goodness-of-fit on $F^2$ | 1.049 | 1.088 | 1.050 |
| R1/ wR2 [I > 2σ (I)] | 0.0262 / 0.0680 | 0.0367 / 0.0855 | 0.0741 / 0.1173 |
| R1/ wR2 (all data) | 0.0278/0.0690 | 0.0400/0.0874 | 0.1311/0.1361 |
| Largest diff peak/hole(e Å$^{-3}$) | 0.429/–0.291 | 0.479/–0.176 | 0.378/–0.377 |

| | **1d** | **1e** | **1f** |
|---|---|---|---|
| Empirical formula | $C_{20}H_{20}N_8S_4Cu$ | $C_{21}H_{22}N_8S_4Cu$ | $C_{22}H_{24}N_8S_4Cu$ |
| Formula weight | 564.27 | 578.25 | 592.32 |
| *T*(K)/ $\lambda$(Å) | 298(2), 0.71073 | 298(2), 0.71073 | 298(2), 0.71073 |
| Crystal system | monoclinic | triclinic | triclinic |
| Space group | *P*2(1)*/c* | *P*–1 | *P*–1 |
| a (Å) | 18.1795(12) | 8.9511(5) | 7.1078(10) |
| b (Å) | 7.6567(5) | 11.5301(6) | 7.4995(11) |
| c (Å) | 24.6776(12) | 12.8835(7) | 13.2473(19) |
| α (°) | 90.00 | 104.497(10) | 94.209(2) |
| β (°) | 131.270(3) | 95.597(10) | 97.374(2) |
| γ (°) | 90.00 | 98.225(10) | 107.625(2) |
| Volume (Å$^3$) | 2480.6(3) | 1261.69(12) | 662.71(16) |
| Z, $\rho_{calcd}$ (g cm$^{-3}$) | 4, 1.511 | 2, 1.522 | 1, 1.484 |
| μ (mm$^{-1}$), *F*(000) | 1.243/1156 | 1.224/594 | 1.167/305 |
| goodness-of-fit on $F^2$ | 1.058 | 1.059 | 1.051 |
| R1/ wR2 [I > 2σ (I)] | 0.0398/0.0912 | 0.0244/0.0620 | 0.0410/0.1017 |
| R1/ wR2 (all data) | 0.0472/0.0950 | 0.0252/0.0625 | 0.0458/0.1048 |
| Largest diff peak/hole (e Å$^{-3}$) | 0.311/–0.291 | 0.272/-0.281 | 0.387/ –0.290 |

**Table 2.2.** Supramolecular interaction between hydrogen from the cation to metal from the anion (bond lengths in Å and bond angles in °).

| Compound | D-H···A | d(H···A) | d(D···A) | <(DHA) | Symmetry code |
|---|---|---|---|---|---|
| **1a** | C(17)–H(17C)···Cu1 | 3.14 | 3.943(2) | 140.7 | x, y-1, z |
| **1b** | C(5)–H(5A)···Cu1 | 3.05 | 3.920(4) | 150.9 | x+1, y, z |
| **1c** | C(12)–H(12A)···Cu1 | 2.98 | 3.865(7) | 151.6 | x, y-1, z |
| | C(12)–H(12B)···Cu1 | 3.06 | 3.877(7) | 142.8 | x, y, z |
| **1d** | C(12)–H(12C)···Cu1 | 3.07 | 3.828(3) | 137.2 | x, -y+1.5, z+0.5 |
| | C(20)–H(20C)···Cu1 | 3.11 | 3.708(4) | 121.8 | x, y+1, z+1 |
| **1e** | C(20)–H(20)···Cu1 | 2.91 | 3.395(18) | 112.6 | 1-x, 1-y, 1-z |
| **1f** | C(8)–H(8C)···Cu1 | 2.72 | 3.614(4) | 156.2 | x, y, z |

**Table 2.3**. Geometrical parameters of the C–H···S and C–H···N hydrogen bonds (Å, °) involved in supramolecular networks of compounds **1a–1f**.[a] D=donor; A=acceptor.

| D-H···A | d(D-H) | d(H···A) | d(D···A) | <(DHA) |
|---|---|---|---|---|
| | | **Compound-1a** | | |
| C(16)-H(16)...N(1)#1 | 0.95 | 2.51 | 3.348(3) | 147.6 |
| C(11)-H(11)...N(1)#1 | 0.95 | 2.37 | 3.304(3) | 168.9 |
| C(12)-H(12)...N(2)#1 | 0.95 | 2.34 | 3.177(3) | 147.0 |
| C(13)-H(13A)...N(2)#2 | 0.99 | 2.70 | 3.545(3) | 143.9 |
| C(14)-H(14)...N(4)#3 | 0.95 | 2.49 | 3.114(3) | 123.1 |
| C(14)-H(14)...N(3)#3 | 0.95 | 2.67 | 3.412(3) | 135.2 |
| C(13)-H(13B)...N(3)#3 | 0.99 | 2.70 | 3.413(3) | 129.0 |
| C(17)-H(17A)...S(4)#4 | 0.98 | 2.95 | 3.624(2) | 126.8 |
| C(9)-H(9B)...S(1)#5 | 0.98 | 2.89 | 3.852(2) | 168.8 |
| | | **Compound-1b** | | |
| C(8)-H(8)...N(2)#6 | 0.93 | 2.75 | 3.498(5) | 138.0 |
| C(5)-H(5B)...N(1)#6 | 0.96 | 2.70 | 3.393(5) | 129.3 |
| C(6)-H(6)...N(1)#7 | 0.93 | 2.52 | 3.340(5) | 147.1 |
| C(9)-H(9B)...N(1)#7 | 0.97 | 2.74 | 3.508(5) | 136.1 |
| C(7)-H(7)...S(1)#8 | 0.93 | 2.84 | 3.614(4) | 141.3 |
| C(5)-H(5B)...S(1)#9 | 0.96 | 2.88 | 3.619(5) | 134.6 |

| | | | | |
|---|---|---|---|---|
| | | **Compound-1c** | | |
| C(13)-H(13B)...S(2)#10 | 0.97 | 2.99 | 3.549(6) | 118.0 |
| C(10)-H(10)...S(4)#11 | 0.93 | 2.98 | 3.609(6) | 126.5 |
| C(19)-H(19)...S(1)#11 | 0.93 | 2.93 | 3.828(7) | 164.1 |
| C(17)-H(17A)...N(3)#11 | 0.96 | 2.72 | 3.407(9) | 128.9 |
| C(16)-H(16)...N(3)#11 | 0.93 | 2.53 | 3.263(9) | 135.8 |
| C(9)-H(9)...N(2)#10 | 0.93 | 2.63 | 3.459(9) | 148.7 |
| C(18)-H(18B)...N(4)#12 | 0.96 | 2.61 | 3.395(10) | 138.9 |
| | | **Compound-1d** | | |
| C(12)-H(12A)...N(2)#13 | 0.96 | 2.69 | 3.327(4) | 124.5 |
| C(12)-H(12B)...N(1)#13 | 0.96 | 2.57 | 3.298(4) | 132.9 |
| C(12)-H(12A)...S(2)#14 | 0.96 | 2.87 | 3.645(4) | 139.0 |
| C(11)-H(11)...S(4)#15 | 0.93 | 3.00 | 3.631(3) | 126.7 |
| C(11)-H(11)...S(2)#15 | 0.93 | 2.95 | 3.751(3) | 144.9 |
| C(9)-H(9)...N(3)#16 | 0.93 | 2.38 | 3.213(4) | 149.0 |
| C(13)-H(13A)...N(1)#17 | 0.97 | 2.50 | 3.373(4) | 149.2 |
| C(15)-H(15B)...N(1)#17 | 0.97 | 2.80 | 3.645(4) | 146.3 |
| C(17)-H(17)...N(2)#15 | 0.93 | 2.48 | 3.303(4) | 147.1 |
| C(16)-H(16B)...N(4)#18 | 0.97 | 2.52 | 3.482(5) | 170.5 |
| C(20)-H(20B)...N(4)#1 | 0.96 | 2.64 | 3.412(4) | 137.3 |
| | | **Compoun-1e** | | |
| C(21)-H(21C)...S(1)#19 | 0.98 | 2.70 | 3.5550(19) | 146.1 |
| C(19)-H(19)...N(4)#20 | 0.95 | 2.60 | 3.416(2) | 143.6 |
| C(20)-H(20)...N(2)#2 | 0.95 | 2.65 | 3.242(2) | 121.1 |
| C(20)-H(20)...S(2)#15 | 0.95 | 2.75 | 3.6352(18) | 155.4 |
| C(18)-H(18)...S(1)#9 | 0.95 | 2.77 | 3.661(2) | 156.3 |
| C(15)-H(15B)...S(3)#9 | 0.99 | 2.97 | 3.9456(19) | 166.9 |
| C(12)-H(12)...N(3)#9 | 0.95 | 2.50 | 3.350(2) | 149.3 |
| C(11)-H(11)...N(4)#11 | 0.95 | 2.46 | 3.234(2) | 138.4 |
| C(9)-H(9B)...N(1)#15 | 0.98 | 2.70 | 3.431(3) | 131.8 |
| C(14)-H(14A)...S(4)#2 | 0.99 | 2.91 | 3.624(2) | 130.1 |
| | | **Compound-1f** | | |
| C(6)-H(6)...S(2)#2 | 0.93 | 2.84 | 3.659(3) | 147.5 |
| C(7)-H(7)...N(2)#11 | 0.93 | 2.57 | 3.411(4) | 151.4 |
| C(5)-H(5)...N(1)#4 | 0.93 | 2.45 | 3.367(4) | 168.5 |

[a]Symmetry transformations used to generate equivalent atoms
#1 -x,-y+1,-z+1 #2 x+1,y,z #3 -x+1,-y+2,-z+2 #4 x-1,y-1,z #5 -x+1,-y+2,-z+1
#6 -x+3/2,y+1/2,-z+1/2 #7 x+1/2,y+1/2,z #8 -x+1,-y+1,-z #9 x+1,y+1,z
#10 -x,y-1/2,-z+1/2 #11 -x,-y+1,-z #12 -x-1,-y+1,-z #13 -x+1,y+1/2,-z+1/2
#14 x,-y+1/2,z+1/2 #15 -x+1,-y+1,-z+1 #16 -x,y+1/2,-z+1/2 #17 x,y,z+1
#18 x,-y+3/2,z+1/2 #19 -x+2,-y+1,-z+1 #20 x+2,y+1,z+1

**Table 2.4.** Crystal data and structural refinement parameters for compounds **2a–2e**.

| | **2a** | **2b** | **2c** |
|---|---|---|---|
| Empirical formula | $C_{19}H_{17}N_9S_4Ni$ | $C_{18}H_{16}N_8S_4Ni$ | $C_{19}H_{18}N_8S_4Ni$ |
| Formula weight | 558.37 | 531.36 | 545.36 |
| $T$(K) / $\lambda$(Å) | 298(2), 0.71073 | 298(2), 0.71073 | 298(2), 0.71073 |
| Crystal system | monoclinic | triclinic | monoclinic |
| Space group | *P*2(1)*/c* | *P*-1 | *P*2(1)*/c* |
| a (Å) | 6.908(5) | 7.284(16) | 9.193(7) |
| b (Å) | 18.176(12) | 9.374(2) | 11.868(9) |
| c (Å) | 19.715(13) | 9.580(2) | 22.330(17) |
| α (°) | 90.00 | 106.632(3) | 90.000 |
| β (°) | 96.880(10) | 109.505(3) | 101.113(10) |
| γ (°) | 90.00 | 98.045(3) | 90.000 |
| Volume (Å$^3$) | 2457.8(3) | 57.04(2) | 2391.0(3) |
| Z, $\rho_{calcd}$ (g cm$^{-3}$) | 4, 1.509 | 1, 1.547 | 4, 1.515 |
| μ (mm$^{-1}$), *F*(000) | 1.156/1144 | 1.240/272 | 1.185/1120 |
| goodness-of-fit on $F^2$ | 1.128 | 1.368 | 1.071 |
| R1/ wR2 [I > 2σ (I)] | 0.0425 / 0.0888 | 0.0846 / 0.1792 | 0.0466 / 0.1090 |
| R1/ wR2 (all data) | 0.0525/0.0929 | 0.0908/0.1819 | 0.0579/0.1154 |
| Largest diff peak/hole(e Å$^{-3}$) | 0.525/–0.303 | 0.971/–0.427 | 0.503/–0.320 |

| | **2d** | **2e** |
|---|---|---|
| Empirical formula | $C_{20}H_{20}N_8S_4Ni$ | $C_{21}H_{22}N_8S_4Ni$ |
| Formula weight | 559.41 | 573.42 |
| $T$(K)/ $\lambda$(Å) | 298(2), 0.71073 | 298(2), 0.71073 |
| Crystal system | triclinic | monoclinic |
| Space group | *P*-1 | *C2/c* |
| a (Å) | 7.408(15) | 19.069(4) |
| b (Å) | 9.595(2) | 7.327(15) |
| c (Å) | 9.624(2) | 18.085(4) |
| α (°) | 89.718(3) | 90.00 |
| β (°) | 69.364(3) | 91.726(3) |
| γ (°) | 75.416(3) | 90.00 |
| Volume (Å$^3$) | 616.9(2) | 2525.7(9) |
| Z, $\rho_{calcd}$ (g cm$^{-3}$) | 1, 1.506 | 4, 1.508 |
| μ (mm$^{-1}$), *F*(000) | 1.150/288 | 1.126/1184 |
| goodness-of-fit on $F^2$ | 0.990 | 1.063 |
| R1/ wR2 [I > 2σ (I)] | 0.0587/0.1128 | 0.0364/0.0969 |
| R1/ wR2 (all data) | 0.0961/0.1254 | 0.0377/0.0982 |
| Largest diff peak/hole (e Å$^{-3}$) | 0.491/–0.276 | 0.373/-0.456 |

**Table 2.5**. Geometrical parameters of the C–H···S and C–H···N hydrogen bonds (Å, °) involved in supramolecular networks of compounds **2a–2e**.[a] D=donor; A=acceptor.

| D-H···A | d(D-H) | d(H···A) | d(D···A) | <(DHA) |
|---|---|---|---|---|
| | | **Compound-2a** | | |
| C(9)-H(9A)...Ni(1) | 1.05(7) | 3.41(6) | 3.885(4) | 110(4) |
| C(13)-H(13B)...S(4)#1 | 0.97 | 2.75 | 3.545(3) | 140.1 |
| C(11)-H(11)...N(3)#2 | 0.93 | 2.60 | 3.415(4) | 146.7 |
| C(14)-H(14)...N(3)#2 | 0.93 | 2.66 | 3.443(4) | 142.8 |
| C(12)-H(12)...N(2)#3 | 0.93 | 2.33 | 3.227(4) | 162.7 |
| C(16)-H(16)...N(2)#3 | 0.93 | 2.77 | 3.551(4) | 142.4 |
| C(16)-H(16)...N(1)#3 | 0.93 | 2.77 | 3.427(4) | 128.5 |
| C(17)-H(17B)...N(3)#4 | 0.96 | 2.62 | 3.516(4) | 156.0 |
| C(15)-H(15)...N(9)#5 | 0.93 | 2.70 | 3.454(5) | 138.9 |
| C(15)-H(15)...N(9)#6 | 0.93 | 2.73 | 3.390(4) | 128.6 |
| | | **Compound-2b** | | |
| C(9)-H(9B)...N(2)#7 | 0.97 | 2.77 | 3.549(12) | 137.5 |
| C(6)-H(6)...N(2)#7 | 0.93 | 2.49 | 3.316(11) | 148.4 |
| C(5)-H(5B)...N(1)#8 | 0.96 | 2.77 | 3.520(12) | 135.1 |
| C(7)-H(7)...S(2)#9 | 0.93 | 2.81 | 3.556(9) | 137.5 |
| C(5)-H(5C)...Ni(1) | 0.96 | 3.47 | 4.388(9) | 160.5 |
| | | **Compound-2c** | | |
| C(1)-H(1)...Ni(1)#10 | 0.93 | 3.06 | 3.516(3) | 111.8 |
| C(12)-H(12B)...Ni(1)#6 | 0.97 | 3.11 | 4.034(3) | 159.6 |
| C(16)-H(16)...N(8)#4 | 0.93 | 2.71 | 3.413(5) | 132.8 |
| C(1)-H(1)...S(3)#1 | 0.93 | 2.96 | 3.649(3) | 132.1 |
| C(11)-H(11A)...N(6)#1 | 0.97 | 2.72 | 3.388(5) | 126.3 |
| C(18)-H(18)...N(8)#10 | 0.93 | 2.78 | 3.690(5) | 166.2 |
| C(17)-H(17)...S(4)#6 | 0.93 | 2.93 | 3.782(4) | 153.3 |
| C(13)-H(13)...N(5)#3 | 0.93 | 2.59 | 3.400(5) | 145.9 |
| | | **Compound-2d** | | |
| C(13)-H(13A)...Ni(1)#11 | 0.96 | 3.11 | 3.885(5) | 139.5 |
| C(15)-H(15)...S(2)#7 | 0.93 | 2.77 | 3.681(5) | 166.1 |
| C(16)-H(16A)...N(5)#12 | 0.97 | 2.73 | 3.616(7) | 151.3 |
| C(6)-H(6)...N(6) | 0.93 | 2.56 | 3.285(7) | 135.2 |
| C(13)-H(13C)...S(2)#13 | 0.96 | 2.82 | 3.737(6) | 159.9 |
| | | **Compoun-2e** | | |
| C(5)-H(5)...Ni(1)#14 | 0.95 | 3.14 | 3.834(2) | 131.6 |
| C(8)-H(8B)...N(1)#15 | 0.99 | 2.69 | 3.321(3) | 121.8 |
| C(6)-H(6)...S(2)#16 | 0.95 | 2.89 | 3.729(3) | 147.3 |
| C(10)-H(10A)...S(3)#17 | 0.98 | 2.91 | 3.772(2) | 147.4 |
| C(11)-H(11)...N(2) | 0.95 | 2.63 | 3.367(3) | 134.4 |
| C(10)-H(10B)...N(2) | 0.98 | 2.71 | 3.414(3) | 129.3 |

[a]Symmetry transformations used to generate equivalent atoms:
#1 x-1,y,z #2 -x+1,y-1/2,-z+3/2 #3 -x+1,y+1/2,-z+3/2 #4 x,-y+3/2,z+1/2 #5 x+1,y,z+1 #6 -x+1,-y+1,-z+1 #7 -x+1,-y,-z+1 #8 x,y,z-1 #9 x+1,y+1,z #10 -x,-y+1,-z+1
#11 x,y,z+1 #12 x+1,y-1,z #13 x-1,y,z+1 #14 -x+1/2,y+1/2,-z+1/2
#15 -x+1/2,-y+1/2,-z+1 #16 -x+1,y,-z+1/2 #17 -x+1/2,y-1/2,-z+1/2

**Table 2.6.** EPR data of the complexes **1a-1f.**

| Name of Compound | Ambient Temp. | | Liq. Nitrogen Temp. | |
|---|---|---|---|---|
| | $g_{\parallel}$ | $g_{\perp}$ | $g_{\parallel}$ | $g_{\perp}$ |
| 1a | 2.100 | 2.034 | 2.088 | 2.025 |
| 1b | 2.083 | 2.023 | 2.082 | 2.023 |
| 1c | 2.091 | 2.024 | 2.091 | 2.022 |
| 1d | – | 2.030 | – | 2.030 |
| 1e | 2.088 | 2.026 | 2.089 | 2.026 |
| 1f | 2.084 | 2.028 | 2.083 | 2.025 |

## 2.5. References

(1) (a) McCleverty, J. A. *Prog. Inorg. Chem.* **1968**, *10*, 49. (b) Coucouvanis, D. *Prog. Inorg. Chem.* **1970**, *11*, 233. (c) Eisenberg, R. *Prog. Inorg. Chem.* **1971**, *12*, 295. (d) Alcacer, L.; Novais in *Extended Linear Chain Compounds* (Ed.: Miller, J. S), Plenum Press, New York, 1983, Vol. 3, ch. 6, p. 319. (e) Alvarez, S.; Ramon, V.; Hoffman, R. *J.Am. Chem. Soc.* **1985**, *107*, 6253. (f) *Progess in Inorganic Chemistry*, vol. 52, *Dithiolene Chemistry*: *Synthesis Properties, and Applications* (Eds.: Karlin, K. D.; Tiefel, E. I), John Wiley & Sons, New York, 2004.

(2) (a) Belo, D.; Almeida, M. *Coord. Chem. Rev.* **2010**, *254*, 1479. (b) Clemenson, P. I. *Coord. Chem. Rev.* **1990**, *106*, 171. (c) Pullen, A. E.; Olk, R.-M. *Coord. Chem. Rev.* **1999**, *188*, 211. (d) Underhill, A. E.; Ahmad, M. M. *J. Chem. Soc., Chem. Commun.* **1981**, 67. (e) Kobayashi, A.; Sasaki, Y.; Kobayashi, H.; Underhill, A. E.; Ahmad, M. M. *J. Chem. Soc., Chem. Commun.* **1982**, 390. (f) Coomber, A. T.; Beljonne, D.; Friend, R. H.; Bredas, J. L.; Charlton, A.; Robertson, N.; Underhill, A. E.; Kurmoo, M.; Day, P. *Nature* **1996**, *380*, 144. (g) Bonneval, B. G.-D.; Ching, K. I. M.-C.; Alary, F.; Bui, T.-T.; Valade, L. *Coord. Chem. Rev.* **2010**, *254*, 1457.

(3) (a) Robertson, N.; Cronin, L. *Coord. Chem. Rev.* **2002**, *227*, 93. (b) Siedle, A. R.; Candela, G. A.; Finnegan, T. F.; Van DuynE, R. P.; Cape, T.; Kokoszka, G. F.; Woyciejes, P. M.; Hashmall, J. A. *Inorg. Chem.* **1981**, *20*, 2635. (c) Ahmad, M. M.; Turner, D. J.; Underhill, A. E.; Jacobsen, C. S.; Mortensen, K.; Carneiro, K. *Phys. Rev. B* **1984**, *29*, 4796. (d) Belo, D.; Figueira, M. J.; Santos, I. C.; Gama, V.; Pereira, L. C.; Henriques, R. T.; Almeida, M. *Polyhedron* **2005**, *24*, 2035. (e) Pullen, A. E.; Faulmann, C.; Pokhodnya, K. I.; Cassoux, P.; Tokumota, M. *Inorg. Chem.* **1998**, *37*, 6714.

(4) (a) Staniland, S. S.; Fujita, W.; Umezone, Y.; Awaga, K.; Camp, P. J.; Clark, S. J.; Robertson, N. *Inorg. Chem.* **2005**, *44*, 546. (b) Ren, X.; Meng, Q.; Song, Y.; Hu, C.; Lu, C.; Chen, X.; Xue, Z. *Inorg. Chem.* **2002**, *41*, 5931. (c) Ni, C.; Tian, Z.; Ni, Z.; Dang, D.; Li, Y.; Song, Y.; Meng, Q. *Inorg. Chim. Acta* **2006**, *359*, 3927. (d) Robertson, N.; Bergemann, C.; Becher, H.; Agarwal, P.; Julian, S. R.; Friend, R. H.; Hatton, N. J.; Underhill, A. E.; Kobayashi, A. *J. Mater. Chem.* **1999**, *9*, 1713. (e)

Nishijo, J.; Ogura, E.; Yamaura, J.; Miyazaki, A.; Enoki, T.; Takano, T.; Kuwatani, Y.; Iyoda, M. *Synth. Met.* **2003**, *133-134*, 539. (f) Muller-Westerhoff, U. T.; Vance, B.; Yoon, D. I. *Tetrahedron* **1991**, *47*, 909. (g) Kato, R. *Chem. Rev*. **2004**, *104*, 5319.

(5) (a) Yao, B.-Q.; Sun, J.-S.; Tian, Z.-F.; Ren, X.-M.; Gu, D.-W.; Shen, L.-J.; Xie, J. *Polyhedron* **2008**, *27*, 2833. (b) Bigoli, F.; Cassoux, P.; Deplano, P.; Mercuri, M. L.; Pellinghelli, M. A.; Pintus, G.; Serpe, A.; Trogu, E. F. *J. Chem. Soc., Dalton Trans*. **2000**, 4639. (c) Bremi, J.; D'Agostino, E.; Gramlich, V.; Caseri, W.; Smith, P. *Inorg. Chim. Acta* **2002**, *335*, 15.

(6) (a) Gao, X.-K.; Dou, J.-M.; Li, D.-C.; Dong, F.-Y.; Wang. *J. Chem. Cryst*. **2005**, *35*, 345. (b) Ni, C.; Zheng, Y.; Yang, L.; Li, Y. *J. Coord. Chem*. **2006**, *59*, 1037. (c) YunXia, S.; LiLi, W.; Huan, Z.; QingJin, M. *Sci. China Ser. B-Chem.* **2007**, *50*, 607. (d) Ren, X.; Ma, J.; Lu, C.; Yang, S.; Meng, Q.; Wu, P. *Dalton Trans*. **2003**, 1345. (e) Dang, D.; Ni, C.; Ni, Z.; Li, Y.; Meng, Q.; Yao, Y. *J. Coord. Chem*. **2005**, 58, 195. (f) Ren, X. M.; Okudera, H.; Xie, J. L.; Meng, Q. J. *J. Mol. Str*. **2005**, *733*, 119. (g) Singh, N.; Singh, V. K. *International J. Inorg. Mater*. **2000**, *2*, 167.

(7) (a) Stach, J.; Kirmse, R.l Sieler, J.; Abram, U.; Dietzsch, W.; Bottcher, R.; Hansen, L. K.; Vergoossen, H.; Gribnau, M.; Keijzers, C. P. *Inorg. Chem.* **1986**, *25*, 1369. (b) Bereman, R. D.; Lu, H. *Inorg. Chim. Acta* **1993**, *204*, 53. (c) Hoyer, E.; Dietzxch, W.; Schroth, W. *Z. Chem.* **1971**, *11*, 41. (d) Coucouvanis, D.; Holah, D. G.; Hollander, F. J. *Inorg. Chem.* **1975**, *14*, 2657. (e) Burns, R. P.; McAuliffe, C. A. *Adv. Inorg. Chem. Radiochem.* **1979**, *22*, 303. (f) Maki, A. H.; Edelstein, N.; Davison, A.; Holm, R. H. *J. Am. Chem. Soc*. **1964**, *86*, 4580. (g) Kirmse, R.; Stach, J.; Dietzsch, W.; Steimecke, G.; Hoyer, E. *Inorg. Chem*. **1980**, *19*, 2679.

(8) (a) Venkatalakshmi, N.; Varghese, B.; Lalitha, S.; Williams, R. F. X.; Manoharan, P. T. *J. Am. Chem. Soc*. **1989**, *111*, 5748. (b) Ren, X. M.; Ni, Z. P.; Noto, S.; Akutagawa, T.; Nishihara, S.; Nakamura, T.; Sui, Y. X.; Song, Y. *Cryst. Growth Des*. **2006**, *6*, 2530. (c) Kishore, R.; Tripuramallu, B. K.; Durgaprasad, G.; Das, S. K. *J. Mol. Str*. **2011**, *990*, 37. (d) Belo, D.; Figueira, M. J.; Santos, I. C.; Gama, V.; Pereira, L. C.; Henriques, R. T.; Almeida, M. *Polyhedron* **2005**, *24*, 2035.

(9) (a) Snaathorst, D.; Doesburg, H. M.; Perenboom, J. A. A. J.; Keijzers, C. P. *Inorg. Chem.* **1981**, *20*, 2526. (b) Lundquist, O.; Anderson, L.; Sieler, J.; Steimeeke, G.; Hoyer, E. *Acta Chem. Scand., Ser. A* **1982**, *36*, 855. (c) Hunter, C.; Weakly, T. J. R. *J. Chem. Soc., Dalton Trans.* **1983**, 1067. (d) Mahadevan, C.; Seshasayee, M. *J. Crystallogr. Spectrosc. Res.* **1984**, *14*, 215.

(10) Huertas, S.; Hissler, M.; McGarrach, J. E.; Lachicotte, R. J.; E. *Inorg. Chem.* **2001**, *40*, 1183.

(11) Maganas, D.; Grigoropoulos, A.; Staniland, S. S.; Chatziefthimiou, S. D.; Harrison, A.; Robertson, N.; Kyritsis, P.; Neese, F. *Inorg. Chem.* **2010**, *49*, 5079.

(12) (a) Martin, E. M.; Bereman, R. D.; Singh, P. *Inorg. Chem.* **1991**, *30*, 957. (b) Bu, X.-H.; Chen, W.; Lu, S.-L.; Zhang, R.-H.; Liao, D.-Z.; Bu, W.-M.; Shionoya, M.; Brisse, F.; Ribas, J. *Angew. Chem. Int. Ed*. **2001**, *40*, 3201. (c) Bu, X.-H.; Chen, W.; Hou, W.-F.; Du, M.; Zhang, R.-H.; Brisse, F. *Inorg. Chem*. **2002**, *41*, 3477. (d) Goodgame, D. M. L.; Grachvogel, D. A.; Hussain, I.; White, A. J. P.; Williams, D. J. *Inorg. Chem*. **1999**, *38*, 2057.

(13) Arion, V. B.; Rapta, P.; Telser, J.; Shova, S. S.; Breza, M.; Luspai, K.; Kozisek, J.; *Inorg. Chem*. **2011**, *50*, 2918.

(14) (a) Moigne, C. L.; Picaud, T.; Boussac, A.; Loock, B.; Momenteau, M.; Desbois, A. *Inorg. Chem*. **2003**, *42*, 6081. (b) Collins, D. M.; Countryman, R.; Hoard, J. L. *J. Am. Chem. Soc*. **1972**, *94*, 2066. (c) Little, R. G.; Dymock, K. R.; Ibers, J. A. *J. Am. Chem. Soc*. **1975**, *97*, 4532. (d) Ogura, H.; Yatsunyk, L.; Medforth, C. J.; Smith, K. M.; Barkigia, K. M.; Renner, M. W.; Melamed, D.; Walker, F. A. *J. Am. Chem. Soc*. **2001**, *123*, 6564.

(15) (a) Song, X.-Z.; Jentzen, W.; Jia, S.-L.; Jaquinod, L.; Nurco, D. J.; Medforth, C. J.; Smith, K. M.; Shelnutt, J. A. *J. Am. Chem. Soc*. **1996**, *118*, 12975. (b) Haddad, R. E.; Gazeau, S.; Pecaut, J.; Marchon, J.-C.; Medforth, C. J.; Shelnutt, J. A. *J. Am. Chem. Soc*. **2003**, *125*, 1253.

(16) (a) White, D. J.; Cronin, L.; Parsons, S.; Robertson, N.; Tasker, P. A.; Bisson, A. P. *Chem. Commun*. **1999**, 1107. (b) McMaster, J.; Beddoes, R. L.; Collison, D.;

Eardley, D. R.; Helliwell, M.; Garner, C. D. *Chem.-Eur. J.* **1996**, *2*, 685-693. (c) Braga, D.; Grepioni, F. *J. Chem. Soc.; Dalton Trans*. **1999**, 1.

(17) (a) Huynh, H. V.; Han, Y.; Ho, J. H. H.; Tan, G. K. *Organometallics* **2006**, *25*, 3267. (b) Braga, D.; Grepioni, F.; Tedesco, E.; Biradha, K.; Desiraju, G. R. *Organometallics* **1997**, *16*, 1846. (c) Zhang, Y.; Lewis, J. C.; Bergman, R. G.; Ellman, J. A.; Oldfield, E. *Organometallics* **2006**, *25*, 3515. (c) Crabtree, R. H.; Eisenstein O.; Sini, G.; Peris, E. *J. Organomet. Chem.* **1998**, *567*, 7.

(18) (a) Schiavo, S. L.; Nicolo, F.; Scopelliti, R.; Tresoldi, G.; Piraino, P. *Inorg. Chim. Acta* **2000**, *304*, 108. (b) Dehand, J.; Fisher, J.; Pfeffer, M.; Mitschler, A.; Zinsius, M. *Inorg. Chem*. **1976**, *15*, 2675. (c) Brammer, L.; Charnock. J. M.; Goggin, P. L.; Goodfellow, R. J.; OPrpen, A. G.; Koetzle, T. F. *J. Chem. Soc.; Dalton Trans*. **1991**, 1789. (d) Pei, W.-B.; Liu, J.-L.; Wu, J.-S.; Ren, X.-M.; Gu, D.-W.; Shen, L.-J.; Meng, Q.-J. *J. Mol. Str*. **2009**, *918*, 160.

(19) Chang, J.-C.; Ho, W.-Y.; Sun, I.-W.; Chou, Y.-K.; Hsieh, H.-H.; Wu, T.-Y. *Polyhedron* **2011**, *30*, 497.

(20) Locke, J.; McCleverty, J. A. *Inorg. Chem*. **1966**, *5*, 1157.

(21) (a) *SAINT: Software for the CCD Detector System*; Bruker Analytical X-ray Systems, Inc.: Madison, WI, **1998** (b) *SADABS: Program for Absorption Correction;* G. M. Sheldrick University of Gottingen: Gottingen, Germany, **1997**. (c) *SHELXS-97: Program for Structure Solution;* G. M. Sheldrick, University of Gottingen: Gottingen, Germany, **1997**. (d) *SHELXL-97: Program for Crystal Structure Analysis;* G. M. Sheldrick University of Gottingen: Gottingen, Germany, **1997**.

(22) (a) Zhou, H.; Wen, L. L.; Ren, X. M.; Meng, Q. J. *J. Mol. Str*. **2006**, *787*, 31. (b) Dang, D.; Bai, Y.; Wen, L.; Tian, Z.; Li, Y.; Meng, Q. *J. Mol. Str*. **2005**, *753*, 99. (c) Dang, D.; Ni, C.; Bai, Y.; Tian, Z.; Wen, L.; Meng, Q.; Gao, S. *J. Mol. Str*. **2005**, *743*, 197.

(23) (a) Huang, Q.; Lin, J.-H.; Liang, L.-B.; Chen, X.; Zuo, H.-R.; Zhou, J.-R.; Yang, L.-M.; Ni, C.-L.; Hu, X.-L. *Inorg. Chim. Acta* **2010**, *363*, 2546. (b) Kiani, S.; Long, J. R.; Stavropoulos, P. *Inorg. Chim. Acta* **1997**, *263*, 357.

(24) (a) Shupack, S. I.; Billig, E.; Clark, R. J. H.; Williams, R.; Gray, H. B. *J. Am. Chem. Soc*. **1964**, *86*, 4594. (b) Schrauzer, G. N.; Mayweg, V. P. *J. Am Chem. Soc*. **1965**, *87*, 3585.

(25) Madhu, V.; Das, S. K. *Polyhedron* **2004**, *23*, 1235.

(26) (a) Dietzsch, W.; Lerchner, J.; Reinhold, J.; Stach, J.; Kirmse, R.; Stimecke, G.; Hoyer, E. *J. Inorg. Nucl. Chem*. **1980**, *42*, 509. (b) Persaud, L.; Langford, C. H. *Inorg. Chem*. **1985**, *24*, 3562. (b) Mines, T. E.; Geiger, W. E. *Inorg. Chem*. **1973**, *12*, 1189.

(27) Schmitt, R. D.; Maki, A. H. *J. Am. Chem. Soc*. **1968**, *90*, 2288.

(28) (a) Kirmse, R.; Dietzsch, W.; Stach, J.; Golic, L.; Bottcher, R.; Brunner, W.; Gribnau, M. C. M.; Keijzers, C. P. *Mol. Phys.* **1986**, *57*, 1139. (b) Reijerse, E. J.; Thiers, A. H.; Kanters, R.; Gribnau, M. C. M.; Keijzers, C. P. *Inorg. Chem*. **1987**, *26*, 2764.

(29) (a) Bilig, E.; Williams, R.; Bernal, I.; Waters, J. H.; Gray, H. B. *Inorg. Chem*. **1964**, *3*, 663. (b) Singh, N.; Prasad, A.; Gupta, S. *Transition Met. Chem.* **2005**, *30*, 383. (c) Tomas, A.; Viossat, B.; Charlot, M.-F.; Girerd, J.-J.; Huy, D. N. *Inorg. Chim. Acta* **2005**, *358*, 3253.

(30) Hathway, B. J.; Wilkinson, G.; Gillard, R. D.; McCleverty, J. A. (Eds), *Comprehensive Coordination Chemistry, Pergamon Press, Oxford England*, **1987**, *5*, 533.

# Synthesis, Crystal Structure and Properties of Ion-Pair Charge Transfer Complexes: Conformational Change in Organic Cation Receptor Through Supramolecular Interactions

3 Chapter

**Abstract:–** A series of new ion-pair complexes $[Bz,R\text{-}BzBimy]_2[M(mnt)_2]$ {$[Bz,R\text{-}BzBimy]^+$ = 1-benzyl-3-(4-R-benzyl)benzimidazolium; M = Cu, R = H (**1a**), $NO_2$ (**1b**) and Br (**1c**); M = Ni, R = H (**2a**), $NO_2$ (**2b**) and Br (**2c**) and $mnt^{2-}$ = maleonitriledithiolate} have been prepared and characterized by single crystal X-ray structure analyses. Due to flexible nature of aryl groups (–$CH_2$–Ar) in benzimidazolium cations (**a** and **b**), the conformational change of aryl groups have been observed in its corresponding metal based dithiolene ion-pair complexes **1a**, **1b** and **2a**, **2b**. We do not observe any change or phenyl groups orientation/conformation change in the organic receptor compound **c** and in metal complex **1c**, **2c**, because in these complexes there are C–H···π and π···π stacking interactions, that are the responsible to control the phenyl groups orientation. Supramolecular interactions (such as S···H, N···H, O···H, Br···Br and N···Br etc.) are accountable for the change in orientation (conformational change) of aryl groups in organic receptor compounds (benzimidazolium salts with tetrafluoroborate) as well as in ion-pair dithiolene complexes. The substituents (H, $NO_2$ and Br), which are present at the *p*-position of one of the phenyl rings in benzimidazolium moiety, are the responsible for the structural diversities in all the metal (copper and nickel) dithiolene complexes. The molecular structures of complexes **2a**, **2b** and **2c** are isostructural to the complexes of **1a**, **1b** and **1c** respectively. Copper-dithiolene complexes exhibit a Z-shaped non-planar geometry with a different angles. All dianionic copper(II) complexes **1a-1c**, are characterized by electron spin resonance spectroscopy. All these complexes exhibit an absorption in the near infrared (NIR) region. The near-IR absorbance bands are observed at 1210 and 862 nm for the copper (**1a-1c**) and nickel (**2a-2c**) complexes respectively, which have been attributed to the charge transfer from the copper dithiolate anion $[Cu(mnt)_2]^{2-}$ to the benzimidazolium cation $[Bz,R\text{-}BzBimy]^+$ and there is a combined transition of d–d, MLCT, π→π* in the $[Ni(mnt)_2]^{2-}$ anion.

The compound $[Hb]_2[Cu(mnt)_2]$ (**1**) [Hb = 1-(4-((1H-imidazol-1-yl)methyl)benzyl)-1H-imidazol-3-ium)] has been synthesized, starting from 1,4-bis((1H-imidazol-1-yl)methyl)benzene, $CuCl_2$ and $Na_2mnt$ in methanol. Compound **1** crystallizes in monoclinic system with *C2/c* space group. In the crystal structure, the interactions between cations and anions *via* bifurcated C–H···$(NC\text{-}mnt)_2$ hydrogen bonds give rise to a two dimensional supramolecular network. It has also been observed that two cation moieties (Hb) are attached by a very short C–H···N hydrogen bonding interaction with H···N distance of 1.74 Å, ∠CHN bond angle of 174.9°. Compound **1** is additionally characterized by cyclic voltammetry, UV-Vis, IR, $^1$H NMR and EPR spectroscopy. Compound **1** exhibits an oxidative response at +0.46 V *vs* Ag/AgCl and a reductive event at –0.67 V *vs* Ag/AgCl.

## 3.1. Introduction

Much efforts have been devoted to the study of bis(1,2-dithiolato) transition metal complexes in the fields of conducting- and magnetic-,[1] nonlinear opticical-,[2] NIR absorbing-materials,[3] catalysis[4] and electrochemical analysis.[5] Non-covalent interactions, intermolecular hydrogen bonding interactions such as S···H, N···H, H···Br, O···H and π···π stacking interactions are attracted attention in view of crystal engineering during last two decades and being utilized to construct functional molecular materials.[6,7] These interactions also plays a crucial role to control the conformation/orientation of molecular self assembly towards the generation of a wide variety of molecular architectures in biological, framework/network systems. The importance of conformational change can be realized from the following facts: (i) Biological: generally particular orientation/conformation of the single native protein (enzyme) has the ability to catalyze the concerned enzymatic reaction (substrate binds to the active site), that can be studied, in some cases, by the circular dichroism spectroscopy.[8] (ii) Frameworks: ligand conformation has a key role in the formation of porous networks of metal organic frameworks (MOFs) and porous coordination polymers (PCPs) architectures.[9,10] When flexibility of the ligand is incompatible with the porous properties, it would lead to a collapse of the framework.[11] One example to explain the importance of ligand orientation/conformation to build network is: *N,N′*-bis(3-pyridyl)urea (**L1**) molecule has various ligating topologies, based on the orientation of the pyridyl groups with respect to urea functionality.[9] Consequently, the MOF architecture (formed from **L1**) is dependent on the ligand conformation (if the L1 has the syn-anti conformation, it gives 1D zigzag polymeric chain, whereas for syn-syn/anti-anti conformation, it gives the metal organic macrocycle). The flexibility of ligands is essential to exhibit some particular properties, such as breathing ability in the solid state, adaptive recognition for coexisting counter ions. However it is very difficult to predict and control the flexibility of networks through flexible ligands. Hence, the conformation control of flexible ligands in networks is an important proposition to researchers. Recently we have reported the factors affecting the conformational modulation of flexible ligands in the coordination polymers and also we described, how the supramolecular interactions play a key role to control the geometry (square planar / distorted square planar) of copper metal in ion-pair dithiolene complexes.[12]

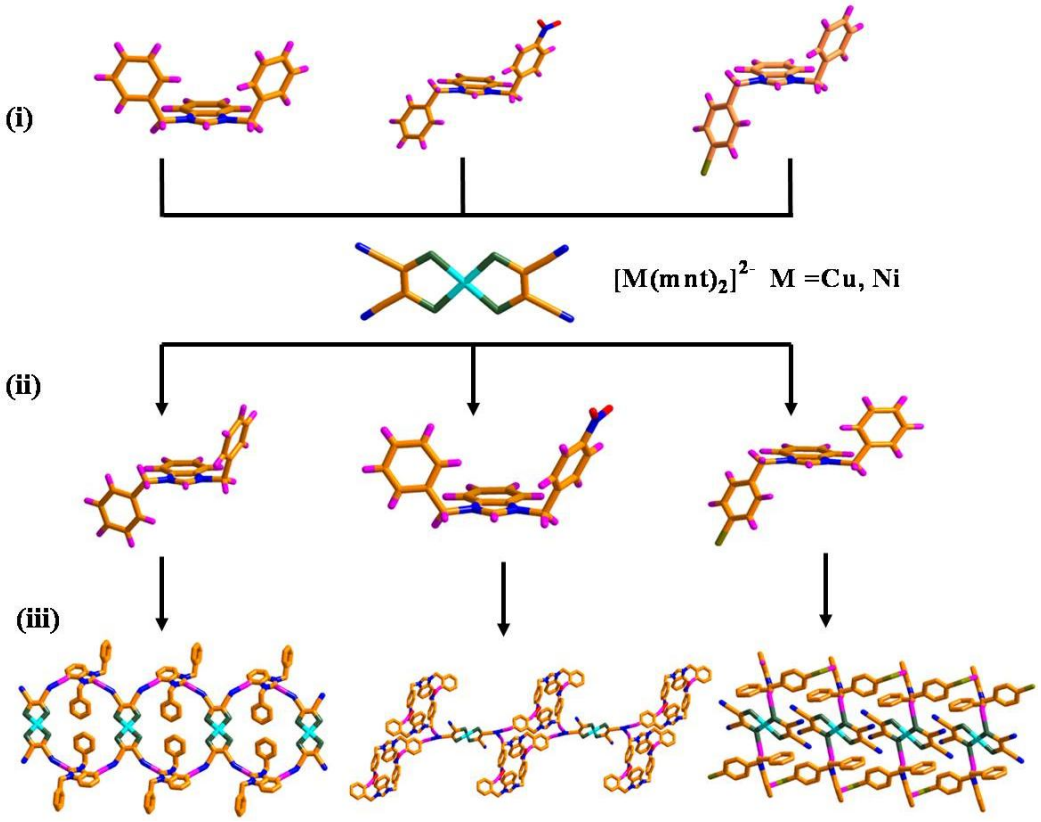


**Scheme 3.1**. (i) Conformation of the benzimidazolium salts (from left to right: **a**–**c**), anions are omitted for clarity, (ii) conformation of the benzimdazolium salts in metal-bis dithiolene ion-pair complexes, complex anion $[M(mnt)_2]^{2-}$ is omitted for clarity, (iii) packing diagrams through N···H; N···H, O···H and S···H, H···Br interactions of the copper-bis(dithiolene) ion-pair complexes of **1a**, **1b** and **1c** respectively (from left to right).

To extend this theme, we focus on the conformational change of organic cation receptors between the salts of tetrafluoroborate and the metal-bis(dithiolate) anions. Here, we report six new ion-pair metal-dithiolato complexes $[Bz,R\text{-}BzBimy]_2[M(mnt)_2]$ (M = Cu (**1**), Ni (**2**); R = H (**1a**, **2a**), $NO_2$ (**1b**, **2b**) and R = Br (**1c**, **2c**)). In this series of complexes, interestingly the two phenyl ($–CH_2–Ar$) groups (which are attached to the nitrogen atoms in the benzimidazole) are in *cis* and *trans* (with respect to the mean plane of benzimidazole ring) positions in organic cation receptors **a** and **b** respectively as tetrafluoroborate salts. When these salts are treated with $Na_2[M(mnt)_2]$, the orientation/conformation of two phenyl groups change their orientation to *trans* and *cis* respectively in their corresponding ion-pair complexes (**1a**, **2a** and **1b**, **2b**), as shown in Scheme 1. This phenomenon can be explained by the supramolecular interactions (hydrogen bonding and π···π stacking interactions) between

the mnt rings of $[M(mnt)]^{2-}$ complex anion and the aromatic ring of organic receptor cation. On the other hand, there is no change in orientation / conformation of two phenyl rings in bromo substituted organic cation receptor compound **c** and its dithiolato complexes **1c** and **2c**, because there are C–H···π interactions, that are present between one of the two phenyl rings and centroid of the chelate ring from $[Cu(mnt)_2]^{2-}$. All these compounds exhibit near-IR electronic absorption bands in their solution and solid states. The near-IR absorption is of special interest in metal based dithiolene complexes, because they are useful in application studies, e.g., in Q-switching laser applications.[12c,d] All the complexes **1a-1c**, **2a-2c** and organic cationic receptors **a-c** are unambiguously characterized by single crystal X-ray structure determinations and further characterized by IR, $^1$H NMR, ESR, cyclic voltammetry, LCMS, UV-vis-NIR.

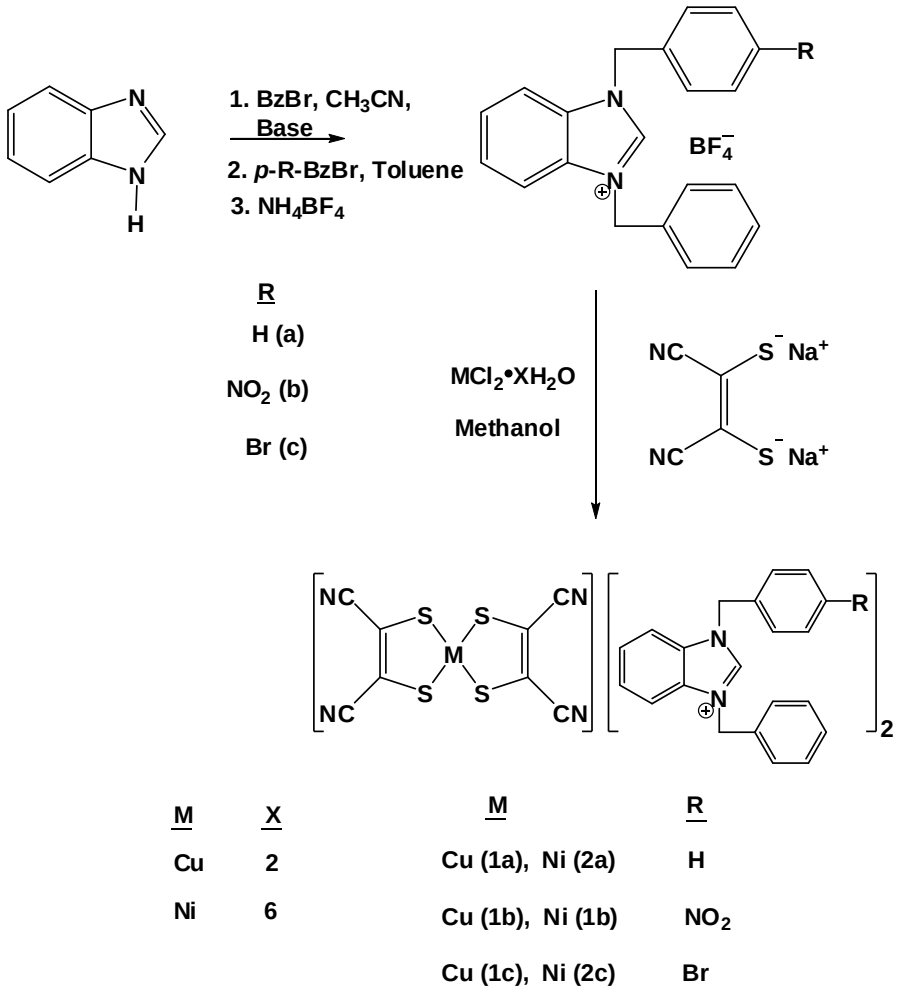


**Scheme 3.2**. Synthetic route for the preparation of organic cation receptor and metal-dithiolene complexes.

IPCT complexes of the type $[NO_2BzPy][M(mnt)_2]$ (M= Ni, Au) have been recently reported with near-IR absorption properties by Xiaoming Ren *et.al.*[13] We have reported IPCT compounds of the type $[Bu_4N][Ni(XPhdt)_2]$ (X= F, Cl, Br, and $NO_2$) that are basically asymmetrically substituted bis(1,2-dithiolato)-Nickel(III) complexes exhibiting near-IR absorption and structural diversity.[13b] In the present study we have found interesting H-bonding interactions that involve the mnt rings of $[M(mnt)]^{2-}$ complex anion and the aromatic rings of organic receptor cation in the crystal structure of compound **1**. This represents a new type of molecular recognition in the area of supramolecular chemistry. In this complex, protonation occurs *in-situ* in one of the imidazole rings of **b** (1,4-bis((1H-imidazol-1-yl)methyl)benzene) in MeOH solution. We wish to report here the synthesis, molecular structure and physical properties of compound $[Hb]_2[Cu(mnt)_2]$ (**1**) [Hb = 1-(4-((1H-imidazol-1-yl)methyl)benzyl)-1H-imidazol-3-ium)]. We have also described the supramolecular features and electrochemical properties of compound **1**.

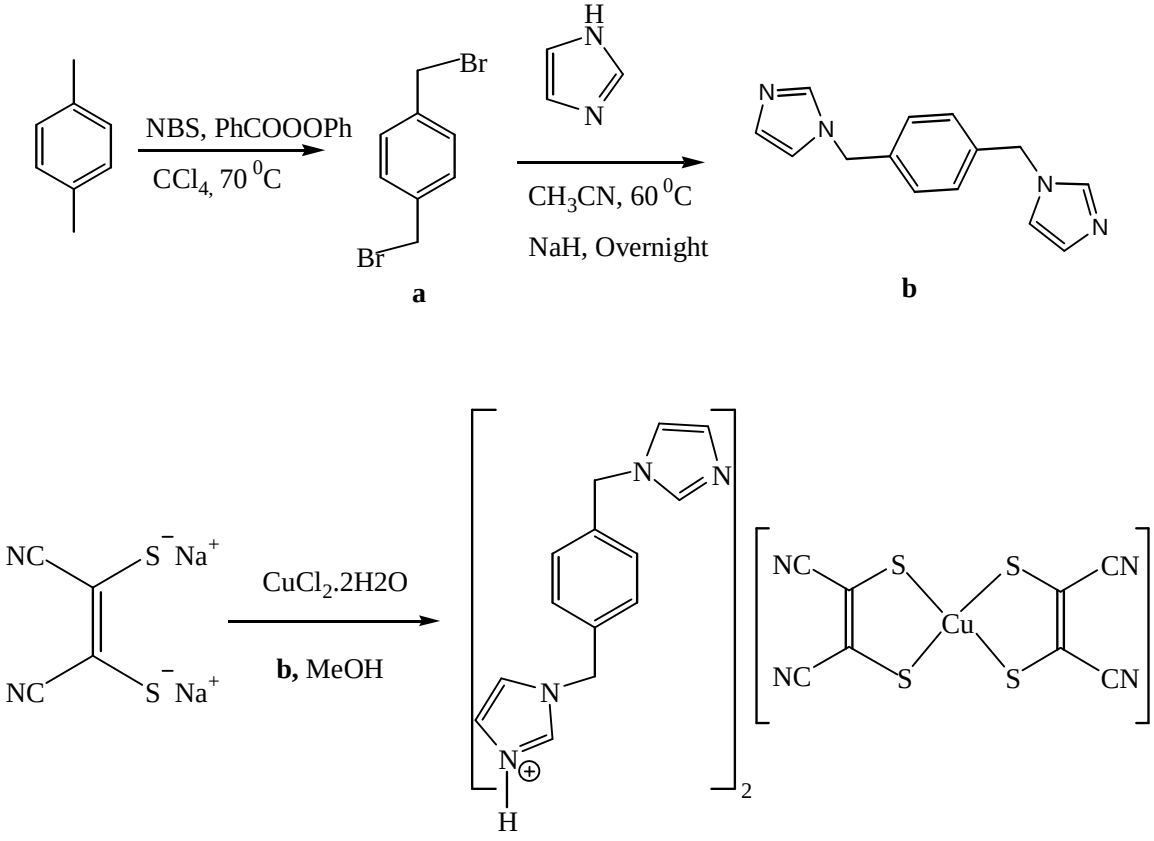


**Scheme 3.3.** Syntheses scheme for the ligand **b** and complex **1**.

## 3.2. Experimental Section

### 3.2.1. Materials and Methods

All chemicals were purchased from commercial sources and used without further purification. Micro analytical (C, H, N) data were obtained with a FLASH EA 1112 Series CHN Analyzer. The IR spectra (with KBr pellets) were recorded in the range of 400-4000 $cm^{-1}$ on a JASCO FT/ IR-5300 spectrometer. Diffuse reflectance and near-IR absorption spectra were recorded on a UV-3600 Shimadzu UV-Vis-NIR spectrophotometer. The electron spin resonance (ESR) spectra were recorded on a (JEOL) JESFA200 ESR spectrometer. $^1H$ NMR spectra was recorded on Bruker DRX- 400 spectrometer using $Si(CH_3)_4$ (TMS) as an internal standard. Solution mass spectra (LCMS) were obtained on a LCMS-2010A Shimadzu spectrometer. A Cypress model CS-1090/CS-1087 electroanalytical system was used for cyclic voltammetic experiments. The electrochemical experiments were measured in acetonitrile solvent containing $[Bu_4N][ClO_4]$ as a supporting electrolyte, using a conventional cell consisting of two platinum wires as working and counter electrodes.

### 3.2.2. Synthesis

**Preparation of Benzimidazolium derivatives**

According to literature procedure,[14] benzimidazole (10 mmol) was suspended in $CH_3CN$ (20 mL); to this, NaOH (10 mmol, 6.25 M) was added for deprotonation and it was continued to stir at room temperature for 30 min. Subsequently benzyl bromide (10 mmol) was added to the reaction mixture. The mixture was stirred overnight at 80 °C, and the solvent was removed. The residue was dissolved in water and extracted with $CH_2Cl_2$; the crude product was obtained after removal of the solvent; it was then dissolved in toluene (30 mL) and another portion of *p*-R-benzyl bromide (R=H, $NO_2$, Br) (10 mmol) was added to it. The reaction mixture was stirred overnight at 90 °C. The white precipitate was filtered off and washed with toluene, diethyl ether and air-dried and finally stored at room temperature.

**General procedure for counter ion exchange (bromide salts to tetrafluoroborate salts):**

1-benzyl-3-(4-R-benzyl)benzimidazolium bromides (2 mmol) were dissolved in hot water and ammoniumtetrafluoro borate (>2 mmol) was added until there is no precipitation; after that, it was extracted with ethyl acetate (2x20 mL) and dried by using $Na_2SO_4$. The resulting white crude product, so obtained after removal of the solvent by rotary evaporator, was crystallized

from hot methanol to obtain single crystals of compounds **a–c**, suitable for X-ray structure analysis. The characterization data for compounds **a–c** are described below.

**1,3-dibenzylbenzimidazolium tetrafluoroborate** (**a**). Yield: 78% (based on Bz-bromide). Anal. Calc. for $C_{21}H_{19}BF_4N_2$: C, 65.31; H, 4.95; N, 7.25%. Found: C, 65.68; H, 4.89; N: 7.58%. LCMS (*m/z)*: 299 (M+). $^1$H NMR (400 MHz, DMSO-$d_6$): $\delta$ 10.02 (s, 1H), 7.98-7.96 (m, 2H), 7.65-7.63 (m, 2 H), 7.52 (d, 4H, J=7.2), 7.46-7.37 (m, 6 H), 5.79 (s, 4H). LCMS-ESI: *m*/*z*= 299 $[M]^+$.

**1-benzyl-3-(4-nitro-benzyl)benzimidazolium tetrafluoroborate** (**b**). Yield: 86% (based on Bz-bromide). Anal. Calc. for $C_{21}H_{18}BF_4N_3O_2$: C, 58.50; H, 4.20; N, 9.74%. Found: C, 58.82; H, 4.27; N: 9.38%. LCMS (*m/z)*: 344 (M+). $^1$H NMR (400MHz, DMSO-$d_6$): $\delta$ 10.01 (s, 1H), 8.29 (d, 2H, J=8.8), 7.97 (s, 2H), 7.91 (s, 2H), 7.77 (d, 2H, J=8.4), 7.65 (t, 2H, J=3.6), 7.54 (d, 2H, J=7.2), 7.43 (t, 3H, J=4.8), 5.96 (s, 2H), 5.80 (s, 2H).

**1-benzyl-3-(4-bromo-benzyl)benzimidazolium tetrafluoroborate** (**c**). Yield: 82% (based on Bz-bromide). Anal. Calc. for $C_{21}H_{18}BF_4N_2Br$: C, 54.23; H, 3.90; N, 6.02%. Found: C, 54.62; H, 3.95; N: 6.48%. LCMS (*m/z)*: 378 (M+). $^1$H NMR (400MHz, DMSO-$d_6$): $\delta$ 9.98 (s, 1H), 7.96 (t, 2H, J= 3.6), 7.64 (t, 4H, J= 3.6), 7.51 (t, 4H, J= 8.4), 7.45-7.39 (m, 3H), 5.78-5.76 (4H).

**General synthetic procedure for the ion pair compounds 1a-c and 2a-c** (see also Scheme 3.2).

To a 10 mL MeOH solution of $Na_2$mnt (2 mmol),[15a] 5 mL MeOH solution of $MCl_2 \cdot XH_2O$ (M = Cu, Ni; X = 2, 6) (1 mmol) was added, stirred for 30 min at room temperature and filtered. To this solution, 15 mL MeOH solution of [Bz,R-BzBimy][$BF_4$] (R = H, $NO_2$, Br; 2 mmol) was added and continued to stirr at room temperature for 4h. Subsequently, it was filtered off. The crude (black colored ppt) product was crystallized from $CH_3CN$/ether by diffusion method to obtain dark-red crystals for compounds **2a–2c**. Compounds **1a–1c** was grown from slow evaporation of MeOH filtrate solution.

**[Bz,H-BzBimy]$_2$[Cu(mnt)$_2$] (1a).** Yield: 52% (based on copper). Anal. Calc. for $C_{50}H_{38}N_8S_4Cu$: C, 63.70; H, 4.06; N, 11.88. Found: C, 63.55; H, 4.15; N: 11.65. IR spectrum (KBr pellet, $\nu$/cm$^{-1}$): 3119, 2191, 1556, 1464, 1145, 1016, 742, 702. LCMS (*m/z)*: 299 ($M^+$).

$^1$H NMR (400 MHz, $\delta$ ppm) (DMSO-$d_6$): 10.17 (s, 1H), 8.014 (dd, 2H, $J_1$= 3.2 Hz, $J_2$ = 2.8 Hz), 7.69-7.65 (m, 2H), 7.573 (d, 4H, $J$ = 7.6 Hz), 7.48-7.40 (m, 6H), 5.84 (s, 4H).

**[Bz,$NO_2$-BzBimy]$_2$[Cu(mnt)$_2$] (1b).** Yield: 46% (based on copper). Anal. Calc. for $C_{50}H_{36}N_{10}O_4S_4Cu$: C, 58.15; H, 3.51; N, 13.56. Found: C, 58.31; H, 3.45; N, 13.68. IR spectrum (KBr, ν/cm$^{-1}$): 3074, 2986, 2920, 2191, 1604, 1562, 1452, 1346, 1249, 1026, 966, 806, 746, 528. LCMS (*m/z*): 344 $(M)^+$. $^1$H NMR (400 MHz, $\delta$ ppm) (DMSO-$d_6$): 10.02 (s, 1H), 8.28 (bs, 2H), 7.98-7.88 (m, 2H), 7.77 (d, 2H, $J$ = 6.8 Hz), 7.65 (s, 2H), 7.54 (s, 2H), 7.44 (d, 3H), 5.97 (s, 2H), 5.81 (s, 2H).

**[Bz,Br-BzBimy]$_2$[Cu(mnt)$_2$] (1c).** Yield: 48% (based on copper). Anal. Calc. for $C_{50}H_{36}N_8Br_2S_4Cu$: C, 54.57; H, 3.29; N, 10.18. Found: C, 54.16; H, 3.34; N, 10.24. IR spectrum (KBr, cm$^{-1}$): 2191, 1633, 1556, 1458, 1369, 1217, 1105, 1010, 758. LCMS (*m/z*): 377, 379 $(M)^+$, $(M+2)^+$. $^1$H NMR (400 MHz, $\delta$ ppm) (DMSO-$d^6$): 10.19 (s, 1H), 7.98 (d, 2H, $J$ = 4 Hz), 7.66 (d, 4H, $J$ = 8 Hz), 7.55 (t, 4H, $J$ =8), 7.46-7.38 (m, 3H), 5.82-5.81 (bs, 4H).

**[Bz,H-BzBimy]$_2$[Ni(mnt)$_2$] (2a).** Yield: 68% (based on nickel). Anal. Calc. for $C_{50}H_{38}N_8S_4Ni$: C, 64.03; H, 4.08; N, 11.94. Found: C, 64.21; H, 4.15; N, 12.16. IR spectrum (KBr, ν/cm$^{-1}$): 3119, 3059, 2191, 1604, 1556, 1485, 1182, 1145, 744, 702. LCMS (*m/z*): 299 $(M)^+$. $^1$H NMR (400 MHz, $\delta$ ppm) (DMSO-$d_6$): 10.00 (s, 1H), 7.94 (dd, 2H, Ar-H),7.63-7.37 (m, 12H, Ar-H), 5.77 (s, 4H, Benzyl).

**[Bz,NO2-BzBimy]$_2$[Ni(mnt)$_2$] (2b).** Yield: 64% (based on nickel). Anal. Calc. for $C_{50}H_{36}N_{10}O_4S_4Ni$: C, 58.43; H, 3.53; N, 13.62. Found: C, 58.36; H, 3.61; N, 13.71. IR spectrum (KBr, ν/cm$^{-1}$): 2924, 2293, 2193, 1604, 1562, 1521, 1479, 1346, 738. LCMS (*m/z*): 344 $(M)^+$. $^1$H NMR (400 MHz, $\delta$ ppm) (DMSO-$d^6$): 10.01 (s, 1H), 8.29 (d, 2H, $J$ = 8.8 Hz), 7.98 (bs,1H), 7.93 (bs, 1H), 7.76 (d, 2H, $J$ = 8.4 Hz), 7.68 (bs, 2H), 7.55 (d, 2H, $J$ = 17.2 Hz), 7.43 (d, 3H, $J$ = 8.0 Hz), 5.95 (s, 2H), 5.79 (s, 2h).

**[Bz,Br-BzBimy]$_2$[Ni(mnt)$_2$] (2c).** Yield: 61% (based on nickel). Anal. Calc. for $C_{50}H_{36}N_8Br_2S_4Ni$: C, 54.81; H, 3.31, N, 10.22. Found: C, 54.76, H, 3.24, N, 10.29. IR spectrum (KBr, ν/cm$^{-1}$): 2193, 1558, 1487, 1406, 1369, 1130, 1070, 806. LCMS (*m/z*): 377, 379 $(M^+)$, $(M+2)^+$. $^1$H NMR (400 MHz, $\delta$ ppm) (DMSO-$d^6$): 10.16 (s, 1H), 7.96 (d, 2H, $J$ = 4 Hz), 7.62 (d, 4H, $J$ = 7 Hz), 7.55 (t, 4H, $J$ =8), 7.44-7.35 (m, 3H), 5.82-5.81 (bs, 4H).

**Synthesis of compound $[Hb]_2[Cu(mnt)_2]$ (1).** The ligand **b** (1,4-bis((1H-imidazol-1-yl)methyl)benzene) has been prepared according to literature procedure.[15b] According to Scheme 3.3, to a 10 mL MeOH solution of $Na_2$mnt (0.465g, 2.5 mmol), 5 mL MeOH solution of $CuCl_2 \cdot 2H_2O$ (0.212 g, 1.25 mmol) was added, stirred for 30 min at room temperature and then filtered. To this filtrate solution, 1,4-bis(imidazol-1-yl-methylene)benzene (**b**) (0.721 g, 2.5 mmol) in 15 mL MeOH was added, and stirring was continued for another 4 h at room temperature, and then it was filtered. Single crystals, suitable for X-ray structure analysis, were grown by slow evaporation of methanol (filtrate) solution. Yield: 0.273 g (30% based on copper). Anal. Calcd. for ($C_{36}H_{30}N_{12}S_4Cu$): C, 52.57; H, 3.67; N, 20.43. Found: C, 52.35; H, 3.76; N, 20.61. $^1$H NMR (400 MHz, $\delta$ ppm) (DMSO-$d_6$): 7.27 (s), 5.2 (s), 8.6 (bs). IR (KBR pellet)($\upsilon$/cm$^{-1}$): 3130, 2193 ($\nu_{C\equiv N}$), 1516 (phen), 1454 ($\nu_{C=C}$), 1296, 1149 ($\nu_{C-C\equiv N}$), 1082, 835, 765, 713, 623.

### 3.2.3. X-ray Diffraction

Data were measured at room temperature for compounds **1a–1c**, **2a–2c**, **a–c** and compound **1** on a Bruker SMART APEX CCD, area detector system [$\lambda$ (Mo K$\alpha$) = 0.7103 Å], graphite monochromator, 2400 frames were recorded with an $\omega$ scan width of 0.3°, each for 10 s, crystal-detector distance 60 mm, collimator 0.5 mm.[16] Data reduction was performed with the SAINTPLUS software,[16a] absorption correction using an empirical method SADABS,[16b] structure solution using SHELXS-97 program[16c] and refined using SHELXL-97 program.[16d] Hydrogen atoms on the aromatic rings were introduced on calculated positions and included in the refinement riding on their respective parent atoms.

## 3.3. Results and discussion

### 3.3.1. Synthesis

We have synthesized a series of ion-pair metal-bis(dithiolene) complexes by the treatment of 1 mmol of metal chlorides ($CuCl_2 \cdot 2H_2O$ and $NiCl_2 \cdot 6H_2O$) and 2 mmol of $Na_2$mnt (disodium maleonitriledithiolate) in methanol with various substituted benzimidazolium derivatives (2 mmol) at room temperature condition. Benzimidazolium derivatives of tetrafluoroborate compounds **a-c** and ion-pair dithiolene complexes **1a-1c, 2a-2c** are characterized by routine

elemental analyses, IR, NMR, UV-Visible-NIR spectroscopic techniques, cyclic voltammetry and unambiguously characterized by single crystal X-ray structure determinations.

### 3.3.2. Description of Crystal Structure

**Compound [Bz,R-BzBimy]$_2$[M(mnt)$_2$] [R= H, M= Cu (1a), Ni (2a)].** Dark red crystals of the compounds **1a** and **2a** are suitable for X-ray structure analysis. Crystallographic analysis reveals that both **1a** and **2a** crystallize in triclinic system with *P*-1 space group. The concerned asymmetric unit contains half of the molecule, which was represented by labeled atoms in ORTEP diagram as shown in Figure 3.1. The basic crystallographic data for compounds **1a** and **2a** are presented in Tables 3.1 and 3.2. In $[Cu(mnt)_2]^{2-}$ of compound **1a**, the four sulfur atoms define a plane; hence the geometry around the copper metal is perfectly square-planar with the average of 90.78(3)° S–Cu–S bond angles within the five membered chelate rings. The average Cu–S, C–S, and C=C bond lengths are 2.262, 1.729 and 1.347 Å respectively in compound **1a**. The overall charge of the metal complex anion $[Cu(mnt)_2]^{2-}$ in compound **1a**, as expected, is –2, and this anionic charge is compensated by a two $[Bz,H\text{-}BzBimy]^{+}$ cations as observed in the crystal structure.

In the crystal structure of organic receptor **a**, the two aryl groups are in the *cis* conformation with respect to the mean plane of benzimidazole ring. Whereas in the crystal structure of metal complex **1a**, these two aryl groups are situated in trans arrangement. This phenomenon (orientation of aryl groups: conformational change) can be attributed by weak supramolecular interactions between the cations and the anion. To explain this situation of conformational change, let us consider the Figure 3.2(a), in which X1 and X2 positions represent the $sp^3$ hybridization of carbon atoms and the Figure 3.2(b), that indicates the orientation of two hydrogen atoms and the phenyl rings (staggered form), attached to X1 and X2 carbon-centers.

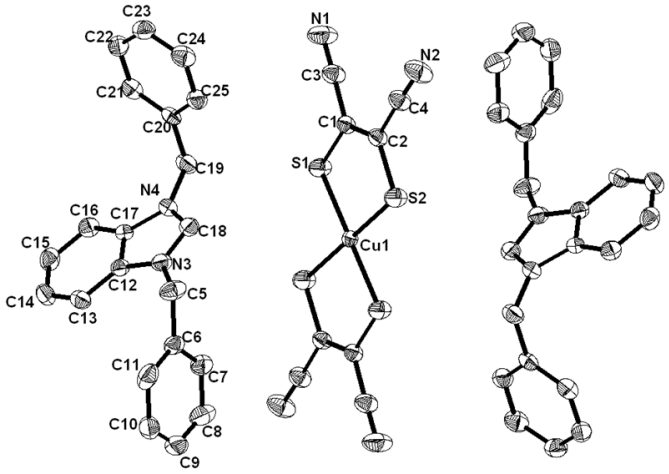


**Figure 3.1.** Thermal ellipsoidal diagram of the compound **1a** (30% probability, hydrogen atoms are omitted for clarity).

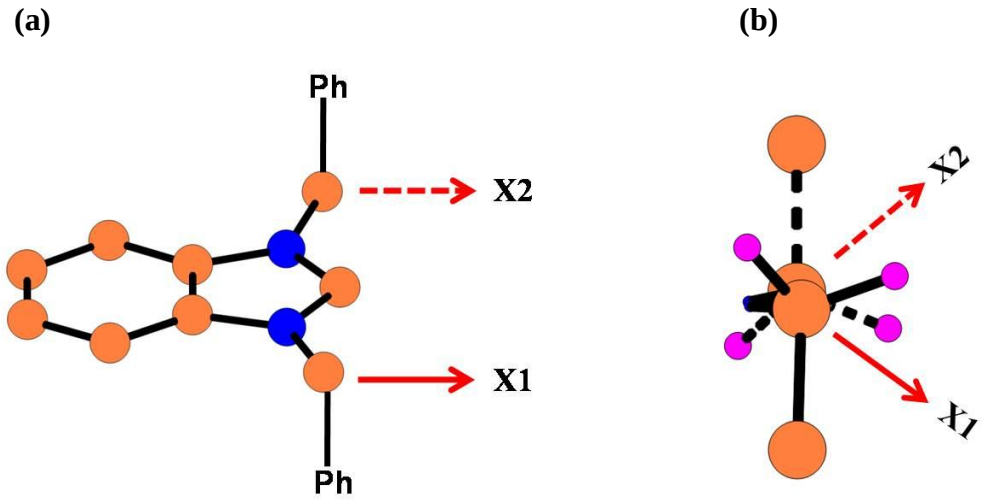


**Figure 3.2.** (a) General representation of the sp3 carbons in benzimidazolium salt, (b) orientation of the hydrogen's at X1, X2 positions of the carbons.

In the crystal structure of compound **a** ($BF_4$ salt of same organic receptor), eight C–H···F hydrogen bonding interactions are present between cation and anion. Through these supramolecular interactions, the alignment of hydrogen atoms, which are belonged to free carbons at X1 and X2 positions, are in a nearly eclipsed form. Hence the two phenyl rings, which are attached to the sp3 hybridized carbons (X1, X2 positions of carbons) are in a cis

arrangement in the crystal structure of compound **a** ($BF_4$ salt). Whereas in the crystal structure of metal dithionate complex **1a**, there are totally four types of C–H···N and C–H···S interactions (less than the sum of the van der Waals radii) (Table 3.3).

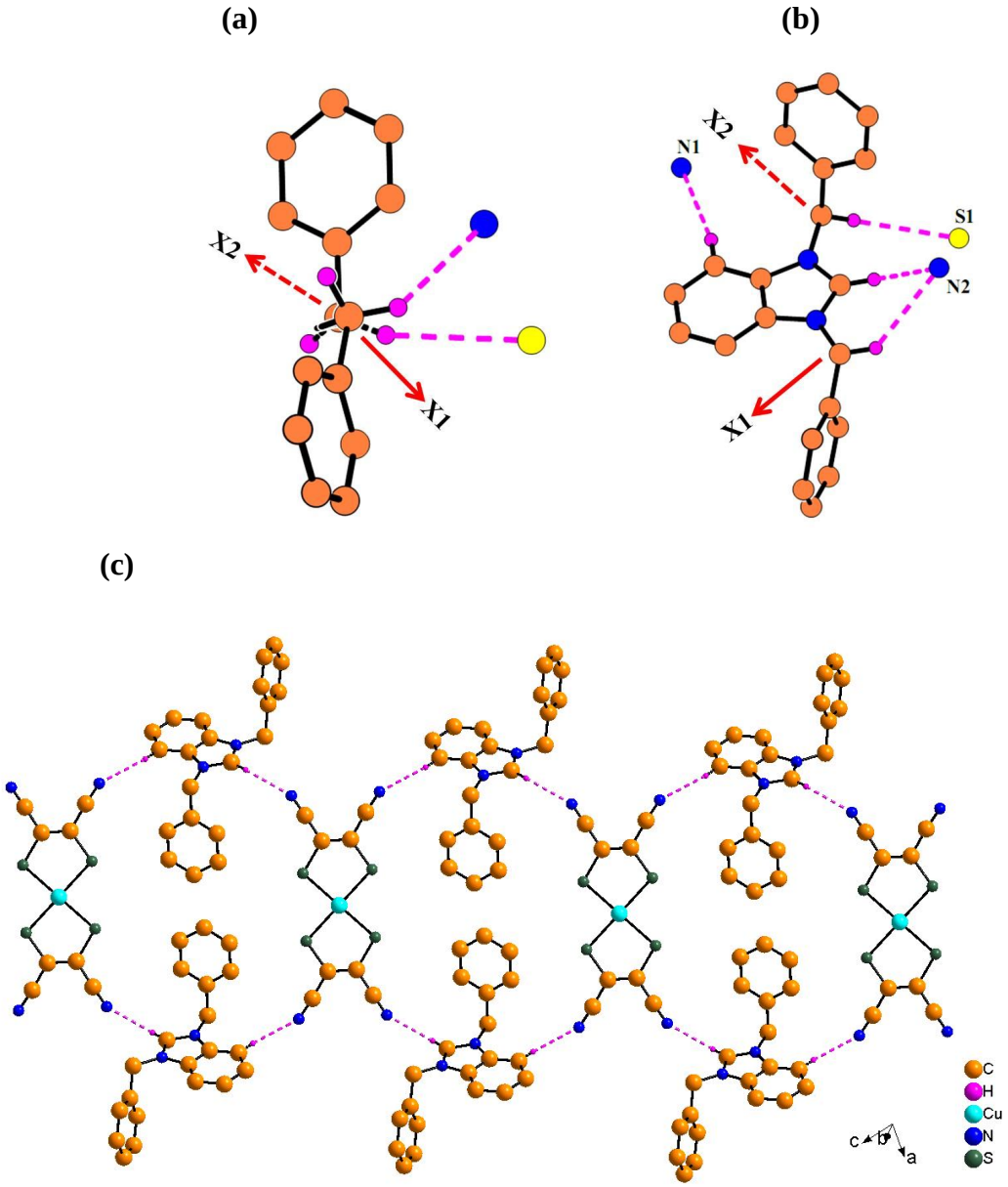


**Figure 3.3**. In compound **1a** (a) orientation of the hydrogen's at X1, X2 positions, (b) hydrogen bonding interactions, (c) packing diagram.

Due to these interactions the hydrogen's positions at X1 and X2 are in nearly in staggered alignment (Figure 3.3a). The C–H···N hydrogen bonding at X1 position is above and the C–H···S interaction at X2 position is below the mean plane of the benzimidazole ring. As a result

of this staggered supramolecular hydrogen bonding interactions (Figure 3.3b), the two phenyl rings are in a trans arrangement in the crystal structure of compound **1a**.

In the crystal structure of organic receptor compound **a**, there is only one type of C–H···Cg (Cg denotes the C2–C7 aryl ring, H···Cg is 3.173 Å) interactions are present. On the other hand, in metal coordination complex **1a**, C–H···Cg, Cg1···Cg1 interactions (Cg, Cg1denotes the centroids of the C20–C25, C12–C17 aryl rings respectively) are present with a distance of 3.761 (H···Cg), 3.749 Å respectively. In the packing diagram of the compound **1a**, the $[Cu(mnt)_2]^{2-}$ anions are arranged in a layer and each anion molecule is connected by the two cations with four C–H···N hydrogen bonding interactions, leading to an 2D network as shown in Figure 3c. The nearest Cu···Cu and Cu···S distances are 7.850 and 6.298 Å respectively. Similar interactions and similar discussion are observed, as expected, in the crystal of compound **2a**.

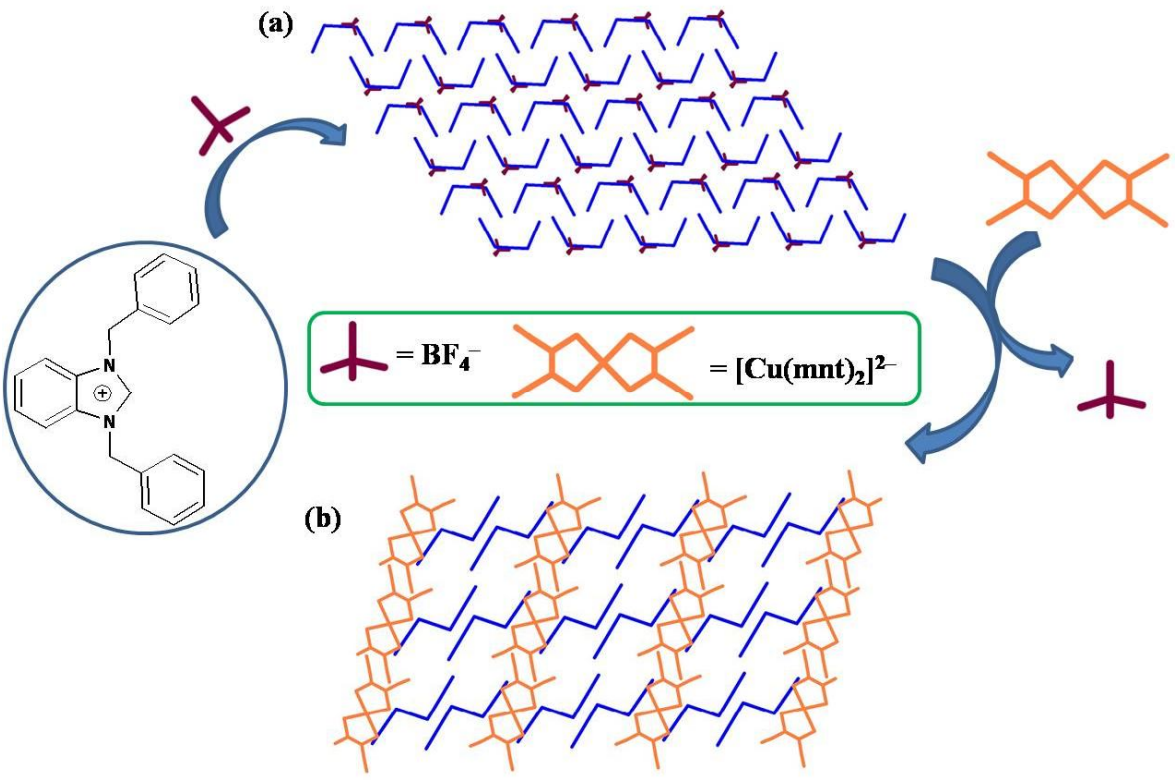


**Figure 3.4.** Topological representation of (a) compound **a**, (b) compound **1a**.

According to topological representation of Figure 3.4(a), the alignment of phenyl groups are in cis arrangement in organic receptor compound **a**. In the crystal structure, all the tetrafluoroborate anions are arranged back and front sides of the benzimidazolium moieties. All the cations are arranged in a CC*CC*CC* (C* is the mirror image of C) fashion. The tetrafluoroborate anion is replaced by the $[Cu(mnt)_2]^{2-}$ anion in compound **1a**, when the alignment of cations are changed to trans conformation. As shown in Figure 4b, all the anions (A) are situated in between the organic cations (C), giving an ACCACCACC type arrangement.

**Compound $[Bz,R\text{-}BzBimy]_2[M(mnt)_2]$ [R= $NO_2$, M= Cu(1b), Ni(2b)].** Dark red crystals of the compounds **1b** and **2b** are crystallized in triclinic space group *P*-1. Thermal ellipsoidal diagram of the compound **1b** is shown in Figure 3.5, in which the relevant asymmetric unit contains half of the molecule represented by labeled atoms. The four sulfur atoms surround the copper ion, providing the square planar coordination geometry with the average S–Cu–S angle of 90.47 Å. In the five membered chelate ring in dithiolene moiety, the average S–Cu, C–S and C=C bond lengths are consistent with those in the crystal structure of compound **1a**.

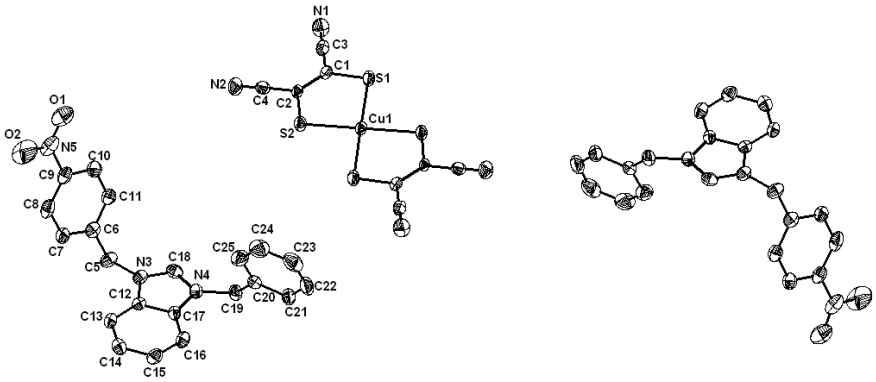


**Figure 3.5.** Ortep diagram of compound **1b** (30% probability, hydrogen atoms are omitted for clarity).

When in the compound **a**, among two phenyl rings, one of the *p*-position in the phenyl ring is substituted with a nitro group, it gives a organic receptor compound **b**. In the crystal structure of compound **b** (i.e $BF_4^-$ salt of cation), the aryl groups are in the trans with respect to the mean plane of benzimidazole ring, whereas the two aryl groups are in the cis alignment in compound **1b**. This conformational modulation can be explained on the basis of weak supramolecular interactions between cation and anions such as H···N, H···S, H···O and H···F, pi-pi stacking interactions. In the crystal structure of compound **b**, there are thirteen C–H···F

hydrogen bonding interactions. In this compound the alignment of hydrogen's which are attached to the carbon atoms at X1 and X2 positions are in the nearly staggered form, in which two hydrogen bonding interactions (H1B···F1, H1B···F4) are above and the remaining two hydrogen bonding interactions (H15B···F4, H15A···F3) are below to the mean plane of benzimidazole ring. Hence the two phenyl rings are in the trans orientation in compound **b**.

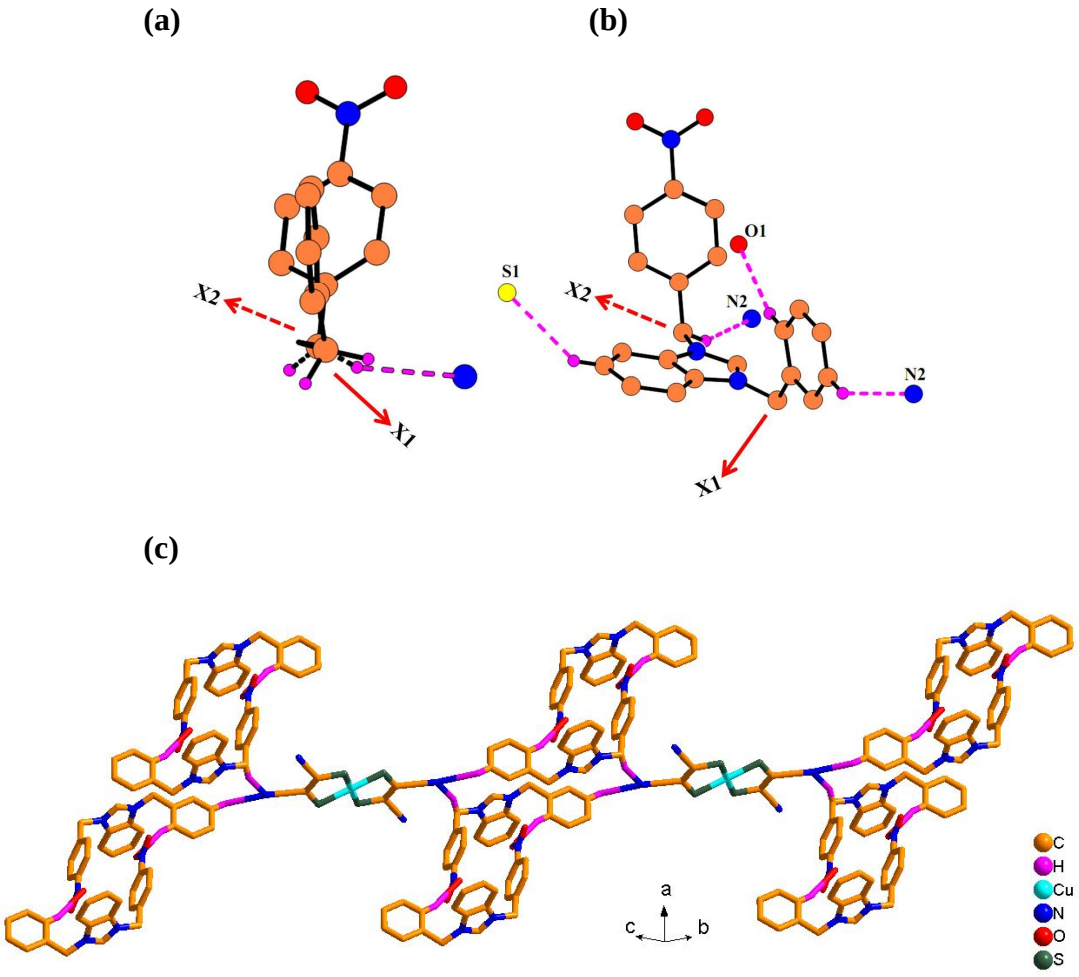


**Figure 3.6.** In compound **1b** (a) hydrogen atoms orientation at X1, X2 positions, (b) hydrogen bonding interactions, (c) packing diagram.

In the crystal structure of compound **1b**, there are totally four C–H···N, C–H···S and C–H···O hydrogen bonding interactions, in which the hydrogen bonding interaction at X2 position is in eclipsed form (Figure 3.6(a)), and the remaining hydrogen bonding interactions (phenyl group attached to carbon at X1 position) are above to the mean plane of benzimidazole ring as

shown in Figure 3.6(b). Due to this type of eclipsed configuration and C–H···O hydrogen bonding interaction, the two aryl groups are in a cis arrangement. All these supramolecular interactions in compound **1b** leads to a dumbbell shaped 2-D network, as shown in Figure 3.6(c). In addition to these interactions, there are C–H···π stacking interactions, that are present in compound **1b** with distances 3.041 Å (H24···Cg1) and 3.128 Å (H16···Cg2) (Cg1 and Cg2 are C12-17 and C6-11 phenyl rings respectively). In compound **2b** also, the orientation of phenyl rings are in cis arrangement, due to the nearly eclipsed hydrogen bonding interactions.

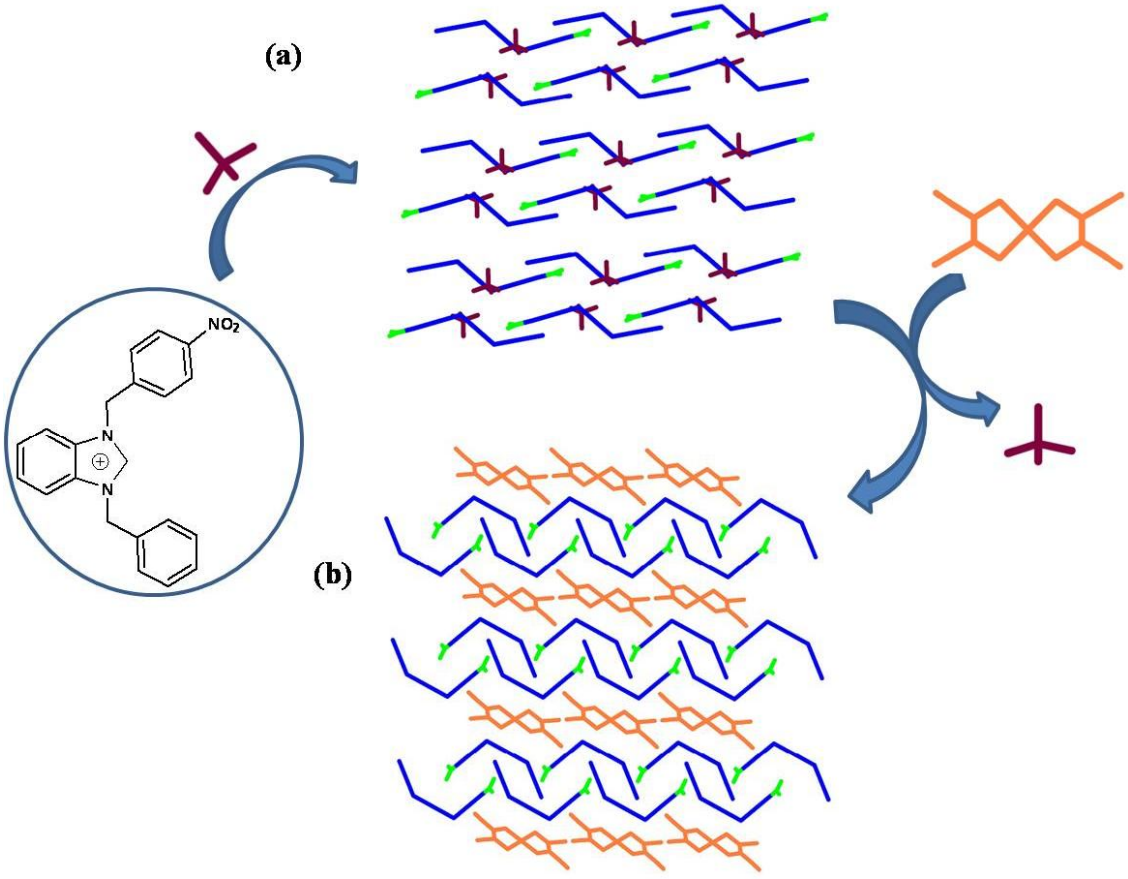


**Figure 3.7.** Topological representation of (a) compound **b**, (b) compound **1b**.

From the Figure 3.7(a), if we consider the horizontal line (H) in the topological representation, all the cations and anions are arranged in a similar manner, and the below horizontal line (H*) is the symmetry (C2) operation of the above horizontal line, it gives a HH*HH*HH* type of super cell along crystallographic *a*-axis for the organic receptor

compound **b**. When the metal-dithiolate anion $[Cu(mnt)_2]^{2-}$ is treated with the compound **b**, it gives metal-dithiolene ion-pair compound **1b.** Now, the alignment of two phenyl groups is changed from trans to cis arrangement in compound **1b.** Anion moieties are indicated by orange color, all the cations are represented by blue color and the substituent group ($-NO_2$) is indicated with green color. In the super cell of compound **1b**, all the anions are situated between the organic cation receptors and the cations are arranged like a chain manner (combination of two horizontal lines) as shown in Figure 3.7(b).

**Compound $[Bz,R\text{-}BzBimy]_2[M(mnt)_2]$ (R= Br, M= Cu (1c), Ni (2c))**. The dark red crystals of compounds **1c** and **2c** were crystallized in triclinic *P*-1 space group. The asymmetric unit of compound **1c** contains half of the molecule represented as the atom labeling description, as shown in Figure 3.8. The geometry around the copper and nickel metal in compounds **1c** and **2c** is perfectly square planar. The Cu–S, S–C and the S–Cu–S bond angles within the five-membered ring are similar to those of above mentioned compounds **1a**, **1b**.

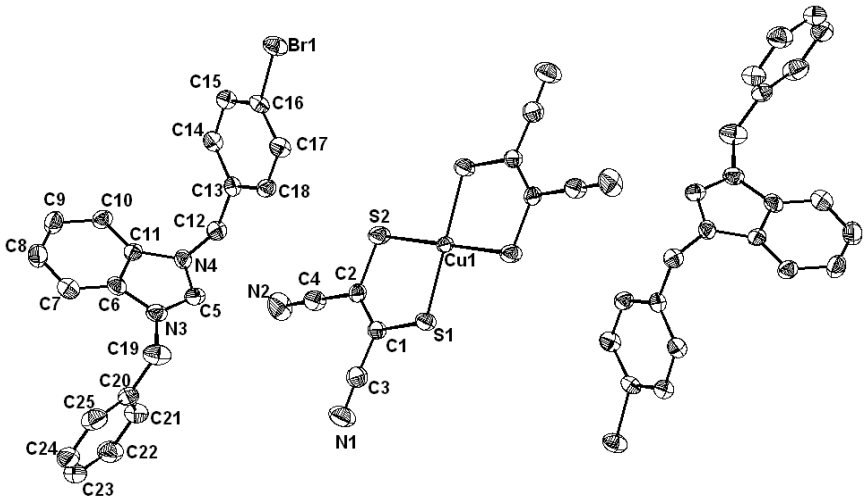


**Figure 3.8.** Ortep diagram of ompound **1c** (30% probability, hydrogen atoms are omitted for clarity).

In the crystal structure of compound **c**, two aryl groups (which are attached to the sp3 carbon atoms) are in the trans alignment. In contrast to the fact observed in **1a**, **2a**, **1b**, **2b**, the two phenyl groups are trans alignment in metal complex **1c**. In this case there is no change in conformation of cation between compound **c** and **1c**, **2c**. This can be explained based on supramolecular hydrogen bonding interactions. In total there are nine C–H···F interactions in

compound **c**. In the relevant crystal structure, the hydrogens that are belonged to carbon atoms at X1 and X2 positions are in a nearly staggered form, in which the hydrogen bond interaction at X1 position is above and at X2 position the two hydrogen bonding interactions are below to the mean plane of benzimidazole ring respectively. Due to these staggered supramolecular interactions, the two phenyl rings are in the trans orientation. In the crystal structure of compound **1c** there are totally six types of hydrogen bonding interactions, as shown in Table 3.3. The hydrogen atoms attached to the sp3 carbon atoms (X1 and X2 positions) are in the nearly staggered form, in which there are only two hydrogen bonding interactions (H12A···Br1, H12B···S1) at X1 position are above the mean plane of benzimidazole ring, as shown in Figure 3.9(a). Here the carbon atom at X2 position is free from hydrogen bonding interactions (Figure 3.9(b)), hence the C–C single bond (–$CH_2$–Ph) can freely rotate to the trans or cis position with respect to the bromo substituted phenyl ring which is attached to the X1 position. In this case, the phenyl ring (C20-C25) attached to the sp3 carbon (at X2 position) atom is more preferably situated in a trans orientation (with respect to the bromo substituted phenyl ring attached to the X1 position) because there are C–H···π (H21···π1 and H24···π1) interactions, present between phenyl and chelate ring from $[Cu(mnt)_2]^{2-}$ anion (π1 indicates the centroid of the Cu1S1C1C2S2). All these hydrogen bonding interactions in compound **1c** give rise to a 2-D network as shown in Figure 3.9(c). Similarly in the crystal structure of compound **2c**, hydrogen's at X1, X2 positions are in the nearly staggered form and also there are C–H···π interactions, observed between the hydrogen atom of phenyl ring (C20-C25) and the chelate ring from $[Cu(mnt)_2]^{2-}$ anion. Hence the two phenyl rings are in the trans geometry, as found in compound **1c**.

In the super cell representation of the organic receptor compound **c**, all the tetrafluoroborate anions are situated in between cation moieties. All the cations are arranged in a related manner in one horizontal line, and the immediate horizontal line is the symmetry operation (C2) of the above line; same trend has been followed for the tetrafluoroborate anions also, as shown in Figure 3.10(a). In the topological representation of the metal complex **1c**, all the anions are arranged in a similar fashion in all the vertical lines and all the cations are located in a trans arrangement along b-axis, as shown in Figure 3.10(b). Thermal ellipsoidal diagrams of the compounds **a**–**c** (Figure 3.11(a–c)), crystallographic data for

compounds **a**–**c** (Table 3.4), hydrogen bonding table for compounds **2a**–**2c**, **a**–**c** were described in Table 3.5 & 3.6.

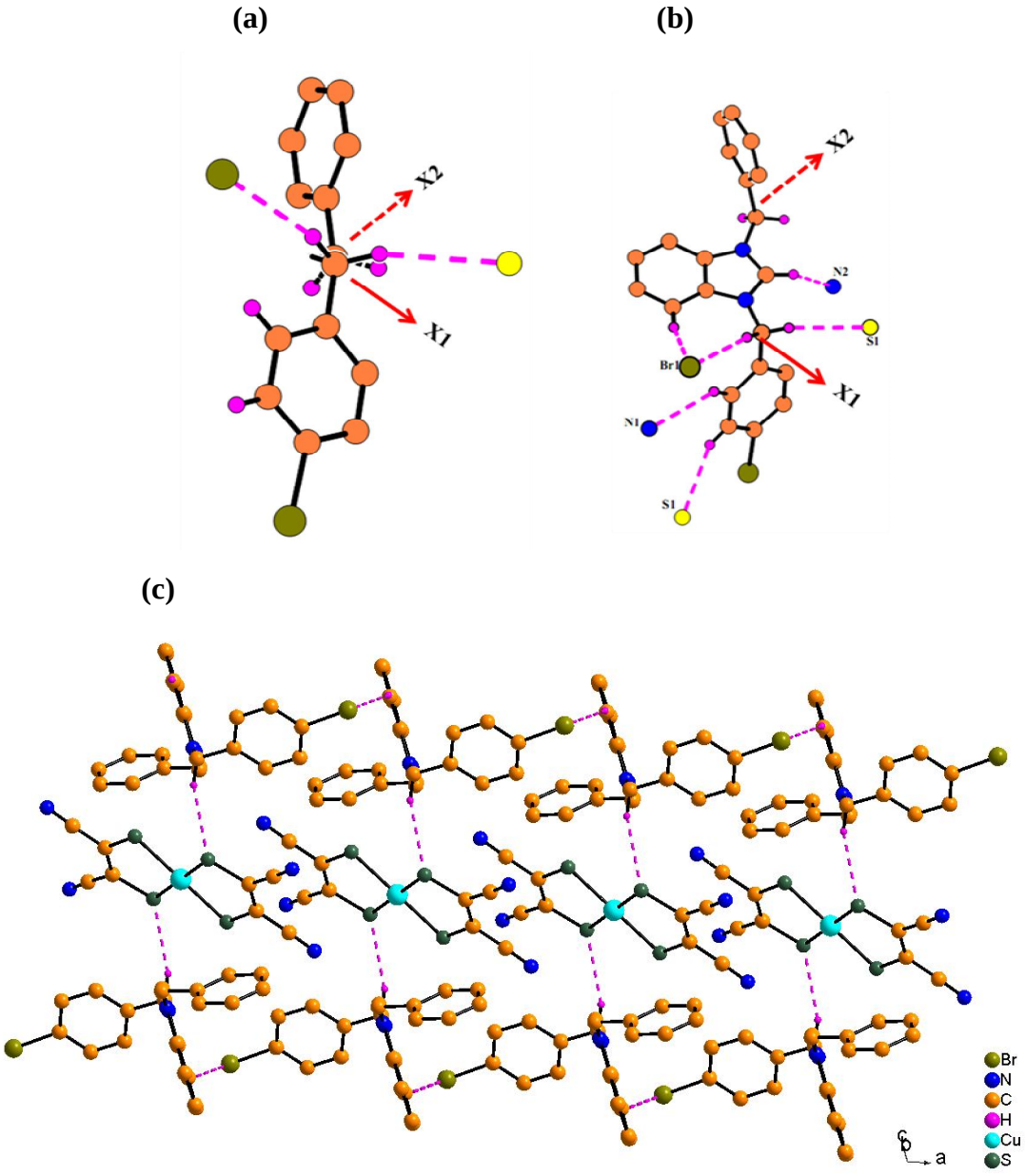


**Figure 3.9.** In compound **1c** (a) orientation of the hydrogen atoms at X1, X2 positions, (b) hydrogen bonding interactions, (c) packing diagram.

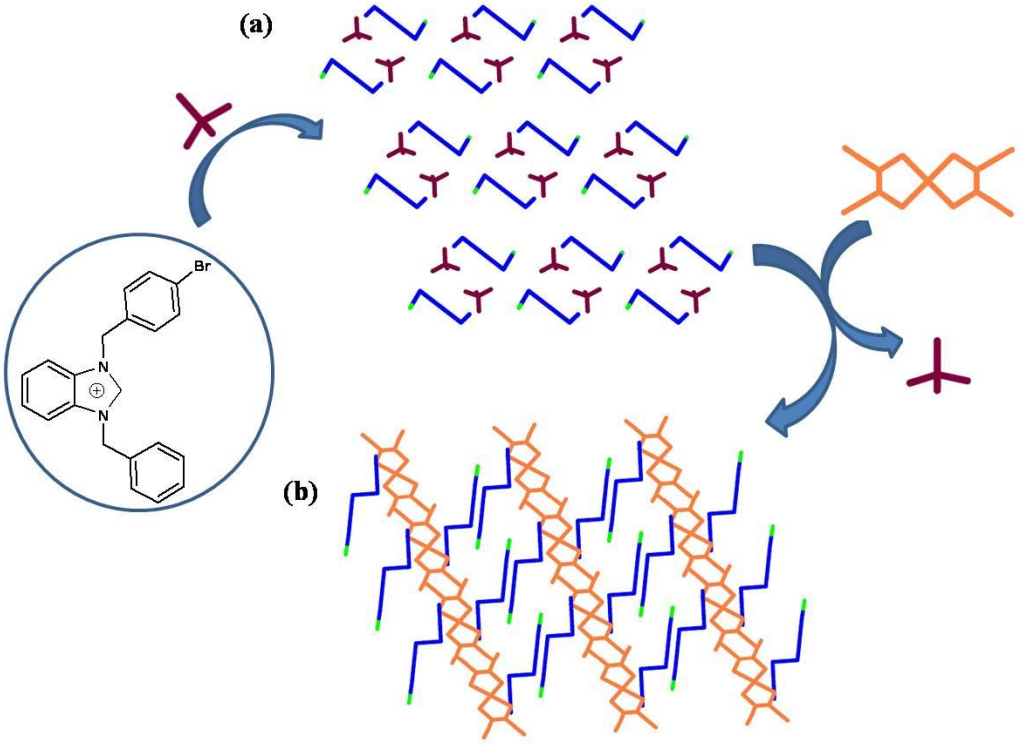


**Figure 3.10.** Topological representation of (a) compound **c**, (b) compound **1c**.

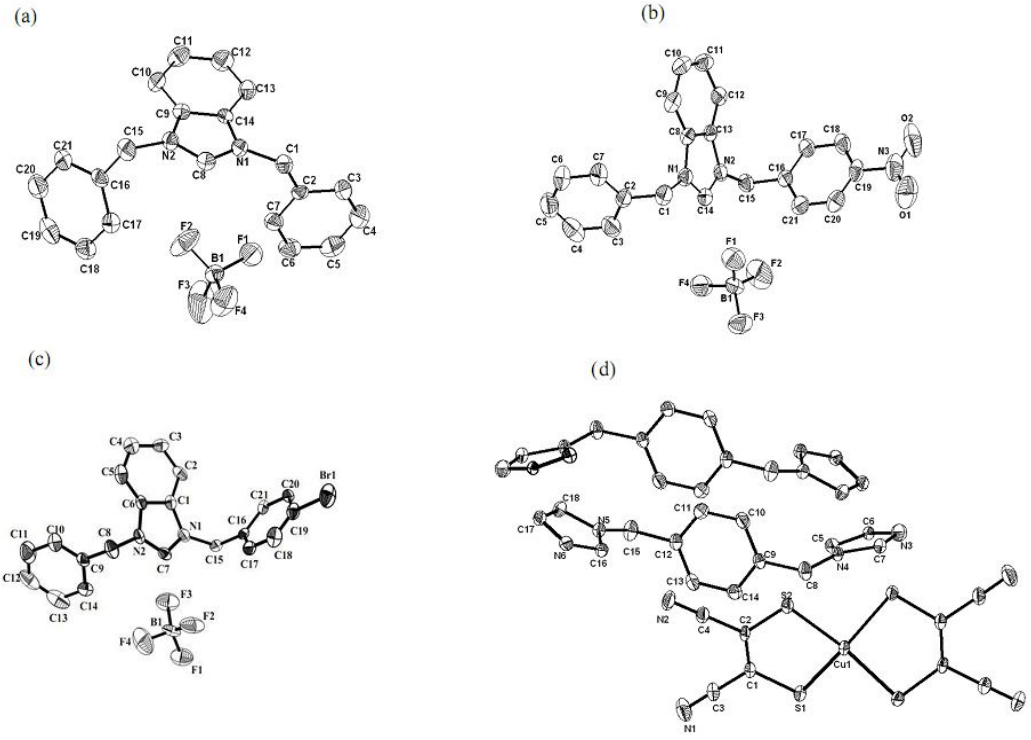


**Figure 3.11.** Ortep diagrams of (a)–(c) compounds **a**–**c**, and (d) compound **1**.

**Compound $[Hb]_2[Cu(mnt)_2]$ (1).** Compound **1** crystallizes in monoclinic system with a space group *C*2/*c*. The thermal ellipsoidal plot of the full molecule is shown in Figure 3.11(d), in which relevant asymmetric unit contains half of the molecule of compound $[Hb]_2[Cu(mnt)_2]$ (represented as labeled atoms). The basic crystallographic data for compound **1** are described in Table 3.7. The overall charge of this Cu(II) complex anion $[Cu(mnt)_2]^{2-}$ in compound **1** as expected is –2, and this anionic charge is compensated by a two $[Hb]^+$ cations. The cation is formed in-situ in methanol solution by protonation of one of the imidazole rings, and further it was confirmed by the broad peak at $\delta$ 8.62 ppm in its $^1$H NMR spectra as shown in Figure 3.12. In the crystal structure, the geometry around copper ion ($Cu^{2+}$) is distorted square planar, in which the copper ion is surrounded by four sulfur atoms of two $mnt^{2-}$ ligand with a dihedral angle of 32.43° between two chelated rings in compound **1**, which is not uncommon to the metal based dithiolene complexes. The non-planarity around the metal ion is caused by dimerization *via* M···S interactions as observed in similar other complexes, $[RBzPy]_2[Fe_2(mnt)_4]$, $[Et_4N]_2[Mn_2(edt)_4]$, $Co_2[S_2C_2(CF_3)_2]_4$.[17a-d] Deviation from planarity were also found in copper based dithiolene complexes $[ClBzPy]_2[Cu(mnt)_2]$, $[DABCOH]_2[Cu(mnt)_2]$ (DABCOH = monoprotonated 1,4-diazabicyclo-[2,2,2]octane) and [TBA][Cu(dcmdtcroc)$_2$] (dcmdtcroc = dithiodicyanomethanecroconato) with dihedral angeles of 27°, 34° (one is mentioned among three) and 36°, respectively.[17e,f] These deviations are generally explained by the weak supramolecular interactions between anion and cations through S···H, N···H interactions. Here, we present a distorted square-planar geometry around the $Cu^{2+}$ ion, caused by the supramolecular interactions between cation and anions through all possible hydrogen bonding sites in the ion-pair complex **1**. In the five member chelated ring, the average Cu–S, C–S, C=C bond lengths and S–Cu–S bond angles are 2.268 (11), 1.736 (4), 1.348 (6) Å and 91.89°, respectively.

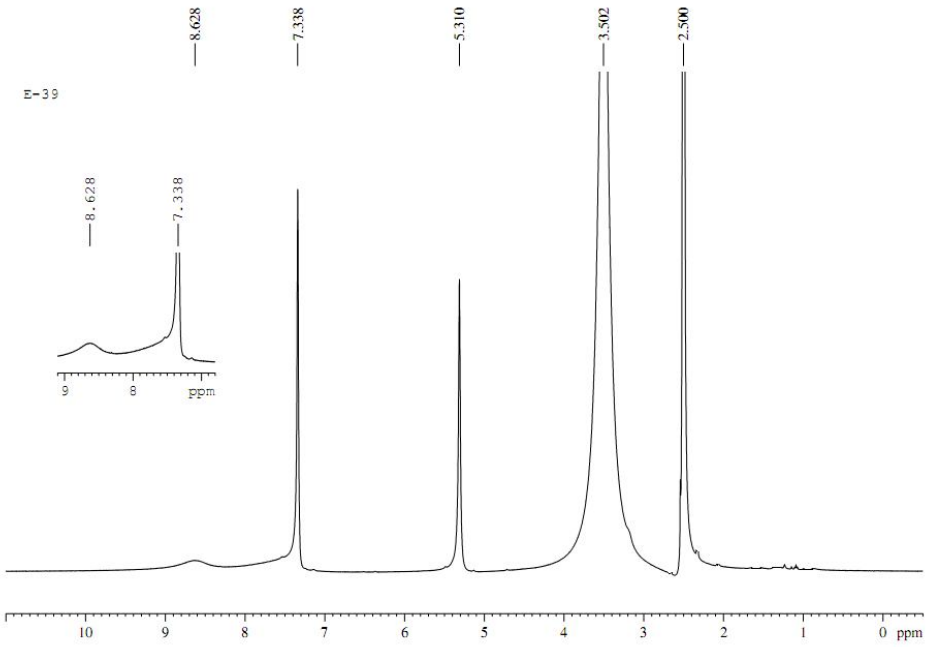


**Figure 3.12.** $^{1}$H NMR spectrum of the compound **1**.

The molecular packing of ion-pair complex **1**, has been characterized by C–H···N hydrogen bonding interactions between cation of the aromatic ring and anion of the $[Cu(mnt)_2]^{2-}$ complex anion, this interactions results in a 2-D supramolecular network (the hydrogen atom on the nitrogen of the cation has not been located) as shown in Figure 3.13(a). Based on CSD literature search on organic molecules[18a,b] and metal based complexes,[18c,d] there are very few reports of C–H···N interactions with H···N distance in the range of 1.60 – 1.80 Å. The relevant ∠CHN bond angle is in the range of 66 – 179°. So far, the shortest H···N distance of 1.79 Å and the shortest ∠CHN bond angle of 67°, reported in the literature, is based on metal dithiolene ion-pair complex.[18e] Some of these reported C–H···N bond distances and corresponding angles are summarized in the Table 3.8 that shows the shortest H···N separation in the present study. Based on literature,[18f] the C–H···N contacts with H···N distances and C–H···N angles are in the range of 1.8 – 3.0 Å and 110 – 180° respectively. Interestingly in compound **1**, there are very strong hydrogen bonding interactions between two cations, in which the C(17)···N(6) distance is 2.66 (5) Å (C–H···N, H···N bond distance is 1.74 Å), which is clearly shorter than the sum of van der Waals radii of the involved nulei (1.70 Å for carbon,

1.55 Å for nitrogen), and the C–H···N angle is 174.9° (which corresponds to a almost linear feature). This shortest hydrogen bonding supramolecular interaction leads to a 1-D chain of the cations as shown in Figure 3.13(b). In the crystal structure of compound **1**, there is a centroid-centroid (Cg-Cg) interaction between two five membered rings ($C_{18}N_4C_{17}C_{16}N_3$ and its symmetry equivalents) of the aromatic cations, with 3.52 Å.

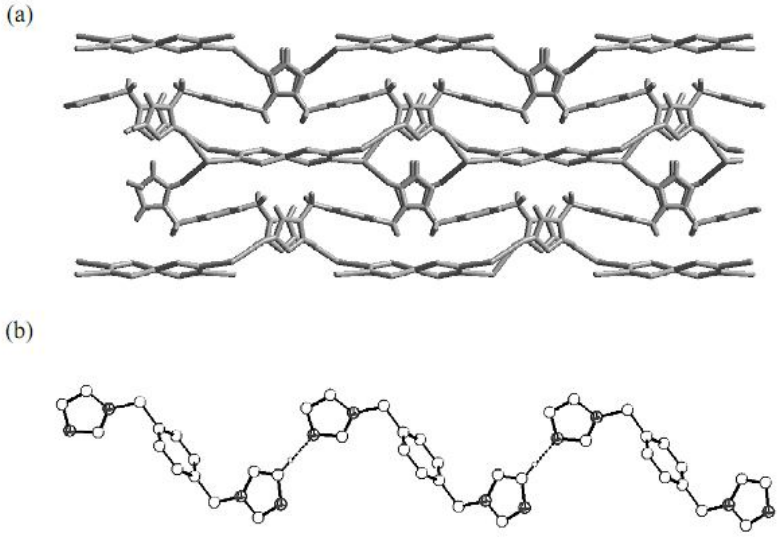


**Figure 3.13**. (a) Supramolecular 2D network between cation and anions through N····H interactions, (b) 1D network between cations N····H interactions.

### 3.3.3. Role of Substituent in Conformational Change of Benzimidazolium cation in Organic cationic receptors and Metal Complexes

In the organic receptor compound **a**, the angle between benzimidazole mean plane and the two phenyl rings (C3-C7, C16-C21 rings) are 86.11, 78.01° and the angle between mean planes for two phenyl rings (C3-C7 and C16-C21) is 50.77°. This indicates the two phenyl rings are not in the parallel to each other as well as one of these phenyl rings (C3-C7) is nearly perpendicular to the benzimidazole mean plane. The torsion angle between two phenyl rings with respect to each other is 5.49°, as shown in Table 3.9. The hydrogen atoms at *p*-position with the labeling atoms H5, H19 are in the two phenyl rings (C2-C7, C16-C21). Among these two phenyl rings, one ring (C2-C7) has C5–H5····Cg1 (Cg1 = C9-C14 ring), another ring (C16-C21) acts as centroid (Cg2) and it has C12–H12····Cg2 interaction with a distance of 3.229 Å, 3.302 Å respectively. When these phenyl rings change their orientation

to trans e.g., in metal complex **1a**, the angle between these two phenyl rings (C6-C11, Cg3 = C20-C25) with respect to benzimidazole ring mean plane changes to 84.87°, 71.84° respectively, and the angle between two phenyl rings changes to 85.55°. This indicates that these two phenyl rings are nearly perpendicular to each other after change their orientation from cis to trans. The torsion angle between two phenyl rings with respect to each other is 166.88°. In the metal complex, the *p*-position hydrogen atoms with the labeling atoms are H9, H23 in the two phenyl rings (C6-C11, C20-C25). Interestingly, in the metal complex, there are no C–H····π interactions to the hydrogen atoms in the *p*-positions as described in organic receptor **a**. Additionally among the two phenyl rings, the ring (C20-C25) acts as centroid (Cg3) for the H14····Cg3, H19A····Cg3 and H19B····Cg3 interactions with a distances of 3.072, 3.326 and 3.171 Å respectively. A π ····π stacking interactions between the two phenyl rings (C13-C18) of adjacent cations is also observed in the crystal packing diagram.

One of the *p*-position of the hydrogen atom is replaced by the nitro group; it gives an organic receptor compound **b**. The torsion angle between two phenyl rings (Cg4 = C16-C21, Cg5 = C2-C7) with respect to each other is 177.86°. The angle between these two phenyl rings with respect to mean plane of benzimidazole ring is 75.23 and 70.79° respectively. In this compound, no C–H····π interactions are observed with the hydrogen atom at *p*-position (C5–H5). However, these two phenyl rings act as centroid for the C–H····π (H7····Cg4, H9····Cg4 and H20····Cg5) interactions within the range of 3.100–3.795 Å. Along with this, there are also π····π stacking interactions, that are present between the centroids of phenyl rings Cg4····Cg4 with a distance of 3.747 Å. When the orientation of these two phenyl rings are altered to cis (with an torsion angle 16.51°) in the metal complex **1b**, now the angle between these two rings (C6-C11, C20-C25) with respect to the mean plane of benzimidazole ring changed to 66.92°, 80.66° respectively, and the angle between mean planes of two phenyl rings becomes 68.86°. In this complex, there is no C–H····π interactions with the hydrogen atom at *p*-position from phenyl ring (C20-C25), even though this ring acts as centroid for the C10–H10····Cg interaction with a distance of 3.048 Å. When we compare the situation of the organic receptor compound **b** with metal complex **1b**, there are very less C–H····π interactions. In this metal complex **1b**, we could not find any π····π stacking interactions between the nitro substituent group of phenyl rings (C6-C11), because the two phenyl rings

(C6-C11, C20-C25) attached to the X1, X2 positions are in the cis alignment. In the metal complex **2b**, the angle between two phenyl rings (C6-C11, C20-C25) is 82.67°. This angle indicates that these two phenyl rings are nearly perpendicular to each other; due to this in metal complex **2b**, we can observe a π····π stacking interactions between the two phenyl rings (C20-C25); in addition to this, there are few C–H····π interactions are also present.

Bromo group is substituted instead of hydrogen atom at *p*-position at one of the phenyl rings in the organic receptor compound **a**, giving rise to a new ligand compound **c**. The angle between two phenyl rings (Cg6 = C9-C14, Cg7 = C16-C21) with respect to the mean plane of benzimidazole ring is 72.03° and 76.39°. The two phenyl rings are situated in a trans alignment with an torsion angle of 177.64° and the angle between these two rings is 80.73°. In the compound **c**, *p*-position atoms are H12 and Br1 in the C9-C14 and C16-C21 phenyl rings respectively. There is only one *p*-position interaction *i.e.* C19–Br1····Cg8 (Cg8 = C1-C6 ring) with a distance of 3.597 Å. The two phenyl rings act as centroid for the C–H····π interactions of H20····Cg6 and H10····Cg7 with a distances of 3.208 Å and 3.824 Å respectively. Apart from these, there are additional π····π stacking interactions, that are observed between the Cg7····Cg7 with a distance of 3.803 Å. When tetrafluoroborate anion was replaced by the $[Cu(mnt)_2]^{2-}$ giving rise to a new metal complex **1c** and the two phenyl rings (Cg9 = C20-C25, Cg10 = C13-C18) are situated in the trans alignment with a 164.89° torsion angle. The angle between these two rings with respect to the mean plane of benzimidazole ring is 88.36°, 74.08° and the angle between these two rings is 77.90°. The *p*-position atoms are (H23, Br1) attached to the two phenyl rings (Cg9 and Cg10) respectively. When we consider the angle (76.39°, 74.08°) between the phenyl ring and the mean plane of benzimidazole ring in the organic receptor compound **c** and metal complex **1c**, the orientation/movement of the bromo substituted phenyl rings (Cg7 and Cg10) are not much influenced even after forming complex. But, the other phenyl ring (Cg9) changes its rotation with a difference of ~16°. Due to this orientation, an extra π····π stacking interaction (compared to organic receptor compound **c**) between the two centroids (Cg9····Cg9) of the phenyl rings is observed including the Cg10····Cg10 interactions with a distance of 3.866 Å, 3.762 Å. In this situation, no interactions with the *p*-position of the atoms (H23, Br1) are observed. However these two phenyl rings act as centroids and gives a C–H····π interactions (H9····Cg9, H7····Cg10) with a

distance of 3.321 and 3.021 Å respectively. Whereas in nickel metal complex **2c**, the angle between two phenyl rings (C12-C17, C20-C25) with respect to the mean plane of benzimidazole ring is 73.33°, 79.54°. The bromo substituted phenyl ring (C20-C25) angle changes to small (~3°) and the other phenyl ring angle is not much rotated (~1°) from the organic receptor compound **c**. Hence, in this complex **2c**, we can't find any π····π stacking interactions, but some C–H····π interactions are observed.

A prominent feature has been observed in the metal-bis(dithiolene) complexes **1a**–**1c** exhibiting Z-shaped non-planar geometry with the ligand fragment bending away from the CuS4 plane with a dihedral angle of 1.94, 16.63 and 3.92 ° respectively (Scheme 3.4). These values are comparable to those of known copper dithiolene complexes,[19] which indicates that non-planar geometry of metal dithiolene complexes depends on the nature of substituent group at *p*-position of the phenyl ring in the organic receptor ligand.

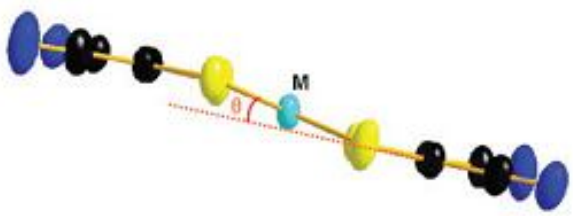


**Scheme 3.4.** Z-shaped nonplanar geometry

### 3.3.4. Theoretical Calculations

To determine the stability of the benzimidazolium cations in different conformations presented in organic receptors and metal complexes in the title compounds, theoretical calculations have been performed, as described in Table 3.10. The molecular geometries of only the ligand were taken from the CIF files of the compounds and the single point calculations have been carried out by using B3LYP with 6-311g** basis set employing the G03 suite of program.[20] As shown in the table the cations $[Bz,H\text{-}BzBimy]^+$, $[Bz,NO_2\text{-}BzBimy]^+$ have almost same energy values (in hartree unit) in both cis and trans conformations in organic receptor and metal complexes respectively. In a similar way, the energy values of the cation $[Bz,Br\text{-}BzBimy]^+$ are almost equivalent in the organic receptor and metal complexes. The theoretical calculations show that the energy barrier to transform from one conformation to another is very less, so that the cation can exist in different

conformations in organic receptors and metal complexes depending upon the supramolecular interactions and short intermolecular contacts due to packing.

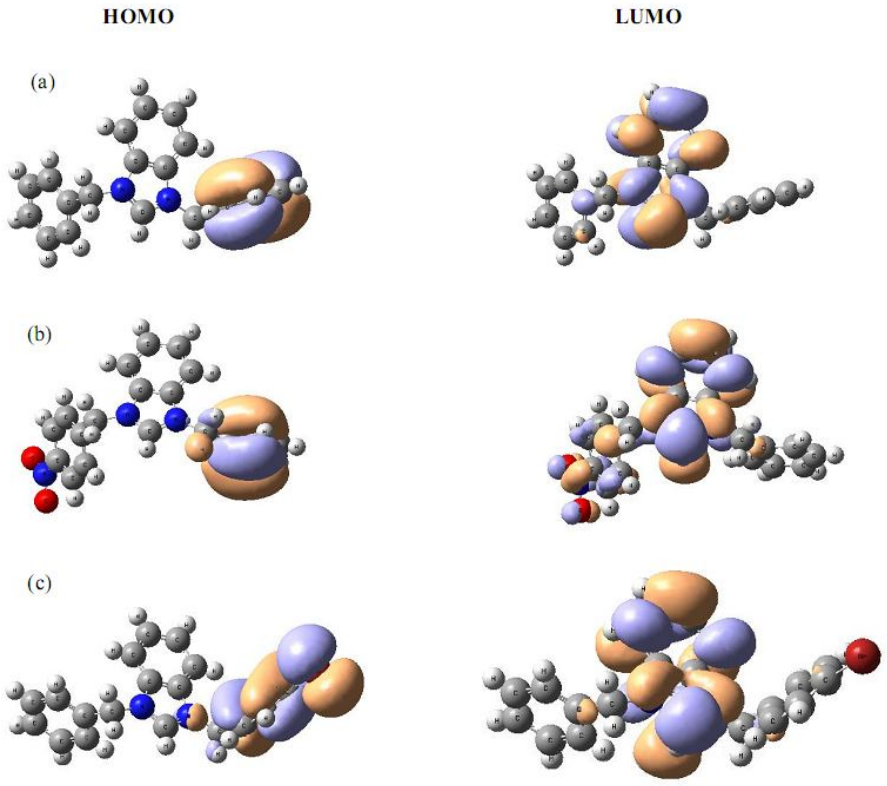


**Figure 3.14.** HOMO and LUMO molecular orbitals of the (a)-(c) compounds **1a–1c**.

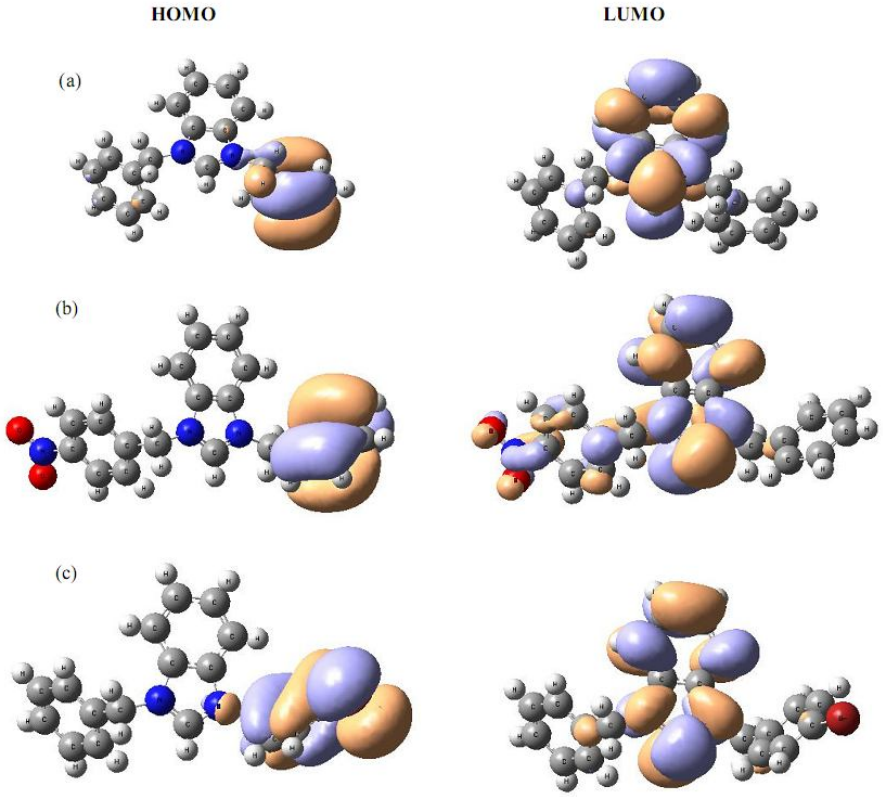


**Figure 3.15.** HOMO and LUMO molecular orbitals of the (a)–(c) compounds **a–c**.

### 3.3.5. Spectroscopic and Electronic Characterization

**Electronic Absorption Spectra.** UV-vis absorption spectra of all these complexes were measured in acetonitrile solutions, this is especially similar to those reported in literatures for other metal dithiolene $[M(mnt)_2]^{n-}$ complexes.[21a-c] For the entire ion-pair complexes **1a-c** and **2a-c**, we have observed five absorption bands in the region between 200-1300 nm, in which there is four intense bands due to allowed tranisiton. Bands at 270, 370 nm are assigned due to the L → M charge transfer transitions of $[M(mnt)_2]^{2-}$ (M = Cu(1), Ni(2)). Bands at 320 nm and 470 nm can be attributed as L → L* and M → L transition, respectively.

Ion-pair dithiolene complexes $[Bz,R\text{-}BzBimy]_2[M(mnt)_2]$ **[**R= H, $NO_2$**,** Br; M= Cu, Ni**]** exhibit strong and moderate absorption bands for nickel and copper complexes in the region of 862 nm and 1210 nm respectively (Figure 3.16). According Langford and Gray,[21a,d,e] metal based dithiolene complexes show an absorption band at 855 nm ($\varepsilon$ = 30 $M^{-1}$ $cm^{-1}$), 1205 nm ($\varepsilon$ = 94 $M^{-1}$ $cm^{-1}$) for nickel, copper dithiolene ion-pair complexes

respectively. We found, that the H-substituted benzimidazolium cation for complex **2a** shows the absorption band at 862 nm in $CH_3CN$ solution ($\varepsilon$ = 683 $M^{-1}$ $cm^{-1}$), whereas for nitro, bromine substituted nickel based **2b**, **2c** ion-pair complexes, the absorption maxima is at 862 nm with less molar extension coefficient ($\varepsilon$ = 308, 670 $M^{-1}$ $cm^{-1}$) compared to the complex **2a**. According to Xiao-Ming Ren *et.al*, there is negligible substituent effect on the LUMO energy level of the cation, so the lower frequency absorbance broad band (~862 nm) can be assigned to combined transitions of partial forbidden d–d, allowed d–π* (MLCT in the $[Ni(mnt)_2]^{2-}$ anion) and π–π* (in the $mnt^{2-}$ ligand) as well as the IPCT transition.[21f] In case of copper complexes, the broad and weak absorption bands appear at ~1210, the molar extension coefficients of the near-IR absorption band for copper complexes **1a**, **1b** and **1c** are 91, 51, and 96 respectively. Absorption spectra described here are characteristics of metal-bis(dithiolene) ion-pair complexes and is generally assigned to π→π* transition between the highest occupied molecular orbital (HOMO) and lowest unoccupied molecular orbital (LUMO). In the solid state, compounds **1a—1c** exhibits a broad band at ~1110 nm in its diffuse reflectance spectra, this absorption band is due to the mixture of d–d transition in $[Cu(mnt)_2]^{2-}$ and IPCT transition. These solid state bands are explained by the intermolecular interactions between anions and cations in the ion-pair complexes. Similarly compound **1** also exhibits broad band at ~1205 nm.

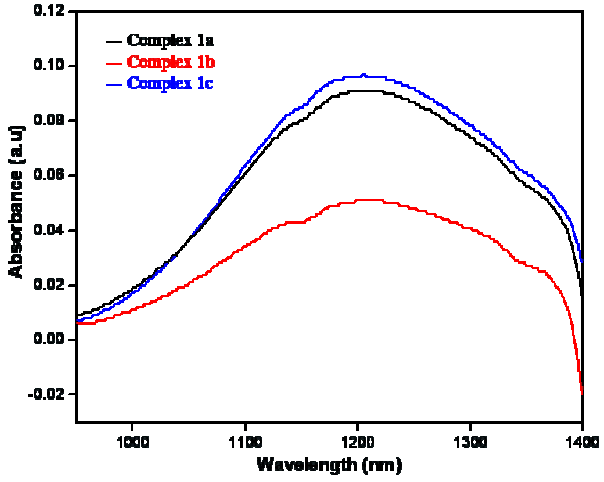


**Figure 3.16.** near-IR absorption spectra of the compounds **1a–1c**.

**3.3.6. Electrochemistry.** The electrochemical behavior of the complexes **1a-1c** and **2a-2c** were recorded in acetonitrile solutions, each containing 0.10 M $[Bu_4N][ClO_4]$ as supporting electrolyte at a platinum working electrode. The results of these complexes are summarized in Table 3.11. Representative cyclic voltammograms for the compounds **1a** and **2a** have been shown in Figure 3.17. All the copper and nickel compounds (**1a**–**1c** and **2a**–**2c**) exhibit a reversible oxidative response at $E_{1/2}$ = +0.44 V, +0.48 V, 0.49 V and +0.42 V, +0.30, +0.24 V vs Ag/AgCl respectively. The present electrochemical data can be explained on the basis of Scheme 4, proposed by McCleverty, Hoyer and others.[22,23] According to this scheme, the oxidative response for compounds **1a**–**1c** and **2a**–**2c** are ascribed due to the couple $[M^{III}(mnt)_2]^{-1}/[M^{II}(mnt)_2]^{-2}$ (M= Cu, Ni). All these oxidative response values of ion-pair dithiolene complexes are comparable to the reported electrochemical data;[12b,24] from this we can say that there is no change in oxidative response by changing the different substituents of counter cation in ion-pair dithiolene complexes. Compound **1** exhibit an quasi-reversible oxidative response at $E_{1/2}$ = +0.46 V ($\Delta E$ = 99 mV) *vs* Ag/AgCl.

**Scheme 4.**

$$[ML_2]^{1-} \underset{-e}{\overset{e}{\rightleftharpoons}} [ML_2]^{2-} \underset{-e}{\overset{e}{\rightleftharpoons}} [ML_2]^{3-}$$

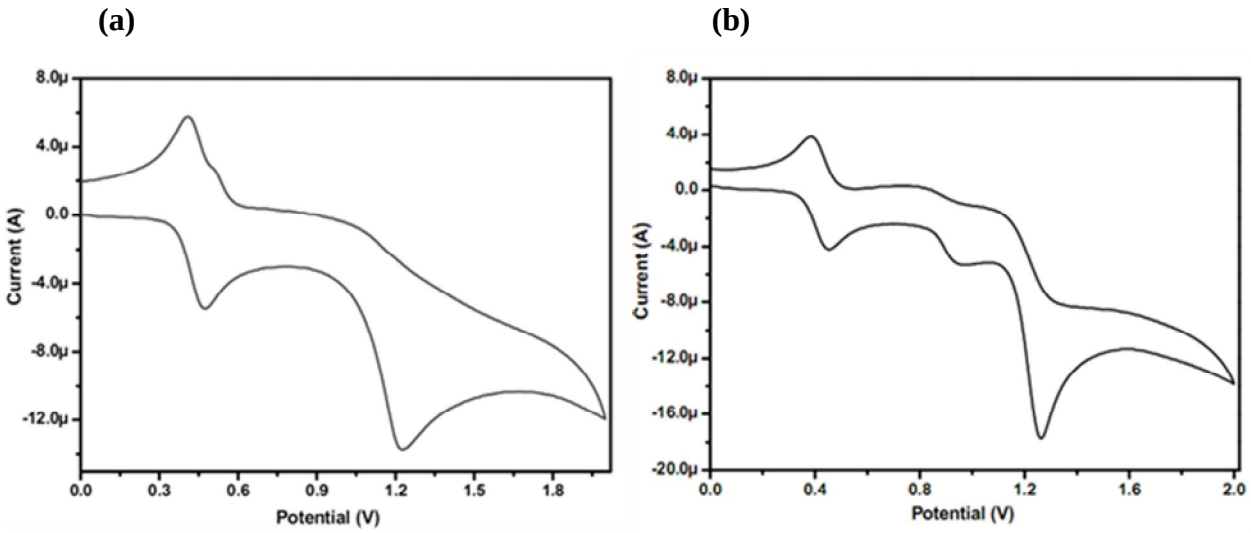


**Figure 3.17.** Cyclic voltammetry of the (a) compound **1a**, (b) compound **2a**.

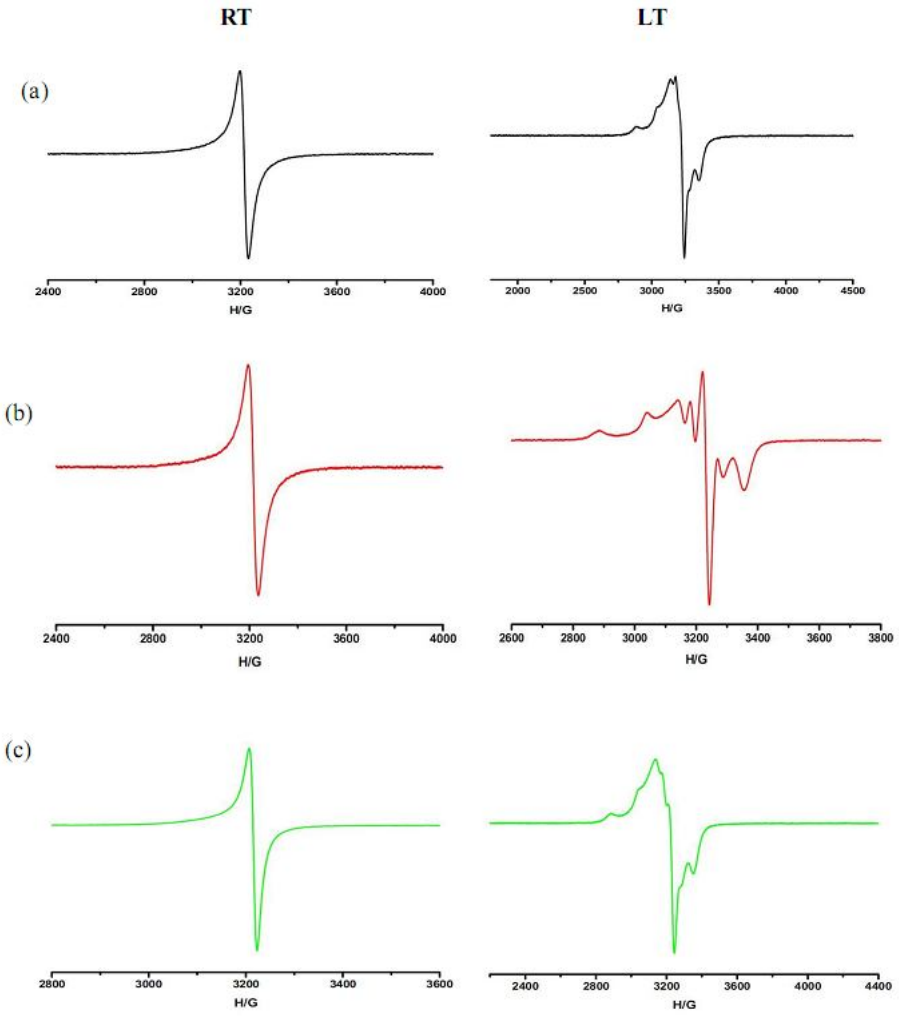


**Figure 3.18.** EPR spectra of the compounds **1a**–**1c** (a) at room temperature, (b) frozen state at liq. nitrogen temperature.

**3.3.7. ESR Spectroscopy**. Figure 3.18 illustrates the representative EPR spectra of complex **1a-1c** in the solid state both at room temperature (Freq. range is: 9155.559 to 9161.153 MHz, Field range is: 324.00 to 400.00 mT) and frozen state at liquid nitrogen temperature (Freq. range: 9135.349 to 3151.168 MHz, Field: 336 mT). All the copper complexes exhibit similar type of peak at room temperature. The ligand hyperfine structure gives an straight information about the environment of the electronic ground state of the complex and the extent to electron spin delocalization over ligand orbitals.[25] We have observed hyperfine splitting in the EPR spectra of compounds **1a-1c** in frozen state at liquid nitrogen temperature. HOMO level of the

$[Cu(mnt)_2]^{2-}$ consists of the $3d_{xy}$ orbital of copper and hybrids of 3s, $3p_x$, and $3p_y$ orbitals of sulfur atoms. These atomic orbitals are overlapped with the $p_z$ orbitals of copper and sulfur, and such combination has a direct effect on the copper hyperfine splitting.[26] The g values of copper complexes **1a**−**1c** at room temperature are $g_\perp$ = 2.034, 2.033 and 2.034 respectively. These values are comparable to those ($g_\parallel$ = 2.090, $g_\perp$ = 2.024 ; and $g_1$ = 2.089, $g_2$ = 2.024, $g_3$ = 2.017) of the non-planar Cu(II)-dithiolene complexes, $[mb]_2[Cu(mnt)_2].Me_2CO$ (mb = methylene blue), $[(Ph)_4As]_2[Cu(mnt)_2]$, respectively.[27] These g values are also equal to those ($g_\parallel$ = 2.08, $g_\perp$ = 2.02; $g_\parallel$ = 2.210, $g_\perp$ = 2.018 ($g_{av}$ = 2.076); and $g_\parallel$ = 2.095, $g_\perp$ = 2.033) of the planar copper-bis(dithiolene) complexes,[28] $[Bu_4N]_2[Cu(mnt)_2]$, $[TBA]_2[Cu(bcd)_2]$ ($bcd^{2-}$ = 1-benzoyl-1-cyanoethylene-2,2-dithiolate) and $[Co(phen)_3][Cu(mnt)_2]$. From these information it can be concluded that there is an unpaired electron in the $d_{x2-y2}$ orbital of copper (II) in the ground state.[29] Similarly type of EPR spectra has been observed for the compound **1**.

## 3.4. Conclusion

In summary, we have prepared copper and nickel based ion-pair dithiolene complexes with different substituent groups at *p*-position in the organic receptor ligands. The conformation of the benzimidazolium cations have been modulated by changing the anions from spherical $BF_4^-$ to the planar $mnt^{2-}$. This type of conformational modulation has been observed in the organic receptors **a**, **b** and metal-bis(dithiolene) complexes **1a**, **1b** and **2a**, **2b**. Staggered/eclipsed hydrogen bonding interactions and other supramolecular interactions are the reasonable factors to control the diversity of cation conformation in organic receptors as well as in metal complexes. However, in metal complexes **1c** and **2c**, no conformational change in the benzimidazolium cation is observed from the organic receptor **c** (i.e. $BF_4^-$ salt as anion). In these two complexes we can observe the C–H···π interactions, that are present between one of the two phenyl groups (which are attached to the X1, X2 positions) and chelate ring from $[M(mnt)_2]^{2-}$ anion. The crystal packing and the orientation of the phenyl groups also depends on the C–H···π interaction. The topological representation clearly indicates the transformation of the benzimidazolium cation between organic receptor compounds (**a**, **b**) and metal complexes (**1a**, **1b**, **2a** and **2b**). All the copper complexes show a

Z-shaped non-planar geometry with different angles which also depends on the substituent groups at *p*-position of phenyl groups.

In compound **1**, the cation is prepared in-situ from MeOH solution, in which only one imidazole ring of **b** (1,4-bis((1H-imidazol-1-yl)methyl)benzene) was protonated. We have demonstrated the shortest C–H···N hydrogen bonding contact among the cations in the crystal structure of compound **1** as far as the relevant literature is concerned. Compound **1** exhibits a broad absorption in the near-IR region at 1205 nm in its diffused reflectance spectrum. The EPR spectroscopy reveals a typical tetragonal feature for a Cu(II) ion in its solid state and hyperfine interactions in solution state. The electrochemical studies show both oxidative and reductive responses corresponding to $Cu^{III}$ / $Cu^{II}$ and $Cu^{II}$ / $Cu^{I}$ couples.

**Table 3.1.** Crystallographic data for copper complexes **1a**, **1b** and **1c**.

| | **Compound 1a** | **Compound 1b** | **Compound 1c** |
|---|---|---|---|
| Empirical formula | $C_{50}H_{38}CuN_8S_4$ | $C_{50}H_{36}CuN_{10}O_4S_4$ | $C_{50}H_{36}Br_2CuN_8S_4$ |
| Formula weight | 942.66 | 1032.72 | 1100.50 |
| Temperature (K) | 298(2) K | 298(2) K | 298(2) K |
| Crystal size (mm) | 0.22 x 0.18 x 0.06 | 0.26 x 0.20 x 0.06 | 0.28 x 0.18 x 0.10 |
| Crystal system | Triclinic | Triclinic | Triclinic |
| space group | *P*-1 | *P*-1 | *P*-1 |
| Z | 1 | 1 | 1 |
| Wavelength(Å) | 0.71073 | 0.71073 | 0.71073 |
| *a* [Å] | 7.850(3) | 9.2802(19) | 7.8620(16) |
| *b* [Å] | 11.924(5) | 10.066(2) | 12.626(3) |
| *c*[Å] | 12.663(5) | 12.719(3) | 13.180(3) |
| α [°] | 77.790(6) | 93.26(3) | 105.262(4) |
| β [°] | 74.257(6) | 91.94(3) | 107.162(4) |
| γ [°] | 84.457(6) | 97.13(3) | 97.026(4) |
| Volume[$Å^3$] | 1114.1(8) | 1176.0(4) | 1177.3(5) |
| Calculated density($Mg/m^{-3}$) | 1.405 | 1.458 | 1.552 |
| Reflections collected/ unique | 10839/3974 | 11180 / 4119 | 11237 / 4152 |
| R(int) | 0.0228 | 0.0374 | 0.0492 |
| F(000) | 487 | 531 | 555 |
| Max. and min. transmission | 0.9579 and 0.8570 | 0.9592 and 0.8390 | 0.7965 and 0.5550 |
| Θ range for data collection | 1.70 to 25.28 | 1.61 to 25.09 | 1.71 to 25.11 |
| Refinement method | Full-matrix least-squares on F2 | | |
| Data / restraints / parameters | 3974 / 0 / 286 | 4119 / 0 / 313 | 4152 / 0 / 295 |
| Goodness-of-fit on $F^2$ | 1.062 | 1.187 | 1.088 |
| $R_1/wR_2$ [I>2sigma(I)] | 0.0418 / 0.0998 | 0.0969/0.1945 | 0.0598/0.1892 |
| $R_1/wR_2$ (all data) | 0.0465 / 0.1029 | 0.1046/0.1980 | 0.0943/0.2112 |
| Largest diff. peak and hole[$e.Å^{-3}$] | 0.378 and -0.202 | 1.068 and -0.450 | 0.838 and -0.433 |

**Table 3.2.** Crystallographic data for nickel complexes **2a**, **2b** and **2c**.

| | **Compound 2a** | **Compound 2b** | **Compound 2c** |
|---|---|---|---|
| Empirical formula | $C_{50}H_{38}N_8NiS_4$ | $C_{50}H_{36}N_{10}NiO_4S_4$ | $C_{50}H_{36}Br_2N_8NiS_4$ |
| Formula weight | 937.83 | 1027.86 | 1095.64 |
| Temperature (K) | 298(2) K | 298(2) K | 298(2) K |
| Crystal size (mm) | 0.26 x 0.22 x 0.14 | 0.28 x 0.20 x 0.08 | 0.40 x 0.36 x 0.12 |
| Crystal system | Triclinic | Triclinic | Triclinic |
| space group | *P*-1 | *P*-1 | *P*-1 |
| Z | 1 | 1 | 1 |
| Wavelength(Å) | 0.71073 | 0.71073 | 0.71073 |
| *a* [Å] | 7.8973(9) | 9.998(5) | 7.992(3) |
| *b* [Å] | 11.9105(13) | 11.735(6) | 12.788(5) |
| *c*[Å] | 12.6120(14) | 12.104(6) | 13.096(5) |
| α [°] | 77.172(2) | 94.856(8) | 64.364(6) |
| β [°] | 74.513(2) | 99.797(8) | 87.050(7) |
| γ [°] | 85.057(2) | 113.317(7) | 84.330(7) |
| Volume[$Å^3$] | 1114.2(2) | 1266.9(11) | 1200.7(8) |
| Calculated density($Mg/m^{-3}$) | 1.398 | 1.347 | 1.515 |
| Reflections collected/ unique | 10639 / 3913 | 12409 / 4698 | 11414/ 4184 |
| R(int) | 0.0340 | 0.0611 | 0.0231 |
| F(000) | 486 | 530 | 554 |
| Max. and min. transmission | 0.9610 and 0.7573 | 0.9534 and 0.8486 | 0.7710 and 0.4616 |
| Θ range for data collection | 1.71 to 25.00 | 1.73 to 25.72 | 1.72 to 24.94 |
| Refinement method | Full-matrix least-squares on $F^2$ | | |
| Data / restraints / parameters | 3913 / 0 / 286 | 4698 / 0 / 313 | 4184/ 0 / 295 |
| Goodness-of-fit on $F^2$ | 0.981 | 0.984 | 1.033 |
| $R_1/wR_2$ [I>2sigma(I)] | 0.0452/ 0.1015 | 0.0534/0.1272 | 0.0422/0.1089 |
| $R_1/wR_2$ (all data) | 0.0688/0.1110 | 0.0868/0.1412 | 0.0541/0.1174 |
| Largest diff. peak and hole[$e.Å^{-3}$] | 0.477 and -0.175 | 0.509 and -0.269 | 0.418 and -0.950 |

**Table 3.3.** Hydrogen bonding parameters for compounds **1a–1c** [Å and deg.].

| D-H...A | d(D-H) | d(H...A) | d(D...A) | <(DHA) |
|---|---|---|---|---|
| **Compound 1a** | | | | |
| C(16)-H(16)...N(1)#2 | 0.93 | 2.59 | 3.508(4) | 168.1 |
| C(5)-H(5B)...N(2)#3 | 0.97 | 2.75 | 3.520(4) | 137.2 |
| C(18)-H(18)...N(2)#3 | 0.93 | 2.44 | 3.199(4) | 138.4 |
| C(19)-H(19B)...S(1) | 0.97 | 2.86 | 3.762(3) | 155.4 |
| **Compound 1b** | | | | |
| C(14)-H(14)...S(1)#4 | 0.93 | 2.86 | 3.615(8) | 138.8 |
| C(5)-H(5B)...N(2)#5 | 0.97 | 2.63 | 3.494(11) | 148.1 |
| C(25)-H(25)...O(1)#6 | 0.93 | 2.57 | 3.446(12) | 157.6 |
| C(22)-H(22)...N(2)#7 | 0.93 | 2.72 | 3.529(11) | 145.8 |
| **Compound 1c** | | | | |
| C(10)-H(10)...Br(1)#8 | 0.93 | 3.12 | 3.960(8) | 151.6 |
| C(14)-H(14)...N(1)#9 | 0.93 | 2.71 | 3.429(11) | 134.7 |
| C(12)-H(12B)...S(1)#2 | 0.97 | 2.76 | 3.692(8) | 162.1 |
| C(15)-H(15)...S(1)#2 | 0.93 | 2.86 | 3.727(7) | 155.8 |
| C(12)-H(12A)...Br(1)#8 | 0.97 | 3.13 | 4.084(8) | 166.4 |
| C(5)-H(5)...N(2) | 0.93 | 2.41 | 3.069(10) | 128.0 |

Symmetry transformations used to generate equivalent atoms:
#2, -x+1, -y+1, -z+1; #3, -x+2, -y+1, -z; #4, x-1, y, z+1; #5, -x+1, -y, -z+1; #6, -x, -y, -z+1; #7, x, y+1, z; #8, x+1, y, z; #9, x, y, z-1.

**Table 3.4.** Crystallographic data for the compounds **a**, **b** and **c**.

| | **Compound a** | **Compound b** | **Compound c** |
|---|---|---|---|
| Empirical formula | $C_{21}H_{19}BF_4N_2$ | $C_{21}H_{18}BF_4N_3O_2$ | $C_{21}H_{18}BrBF_4N_2$ |
| Formula weight | 386.19 | 413.19 | 465.08 |
| Temperature (K) | 298(2) K | 298(2) K | 298(2) K |
| Crystal size (mm) | 0.16 x 0.14 x 0.10 | 0.20 x 0.18 x 0.12 | 0.18 x 0.12 x 0.10 |
| Crystal system | Monoclinic | Triclinic | Triclinic |
| space group | *P*2(1)/*c* | *P*-1 | *P*-1 |
| Z | 4 | 2 | 2 |
| Wavelength(Å) | 0.71073 | 0.71073 | 0.71073 |
| *a* [Å] | 13.476(16) | 9.857(3) | 9.997(2) |
| *b* [Å] | 9.423(11) | 10.493(3) | 10.632(2) |
| *c*[Å] | 19.121(17) | 11.289(3) | 11.501(2) |
| α [°] | 90.00 | 75.795(5) | 74.08(3) |
| β [°] | 127.585(5) | 67.234(5) | 66.49(3) |
| γ [°] | 90.00 | 77.377(5) | 75.69(3) |
| Volume[$Å^3$] | 1924.3(4) | 1033.8(5) | 1064.7(3) |
| Calculated density($Mg/m^{-3}$) | 1.333 | 1.385 | 1.451 |
| Reflections collected/ unique | 17200/3248 | 9696/3555 | 6466/3709 |
| R(int) | 0.0781 | 0.0362 | 0.0749 |
| F(000) | 800 | 444 | 468 |
| Max. and min. transmission | 0.9896 and 0.9384 | 0.9865 and 0.9776 | 0.8271 and 0.7178 |
| Θ range for data collection | 1.91 to 25.03 | 1.99 to 25.14 | 1.97 to 25.45 |
| Refinement method | Full-matrix least-squares on F2 | | |
| Data / restraints / parameters | 3248 / 0 / 253 | 3555 / 0 / 280 | 3709 / 0 / 262 |
| Goodness-of-fit on $F^2$ | 1.099 | 1.002 | 0.913 |
| $R_1/wR_2$ [I>2sigma(I)] | 0.0995 / 0.1866 | 0.0672/0.1536 | 0.0891/0.1891 |
| $R_1/wR_2$ (all data) | 0.1528 / 0.2130 | 0.1264/0.1841 | 0.2321/0.2746 |
| Largest diff. peak and hole[$e.Å^{-3}$] | 0.324 and -0.219 | 0.296 and -0.188 | 0.672 and -0.538 |

**Table 3.5.**Hydrogen bonding parameters for compounds **2a**–**2c** [Å and deg.].

| D-H...A | d(D-H) | d(H...A) | d(D...A) | <(DHA) |
|---|---|---|---|---|
| | **Compound 2a** | | | |
| C(19)-H(19B)...S(1) | 0.97 | 2.89 | 3.781(3) | 153.5 |
| C(6)-H(6)...N(1)#2 | 0.93 | 2.61 | 3.524(4) | 168.6 |
| C(11)-H(11)...N(2)#3 | 0.93 | 2.49 | 3.207(4) | 134.0 |
| C(12)-H(12B)...N(2)#3 | 0.97 | 2.77 | 3.502(4) | 132.4 |
| | **Compound 2b** | | | |
| C(13)-H(13)...N(1)#4 | 0.93 | 2.75 | 3.665(6) | 169.6 |
| C(5)-H(5B)...N(1)#4 | 0.97 | 2.78 | 3.685(6) | 155.4 |
| C(18)-H(18)...N(2)#5 | 0.93 | 2.34 | 3.223(6) | 157.6 |
| C(19)-H(19A)...O(2)#6 | 0.97 | 2.38 | 3.341(6) | 173.3 |
| | **Compound 2c** | | | |
| C(19)-H(19B)...S(1)#1 | 0.97 | 2.95 | 3.802(4) | 147.7 |
| C(22)-H(22)...N(1)#7 | 0.93 | 2.54 | 3.443(5) | 162.6 |
| C(13)-H(13)...N(1)#8 | 0.93 | 2.51 | 3.344(7) | 149.9 |
| C(15)-H(15)...N(1)#9 | 0.93 | 2.53 | 3.380(8) | 151.5 |

Symmetry transformations used to generate equivalent atoms:
#1 -x+1,-y+1,-z+1; #2 x,y,z+1; #3 x+1,y,z; #4 -x+1,-y,-z+1; #5 x-1,y,z; #6 x+1,y+1,z; #7 x+1,y-1,z #8 -x+1,-y+2,-z; #9 -x,-y+2,-z.

**Table 3.6.** Hydrogen bonding parameters for organic receptors **a**–**c** [Å and deg.].

| D-H...A | d(D-H) | d(H...A) | d(D...A) | <(DHA) |
|---|---|---|---|---|
| **Compound a** | | | | |
| C(10)-H(10)...F(3)#1 | 0.93 | 2.60 | 3.447(7) | 152.5 |
| C(1)-H(1B)...F(4)#2 | 0.97 | 2.55 | 3.504(6) | 168.5 |
| C(4)-H(4)...F(3)#3 | 0.93 | 2.57 | 3.339(8) | 140.1 |
| C(1)-H(1A)...F(1) | 0.97 | 2.49 | 3.253(6) | 135.7 |
| C(8)-H(8)...F(1) | 0.93 | 2.53 | 3.241(6) | 133.4 |
| C(8)-H(8)...F(2) | 0.93 | 2.23 | 3.096(6) | 154.3 |
| C(15)-H(15B)...F(2)#4 | 0.97 | 2.35 | 3.132(5) | 137.4 |
| C(19)-H(19)...F(3)#5 | 0.93 | 2.61 | 3.264(8) | 127.7 |
| **Compound b** | | | | |
| C(1)-H(1B)...F(4) | 0.97 | 2.45 | 3.333(4) | 150.7 |
| C(1)-H(1B)...F(1) | 0.97 | 2.70 | 3.503(4) | 140.7 |
| C(14)-H(14)...F(4) | 0.93 | 2.49 | 3.261(4) | 140.8 |
| C(21)-H(21)...F(2) | 0.93 | 2.33 | 3.231(5) | 163.2 |
| C(5)-H(5)...F(1)#6 | 0.93 | 2.52 | 3.446(6) | 175.4 |
| C(3)-H(3)...F(2)#7 | 0.93 | 2.59 | 3.469(5) | 158.2 |
| C(14)-H(14)...F(4)#7 | 0.93 | 2.45 | 3.181(4) | 135.3 |
| C(15)-H(15B)...F(4)#7 | 0.97 | 2.45 | 3.321(4) | 149.4 |
| C(11)-H(11)...F(1)#8 | 0.93 | 2.56 | 3.291(4) | 135.3 |
| C(15)-H(15A)...F(3)#9 | 0.97 | 2.47 | 3.404(4) | 160.8 |
| C(12)-H(12)...F(3)#9 | 0.93 | 2.69 | 3.542(4) | 151.9 |
| C(17)-H(17)...F(3)#9 | 0.93 | 2.57 | 3.404(4) | 149.9 |
| C(12)-H(12)...F(1)#9 | 0.93 | 2.56 | 3.311(4) | 138.7 |
| **Compound c** | | | | |
| C(14)-H(14)...F(4) | 0.93 | 2.59 | 3.421(14) | 148.4 |
| C(7)-H(7)...F(2) | 0.93 | 2.61 | 3.268(12) | 128.5 |
| C(15)-H(15B)...F(2) | 0.97 | 2.40 | 3.285(10) | 152.2 |
| C(12)-H(12)...F(1)#1 | 0.93 | 2.61 | 3.531(14) | 172.5 |
| C(8)-H(8B)...F(2)#2 | 0.97 | 2.56 | 3.410(13) | 146.0 |
| C(17)-H(17)...F(4)#2 | 0.93 | 2.43 | 3.346(12) | 169.5 |
| C(3)-H(3)...F(1)#3 | 0.93 | 2.67 | 3.403(12) | 135.9 |
| C(2)-H(2)...F(1)#4 | 0.93 | 2.56 | 3.299(11) | 137.1 |
| C(15)-H(15A)...F(3)#4 | 0.97 | 2.61 | 3.542(12) | 162.3 |

Symmetry transformations used to generate equivalent atoms:
#1 x,y+1,z; #2 -x+2,y+1/2,-z+3/2; #3 x,-y+1/2,z-1/2; #4 -x+2,-y+1,-z+2; #5 -x+1,y+1/2,-z+3/2; #6 x,y-1,z; #7 -x+1,-y+1,-z+1; #8 -x,-y+1,-z+2; #9 x-1,y,z;

**Table 3.7.** Crystallographic data and structure refinement for compound **1**.

| | |
|---|---|
| Empirical formula | $C_{36}\ H_{30}\ N_{12}\ S_4\ Cu$ |
| Formula weight | 822.50 |
| Temperature (K) | 298(2) |
| Crystal size (mm) | 0.22x 0.18 x 0.16 |
| Crystal system | monoclinic |
| space group | C2/c |
| Z | 4 |
| Wavelength(Å) | 0.71073 A |
| Unit cell dimensions | |
| *a* [Å] | 17.939(3) |
| *b* [Å] | 15.411(3) |
| *c* [Å] | 13.891(3) |
| β [°] | 100.01(3) |
| Volume[$Å^3$] | 3781.8(13) |
| Calculated density($Mg/m^{-3}$) | 1.445 |
| Reflections collected/ unique | 19403/3746 |
| R(int) | 0.0466 |
| F(000) | 1692 |
| Max. and min. transmission | 0.8768 and 0.8361 |
| Theta range for data collection(deg.) | 1.75 to 26.10 |
| Refinement method | Full-matrix least-squares on $F^2$ |
| Data / restraints / parameters | 3746 / 0 / 240 |
| Goodness-of-fit on $F^2$ | 1.082 |
| $R_1/wR_2$ [I>2sigma(I)] | 0.0607/ 0.1393 |
| $R_1/wR_2$ (all data) | 0.0771 / 0.1481 |
| Largest diff. peak and hole | 0.651 and -0.451 $e.Å^{-3}$ |

**Table 3.8.** Selected hydrogen bonds from literature (Å, °)*

| Entry | D–H···A | H···A | ∠DHA | Ref. |
|---|---|---|---|---|
| 1 | C–H···N | 1.61 | 132 | J. Am. Chem. Soc. 129 (2007) 3820. |
| 2 | C–H···N | 1.74 | 114 | Chem. Commun. (2004) 1954. |
| 3 | C–H···N | 1.71 | 102 | Organometallics 27 (2008) 3964. |
| 4 | C–H···N | 1.71 | 135 | Inorg. Chim. Acta. 339 (2002) 461. |
| 5 | C–H···N | 1.77 | 156 | Beilstein J. Org. Chem. 1 (2005) 15. |
| 6 | C–H···N | 1.79 | 66 | Acta Crystallogr. E60 (2004) 960. |
| 7 | C–H···N | 1.74 | 174.9 | Present work |

* Based on CSD literature

**Table 3.9.** Tabulated form of torsion angle in the compounds **a**–**c** and **1a**–**1c**.

| Compound Name | Torsion Angle (°) | Alignment of phenyl rings |
|---|---|---|
| **a** | 5.49 | Cis |
| **b** | 177.86 | Trans |
| **c** | 177.64 | Trans |
| **1a** | 166.88 | Trans |
| **1b** | 16.51 | Cis |
| **1c** | 164.89 | Trans |

**Table 3.10.** Calculated energy values of compounds **1a–1c, 2a–2c** and **a–c**.

| **Cation** | **H(a, 1a, 2a)** | **$NO_2$ (b, 1b, 2b)** | **Br (c, 1c, 2c)** |
|---|---|---|---|
| Organic receptor | 577835.6994(cis) | 706200.1058(trans) | 2192767.2059(trans) |
| Cu-complex | 577834.8353(Trans) | 706202.0653(cis) | 2192769.5060(trans) |
| Ni-complex | 577834.1551(trans) | 706195.5909(cis) | 2192763.1309(trans) |

**Table 3.11.** Cyclic Voltammetry Data*

| **Compound** | **Oxidative response $E_{1/2}$, V($\Delta E_P$, mV)** |
|---|---|
| **1a** | 0.44 (65), 1.23 |
| **1b** | 0.48 (63), 1.23 (61) |
| **1c** | 0.49 (67), 1.22 |
| **2a** | 0.42 (68), 1.26 |
| **2b** | 0.30 (68), 1.16 |
| **2c** | 0.24 (68), 1.04 |

*****Cyclic voltammogram of compounds **1a**, **2a**, **1b**, **2b**, **1c**, and **2c** ($1x10^{-3}$M) in $CH_3CN$

## 3.5. References

(1) (a) Robertson, N.; Cronin, L. *Coord. Chem. Rev*. **2002**, *227*, 93. (b) Jeannin, O.; Clerac, R.; Fourmigue, M. *J. Am. Chem. Soc*. **2006**, *128*, 14649. (c) Uruichi, M.; Yakushi, K.; Yamashita, Y.; Qin, J. *J. Mater. Chem*. **1998**, *8*, 141. (d) Pullen, A. E.; Faulmann, C.; Pokhodnya, K. I.; Cassoux, P.; Tokumoto, M. *Inorg.Chem*. **1998**, *37*, 6714.

(2) (a) Winter, C. S.; Oliver, S. N.; Rush, J. D.; Hill, C. A. S.; Underhill, A. E. *J. Appl. Phys*. **1992**, *71*, 512. (b) Winter, C. S.; Oliver, S. N.; Manning, R. J.; Rush, J. D.; Hill, C. A. S.; Underhill, A. E. *J. Mater. Chem*. **1992**, *2*, 443. (c) Aloukos, P.; Couris, S.; Koutselas, J. B.; Anyfantis, G. C.; Papavassiliou, G. C. *Chem. Phys. Lett*. **2006**, *428*, 109.

(3) (a) Mueller-Westerhoff, U. T.; Vance, B.; Yoon, D. I. *Tetrahedron* **1991**, *47*, 909. (b) Bigoli, F.; Deplano, P.; Mercuri, M. L.; Pellinghelli, M. A.; Pilia, L.; Pintus. G.; Serpe, A.; Trogu, E. F. *Inorg. Chem*. **2002**, *41*, 5241. (c) Aragoni, M. C.; Arca, M.; Devillanova, F. A.; Isaia, F.; Lippolis, V.; Mancini, A.; Pala, L.; Slawin, A. M. Z.; Woollins, J. D. *Inorg. Chem*. **2005**, *44*, 9610. (d) Aragoni, M. C.; Arca, M.; Devillanova, F. A.; Isaia, F.; Lippolis, V.; Mancini, A.; Pala, L.; Verani, G.; Agostinelli, T.; Caironi, M.; Natali, D.; Sampietro. M. *Inorg. Chem. Commun*. **2007**, *10*, 191. (e) Aragoni, M. C.; Arca, M.; Cassano, T.; Denotti, C.; Devillanova, F. A.; Frau, R.; Isaia, F.; Leji, F.; Lippolis, V.; Nitti, L.; Romaniello, P.; Tommasi, R.; Verani. G. *Eur. J. Inorg.Chem*. **2003**, 1939.

(4) (a) Dopke, J. A.; Wilson, S. R.; Rauchfuss, T. B. *Inorg. Chem*. **2000**, *39*, 5014. (b) Madhu, V.; Das, S. K. *Inorg. Chem*. **2006**, *45*, 10037. (c) Llusar, R.; Triguero, S.; Vicent, C.; Sokolov, M. N.; Domercq, B.; Fourmigue, M. *Inorg. Chem*. **2005**, *44*, 8937.

(5) (a) Ollerenshaw, T. J.; Garner, D.; Odell, B.; Clegg, W. *J. Chem. Soc., Dalton Trans*. **1985**, 2161. (b) Lowe, N.D.; Garner, C.D. *J. Chem. Soc., Dalton Trans*. **1993**, 2197. (c) Nomura, M.; Takayama, C.; Kajitani, M. *Inorg. Chem*. **2003**, *42*, 6441. (d) Boyde, S.; Garner, C. D. *J. Chem. Soc., Dalton Trans*. **1991**, 713.

(6) (a) Kiviniemi, S. K.; Sillanpaa, A. S.; Rissanen, M. N.; Lamsa, M. T.; Pursianen, J. *Chem. Commun*. **1999**, 897. (b) Rovira, C. *Chem. Rev*. **2004**, *104*, 5289.

(7) (a) Fujita, W.; Awaga, K. *Science* **1999**, *286*, 261. (b) Ribera, E.; Rovira, C.; Veciana, J.; Tarres, J.; Canadell, E.; Rousseau, R.; Molins, E.; Mas, M.; Schoeffel, J.-P.; Pouget, J.-P.; Morgado, J.; Henriques, R. T.; Almeida, M. *Chem.–Eur. J*. **1999**, *5*, 2025.

(8) Rigos, C. F.; Santos, H. D. L.; Thedei, G.; Ward, R. J.; Ciancaglini, P. *Biochem. Mol. Bio. Edu*. **2003**, *31*, 329.

(9) Kumar, D. K.; Das, A.; Dastidar, P. *Cryst. Growth Des*. **2007**, 7, 205.

(10) Yamada, K.; Tanaka, H.; Yagishita, S.; Adachi, K.; Uemura, T.; Kitagawa, S.; Kawata, S. *Inorg. Chem*. **2006**, *45*, 4322.

(11) Kitagawa, S.; Kondo, M. *Bull.Chem.Soc.Jpn*. **1998**, *71*, 1739.

(12) (a) Tripuramallu, B. K.; Mann, P.; Reddy, S. N.; Das, S. K. *Cryst. Growth Des*. **2012**, *12*, 777. (b) Kishore, R.; Das, S. K. *Cryst. Growth Des*. **2012**, *12*, 3684. (c) Aragoni, M. C.; Arca, M.; Demartin, F.; Devillanova, F. A.; Garau, A.; Isaia, F.; Lelj, F.; Lippolis, V.; Verani, G. *J. Am. Chem. Soc*. **1999,** *121*, 7098. (d) Curreli, S.; Deplano, P.; Faulmann, C.; Ienco, A.; Mealli, C.; Mercuri, M. L.; Pilia, L.; Pintus, G.; Serpe, A.; Trogu, E. F. *Inorg. Chem*. **2004**, *43*, 5069.

(13) (a) Rex, X.; Sui, Y.; Liu, G.; Xie, J. *J. Phys. Chem. A*. **2008**, *112*, 8009. (b) Madhu, V. Das, S. K. *Inorg. Chem*. **2008**, *47*, 5055.

(14) Huynh, H. V.; Wong, L. R.; Ng, P. S. *Organomettallics* **2008**, *27*, 2231.

(15) (a) Locke, J.; McCleverty, J. A. *Inorg. Chem*. **1966**, *5*, 1157. (b) Dhal, P. K.; Arnold, F. H. *Macromolecules* **1992**, *25*, 7051.

(16) (a) *Software for the CCD Detector System*; Bruker Analytical X-Ray Systems, Inc.: Madison, WI, 1998. (b) Sheldrick, G. M., SADABS, *Program for Absorption Correction with the Siemens SMART Area-Detector System*; University of Gottingen: Gottingen, Germany, 1996. (c) Sheldrick, G. M. SHELXS-97, *Program for Solution of Crystal Structures*. University of Gottingen: Gottingen, Germany, 1997. (d) Sheldrick, G. M. SHELXL-97, *Program for Refinement of Crystal Structures*. University of Gottingen: Gottingen, Germany, 1997.

(17) (a) Ren, X.; Wu, P.; Zhang, W.; Meng, Q.; Chen, X. *Trans. Met. Chem.* **2002**, *27*, 394. (b) Costa, T.; Dorfman, J. R.; Hagen, K.S.; Holm, R. H. *Inorg. Chem.* **1983,** *22*, 4091. (c) Christou, G.; Huffman, J. C. *J. Chem. Soc., Chem. Commun*. **1983**, 558. (d) Enemark, J. H.; Lipscomb, W. N. *Inorg. Chem.* **1965**, *4*, 1729. (e) Ren, X. M.; Ni, Z. P.; Noro, S.; Akutagawa, T.; Nishihara, S.; Nakamura, T.; Sui, Y. X.; Song, Y. *Cryst. Growth Des.* **2006**, *6*, 2530. (f) Venkatalakshmi, N.; Varghese, B.; Lalitha, S.; Williams, R. F. X.; Manoharan, P. T. *J. Am. Chem. Soc.* **1989**, *111*, 5748.

(18) (a) Thomas, R.; Gopalan, R. S.; Kulakarni, G. U.; Rao, C. N. R. *Beilstein J. Org. Chem*. **2005**, *1*, 15, doi:10.1186/1860-5397-1-15. (b) Gil-Ramirez, G.; Benet-Buchholz, J.; Escudero-Adan, E. C.; Ballester, P. *J. Am. Chem. Soc.* **2007**, *129*, 3820. (c) Conan, F.; Gall, B. L.; Kerbaol, J.-M.; Stang, S. L.; Sala-pala, J.; Mest, Y. L.; Bacsa, J.; Ouyang, X.; Dunbar, K. R.; Campana, C. F. *Inorg. Chem.* **2004**, *43*, 3673. (d) Redshaw, C.; Warford, L.; Dale, S. H.; Elsegood, M. R. J. *Chem. Commun.* **2004**, 1954. (e) Zhang, H.; Ren, X.-M.; Xie, J.-L.; Li, Y.-Z.; Meng, Q.-J. *Acta Crystallogr. E*60, **2004**, 960. (f) Thalladi, V. R.; Gehrke, A.; Boese, R. *New. J. Chem.* **2000**, *24*, 463.

(19) Wang, F.-M.; Chen, L.-Z.; Liu, Y.-M.; Lu, C.-S.; Duan, X.-Y.; Meng, Q.-J. *J. Coord. Chem*. **2012**, *65*, 87.

(20) (a) Becke, A. D. J. Chem. Phys. **1993**, *98*, 5648. (b) Frisch, M. J.; Trucks, G. W.; Schlegel, et al. GAUSSIAN 03, Revision B. 05, Gaussian Inc., Pittsburgh, PA, 2003.

(21) (a) Shupack, S. I.; Billig, E.; Clark, R. J. H.; Williams, R.; Gray, H. B. *J. Am. Chem. Soc*. **1964**, *86*, 4594. (b) Dang, D.; Bai, Y.; Wen, L.; Tian, Z.; Li, Y.; Meng, Q. *J. Mol. Str*. **2005**, *753*, 99. (c) Dmler, W.; Kisch, H. *New J. Chem*. **1991**, *15*, 649. (d) Persaud, L.; Langford, C. H. *Inorg. Chem*. **1985**, *24*, 3562. (e) Schrauzer, G. N.; Mayweg, V. P. *J. Am. Chem. Soc.* **1965**, *87*, 3585. (f) Yao, B.-Q.; Sun, J.-S.; Tian, Z.-F.; Ren, X.-M.; Gu, D.-W.; Shen, L.-J.; Xie, J. *Polyhedron* **2008**, *27*, 2833.

(22) (a) McCleverty, J. A. *Prog. Inorg. Chem*. **1968**, 10, 49. (b) Dietzsch, W.; Lerchner, J.; Reinhold, J.; Stach, J.; Kirmse, R.; Stimecke, G.; Hoyer, E. *J. inorg. nucl. Chem*. **1979**, *42*, 509.

(23) (a) Persaud, L.; Langford, C. H. *Inorg. Chem.* **1985**, 24, 3562. (b) Mines, T. E.; Geiger, W. E. *Inorg. Chem*. **1973**, *12*, 1189.

(24) Madhu, V.; Das, S. K. Polyhedron **2004**, *23*, 1235.

(25) Schmitt, R. D.; Maki, A. H. *J. Am. Chem. Soc*. **1968**, *90*, 2288.

(26) (a) Kirmse, R.; Dietzsch, W.; Stach, J.; Golic, L.; Bottcher, R.; Brunner, W.; Gribnau, M. C. M.; Keijzers, C. P. *Mol. Phys.* **1986**, *57*, 1139. (b) Reijerse, E. J.; Thiers, A. H.; Kanters, R.; Gribnau, M. C. M.; Keijzers, C. P. *Inorg. Chem.* **1987**, *26*, 2764.

(27) (a) Snaathorst, D.; Doesburg, H. M.; Perenboom, J. A. A. J.; Keijzers, C. P. *Inorg. Chem.* **1981**, *20*, 2526. (b) (a) Stach, J.; Kirmse, R.l Sieler, J.; Abram, U.; Dietzsch, W.; Bottcher, R.; Hansen, L. K.; Vergoossen, H.; Gribnau, M.; Keijzers, C. P. *Inorg. Chem.* **1986**, *25*, 1369.

(28) (a) Bilig, E.; Williams, R.; Bernal, I.; Waters, J. H.; Gray, H. B. *Inorg. Chem*. **1964**, *3*, 663-666. (b) Singh, N.; Prasad, A.; Gupta, S. *Transition Met. Chem*. **2005**, *30*, 383. (c) Singh, N.; Singh, V. K. *International J. Inorg. Mater*. **2000**, *2*, 167.

(29) Hathway, B. J.; Wilkinson, G.; Gillard, R. D.; McCleverty, J. A. (Eds), *Comprehensive Coordination Chemistry*, *Pergamon Press, Oxford England*, **1987**, *5*, 533.

# Synthesis and Characterization of New *N*-heterocyclic 1,2-ene dithiolate Based Nickel(II) Complexes and Intramolecular A-D-A Tetrathiafulvalene-fused Charge Transfer Derivatives

4 Chapter

**Abstract:–** Five new nickel-bis(dithiolene) complexes $(PPh_4)_2[Ni(C_8H_2N_2S_2R_2)_2]$ (R = Pyridin-2-yl (**1**), Pyridin-3-yl (**2**), Thiophen-2-yl (**3**), Furan-2-yl (**4**) and Naphthalen-2-yl (**5**)), have been prepared by the treatment of *N*-heterocyclic based dithiolene ligands with sodium metal in dry methanol. All these dithiolene ligands and metal complexes are characterized by LCMS-, $^1$H NMR- and HRMS-, IR-, UV-vis-NIR-spectroscopy, routine elemental analysis and cyclic voltammetry. Compounds **2** and **3** are structurally characterized by single crystal X-ray crystallography. Complex **2** crystallizes in monoclinic space group *P*2(1)/*c*, whereas complex **3** crystallizes in triclinic space group *P*–1. Both these complexes (**2** and **3**) exhibit a two-dimensional network through C–H···N hydrogen bonding interactions in their crystal packing. Compound **2** undergoes a reversible oxidation ($\Delta E$= 83 mV) at $E_{1/2}$ = +0.21 V *vs* Ag/AgCl, whereas **5** shows quasi-reversible oxidation at $E_{1/2}$ = +0.09 V *vs* Ag/AgCl in dimethylsulfoxide solutions of electrochemical measurements. Interestingly, complex **5** is easily oxidized at very low oxidation potential compared to the other complexes **1**–**4**. The title compounds exhibit absorption in the region of 630–1000 nm, in which complex **5** shows band towards longer wavelength side compared to the remaining complexes **1**–**4**. The positions of the absorption maxima in the electronic absorption spectra of the compounds **1** and **2** depend on the solvent polarity, whereas absorption bands of complexes **3**–**5** are not influenced by the solvent polarity.

## 4.1. Synthesis and characterization of new N-heterocyclic 1,2-ene dithiolate based nickel (II) complexes

### 4.1.1. Introduction

Complexes of dithiolene (1,2-enedithiolate) ligands exhibit significant and diverse properties.[1-6] Among all of these dithiolene complexes, nickel based complexes, for example $[Ni(S_2C_2R_2)_2]^{n-}$ (n = 0–2) attract considerable attention since 1960s because this system has multiple accessible redox states.[7] According to Scheme 4.1, the redox activity of the dithiolene ligands can be explained by the existence of canonical forms; due to the delocalization, metal can exist in variable oxidation states (+4 to 0).[8] This ambiguity is a

classic example of non-innocent behavior[9] of a sulfur donor ligand. Nickel-dithiolene complexes exhibit interesting properties such as metallic-conductivity,[10] optical nonlinearity[11] and facility to reversibly react with olefins through a redox couple foremost to olefin purification,[12] molecular magnets,[13] and strong absorbance in the near-infrared region, appropriate in laser Q-switch dyes.[14] Square planar dithiolene coordination complexes are generally characterized by high extent of electron delocalization within the chelate ring involving the metal ion that appreciably contributes to the low energy electronic transition between the HOMO and the LUMO. This extensive delocalization is responsible for dithiolene complexes to show an absorption band in its near-infrared (NIR) region.[15] For example, there are two nickel dithiolene complexes (shown in Scheme 4.2), in which cyano group and phenyl substituted metal complexes reveal electronic absorption band at 863 and 935 nm respectively. Electron donating capability to metal center is more for phenyl group compared to the cyano group and the band is shifted towards longer wavelengths for the phenyl substituted nickel dithiolene complex. This indicates substituent on dithiolene moiety can influence in the shift of position of electronic absorption band of charge transfer transition, because electron donating/withdrawing substituents play an important role in delocalization of the chelate ring in metal-bis(dithiolene) complexes.[16-21] These facts prompted us to design and synthesize new type of *N*-hetero substituent-based (Pyridin-2-yl, Pyridin-3-yl, Thiophen-2-yl, Furan-2-yl and Naphthalen-2-yl) dithiolene ligands and to synthesize corresponding metal bis(dithiolene) complexes $(PPh_4)_2[Ni(C_8H_2N_2S_2R_2)_2]$ (R = Pyridin-2-yl (**1**), Pyridin-3-yl (**2**), Thiophen-2-yl (**3**), Furan-2-yl (**4**) and Naphthalen-2-yl (**5**)), which enable us to compare the substituent effect on electrochemical studies of the title complexes.

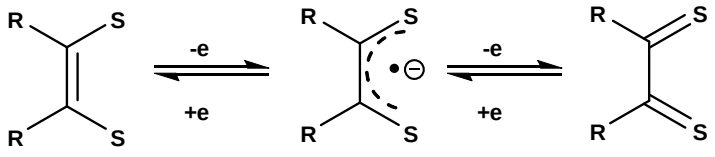


**Scheme 4.1.** Canonical forms of dithiolene ligand

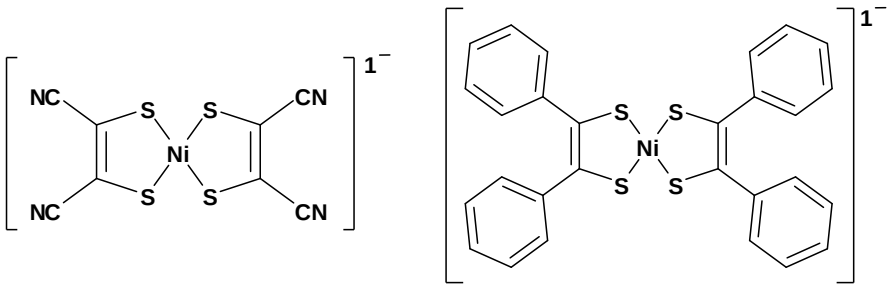


**Scheme 4.2.** Nickel dithiolene complexes

## 4.1.2. Experimental Section

### 4.1.2.1. Materials and Methods

All the reagents for synthesis were commercially available and used as received. 4,5-bis-thiocyanato-banezene-1,2-diamine, 5,6-diaminobenzo[d][1,3]dithiole-2-thione, 1,2-di(pyridine-3-yl)ethane-1,2-dione and 1,2-di(naphthalene-2-yl)ethane-1,2-dione) were prepared according to literature procedures.[22-25] Solvents were dried by standard procedures. Micro-analytical (C, H, N) data were obtained with a FLASH EA 1112 Series CHNS Analyzer. Infrared spectra were recorded as KBr pellets on a JASCO–5300 FT–IR spectrophotometer at 298 K. Electronic absorption spectra of all compounds were recorded on a Shimadzu UV-vis-NIR spectrophotometer. NMR spectra were recorded on Bruker 400 and 500 MHz spectrometer. The chemical shifts ($\delta$) are reported in ppm. A Cypress model CS-1090/CS-1087 electro analytical system was used for cyclic voltammetric experiments. The electrochemical experiments were measured in dimethylsulfoxide containing $[Bu_4N][ClO_4]$ (TBAP) as a supporting electrolyte, using a conventional cell consisting of two platinum wires as working and counter electrodes, and a Ag/AgCl electrode as a reference. Under identical condition, $Fc^+/Fc$ couple was observed at 0.53V. The potentials reported here are uncorrected for junction contributions.

### 4.1.2.2. Synthesis

**General synthetic route for the preparation of the compounds (a-e)**

A mixture of solution containing 5,6-diaminobenzo[*d*][1,3]dithiole-2-thione (1mmol), corresponding 1,2-diketone (1 mmol), and iodine(10 mol%) in $CH_3CN$ (10.0 mL) was stirred at room temperature for 2 h. The resulting yellow colored precipitate was separated by filtration, washed with little $CH_3CN$ and dried in an open air. The characterization data of these compounds were described in the Section 4.2.2.1.

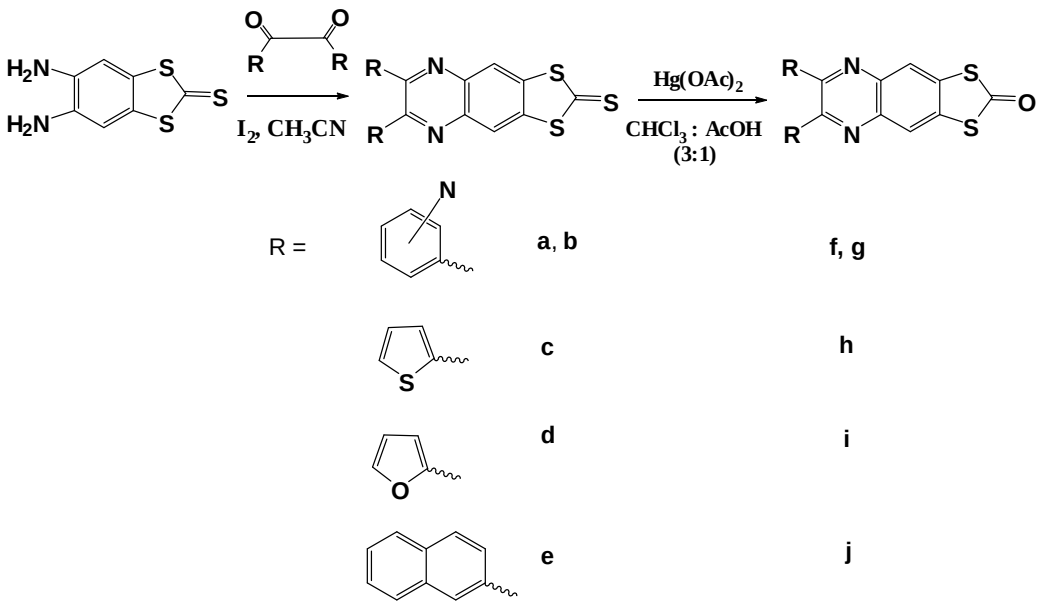


**Scheme 4.3.** Synthetic route for compounds **a**–**e** and **f**–**j.**

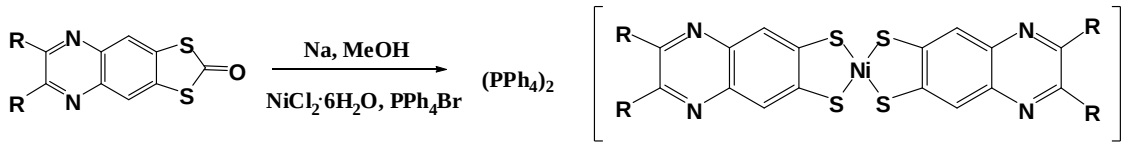


**Scheme 4.4.** Synthetic route for new nickel dithiolene complexes

### General synthetic route for the preparation of the compounds (f-j)

According to literature procedure,[26] to a solution of corresponding **a-e** (1 mmol) in chloroform and acetic acid (3:1), $Hg(OAc)_2$ (3 mmol) was added and it was stirred for 12 h at room temperature under nitrogen atmosphere (Scheme 4.3). The precipitate was filtered off by using celite and washed with chloroform. The filtrate was neutralized with $NaHCO_3$ solution, and extracted with dichloromethane solvent and dried over $Na_2SO_4$. The solvent was removed by rotary evaporator which produces pale yellow colored compound as product. The characterization data for ***f-j*** are described below:

**6,7-Di-pyridin-2-yl-1,3-dithia-5,8-diaza-cyclopenta[*b*]naphthal-2-one** (**f**): (Yield: 92%). $^1$H NMR (400 MHz, δ ppm) (DMSO-$d^6$): 7.40-7.43 (m, 2H), 8.01-8.06 (m, 4H), 8.30 (s, 2H), 8.75 (s, 2H). LC-MS (ESI): *m/z*: 375 $(M+H)^+$. Anal. Calc. for $C_{19}H_{10}N_4OS_2$: C 60.95, H 2.69, N 14.96. Found: C 61.22, H 2.76, N 15.32 %.

**6,7-Di-pyridin-3-yl-1,3-dithia-5,8-diaza-cyclopenta[*b*]naphthalen-2-one** (**g**): (Yield: 94%). $^1$H NMR (400 MHz, δ ppm) (DMSO-$d^6$): 7.40-7.44 (m, 2H), 8.01-8.05 (m, 4H), 8.30 (s, 2H), 8.75 (s, 2H). LC-MS (ESI): *m/z*: 375 $(M+H)^+$. Anal. Calc. for $C_{19}H_{10}N_4OS_2$: C 60.95, H 2.69, N 14.96. Found: C 61.22, H 2.76, N 15.31 %.

**6,7-Di-thiophen-2-yl-1,3-dithia-5,8-diaza-cyclopenta[*b*]naphthalene-2-one (h):** (Yield: 92%). $^1$H NMR (400 MHz, δ ppm) (DMSO-$d^6$): 7.11-7.14 (m, 2H), 7.26-7.27 (m, 2H), 7.83-7.84 (d, 2H), 8.57 (s, 2H). LC-MS (ESI): *m/z*: 385 $(M+H)^+$. Anal. Calc. for $C_{17}H_8N_2OS_4$: C 53.10, H 2.10, N 7.29. Found: C 53.42, H 2.17, N 7.68 %.

**6,7-Di-furan-2-yl-1,3-dithia-5,8-diaza-cyclopenta[*b*]naphthalen-2-one (i):** (Yield: 91%). $^1$H NMR (400 MHz, δ ppm) (DMSO-$d^6$): 6.72-6.79 (m, 4H), 7.92 (s, 2H), 8.58 (s, 2H). LC-MS (ESI): *m/z*: 353 $(M+H)^+$. Anal. Calc. for $C_{17}H_8N_2O_3S_2$: C 57.94, H 2.29, N 7.95. Found: C 58.26, H 2.37, N 8.38 %.

**6,7-Di-naphthalen-2-yl-1,3-dithia-5,8-diaza-cyclopenta[*b*]naphthalen-2-one (j):** (Yield: 91%). $^1$H NMR (400 MHz, δ ppm) (DMSO-$d^6$): 7.45-7.57 (m, 3H), 7.86-7.88 (m, 4H), 8.16-8.22 (m, 2H), 8.76 (s, 1H). LC-MS (ESI): *m/z*: 473 $(M+H)^+$. Anal. Calc. for $C_{29}H_{16}N_2OS_2$: C 73.70, H 3.41, N 5.93. Found: C 74.03, H 3.45, N 6.42 %.

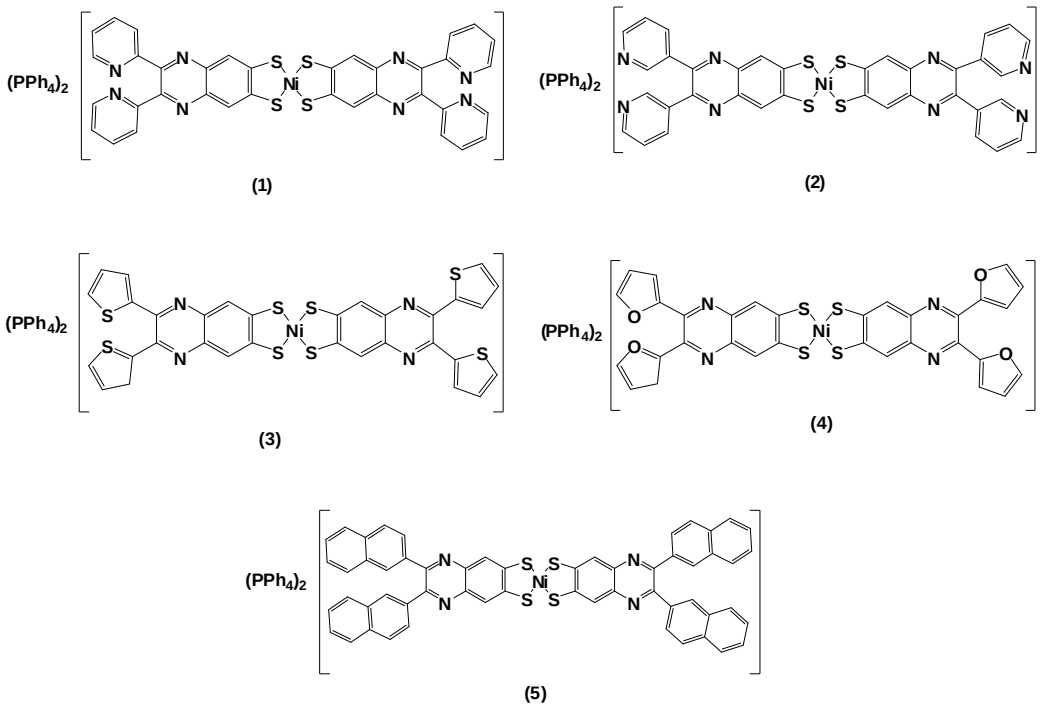


**Scheme 4.5**. Structural representation of synthesized nickel dithiolene complexes

**General procedure for the synthesis of nickel dithiolene coordination complexes 1–5**

Sodium metal was added to the 10 mL methanol solution of **f-g** (2 mmol); after getting clear solution, $NiCl_2 \cdot 6H_2O$ (1 mmol) was added and it was stirred for 10 min, followed by the addition of $[PPh_4]Br$ (tetraphenylphosphonium bromide) (2 mmol) and continue to stirred for an additional 15 min by the addition of 10 mL water, whereby the precipitate was obtained which was filtered and air dried (Scheme 4.4). All these compounds were recrystalized from respective acetonitrile solutions. Compounds **2** and **3** are crystallized by mixed solvent of (acetonitrile+methanol)/diethyl ether and acetonitrile/diethyl ether diffusion method. Compounds **1**, **4** and **5** are also crystallized by diffusion method of acetonitrile/ether solutions, but we could not collect the single X-ray crystallography data because of too tiny crystals. The characterization data for compounds **1**-**5** are described below. Compounds **2** and **3** are additionally characterized by single crystal X-ray crystallography.

**Compound 1**: Yield: 0.124 g (62% based on nickel metal). HRMS: calc: 750.0047, found: 750.0047 (*m/z*). Anal. Calc. for $C_{84}H_{60}N_8NiP_2S_4$: C 70.54, H 4.22, N 7.83 %. Found: C 70.83, H 4.29, N 8.19 %. IR (KBr, $\nu/cm^{-1}$): 3468, 3051, 2922, 2852, 1635, 1585, 1473, 1431, 1348, 1207, 1087, 995, 860. $^1H$ NMR (400 MHz, $\delta$ ppm) ($CD_3CN$): 8.12-2.11 (m, 1H), 8.04-7.89 (m, 13H), 7.77-7.65 (m, 40H), 7.62-7.60 (m, 3H), 7.47-7.42 (m, 3H).

**Compound 2**: Yield: 0.103 g (58% based on nickel metal). HRMS: calc. 750.0047, found: 750.0047 (*m/z*). Anal. Calc. for Anal. Calc. for $C_{84}H_{60}N_8NiP_2S_4$: C 70.54, H 4.22, N 7.83 % Found: C 70.83, H 4.29, N 8.19 %. IR (KBr, $\nu/cm^{-1}$): 3435, 3049, 2922, 2851, 1583, 1481, 1327, 1205, 1078, 997, 850. $^1H$ NMR (500 MHz, $\delta$ ppm) ($CD_3CN$): 8.06-8.03 (m, 12H), 7.89-7.85 (m, 21H), 7.83-7.78 (m, 23H), 7.72 (s, 4H).

**Compound 3**: Yield: 0.135 g (68% based on nickel metal). HRMS: calc: 770.8572, found: 769.8494 $(M-H)^+$. Anal. Calc. for $C_{80}H_{56}N_4NiP_2S_8$: C 66.24, H 3.89, N 3.86 %. Found: C 66.42, H 3.96, N 4.19 %. IR (KBr, $\nu/cm^{-1}$): 3437, 2922, 2851, 1641, 1581, 1514, 1483, 1431, 1358, 1203, 1080, 995, 848. $^1H$ NMR (500 MHz, $\delta$ ppm) ($CD_3CN$): 8.06-8.01 (m, 15H), 7.86-7.54 (m, 33H), 7.43-7.21 (m, 3H), 7.16-7.13 (m, 5H).

**Compound 4**: Yield: 0.122g (58% based on nickel metal). HRMS: calc: 706.9486, found: 705.9408 $(M-H)^+$. Anal. Calc. for $C_{80}H_{56}N_4NiO_4P_2S_4$: C 69.31, H 4.07, N 4.04 %. Found: C 69.55, H 4.13, N 4.49 %. IR (KBr, $\nu/cm^{-1}$): 3416, 2922, 2851, 1581, 1481, 1425, 1327, 1251, 1205, 1157, 1078, 997, 887. $^1H$ NMR (400 MHz, $\delta$ ppm) ($CD_3CN$): 7.93-7.86 (m,

5H), 7.77-7.70 (m, 15H), 7.69-7.65 (m, 7H), 7.63-7.60 (m, 5H), 7.47-7.42 (m, 14H), 7.26-7.22 (m, 8H), 7.17-7.15 (m, 2H).

**Compound 5**: Yield: 0.132g (62% based on nickel metal). HRMS: calc: 946.0863, found: 946.0863 (*m/z*). Anal. Calc. for $C_{104}H_{72}N_4NiP_2S_4$: C 76.79, H 4.46, N 3.44%. Found: C 76.98, H 4.52, N 3.73 %. IR (KBr, ν/cm$^{-1}$): 3439, 3053, 2962, 2924, 2852, 1658, 1624, 1593, 1433, 1352, 1261, 1176, 1082, 906, 860. $^1$H NMR (500 MHz, $\delta$ ppm) ($CD_3CN$): 8.24-8.22 (m, 8H), 8.17-8.13 (m, 8H), 8.11-8.08 (m, 3H), 8.05-7.99 (m, 10H), 7.92-7.84 (m, 17H), 7.82-7.78 (m, 12H), 7.76-7.70 (m, 7H), 7.67-7.61 (m, 7H).

### 4.1.2.3. Crystal structure determination

Crystal data of compound **2** was measured at 298(2) K on Oxford Gemini Diffractometer equipped with EOS CCD detector. Monochromatic Mo–Kα radiation (λ = 0.71073 Å) was used for the measurements. Absorption corrections using multi ψ–scans were applied. Single crystals, suitable for facile structural determination for the compound **3**, was measured at 100(2) K on a three circle Bruker SMART APEX CCD area detector system under Mo–Kα (λ = 0.71073 Å) graphite monochromatic X–ray beam, 2400 frames were recorded with an ω scan width of 0.3$^o$, each for 10 s, crystal-detector distance 60 mm, collimator 0.5 mm. Data reduction performed by using SAINTPLUS.[27] Empirical absorption corrections were performed by using equivalent reflections performed program SADABS.[27] The structures were solved by direct methods and least-square refinement on $F^2$ for the compounds **2** and **3** by using SHELXS-97.[28] All non-hydrogen atoms were refined anisotropically. The hydrogen atoms were included in the structure factor calculation by using a riding model. The crystallographic parameters, data collection and structure refinement of the compounds **2**–**3** are summarized in Table 4.1. Hydrogen boding data of the compounds **2**–**3** are described in Table 4.2. In the crystal structure of complex **2**, the disordered solvent contributions were removed by the SQUEEZE[29] command in the Platon program.

**(a)**

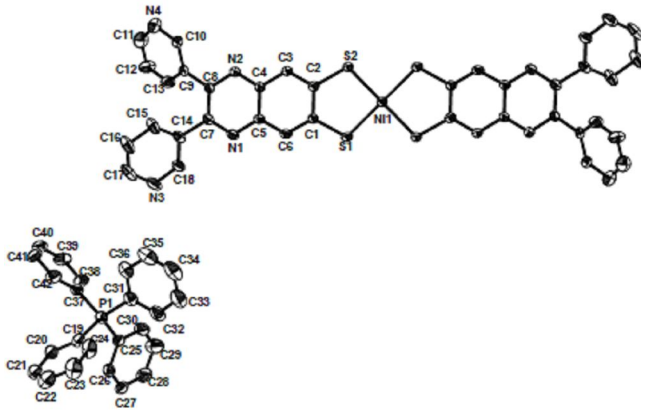


**(b)**

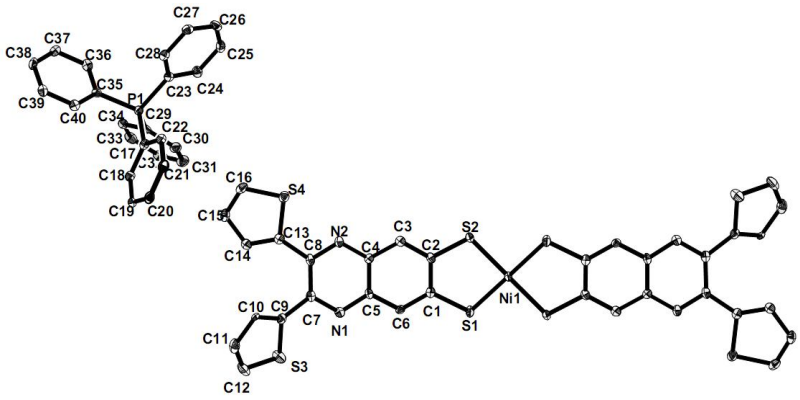


**Figure 4.1.** Thermal ellipsoidal diagrams of the (a) compound **2** (20% probability), (b) compound **3** (40% probability, Hydrogen atoms are omitted for clarity).

## 4.1.3. Results and discussion

### 4.1.3.1. Synthesis

Compounds **1-5** have been synthesized by the reaction of one equivalent $NiCl_2 \cdot 6H_2O$ with two equivalents of di-substituted-1,3-dithia-5,8-diaza-cyclopenta[*b*]naphthalen-2-one (**f-j**) in MeOH treated with sodium metal at ambient temperature condition and then precipitated by adding tetraphenylphosphonium bromide, yielding the microcrystalline form of compounds **1-5** in reasonable yield. Diagrammatic representations of the compounds **1**–**5** have been shown in Scheme 4.5.

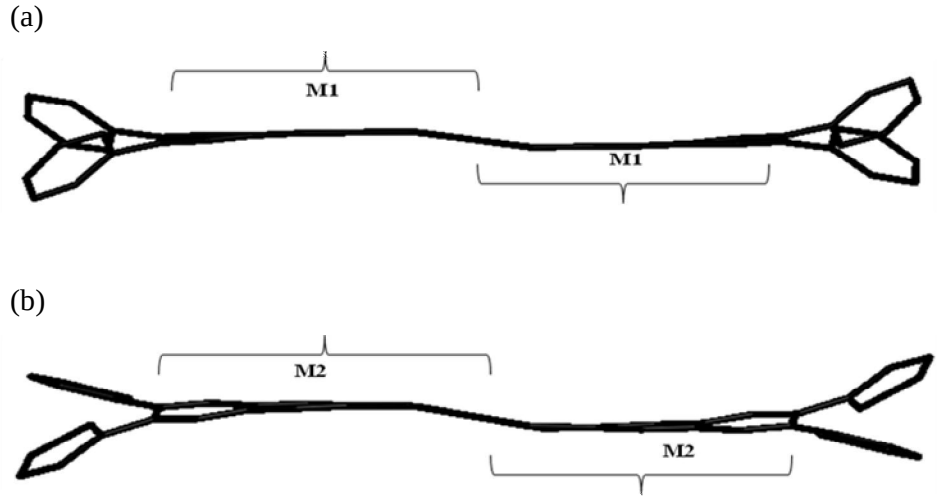


**Figure 4.2.** (a) Mean plane (M1) of the half dithiolene unit (Ni1S1C1C6C5N1C7C8N2C4C3C2S2) in compound **2** and (b) mean plane (M2) of the half dithiolene unit (Ni1S1C1C6C5N1C7C8N2C4C3C2S2) in compound **3**.

### 4.1.3.2. Description of Crystal Structures

Black coloured block-shaped-crystals of compound $(PPh_4)_2[Ni(C_{18}H_{10}N_4S_2)_2]$ (**2**) were crystallized in monoclinic space group *P(2)/c*, whereas compound $(PPh_4)_2[Ni(C_{16}H_8N_2S_4)_2]$ **(3)** was crystallized in triclinic space group *P*-1. The asymmetric unit in the crystal structure of compounds **2** and **3** (represented as labelled atoms in Figure 4.1) contains half molecule of nickel-dithiolene moiety and one tetraphenylphosphonium cation. The average Ni–S bond distances in the crystal structure of compound **2** is 2.173 Å, whereas in compound **3**, it is 2.163 Å. The distance between two mean planes of chelate rings Ni1S1C1C2S2 in $[Ni(C_{18}H_{10}N_4S_2)_2]^{2-}$ (**2**) and $[Ni(C_{16}H_8N_2S_4)_2]^{2-}$ (**3**) are 0.149 Å and 0.172 Å respectively. The dihedral angle between two S1NiS2 planes in both the compounds **2** and **3** is 0°, that is, the $c_1$–Ni–$c_2$ angle is 180° (c1 and c2 are the midpoints of the sulphur atoms in the five-membered chelate rings), which indicates the geometry around nickel metal centre is perfectly square planar in both compounds. The angle between two pyridin-2-yl rings (C14C15C16C17N3C18 and C9C10N4C11C12C13) in compound **2** is 62.20°, and angle between two thiophen-2-yl rings (C9C10C11C12S3 and C13S4C14C15C16) is 51.96° in compound **3**. This indicates that, due to the large size of the pyridin-2-yl rings (steric effect) the concerned angle is more in compound **2** compared to that in compound **3**. The bending angles (η) between {S1Ni1S2} and

{S1C1C2S2} planes present in the {Ni1S1C1C2S2} dithiolate-chelated ring are 9.78° and 11.31° in compounds **2** and **3** respectively. The distance between two mean planes in compound **2** is 0.423 Å (M1 in Figure 4.2), whereas in compound **3** this distance (M2) between two mean planes is 0.526 Å. As shown in Figure 4.2, the half moiety of M1, which is present in compound **2**, is more planar than the half moiety of M2 which is present in compound **3**. A prominent feature of the structure for these two complexes is that $[Ni(C_8H_2N_2S_2R_2)_2]^{2-}$ (R = pyridin-3-yl and naphthalen-2-yl) exhibit Z-shaped non-planar geometry with the ligand fragment bent away from the NiS4 plane with a dihedral angle of 11.14° in compound **2** and 14.28° in compound **3** (Scheme 4.6); these values are comparable to those of known copper dithiolene complexes.[30]

(a)

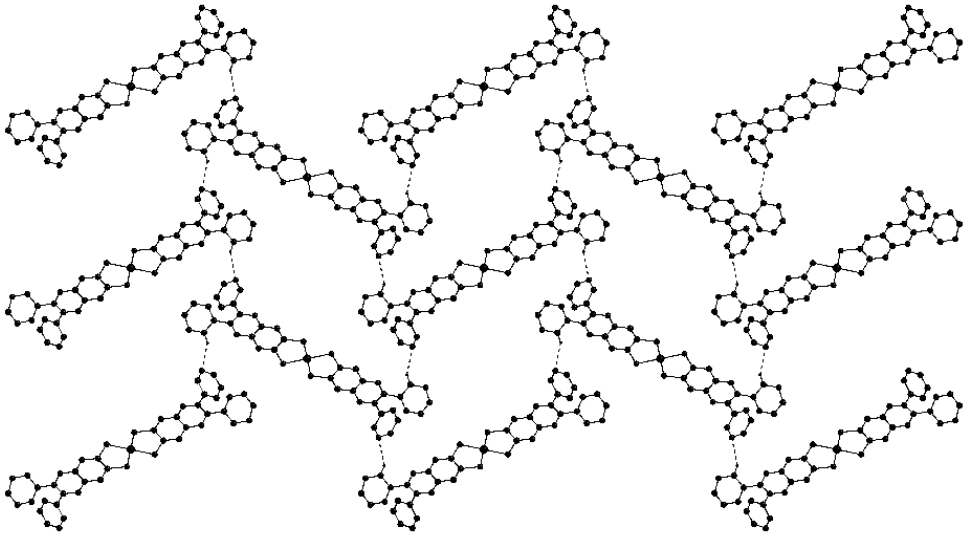

(b)

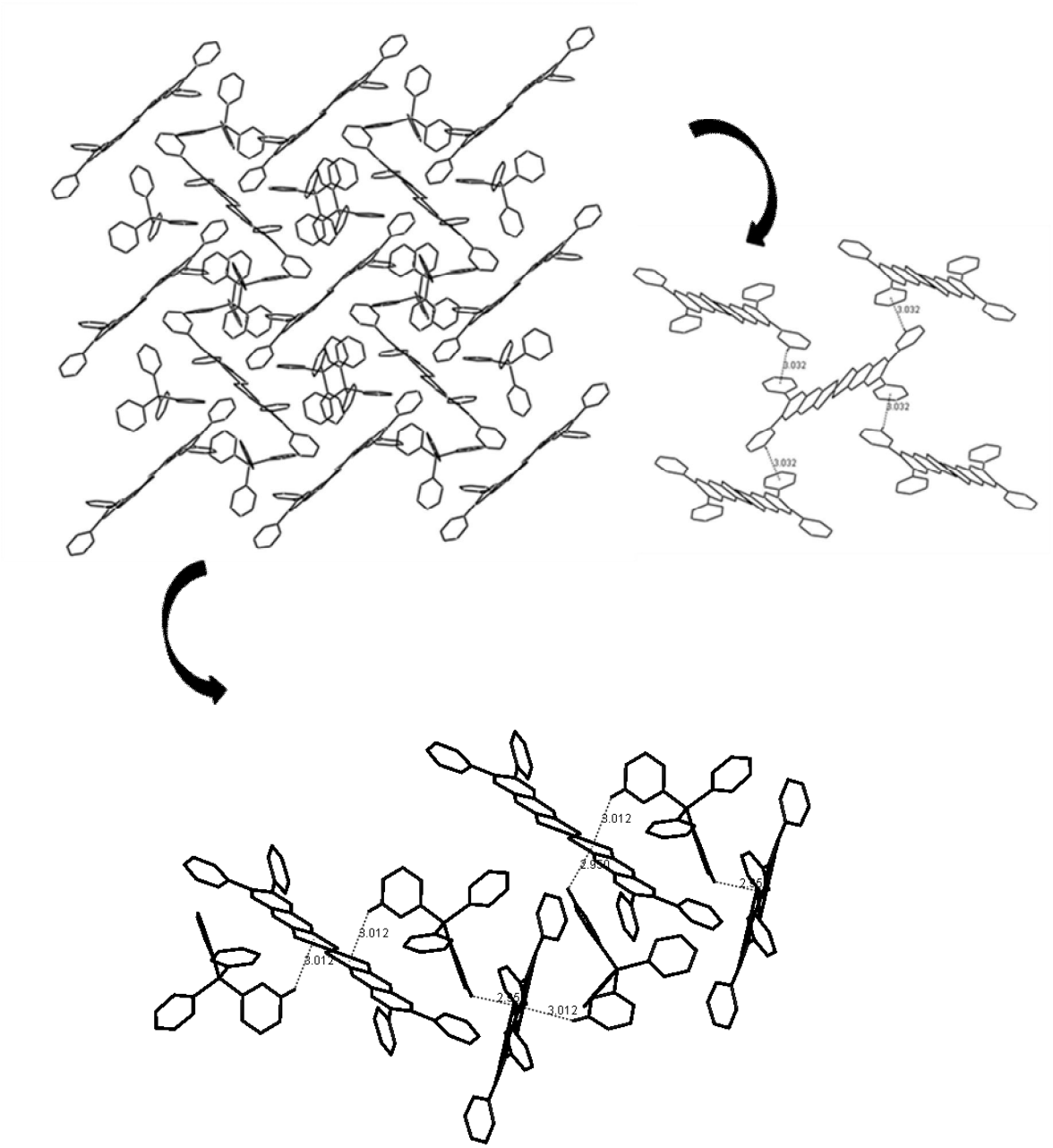

(c)

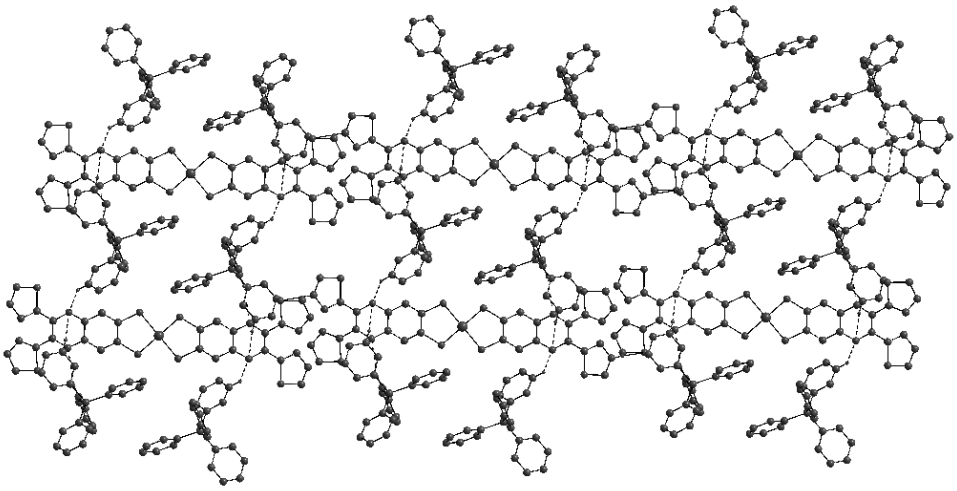

**Figure 4.3.** (a) Molecular packing diagram of the compound **2** characterized by C−H···N weak interactions resulting in two dimensional supramolecular chain, (b) C–H····π interactions between pyridyl rings from the anion moiety and C–H···π interactions between centroid of the metal chelate ring and cation (tetraphenylphosphonium), (c) Two-dimensional supramolecular network through C−H···N hydrogen bonding interactions in the crystal structure of compound **3**.

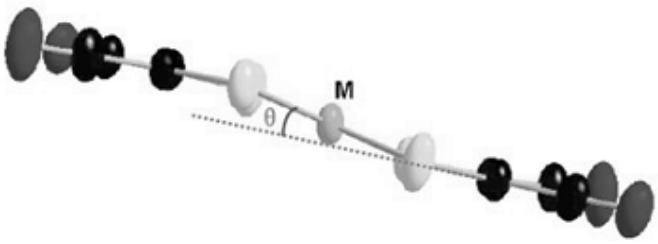


**Scheme 4.6**. Z-shaped nonplanar geometry.

The interactions between pyridine moieties with a distance 2.52 Å (H···A) of C(10)–H···N(3) hydrogen bond in compound **2** lead to a two dimensional network; compound **3** also offers 2-D network through C–H···N supramolecular interactions as shown in Figure 4.3. In compound **2**, there are additional C(16)–H····π (H16····Cg, Cg = C9C10C11C12C13N4) interactions between pyridine moieties with a distance of 3.032 Å; these interactions involve four anionic moieties around one anionic moiety, as shown in Figure 4.3(b). In addition to this, there are other C–H···π interactions C–H(29)····Cg and C–H(34)····Cg (H····Cg = 3.012 and 2.950 Å respectively), that are present between phenyl moiety (from tetraphenylphosphonium cation) and the centroid (Cg) of the Ni1S1C1C2S2 chelate ring system.

**4.1.3.3. UV-Vis absorption spectra for compounds 1–5**

Figure 4.4 shows the electronic absorption spectra of the complexes **1–5**. UV-vis-NIR absorption spectra measurements were carried out in acetonitrile solutions at ambient temperature. The observed absorption maxima of the complexes from **1** to **5** are found at 635, 639, 665, 649 and 892 nm respectively. As the nature of the substituent of each complex varies, it is obvious to expect changes in its corresponding absorption maximum. The extent of the relative shift in the absorption maximum of each complex is explained based on the extent of delocalization induced by the substituent. The absorption spectra of complexes **1** and **2** did not deviate much from one another and the close proximity of their maxima is due to the identical in nature of the pyridin-2-yl and pryridin-3-yl substituents. However, it is noticed that simple exchange of furan-2-yl by thiophen-2-yl enhances the extent of electron delocalization and responsible for the red shift of the absorption maximum of complex **3** (665 nm) compared to complex **4** (649 nm). Extending π-electron cloud by introducing naphthalene substituent in complex **5** drastically shifts the absorption maximum of the complex into the near IR region with absorption maximum at 892 nm. These bands can be attributed to the charge transfer transitions (CT) involving electronic excitation from a HOMO which is a mixture of dithiolate (π) and metal (d) orbital character to a LUMO which is a π* orbital of the dithiolate.[31,32] The influence of different substituents with different electron delocalization capabilities on the spectral properties of the nickel complexes is known in literature and the results observed in the present study are in accord with the mechanisms explained (in literature) that are based on the delocalization effects of the substituents.[15,33]

Interestingly, complexes **1** and **2** in the present case show negative solvatochromic behavior with a blue shift in the spectral maximum with increase in solvent polarity. Figure 4.5 represents the negative solvatochromic behavior of complex **2** with a change in the absorption maximum from 714 nm in chloroform to 639 nm in acetonitrile. The unusual behavior of these complexes indicates more charge transfer nature of the ground state than the excited state.[34-36] Increase in polarity of the solvent stabilizes the ground state more than the excited state, which further increases the energy gap between the HOMOs and LUMOs in dithiolene complexes **1** and **2**. The increase in energy gap with increase in solvent polarity imparts blue shift to the observed absorption maximum. Like most of the organic molecules and inorganic complexes, the solvatochromic behavior of the dithiolene complexes is also associated with several solvent factors such as coulomb,

directional, inductive, dispersion, charge-transfer, hydrogen-bonding forces, etc.[37-39] Thus in the present study also, the nature of the solvent-complex interactions will depend on these factors. Unlike compounds **1** and **2**, complexes **3**–**5** did not show any solvatochromic behavior, solvatochromic spectrum of the compound **5** as shown in Figure 4.6.

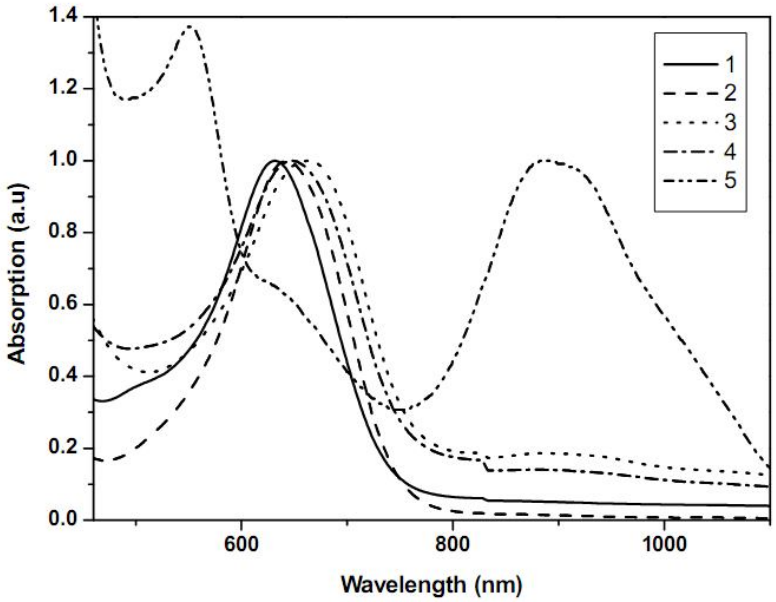


**Figure 4.4.** Normalised electronic absorption spectra of compounds **1**–**5** in acetonitrile solution.

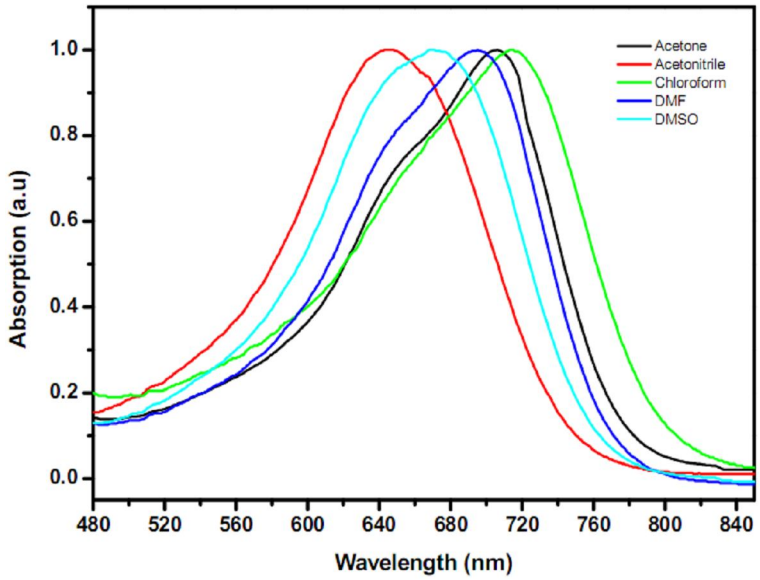


**Figure 4.5.** Normalized absorption spectra of compound **2** in different solvents at room temperature.

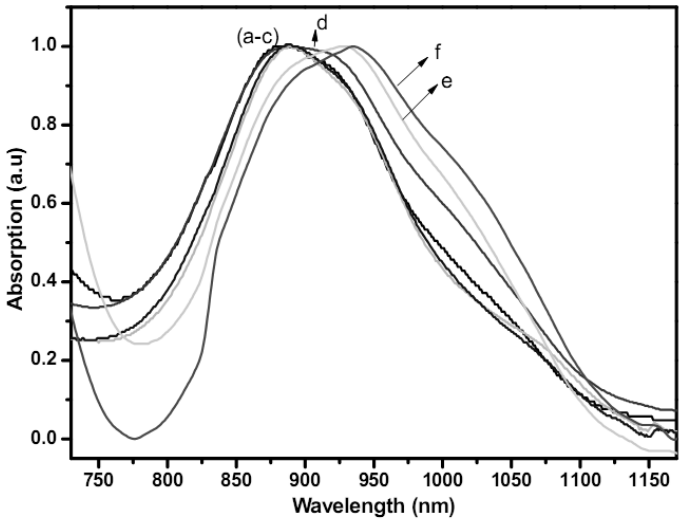


**Figure 4.6.** Normalised electronic absorption spectra for compound **5** in (a) Acetone, (b) DCM, (c) $CHCl_3$, (d) $CH_3CN$, (e) DMF and (f) DMSO solutions.

### 4.1.3.4. Electrochemistry

The electrochemical behavior of the complexes **1**–**5** were performed in dimethylsulfoxide solution, which contains $[Bu_4N][ClO_4]$ (TBAP) as supporting electrolyte (at plantinum working electrode). A representative cyclic voltammogram of compound **2** is as shown in Figure 4.7. This shows an reversible oxidative response at $E_{1/2}$ = +0.21 V (ΔE = 83 mV) vs. Ag/AgCl (under identical condition, $Fc^+/Fc$ couple is observed at 0.53 V) which corresponds the $[Ni(C_8H_2N_2S_2R_2)_2]^{1-}$ / $[Ni(C_8H_2N_2S_2R_2)_2]^{2-}$ (R = naphthalen-2-yl) redox couple for the compound **2**. Compound **1** exhibits reversible oxidative response at $E_{1/2}$ = 0.17 V (92 mV), whereas compounds **3**–**5** exhibit quasi reversible oxidative responses at $E_{1/2}$ = 0.18 V (120 mV), 0.17 V (132 mV), 0.09 V (111 mV) respectively (see Figure 4.8). According to literature,[40-43] usually $Ni^{II}$-bis(dithiolene) complexes exhibit oxidative response within the range of $E_{1/2}$ = +0.12 V to +0.41 V. In the present study, among all compounds **1–5**, compound **5** is easily oxidized ($E_{1/2}$ = 0.09 V) than other compounds **1–4** and this value is very less compared to the previously reported literature values. Probably the electron drift from metal center to the substituent naphthalene ring by resonance effect is responsible for this low oxidation potential of compound **5**.

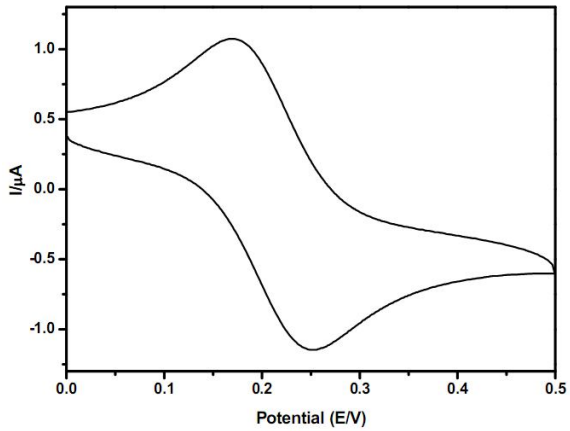


**Figure 4.7.** Cyclic voltammogram of compound **2** in TBAP/DMSO at scan rate 50 $mVs^{-1}$.

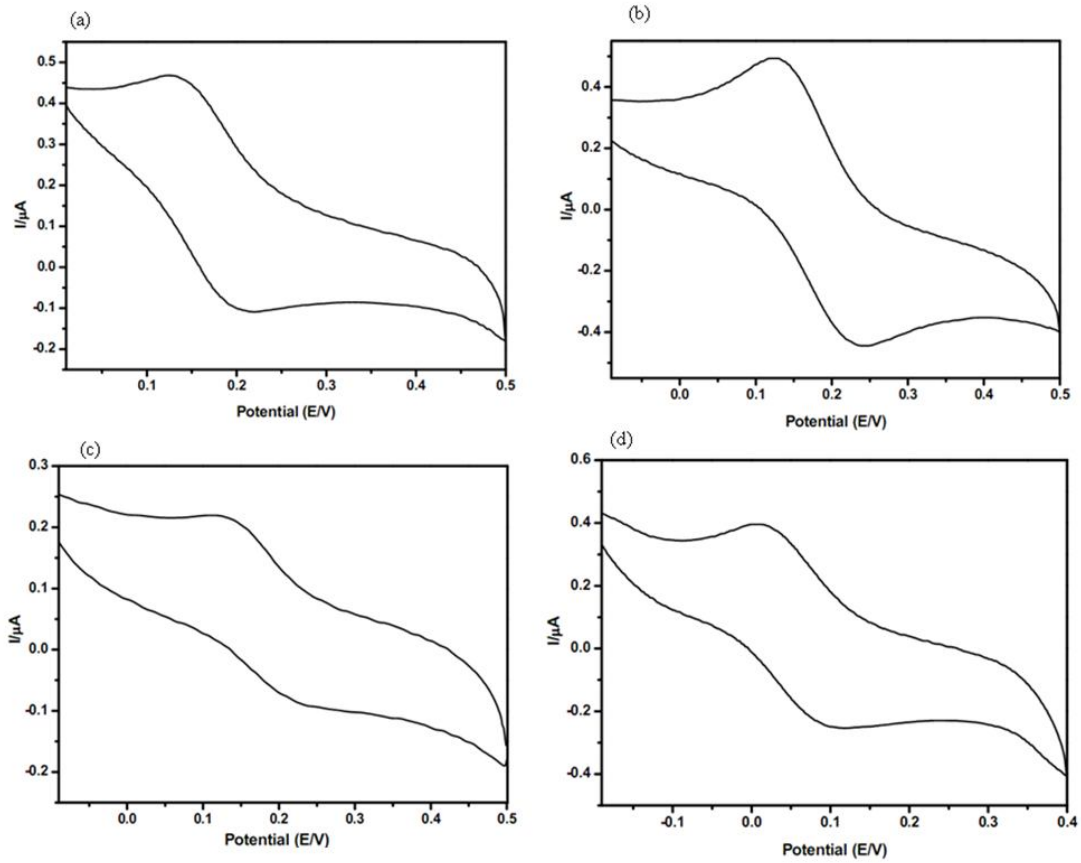


**Figure 4.8.** Cyclic voltammograms of the complexes (a) **1**, (b) **3**, (c) **4** and (d) **5** at scan rate 50 $mVs^{-1}$.

## 4.2. Tetrathiafulvalene Derivatives

### 4.2.1. Introduction

Electrochemically amphoteric compounds are of the current interests owing to their potential applications in molecular electronics and optoelectronics, where by the organic compounds possessing a high degree of conjugation; these systems are particularly interesting for advanced electronic application.[44] In this context, the effective intermolecular orbital overlap between π–stacked assemblies, which is highly sensitive to chemical modifications of the TTF framework, plays a crucial role in the electric conductivity. Based on literature, TTF-imidazole systems exhibit exceptional electronic and structural modulation effects through protonated hydrogen bonds, leading to a number of highly conductive CT complexes with various substituents on acceptor moieties.[45] Accordingly efforts have been directed to the design and synthesis of molecular systems composed of building blocks that give rise to electron donor (D) and acceptor (A) interaction amongst all kinds of the molecular electron donor moieties *e.g.*, tetrathiafulvalene(TTF) unit and its derivatives. Upon protonation on the acceptor moieties, it gives an cationic species, thus leading to more CT bands with less energy gap between HOMO and LUMO orbitals; these materials are used as conducting and superconducting materials.[46] Herein, we report five heterocyclic based tetrathiafulvalene derivates with the molecular formulae $[(C_9H_4N_2S_2R_2)_2]$ (R = pyridin-2-yl (**6**), pyridin-3-yl (**7**), furan-2-yl (**8**) and naphthalen-2-yl (**9**)). All these TTF molecules are characterized by the HRMS, UV-Vis, $^1$H NMR and routine elemental analysis.

### 4.2.2. Experimental section

#### 4.2.2.1. Synthesis

**General synthetic route for the preparation of the compounds (a-e):** A mixture of solution containing 5,6-diaminobenzo[d][1,3]dithiole-2-thione (1mmol), corresponding 1,2diketone (1mmol), and iodine(10 mol%) in $CH_3CN$ (10.0 mL) was stirred at room temperature for 2 h. The resulting yellow colored precipitate was separated by filtration, washed with little $CH_3CN$ and dried in an open air.

*6,7-Di-pyridin-2-yl-1,3-dithia-5,8-diaza-cyclopenta[b]naphthalene-2-thione* (**a**): (Yield: 90%). $^1$H NMR (400 MHz, δ ppm) (DMSO-$d^6$): 7.39-7.42 (m, 2H), 8.00-8.05 (m, 4H),

8.31 (s, 2H), 8.76 (s, 2H). LC-MS (ESI): *m/z*: 391 $(M+H)^+$. Anal. Calc. for $C_{19}H_{10}N_4S_3$: C 58.44, H 2.58, N 14.35. Found: C 58.68, H 2.63, N 14.72 %.

*6,7-Di-pyridin-3-yl-1,3-dithia-5,8-diaza-cyclopenta[b]naphthalene-2-thione* (**b**): (Yield: 93%). $^1$H NMR (400 MHz, δ ppm) (DMSO-$d^6$): 7.39-7.42 (m, 2H), 8.00-8.05 (m, 4H), 8.31 (s, 2H), 8.76 (s, 2H). LC-MS (ESI): *m/z*: 391 $(M+H)^+$. Anal. Calc. for $C_{19}H_{10}N_4S_3$: C 58.44, H 2.58, N 14.35. Found: C 58.68, H 2.63, N 14.72 %.

*6,7-Di-thiophen-2-yl-1,3-dithia-5,8-diaza-cyclopenta[b]naphthalene-2-thione* **(c):** (Yield: 92%). $^1$H NMR (400 MHz, δ ppm) (DMSO-$d^6$): 7.12-7.14 (m, 2H), 7.27-7.28 (m, 2H), 7.84-7.85 (d, 2H), 8.56 (s, 2H). LC-MS (ESI): *m/z*: 400 $(M+H)^+$ . Anal. Calc. for $C_{17}H_8N_2S_5$: C 50.97, H 2.01, N 6.99. Found: C 51.23, H 2.06, N 6.52 %.

*6,7-Di-furan-2-yl-1,3-dithia-5,8-diaza-cyclopenta[b]naphthalene-2-thione* (**d**): (Yield: 92%). $^1$H NMR (400 MHz, δ ppm) (DMSO-$d^6$): 6.73-6.79 (m, 4H), 7.94 (s, 2H), 8.59 (s, 2H). LC-MS (ESI): *m/z*: 369 $(M+H)^+$. Anal. Calc. for $C_{17}H_8N_2O_2S_3$: C 55.42, H 2.19, N 7.60. Found: C 55.81, H 2.26, N 7.26 %.

*6,7-Di-naphthalen-2-yl-1,3-dithia-5,8-diaza-cyclopenta[b]naphthalene-2-thione* (**e**): (Yield: 92%). $^1$H NMR (400 MHz, δ ppm) (DMSO-$d^6$): 7.44-7.56 (m, 3H), 7.86-7.89 (m, 4H), 8.16-8.21 (m, 2H), 8.75 (s, 1H). LC-MS (ESI): *m/z*: 489 $(M+H)^+$. Anal. Calc. for $C_{29}H_{16}N_2S_3$: C 71.28, H 3.30, N 5.73. Found: C 71.57, H 3.36, N 6.08 %.

**General synthetic route for the preparation of the TTF derivatives (6-9):** Based on literature,[46e] a solution of compounds **f**, **g** and **i**, **j** (0.320 mmol) in triethylphosphite (3 mL) was refluxed at 130–140 °C for 2 h under $N_2$ atmosphere. After cooling to room temperature, MeOH (15 mL) was added and the resulting orange precipitate was filtered off.

*6,7,6′,7′-tetra(pyridin-2-yl)-[2,2′]bi[1,3-dithia-5,8-diaza-cyclopenta[b]napthalenylidene] (**6**):* Yield: 48%. $^1$H NMR (400 MHz, $CDCl_3$, δ ppm): 8.56 (d, 4H), 8.38 (d, 4H), 7.84 (m, 4H), 7.34-7.30 (m, 4H), 7.5 (s, 4H). $^{13}$C NMR (100 MHz, $CDCl_3$): δ 154.1, 148.6, 145.2,

137.6, 133.8, 133.6, 131.6, 127.2, 120.0. HRMS: Calc. 716.0694. Found: 717.0772. Anal. Calc. for $C_{38}H_{20}N_8S_4$: C 63.67, H 2.81, N 15.63. Found: C 63.36, H 2.76, N 15.21.

*6,7,6′,7′-tetra(pyridin-2-yl)-[2,2′]bi[1,3-dithia-5,8-diaza-cyclopenta[b]napthalenylidene] **(7):*** Yield: 52%. $^1$H NMR (CDCl3, δ ppm): 9.21 (s, 4H), 8.66 (d, 4H), 8.38 (d, 4H), 7.76 (s, 4H), 7.51 (m, 4H). $^{13}$C NMR (100 MHz, $CDCl_3$): δ 154.3, 146.9, 146.4, 137.6, 134.3, 133.6, 132.8, 127.2, 120.0. HRMS: Calc. 716.0694. Found: 717.0773. Anal. Calc. for $C_{38}H_{20}N_8S_4$: C 63.67, H 2.81, N 15.63. Found: C 63.36, H 2.76, N 15.21.

*6,7,6′,7′-tetra(furan-2-yl)-[2,2′]bi[1,3-dithia-5,8-diaza-cyclopenta[b]naphthalenylidene] **(8):*** Yield: 46%. $^1$H NMR: (400 MHz, $CDCl_3$): δ 7.82 (d, 4H), 7.78 (s, 4H), 7.46-6.84 (m, 8H). $^{13}$C NMR: (100 MHz, $CDCl_3$): δ 156, 144.2, 141.7, 137.6, 134.6, 127.4, 111.4, 106.8, 119.6. HRMS: Calc. 672.0054. Found: 673.0086. Anal. Calc. for $C_{34}H_{16}N_4O_4S_4$: Calc. C 60.70, H 2.40, N 8.33. Found C 60.34, H 2.34, N 8.79.

*6,7,6',7'-tetra(naphthalen-2-yl)-[2,2']bi[1,3-dithia-5,8-diaza-cyclopenta[b]napthalenylidene] **(9):*** Yield: 54%. $^1$H NMR: (400 MHz, $CDCl_3$): δ 8.42-7.96 (m, 16H), 7.84 (d, 4H), 7.61-7.56 (m, 8H), 7.6 (s, 4H). 13C NMR (100 MHz, $CDCl_3$): δ 137.8, 134.6, 134.1, 133.6, 132.8, 131.0, 128.2, 128, 127.9, 127.2, 126.6, 126, 125.4, 125.0, 121.4. HRMS: Calc. 912.1510. Found: 913.1518. Anal. Calc. for $C_{58}H_{32}N_4S_4$: C 76.29, H 3.53, N 6.14. Found: C 76.72, H 3.47, N 6.53.

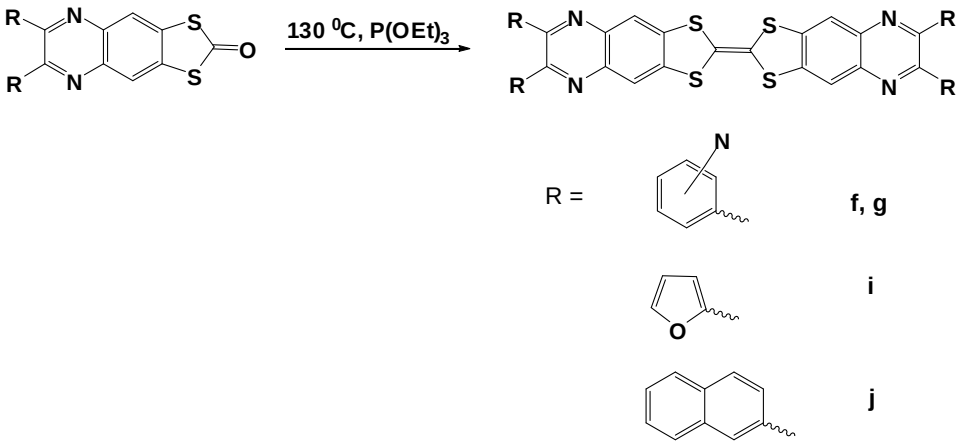


**Scheme 4.7.** Synthetic route for new heterocyclic tetrathiafulvalene derivatives

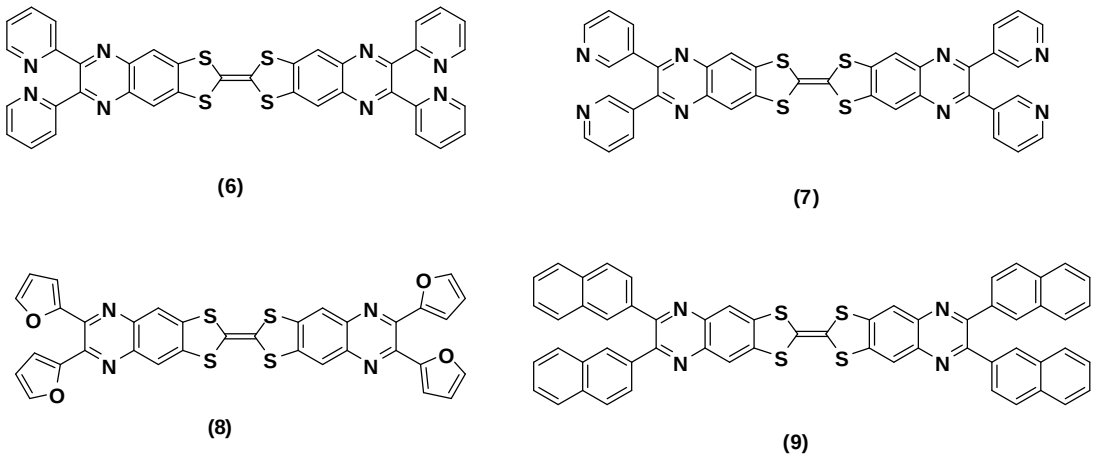


**Scheme 4.8.** Structural representation of synthesized TTF derivatives **6**-**9**.

## 4.2.3. Results and discussion:

The UV-vis absorption spectral measurements of the compounds **6–9** are carried out in $CHCl_3$ at an ambient temperature (298 K). As shown in Figure 4.9, absorption spectra of all the compounds exhibit two peaks at 281 and 471 nm. The lowest energy band in the 400 – 800 nm region corresponds to intramolecular charge transfer (ICT) transition from the TTF unit to the substituted (R = pyridin-2-yl (**6**), pyridin-3-yl (**7**), furan-2-yl (**8**) and naphthalen-2-yl (**9**)) pyrazine unit.[47] $\pi$–$\pi$* transition between TTF and substituted pyrazine core unit is believed to be responsible for the strong absorption band in the UV region in their electronic absorption spectra.[47]

As shown in Figure 4.9, all these A–D–A compounds are found to be acid sensitive and addition of hydrochloric acid induces changes in the absorption spectral properties with the appearance of new bands between 300 and 670 nm. Except for compound **6**, 11.6 M HCl is directly used for the titration experiments of compounds **7**-**9**. Figure 4.9(a) shows the effect of acid on the spectral properties of compound 6 in $CHCl_3$. Addition of different volumes of acid (2.3 M) to 4 x $10^{-5}$ M to compound **6** solution leads to shift in the 281 and 471 nm bands to 305 and 502 nm respectively. It has already been demonstrated experimentally and theoretically that benzimidazole nitrogen atoms have higher proton affinity than pyridine-2-yl moiety.[48] Based on this literature report, we anticipate that protonation, in case of compound **6**, starts with pyridine nitrogen atoms followed by nitrogen atoms on the pyrazine moiety. Similar is the case with TTF derivative of compound **7**. The order of electron donating capacity of the substituents to

the pyrazine moiety is as follows: furan-2-yl > naphthalen-2-yl > pyridin-2/3-yl.[49] After adding acid, spectral changes have also been observed in case of furan-2-yl substituent of the compound **8**, with peak shift from 492 nm to 663 nm. Addition of acid to naphthalene-2-yl substituent of compound **9** results in the shift of 270 and 474 nm bands to 307 and 634 nm respectively. Though the present experiments reveal that all these TTF derivatives are acid sensitive, studies to establish the complete picture of protonation of TTF derivatives and the nature of nitrogens that get protonated are presently progress in our laboratory.

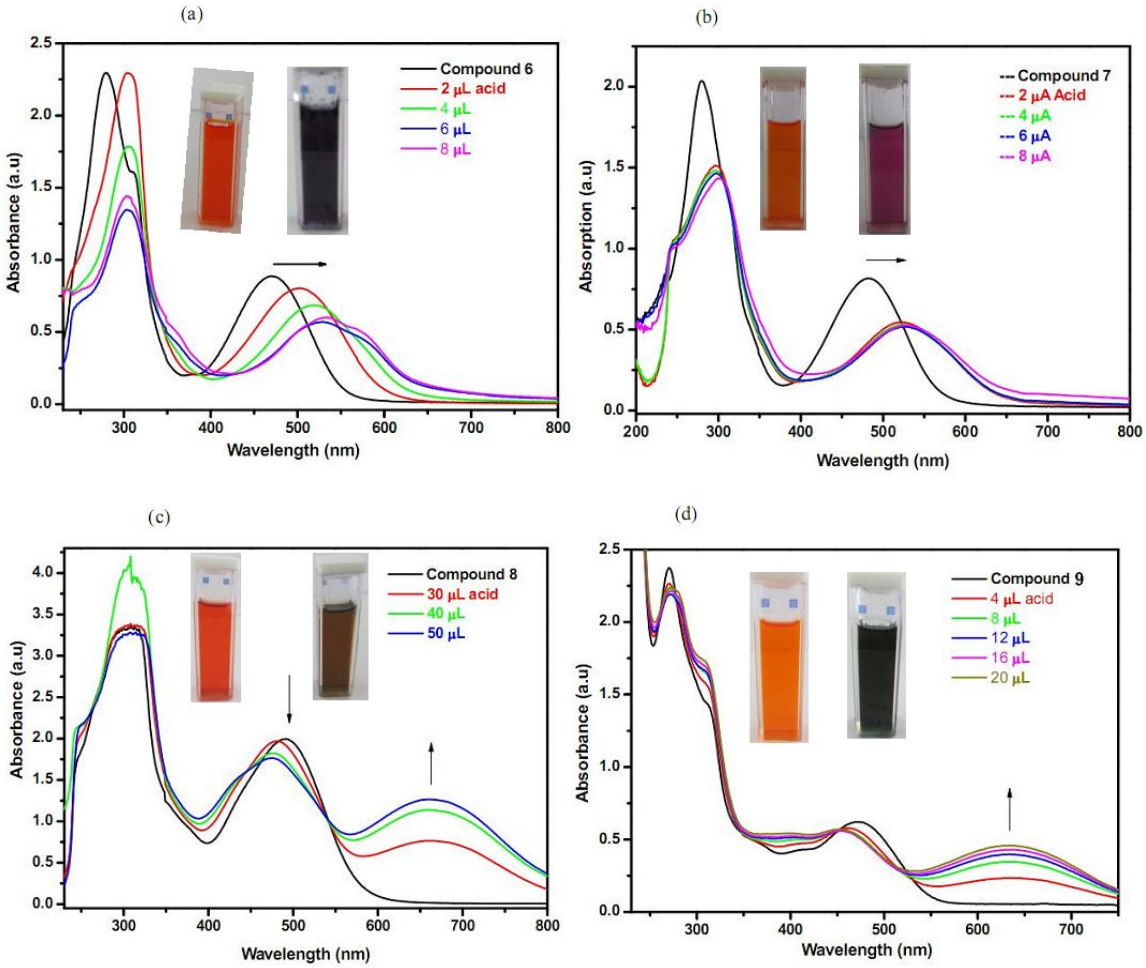


**Figure 4.9.** All spectra were recorded in $CHCl_3$ solvent , (a) absorption spectra of compound **6** ($4x10^{-5}$ M) vs HCl ($23x10^{-1}$M), (b) compound **7** ($7.5x10^{-5}$M) vs HCl (11.6 M), (c) compound **8** ($33x10^{-5}$M) vs HCl (11.6 M), (d) compound **9** ($4x10^{-5}$ M) vs HCl (11.6 M). Insets show the photographs of the compounds before and after acid treatment.

## 4.3. Conclusion

We have described here *N*-heterocyclic based nickel bis(dithiolene) complexes $(PPh_4)_2[Ni(C_8H_2N_2S_2R_2)_2]$ (R = Pyridin-2-yl (**1**), Pyridin-3-yl (**2**), Thiophen-2-yl (**3**), Furan-2-yl (**4**) and Naphthalen-2-yl (**5**)). Complexes **2** and **3** have been characterized by X-ray crystallography; the relevant analysis shows supramolecular weak interactions in the crystal structures and the distortion in square-planar geometry around the metal ion in terms of dihedral angle ($\lambda$) between two SMS planes and bending angle ($\eta$) (between the SMS and CSSC planes) of dithiolene chelate ring system. We have compared the effect of dithiolene-substituents on the electronic absorption spectral shift. The more electron donating group / more delocalization dithiolene core moiety exhibits band at near-IR region, hence there is a red shift (892 nm) for the naphthlen-2-yl substituent group of dithiolene complex **5**. Charge transfer absorption band in compounds **1** and **2** (635 and 639 nm) are influenced by the solvent polarity, and hence it shows a negative solvatochromism (absorption band is shifted towards blue shift for the more polar solvent). An important aspect of the present study is that compound **5** is oxidized electrochemically at a very low oxidation potential meaning that complex $(PPh_4)_2[Ni^{II}(C_8H_2N_2S_2R_2)_2]$ (**5**) (R = naphthalen-2-yl) would be easily oxidized to corresponding Ni(III) compound $(PPh_4)[Ni^{III}(C_8H_2N_2S_2R_2)_2]$. *N*-heterocyclic based intramolecular TTF derivatives has been prepared characterized by HRMS techniques. All these TTF derivatives (**6**–**9**) exhibit bands nearly at 281 and 471 nm. After titration with acid we can observe new shifting peaks within the range of 300–680 nm, due to the protonation of the pyrazine nitrogen atoms.

**Table 4.1**. Crystal data and structural refinement for compounds **2** and **3**.

| | **2** | **3** |
|---|---|---|
| Empirical formula | $C_{80}H_{60}NiN_8S_4P_2$ | $C_{80}H_{56}N_4NiP_2S_8$ |
| Formula weight | 1430.29 | 1450.42 |
| Temperature (K) | 298K | 100K |
| Crystal size (mm) | 0.24 x 0.22 x 0.18 | 0.28X0.26X0.22 |
| Crystal system | Monoclinic | Triclinic |
| space group | *P2(1)/c* | *P*-1 |
| Z | 2 | 1 |
| Wavelength (Å) | 0.71073 | 0.71073 |
| *a* [Å] | 15.506(5) | 9.364(10) |
| *b* [Å] | 15.916(5) | 10.592(11) |
| *c* [Å] | 15.090(4) | 17.983(19) |
| α [°] | 90.00 | 78.44(2) |
| β [°] | 90.97(2) | 76.54(2) |
| γ [°] | 90.00 | 73.63(2) |
| Volume [$Å^3$] | 3723.95(19) | 1647.0(3) |
| Calculated density ($Mg/m^{-3}$) | 1.276 | 1.462 |
| Reflections collected/ unique | 14890/6451 | 15756/ 5783 |
| R(int) | 0.0357 | 0.0485 |
| F(000) | 1484 | 750 |
| Max. and min. transmission | 0.9208 and 0.8964 | 0.8705 and 0.8393 |
| θ range for data collection(deg.) | 2.70 to 25.00 | 2.03 to 25.00 |
| Data / restraints / parameters | 6451 / 0 / 448 | 5783 / 0 / 430 |
| Goodness-of-fit on $F^2$ | 0.821 | 1.208 |
| $R_1/wR_2$ [I>2sigma(I)] | 0.0550/ 0.1484 | 0.0704/ 0.1401 |
| $R_1/wR_2$ (all data) | 0.0911 / 0.1761 | 0.0858/ 0.1464 |
| Largest diff. peak and hole [$e.Å^{-3}$] | 0.330 and -0.247 | 0.962 and -0.474 |

**Table 4.2**. Hydrogen bonding parameters for compounds **2** and **3** [Å and deg.].

| D-H...A | d(D-H) | d(H...A) | d(D...A) | <(DHA) |
|---|---|---|---|---|
| Compound **2** | | | | |
| C(10)-H(10) ...N(3)#1 | 0.93 | 2.52 | 3.363(6) | 150.2 |
| C(39)-H(39) ...N(3)#2 | 0.93 | 2.92 | 3.653(7) | 136.5 |
| Compound **3** | | | | |
| C(31)-H(31)...N(1)#3 | 0.93 | 2.85 | 3.529(6) | 131.1 |
| C(22)-H(22)...N(2)#2 | 0.93 | 2.85 | 3.656(6) | 145.9 |
| C(27)-H(27)...N(1)#2 | 0.93 | 2.86 | 3.699(6) | 151.3 |
| C(11)-H(11)...S(4)#4 | 0.93 | 3.02 | 3.862(5) | 151.0 |

Symmetry transformations used to generate equivalent atoms:

#1 -x,y+0.5,-z+0.5 #2 -x,-y+1,-z+1 #3 -x+1,-y,-z+1 #4 -x,-y,-z+1

## 4.4. References


[1] Burns, R. P.; McAuliffe, C. A. *Adv. Inorg. Chem. Radiochem.***1979**, *22*, 303.

[2] Roberston, N.; Cronin, L. *Coord.Chem.Rev.***2002**, *227*, 93.

[3] McCleverty, J. A. *Prog. Inorg. Chem.***1969**, *10*, 49.

[4] Eisenberg, R. *Prog. Inorg. Chem.* **1970**, *12*, 295.

[5] Mueller-Westerhoff, U.T.; Vance, B.; In Comprehensive Coordination Chemistry Wilkinson, G.; Gillard, R.D.; McCleverty, J.A. *Eds.Pergamon: Osford*.**1987**, *2*, 16.

[6] Pullen, A. E.; Faulmann, C.; Pokhodnya, K. I.; Cassous, P.; Tokumoto, M. *Inorg. Chem.* **1988**, *37*, 6714.

[7] Davison, A.; Edelstein, N.; Holm, R. H.; Maki, A. H. *J. Am. Chem. Soc.* **1963,** *85*, 2029.

[8] Adams, H.; Coffey, A. M.; Morris, M. J.; Morris, S. A. *Inorg. Chem.* **2009**, *48*, 11945.

[9] Ward, M. D.; McCleverty, J. A. *J. Chem. Soc., Dalton Trans.* **2002**, 275.

[10] Tanaka, H.; Okano, Y.; Kobayashi, H.; Suzuki, W.; Kobayashi, A. *Science* **2001**, *291*, 285.

[11] Oliver, S. N.; Kershaw, S. V.; Underhill, A. E.; Hill, C. A. S.; Charlton, A.; MCLC S&T Sect B: *Nonlinear Opt.* **1995**, *10*, 87.

[12] Wang, K.; Stiefel, E. I. *Science* **2001**, *291*, 106.

[13] Fourmigue, M. *Acc. Chem. Res.* **2004**, *37*, 179.

[14] Mueller-Westerhoff, U. T.; Vance, B.; Yoon, D. I. *Tetrahedron* **1991**, *47*, 909.

[15] Basu, P.; Nigam, A.; Mogesa, B.; Denti, S.; Nemykin, V. N. *Inorg. Chim. Acta.* **2010**, *363*, 2857.

[16] Bui, T.-T.; Thieubaut, O.; Grelet, E.; Achard. M.-F.; Bonneval, B. G.-de.; Ching, K. I. M.-C. *Eur. J. Inorg. Chem.* **2011**, 2663.

[17] Rabaca, S.; Cerdeira, A. C.; Oliveira, S.; Santos, I. C.; Henriques, R. T.; Pereira, L. C. J.; Coutinho, J. T.; Almeida, M. *Polyhedron* **2012**, *39* , 91.

[18] Lee, H.-J.; Noh, D.-Y. *Polyhedron* **2000**, *19*, 425.

[19] Rabaca, S.; Cerdeira, A. C.; Neves, A. I. S.; Dias, S. I. G.; Mezier, C.; Santos, I. C.; Pereira, L. C. J.; Fourmigue, M.; Henriques, R. T.; Almeida, M. *Polyhedron* **2009**, *28*, 1069.

[20] Tian-Ming, Y.; Jing-lin, Z.; Xiao-Zeng, Y. *Polyhedron* **1995**, *14*, 1487.

[21] Zuo, J.-L.; Yao, T.-M.; You, F.; You, X.-Z.; Fun, H.-K.; Yip, B.-C. *J. Mater. Chem*. **1996**, *6*, 1633.

[22] Brusso, J. L.; Clements, O. P.; Haddon, R. C.; Itkis, M. E.; Leitch, A. A.; Oakley, R. T.; Reed, R. W.; Richardson, J. F. *J. Am. Chem. Soc*. **2004**, *126*, 8256.

[23] Jia, C.; Liu, S.-X.; Tanner, C.; Leiggener, C.; Neels, A.; Sanguinet, L.; Levillain, E.; Leutwyler, S.; Hauser, A.; Decurtins, X.; *Chem.-Eur. J*. **2007**, *13*, 3804.

[24] Morkved, E. H.; Andreassen, T.; Novakova, V.; Zimcik, P.; *Dyes and Pigments* **2009**, *82*, 276.

[25] Harrington, L. E.; Britten, J. F.; Hughes, D. W.; Bain, A. D.; Thepot, J.-Y.; McGlinchey, M. J.; *J. Organomet. Chem.* **2002**, *656*, 243.

[26] Bolligarla, R.; Das, S. K. *Tetrahedron Lett.* **2011**, *52*, 2496.

[27] Bruker. *SADABS, SMART, SAINT and SHELXTL*, 2000 (Bruker AXS Inc., Madison, Wisconsin, USA).

[28] Sheldrick, G. M. *Acta Cryst. Sect.* **2008,** *A 64*, 112.

[29] Sluis, P. V. D.; Speak, A. L. *Acta Crystallography.* **1990**, *A46* , 194.

[30] Wang, F.-M.; Chen, L.-Z.; Liu, Y.-M.; Lu, C.-S.; Duan, X.-Y.; Meng, Q.-J. *J. Coord. Chem*. **2012**, *65*, 87.

[31] Cummings, S. D.; Eisenberg, R. *Inorg. Chem.* **1995**, *34*, 2007.

[32] Shupack, S. I.; Billig, E.; Clark, R. J. H.; Williams, R.; Gray, H. B. *J. Am. Chem. Soc.* **1964**, *86*, 4594.

[33] Horie, H.; Takagi, A.; Hasebe, H.; Ozawa, T.; Ohta, K. *J. Mater. Chem.* **2001**, *11*, 1063.

[34] Reichardt, C. *Chem. Rev*. **1994**, *94* , 2319.

[35] Reichardt, C. *Chem. Soc. Rev*. **1992**, *21*, 147.

[36] Cha, S.; Choi, M. G.; Jeon H. R.; Chang, S.-K. *Sens. Accuators B: Chem*. **2011**, *157*, 14.

[37] Deplano, P.; Mercuri, M. L.; Pintus, G.; Trogu, E. F. *Comments on Inorg. Chem.* **2001**, *22*, 353.

[38] Reichardt, C. *Angew. Chem. Int. Ed.* **1965,** *4*, 29.

[39] Liptay, W. *Angew. Chem. Int. Ed*. **1969**, *8*, 177.

[40] Bolligarla, R.; Das, S. K. *Eur. J. Inorg. Chem.* **2012**, 2933.

[41] Bolligarla, R.; Durgaprasad, G.; Das, S. K. *Inorg. Chem. Commun*. **2011**, *14*, 809.

[42] Bolligarla, R.; Durgaprasad, G.; Das, S. K. *Inorg*. *Chem. Commun*. **2009,** *12*, 355.

[43] Bolligarla, R.; Kishore, R.; Durgaprasad, G. Inorg. *Chim .Acta* **2010**, *363*, 3061.

[44] (a) Carroll, R. L.; Gorman, C. B. *Angew. Chem*. **2002**, *114*, 4556. (b) Tsiperman, E.; Becker, J. Y.; Khodorkovsky, V.; Shames, A.; Shapiro, L. *Angew.Chem.* **2005**, *117*, 4083.

[45] (a) Murata, T.; Morita, Y.; Yakiyama, Y.; Fukui, K.; Yamochi, H.; Saito, G.; Nakasuji, K. *J. Am. Chem. Soc*. **2007**, *129*,10837. (b) Murata, T.; Morita, Y.; Fukui, K.; Sato, K.; Shiomi, D.; Takui, T.; Maesato, M.; Yamochi, H.; Saito, G.; Nakasuji, K. *Angew.Chem.* **2004**, *116*, 6503. (c) Morita, Y.; Yamamoto, Y.; Yakiyama, Y.; Murata, T.; Nakasuji, K. *Chem Lett*. **2008**, *37*, 24.

[46] (a) TTF Chemistry : Fundamentals and Applications of Tetrathiafulva-lene (Eds. : J.-I. Yamada, T. Sugimoto), Springer, Berlin, Germany,2004; (b) V. Khodorkovsky, J. Y. Becker, Organic Conductors: Fun-damentals and Applications(Ed. : J. P. Farges), Marcel Dekker, NewYork, NY, 1994, chap. 3. (c) J. M. William, J. R. Ferraro, R. J. Thorn,K. D. Carlson, U. Geiser, H. H. Wang, A. M. Kini, M. H. Whangbo,Organic Superconductors (Including Fullerenes): Synthesis Structure, Properties, and Theory, Prentice Hall, Englewoods Cliffs, NJ, 1992. (d) G. Saito, Y. Yoshida,Bull. *Chem. Soc. Jpn*. **2007**, *80*, 1. (e) Bolligarla, R.; Das, S. K. *Tetrahedron Lett*. **2011**, *52*, 2496.

[47] (a) Wu, J.; Dupont, N.; Liu, S.-X.; Neels, a.; Hauser A.; Decurtins, S. *Chem. Asian J*. **2009**, *4*, 392. (b) C. J. Chang, C. H. Yang, K. Chen, Y. Chi, C. F. Shu, M. L. Ho, Y. S.Yeh, P. T. Chou,Dalton Trans. **2007**, 1881.

[48] (a) J. Smets, W. McCarthy, G. Maes, L. Adamowicz, *J. Mol. Struct.* **1999**, *476*, 27. (b) Novo, M.; Mosquera, M.; Prieto, F. R. *Can. Chem.* **1992**, *70*, 823.

[49] Lumma, Jr. W. C.; Baldwin, J. J.; Bicking, J. B.; Bolhofer, W. A.; Hoffman, J. M.; Phillips, B. T.; Robb, C. M.; Torchiana, M. L.; Schlegel, H. B. *J. Med*. *Chem.* **1984**, *27*, 1047.

# Synthesis, Structural Characterization and Properties of New *N*-heterocyclic Carbene Ag(I) Complexes

5 Chapter

**Abstract:–** The syntheses, crystal structures and properties of new *N*-heterocyclic carbene complexes [{1-(2,3,5,6- tetra methyl benzyl)-3-benzylbimy}AgCl] (**2a**), [{1-(benzyl)-3-benzylbimy}$_2$Ag][$BF_4$] (**2b**), [{1-(benzyl)-3-butylbimy}AgBr]$_2$ (**2c**), [{1-(benzyl)-3-(4-nitro-benzyl)bimy}AgBr] (**2d**), [{1-(benzyl)-3-(4-bromo-benzyl)bimy}AgBr] (**2e**), [{1-(benzyl)-3-(4-nitro-benzyl)bimy}$_2$Ag][$BF_4$] (**2f**), [{1-(benzyl)-3-(4-bromo-benzyl)bimy}$_2$Ag][$BF_4$] (**2g**) (bimy = benzimidazol-2-ylidene), and [{1-(10-bromo-9-anthracenylmethyl)-3-butylimy}AgBr] (**2h**) (imy = imidazol-2-ylidene) have been described. Compounds **2a-2h** have been characterized by IR-, $^1$H NMR-, UV-visible- LC/MS-spectral and electrochemical studies including elemental analysis. Compounds **2a-2c** and **2h** are unambiguously characterized by single crystal X-ray crystallography.

## 5.1. Introduction

The most *N*-Heterocyclic carbenes (NHCs) are commonly derived from imidazolium/benzimidzolium salts. Generally NHCs have attracted considerable attention because of their ability to coordinate very strongly to transition metals and main-group elements.[1,2] In 1968, Ofele and Wanzlick first pioneered the metalation of imidazol-2-ylidenes, that are popularly known as *N*-Heterocyclic carbenes.[3,4] NHCs (as ligands) are considered to be better σ donors (i. e., Lewis bases) than most phosphines.[5] NHCs, that are air-stable, are significantly simpler to synthesize. Even though, these are not realized with $d^{10}$ ions, they have potential for metal-ligand back-bonding interactions.[6] While some of these carbenes are isolable, some are less stable that can be generated by in-situ.[7-11] Transition metal-NHC complexes have several applications in the areas of catalysis of organic reactions (most notably the Heck and Suzuki C–C coupling reactions),[12-20] supramolecular- and, materials-chemistry.[21-23] Silver-NHC complexes are generally prepared by a one-pot reaction of an imidazolium/benzimidazolium salt with $Ag_2O$, which can be easily derived. There are

some reports on benzimidazole-2-ylidene and imidazole-2-ylidene complexes of silver.[24-30] In fact, silver-NHC complexes have drawn significant interest, particularly because of their ability to act as effective carbene transfer agent for the syntheses of Ni-, Pd-, Pt-, Cu-, Au-, Rh-, Ir- and Ru-carbene complexes; indeed, this route is the only method for the effective preparation of metal-carbene metal complexes.[31-32] In addition, silver carbene metal complexes are well noted as efficient fluorescent switches; they show biological activity and have also been used as antimicrobial and antimitochondrial agents.[33-40] Herein we wish to report the syntheses of silver-NHC complexes [{1-(2,3,5,6- tetra methyl benzyl)-3-benzylbimy}AgCl] (**2a**), [{1-(benzyl)-3-benzylbimy}$_2$Ag][$BF_4$] (**2b**), [{1-(benzyl)-3-butylbimy}AgBr]$_2$ (**2c**), [{1-(benzyl)-3-(4-nitro-benzyl)bimy}AgBr] (**2d**), [{1-(benzyl)-3-(4-bromo-benzyl)bimy}AgBr] (**2e**), [{1-(benzyl)-3-(4-nitro-benzyl)bimy}$_2$Ag][$BF_4$] (**2f**), [{1-(benzyl)-3-(4-bromo-benzyl)bimy}$_2$Ag][$BF_4$] (**2g**) (bimy = benzimidazol-2-ylidene), and [{1-(10-bromo-9-anthracenylmethyl)-3-butylimy}AgBr] (**2h**). Among this **2a**–**2h**, the compounds **2a**, **2b**, **2c** and **2h** are unambiguously characterized by single crystal X-ray crystallography. All compounds **2a**–**2h** have been further characterized by routine elemental analysis, UV-vis electronic absorption-, $^1$H NMR- , and LC/MS -spectroscopic techniques.

## 5.2. Experimental Section

### 5.2.1. Materials and Methods

All the chemicals for synthesis were commercially available and used as received. Benzimidazolium/imidazolium salts of bromide/tetrafluoroborate were prepared according to literature procedure.[69,70] Syntheses of metal complexes were performed under light sensitive care. The general procedure is schematically shown in Scheme 5.1. Solvents were dried by standard procedures. Micro analytical (C, H, N) data were obtained with a FLASH EA 1112 Series CHNS Analyzer. $^1$H NMR spectra of compounds were recorded on Bruker DRX- 400 spectrometer using $Si(CH_3)_4$ [TMS] as an internal standard. Electronic absorption spectra of solutions were recorded on a Cary 100 Bio UV-Vis spectrophotometer.

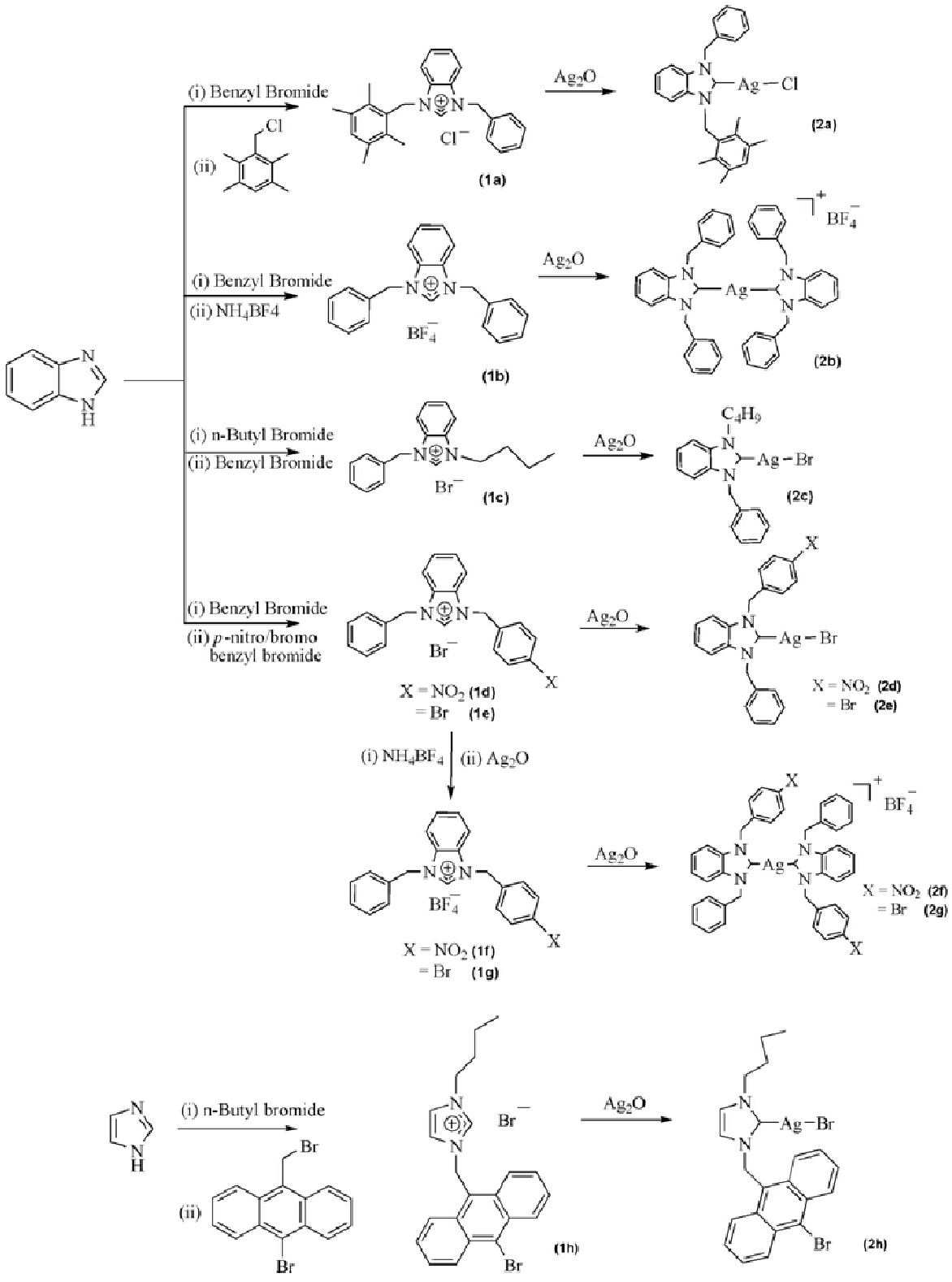


**Scheme 5.1.** Synthetic procedure to prepare silver-carbene complexes **2a**–**2h**.

### 5.2.2. Synthesis

**General method for the benzimidazolium/imidazolium salts:**

To a round-bottom flask containing benzimidazole/imidazole (1.0 mmol) in THF solution were added sodium hydroxide (2.2 mmol), tetrabutylammonium bromide (0.2 mmol), and benzyl/alkyl halide (1.1 mmol). The reaction mixture was refluxed for 4h and then cooled to room temperature and solvent was removed by rotary evaporator. Water was added to the mixture and solvent extract with dichloromethane, dried over by sodium sulphate and solvent was removed by rotary evaporator. To this product, benzyl/anthracenyl halide was added in THF solution and kept reflux for overnight, and filtered the compound, dried the compound by air.

*3-Benzyl-1-(2,3,5,6-tetramethyl-benzyl)-3H-benzoimidazol-1-ium chloride (**1a**)*:

Yield: (0.794 g). $^1$H NMR (400 MHz, $\delta$ ppm) (DMSO-$d_6$): 10.01 (s, 1H), 7.92 (m, 4H), 7.43 (m, 6H), 5.64 (d, 4H), 2.21 (m, 12H). Anal. Calc. for $C_{25}H_{27}ClN_2$: C 76.80, H 6.96, N 7.17. Found: C 77.15, H 7.02, N 7.35 %.

*1,3-Dibenzylbenzimidazolium tetrafluoroborate (**1b**)*:

Yield: 0.750g. $^1$H NMR (400 MHz, DMSO-$d_6$): $\delta$ 10.02 (s, 1 H), 7.98-7.96 (m, 2H), 7.65-7.63 (m, 2 H), 7.52 (d, 4H), 7.46-7.37 (m, 6 H), 5.79 (s, 4H). Anal. Calc. for $C_{21}H_{19}BF_4N_2$: C 65.31, H 4.96, N 7.25. Found: C 65.69, H 5.03, N 7.69 %.

*3-Benzyl-1-butyl-3-H-benzimidazol-1-ium bromide (**1c**)*:

Yield: 0.894 g. $^1$H NMR (400 MHz, $\delta$ ppm) (DMSO-$d_6$): 10.01 (s, 1H), 7.89 (s, 1H), 7.75 (s, 1H), 7.43 (m, 7H), 5.78 (s, 2H), 4.53 (s, 2H), 1.87 (s, 2H), 1.34 (s, 2H), 0.91 (s, 3H). Anal. Calc. for $C_{18}H_{21}BrN_2$: C 62.61, H 6.13, N 8.11. Found: C 62.96, H 6.19, N 8.42 %.

*1-Benzyl-3-(4-Nitro-benzyl)benzimidazolium bromide (**1d**)*:

Yield: 0.862g. $^1$H NMR (400MHz, DMSO-$d_6$): $\delta$ 9.98 (s, 1H), 7.77 (s, 2H), 7.54 (d, 4H), 7.37 (m, 7H), 5.79 (d, 4H). Anal. Calc. for $C_{21}H_{18}BrN_3O_2$: C 59.45, H 4.28, N 9.90. Found: C 59.12, H 4.35, N 10.22 %.

*1-Benzyl-3-(4-Bromo-benzyl)benzimidazolium Bromide (**1e**)*:

Yield: 0.960g. $^1$H NMR (400MHz, DMSO-$d_6$): $\delta$ 9.98 (s, 1H), 7.96 (t, 2H, J= 3.6), 7.64 (t, 4H, J= 3.6), 7.51 (t, 4H, J= 8.4), 7.45-7.39 (m, 3H), 5.78-5.76 (4H). Anal. Calc. for $C_{21}H_{18}Br_2N_2$: C 55.05, H 3.96, N 6.11. Found: C 55.39, H 4.03, N 6.42 %.

*1-Benzyl-3-(4-Nitro-benzyl)benzimidazolium tetrafluoroborate (**1f**)*:

Yield: 0.862g. $^1$H NMR (400MHz, DMSO-$d_6$): $\delta$ 10.01 (s, 1H), 8.29 (d, 2H, J=8.8), 7.97 (s, 2H), 7.91 (s, 2H), 7.77 (d, 2H, J=8.4), 7.65 (t, 2H, J=3.6), 7.54 (d, 2H, J=7.2), 7.43 (t, 3H, J=4.8), 5.96 (s, 2H), 5.80 (s, 2H). Anal. Calc. for $C_{21}H_{18}BF_4N_3O_2$: C 58.49, H 4.21, N 9.75. Found: C 58.85, H 4.28, N 10.04 %.

*1-Benzyl-3-(4-Bromo-benzyl)benzimidazolium tetrafluoroborate (**1g**)*:

Yield: 0.794 g. $^1$H NMR (400 MHz, $\delta$ ppm) (DMSO-$d_6$): 9.99 (s, 1H), 7.72 (m, 2H), 7.26-7.39 (m, 11H), 5.78 (d, 4H). Anal. Calc. for $C_{21}H_{18}BF_4N_2Br$: C 54.23, H 3.90, N 6.02. Found: C 54.58, H 3.95, N 6.34 %.

*3-Benzyl-1-(10-bromo-anthracen-9-ylmethyl)-3H-imidazol-1-ium bromide (**1h**)*: Yield: 0.784 g. $^1$H NMR (400 MHz, $\delta$ ppm) (DMSO-$d_6$): 9.87 (s, 1H), 8.67-8.34 (m, 4H), 7.67-7.32 (m, 6H), 6.12 (m, 2H), 3.53 (s, 2H), 1.50 (s, 2H), 0.98 (s, 2H), 0.67 (s, 3H). Anal. Calc. for $C_{22}H_{22}Br_2N_2$: C 55.72, H 4.68, N 5.91. Found: C 55.96, H 4.75, N 6.29 %.

**Preparation of the silver-carbene complexes (2a–2h)**

*[($C_{25}H_{26}N_2$)AgCl]* **(2a)**

A stirred suspension of KOBu$^t$ (0.04 g, 0.3 mmol), 3-Benzyl-1-(2,3,5,6-tetramethyl-benzyl)-3H-benzoimidazol-1-ium chloride (**1a**) (0.160 g, 0.3 mmol) and silver oxide (0.04 g, 0.15 mmol) in $CH_2Cl_2$ (15 mL) was stirred at room temperature for 4 h. After completion of this reaction, it was filtered through celite and solvent was concentrated to 3 mL by rotary evaporator and subsequently diethylether (2 mL) was added to give white solid. Yield: (0.08 g). $^1$H NMR (400 MHz, $\delta$ ppm) (DMSO-$d_6$): 2.21 (m, 12H), 5.64 (d, 4H), 7.43 (m, 6H), 7.92 (m, 4H). MS (ESI): *m/z* 496. Anal. Calc. for $C_{25}H_{26}N_2AgCl$: C 60.32, H 5.26, N 5.63. Found: C 60.55, H 5.21, N 5.97 %.

*[($C_{21}H_{18}N_2$)$_2$Ag][$BF_4$]* **(2b)**

This complex was prepared in a manner analogous to that of **2a**. In this case, the reactants are: 1,3-dibenzylbenzimidazolium tetrafluoroborate (**1b**) (0.772 g, 2 mmol), KOBu$^t$ (0.11 g, 1 mmol) and silver oxide (0.232 g, 1 mmol). Complex **2b** was obtained as a white powder. Yield: (0.54 g). $^1$H NMR (400 MHz, $\delta$ ppm) (DMSO-$d_6$): 5.78 (s, 8H), 7.30 (m,

20H), 7.44 (s, 4H), 7.78 (s, 4H). MS (ESI): *m/z*: 702 $(M-H)^+$. Anal. Calc. for $C_{42}H_{36}N_4AgBF_4$: C 63.74, H 4.58, N 7.08. Found: C 64.09, H 4.52, N 6.67 %.

*$[(C_{18}H_{20}N_2)AgBr]_2$* (**2c**)

This complex was prepared in a manner analogous to that of **2a**. The starting precursors are: 3-benzyl-1-butyl-3-H-benzimidazol-1-ium bromide (**1c**) (0.373 g, 1 mmol), $KOBu^t$ (0.11 g, 1 mmol) and silver oxide (0.116 g, 0.5 mmol). Complex **2c** was obtained as a white powder. Yield: (0.22 g). $^1$H NMR (400 MHz, $\delta$ ppm) (DMSO-$d_6$): 0.91 (s, 6H), 1.34 (s, 4H), 1.87 (s, 4H), 4.53 (s, 4H), 5.78 (s, 4H), 7.43 (m, 14H), 7.75 (s, 2H), 7.89 (s, 2H). MS (ESI): *m/z*: 635 ($[L_2Ag]^+$, 100%). Anal. Calc. for $C_{36}H_{40}Ag_2Br_2N_4$: C 47.82, H 4.46, N 6.20. Found: C 47.49, H 4.39, N 6.67 %.

*$[(C_{21}H_{17}N_3O_2)AgBr]$* (**2d**)

1-Benzyl-3-(4-nitro-benzyl)benzimidazolium bromide (**1d**) (0.212 g, 0.5 mmol) was taken in $CH_2Cl_2$ (20 mL); to this, silver oxide (0.058 g, 0.25 mmol) was added. It was then stirred for 4 h at ambient temperature. After completion of this reaction, it was fileterd through celite and solvent was concentrated to 3 mL. Subsequently, diethylether (2 mL) was added to give a white powder. Yield: (0.124 g). $^1$H NMR (400 MHz, $\delta$ ppm) (DMSO-$d_6$): 5.78 (d, 4H), 7.36 (m, 7H), 7.56 (d, 4H), 7.76 (s, 2H). MS (ESI): *m/z*: 529. Anal. Calc. for $C_{21}H_{17}N_3O_2AgBr$: C 47.49, H 3.23, N 7.91. Found: C 47.85, H 3.28, N 7.54 %.

*$[(C_{21}H_{17}N_2Br)AgBr]$* (**2e**)

1-Benzyl-3-(4-Bromo-benzyl)benzimidazolium bromide (**1e)** (0.343 g, 0.74 mmol) was taken in $CH_2Cl_2$ (20 mL). It was then treated with silver oxide (0.088 g, 0.37 mmol). The resulting reaction mixture was stirred for 8 h at an ambint temperature. After completion of this reaction, it was fileterd through celite and remove the solvent by rotary evaporator. The final product was then washed with diethyl ether and air dried. Yield: (0.144 g). $^1$H NMR (400 MHz, $\delta$ ppm) (DMSO-$d_6$): 5.80 (s, 2H), 5.97 (s, 2H), 7.37 (m, 7H), 7.54 (d, 2H), 7.76 (m, 2H), 8.19 (d, 2H). MS (ESI): *m/z*: 562. Anal. Calc. for $C_{21}H_{17}N_2AgBr_2$: C 44.64, H 3.03, N 4.96. Found: C 44.35, H 3.09, N 5.38 %.

*$[(C_{21}H_{17}N_3O_2)_2Ag][BF_4]$* **(2f)**

1-Benzyl-3-(4-nitro-benzyl)benzimidazolium tetrafluoroborate (**1f**) (0.431 g, 1 mmol) and silver oxide (0.116 g, 0.5 mmol) were taken in acetonitrile (20 mL); the resulting reaction mixture was then refluxed for overnight. After cooling the solvent, it was filtered through celite and solvnet was concentrated to 3 mL by rotary evaporator. Diethylether (3 mL) was added to give white product. Yield: (0.231 g). $^1$H NMR (400 MHz, $\delta$ ppm) (DMSO-$d_6$): 5.76 (s, 4H), 5.92 (s, 4H), 7.28-7.39 (m, 14H), 7.49 (d, 4H), (7.70 (m, 4H), 8.12 (d, 4H). MS (ESI): *m/z*: 793. Anal. Calc. for $C_{42}H_{34}N_6O_4AgBF_4$: C 57.23, H 3.89, N 9.53. Found: C 57.57, H 3.84, N 9.97 %.

*$[(C_{21}H_{17}N_2Br)_2Ag][BF_4]$* (**2g**)

This complex was prepared in a manner analogous to that of **2f**. The starting precursors are: 1-benzyl-3-(4-Bromo-benzyl)benzimidazolium tetrafluoroborate (**1g)** (0.165 g, 0.35 mmol) and silver oxide (0.04 g, 0.17 mmol). Complex **2g** was obtained as a white powder. Yield: (0.115 g). $^1$H NMR (400 MHz, $\delta$ ppm) (DMSO-$d_6$): 5.75 (d, 8H), 7.28-7.38 (m, 22H), 7.70 (m, 4H). MS (ESI): *m/z*: 859. Anal. Calc. for $C_{42}H_{34}N_4Br_2AgBF_4$: C 53.14, H 3.61, N 5.90. Found: C 53.54, H 3.18, N 6.39 %.

*$[(C_{22}H_{21}N_2Br)AgBr]$* (**2h**)

3-Benzyl-1-(10-bromo-anthracen-9-ylmethyl)-3H-imidazol-1-ium bromide (**1h**) (0.271 g, 0.5 mmol) was taken in $CH_2Cl_2$ (25 mL); to this, silver oxide (0.06 g, 0.25 mmol) was added added. It was then stirred for over night at ambient temperature. After completion of this reaction, it was fileterd through celite. The solvent was then concentrated to 3 mL by rotary evaporator. Finally, diethylether was added to give brown powder. Yield: (0.128 g). $^1$H NMR (400 MHz, $\delta$ ppm) (DMSO-$d_6$): 0.67 (s, 3H), 1.01 (s, 2H), 1.50 (s, 2H), 3.73 (s, 2H), 6.22 (m, 2H), 7.67-7.32 (m, 6H), 8.69-8.36 (m, 4H). MS (ESI): *m/z*: 578. Anal. Calc. for $C_{22}H_{21}N_2AgBr_2$: C 45.47, H 3.64, N 4.82. Found: C 45.82, H 3.57, N 4.39 %.

### 5.2.3. Crystal structure determination

Single crystals, suitable for facile structural determination for the compounds **2a**–**2c** and **2h**, were measured on a three circle Bruker SMART APEX CCD area detector system under Mo–Kα ($\lambda$ = 0.71073 Å) graphite monochromatic X–ray beam. The frames were recorded with an ω scan width of 0.3º, each for 10 s, crystal-detector distance 60 mm, collimator 0.5 mm. Data reduction performed by using SAINTPLUS.[71] Empirical absorption corrections using equivalent reflections performed program SADABS.[71] The Structures were solved by direct methods and least-square refinement on $F^2$ for all the compounds **1**–**3** by using SHELXS-97.[72] All non-hydrogen atoms were refined anisotropically. The hydrogen atoms were included in the structure factor calculation by using a riding model. The crystallographic parameters, data collection and structure refinement of the compounds **2a**–**2c**, and **2h** are summarized in Table 5.1. Selected bond lengths and angles for the compounds **2a**–**2c**, and **2h** are listed in Table 5.2. The hydrogen bonds for the compounds **2a**–**2c**, and **2h** are shown Table 5.3. The anisotropic displacement parameters of carbon atom C22 are non-positive definite, indicating the unresolved disorder, also the maximum and minimum main axis ADP ratio of the carbon atoms C1, C2 and C4 are more than 5.0 indicating the unresolved disorder. However, no proper model (by applying restraints ISOR or SIMU to displacement parameters) was used to resolve this problem. Even though, we collected data for the compound **2c** at 100 K and with a better quality of crystal we could not resolve the disorder problem.

## 5.3. Results and Discussion

### 5.3.1. Synthesis and spectroscopic characterization

Benzimidazolium/imidazolium halides were prepared according to Scheme 5.1. Compounds of benzimidazolium halides **1d** and **1e** are changed to corresponding benzimidazolium tetrafluoroborate **1f** and **1g** respectively by an anionic exchange reaction with $NH_4BF_4$. The precursors **1b**, **1f** and **1g** are soluble in organic solvents, such as, $CH_2Cl_2$, $CH_3OH$, and $CH_3CN$, and insoluble in diethyl ether, hydrocarbon solvents. The direct reaction of benzimidazolium/imidazolium halides with silver oxide in presence of $KOBu^t$ in $CH_2Cl_2$, furnishes the complexes [{1-(2,3,5,6- tetra methyl benzyl)-3-benzylbimy}AgCl] (**2a**), [{1-

(benzyl)-3-benzylbimy}$_2$Ag][$BF_4$] (**2b**), [{1-(benzyl)-3-butylbimy}AgBr]$_2$ (**2c**). The remaining carbene complexes have been prepared without using base by refluxing the acetonitrile solution of benzimidazolium/imidazolium halides and silver oxide affording complexes [{1-(benzyl)-3-(4-nitro-benzyl)bimy}AgBr] (**2d**), [{1-(benzyl)-3-(4-bromo-benzyl)bimy}AgBr] (**2e**), [{1-(10-bromo-9-anthracenylmethyl)-3-butylimy}AgBr] (**2h**), and [{1-(benzyl)-3-(4-nitro-benzyl)bimy}$_2$Ag][$BF_4$] (**2f**), [{1-(benzyl)-3-(4-bromo-benzyl)bimy}$_2$Ag][$BF_4$] (**2g**). All these complexes are stable to air, moisture, and sensitive to sonication, higher temperature. Benzimidazolium/imidazolium halides were deprotaned by the use of strong base KOBu$^t$, and for the preparation of some of the complexes (**2d-2g**), silver oxide acts as a base. The $^1$H NMR spectra of these carbene complexes **2a**–**2h** do not show a low-field signal within the range of 9.50-10.00 ppm, and the chemical shifts of other hydrogens are similar to those of benzimidazolium/imidazolium halide derivatives of **1a**–**1h**. We could not record the $^{13}$C NMR spectra for carbene peak because of its poor solubility in dueterated organic solvents. The colorless, air-stable crystals of **2a-2c** and **2h**, suitable for single X-ray crystallography, are obtained by slow diffusion of $Et_2O$ into their respective $CH_2Cl_2$ soltutions, and methanol into its 1,2-dichloromethane solution, respectively.

Thermal ellipsoidal diagrams and the crystal packing of the complexes **2a**–**2c,** and **2h** are depicted in Figures. 5.1 to 5.4 respectively. The internal angle (N–C–N) at the carbene center is within the range of 104.48˚ to 105.88˚, which is similar to that of some known similar silver complexes.[40-42] In carbene complexes, the bond between metal and carbene carbon is arised by carbene-metal σ-donation as well as π-back donation from the d-orbitals of metal to the carbene carbon;[43-49] thus the carbon-metal bond has a partial double bond character. The Ag–$C_{carbene}$ bond distances in complexes **2a**–**2c**, and **2h** are 2.082, 2.089, 2.129, and 2.062 Å respectively. This indicates that the partial double bond character between carbene carbon and metal is more in complex **2h** compared to those in remaing **2a–2c** complexes. In the crystal structure of complex **2c**, the Ag-benzimy (bimy) bond distance (Ag1–C19 = 2.129 Å) indicates very little π-back-donation and accordingly this metal-benzimy complex shows very little metal-carbene double bond character,[50,51] which is in consistent with known silver-NHC complexes.[52-59] There are only few reports on anthracene moiety associated benzimidazole and imidazole type silver carbene complexes. In

these compouds, the Ag–$C_{carbene}$ bond distances are within the range of 2.073–2.088 Å (benzimidazole type) and 2.084–2.182 Å (imidazole type).[40,58,60-62] As per this reported data, the shortest Ag–$C_{carbene}$ bond (2.062 Å) in the present study (compound **2h,** among related literature).

The electronic absorption spectra of complexes **2a**–**2h** are measured in dichloromethane. As shown in the Figure 5.5(a), the complexes of **2a**–**2g** exhibit two bands at 230 nm and 270–285 nm respectively; the compound **2h** exhibits two bands at 250 nm, and 360–400 nm respectively. The fluorescent emission spectra of **1h** and **2h** in dichloromethane solutions are shown in Figure 5.5(b). Both lignad **1h** and complex **2h** exhibit a structured fluoroscene emission spectrum in the region of 386–440 nm. Thus the emission intensity of **1h** is enhanced to some extent after its complexation with silver.

### 5.3.2. Description of crystal structures

*[{1-(2,3,5,6- tetra methyl benzyl)-3-benzylbimy}AgCl]*: *[($C_{25}H_{26}N_2$)AgCl]* **(2a)**

The crystals of complex **2a**, suitable for single crystal X-ray structure determination, were obtained from diffusion of $Et_2O$ into dichloromethane solution. Crystallographic analysis reveals that complex **2a** crystallizes in triclinic system with *P*-1 space group. The angle between <C1AgCl1 is 175.01°, which indicates the near-linear structure of the C–Ag–C moiety as shown in Figure 5.1(a). In its crystal structure, the chlorine atom is situated with a distance of 0.4 Å from the benzimidazole moiety plane. The two aryl rings are attached to the imidazole ring through two nitrogen atoms. The angle between the mean planes of benzimadazole moiety and phenyl moiety is 85.17° and that of benzimadazole moiety and tetra methyl phenyl moiety is 89.23° (Figure 5.1(a)). The orientation of the two phenyl rings is in trans direction with respect to the benzimadazole moiety. The supramolecular interaction between halogen and a hydrogen ($C_2$–$H_5$···$Cl_1$) is 2.780 Å. This intermolecular interaction leads to a 2D network, as shown in Figure 5.1(b). In the crystal packing, there are C–H···π interactions with a distance of 2.78 Å between the centroid (Cg = C9C10C11C12C13C14) of the tetra methyl phenyl ring and the hydrogen atom from the benzyl carbon atom (C8–H8B), as shown in Figure 5.1(c).

(a)

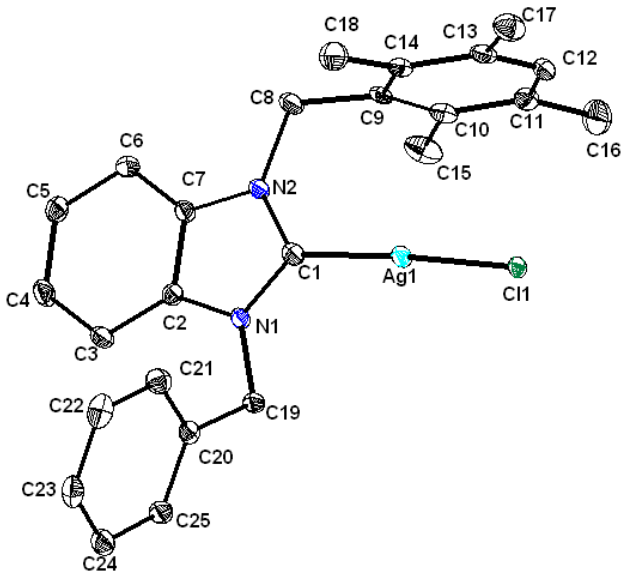
C18
C14
C13
C17
C12
C8
C9
C10
C11
C16
C15
C6
C7
N2
C5
C1
Ag1
Cl1
C4
C2
N1
C3
C21
C22
C19
C20
C23
C25
C24

(b)

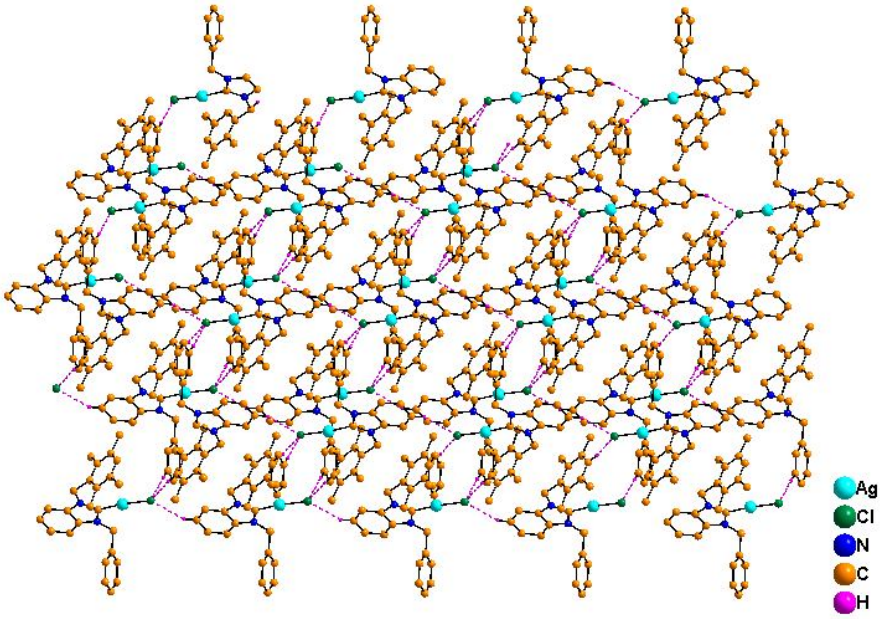
Ag
Cl
N
C
H

**(c)**

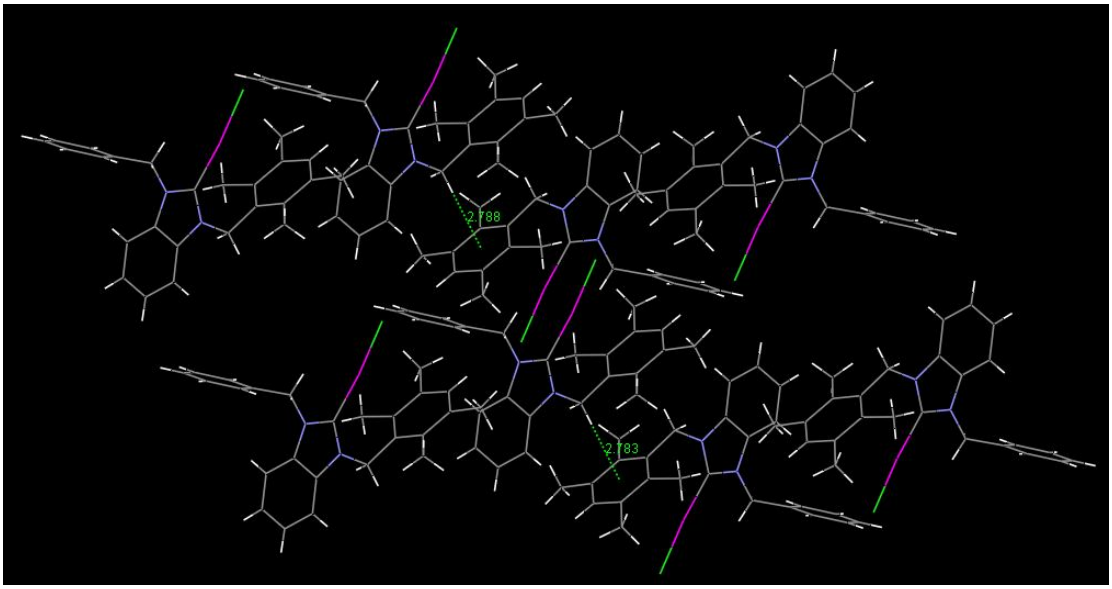


**Figure 5.1.** (a) Thermal ellipsoidal (40 % probability) plot of compound **2a** and (b) packing diagram in the crystal structure of **2a** (hydrogen atoms are omitted for clarity), (c) C–H···π interactions in compound **2a.**

*[{1-(benzyl)-3-benzylbimy}$_2$Ag][BF$_4$]*: *[(C$_{21}$H$_{18}$N$_2$)$_2$Ag][BF$_4$]* **(2b)**

The compound **2b** was crystallized in triclinic space group *P*-1. Thermal ellipsoidal diagram of the compound **2b** has been shown in Figure 5.2(a). In the crystal structure, the silver ion is connected to two carbene moieties with a distance of 2.089 Å. Out of four phenyl rings, two are situated at above, and the remaining two are at below the plane of the benzimidazole moiety in compound **2b**. The angle between mean planes of the two benzimidazole moieties is 0.60° indicating that the planes of two benzimidazole moieties are slightly deviated from their co-planarity nature. The angle <C1AgC22 (Figure 5.2(a)) of 177.88° indicates the near-linear structure of C–Ag–C bonds. The dihedral angle between the planes of phenyl rings presented on the benzimidazole moiety i.e. (C9C10C11C12C13C14) and (C16C17C18C19C20C21) is 88.28°, while in the other benzimidazole moiety, it is 81.13° [i.e. angle between (C30C31C32C33C34C35) and (C37C38C39C40C41C42)]. This suggests that the two benzimidazole moieties, which are connected by the silver ion, are in a different alignment. There is a π···π stacking interaction between two benzimidazole moieties with a distance of

3.579 Å. The supramolecular interactions between fluorine atoms (of $BF_4^-$ anion) and hydrogen atom (from organic component) afford a 2D-network as shown in Figure 5.2(b); in the relevant crystal packing, the "Z" type interaction-patterns are observed which are shown in purple color dotted lines.

(a)

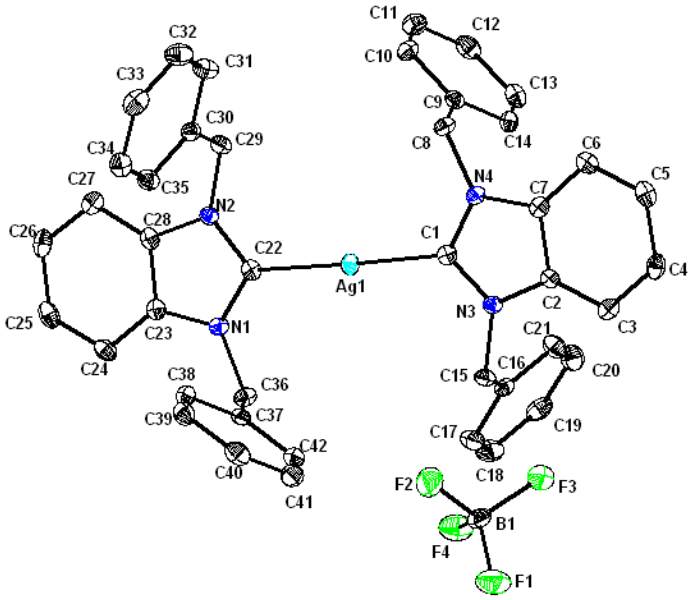


(b)

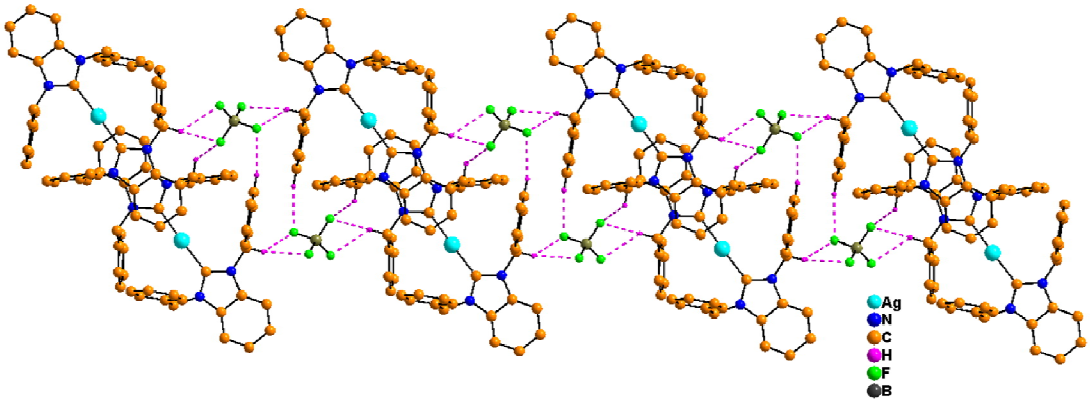


**Figure 5.2.** (a) Thermal ellipsoidal (50 % probability) plot of **2b**, and (b) packing diagram in the crystal structure of compound **2b** (hydrogen atoms are omitted for clarity).

*[{1-(benzyl)-3-butylbimy}AgBr]$_2$*: *[($C_{18}H_{20}N_2$)AgBr]$_2$* (**2c**)

The crystals of complex **2c** crystallize in monoclinic space group *P*2(1). In the crystal structure, the complex unit *[($C_{18}H_{20}N_2$)AgBr]* (Figure 5.3(a)) interacts with another complex unit *[($C_{18}H_{20}N_2$)AgBr]* (both these complex units appear in the asymmetric unit) through Ag···Br weak bonds to form a supramolecular dimer (Figure 5.3(b)).

(a)

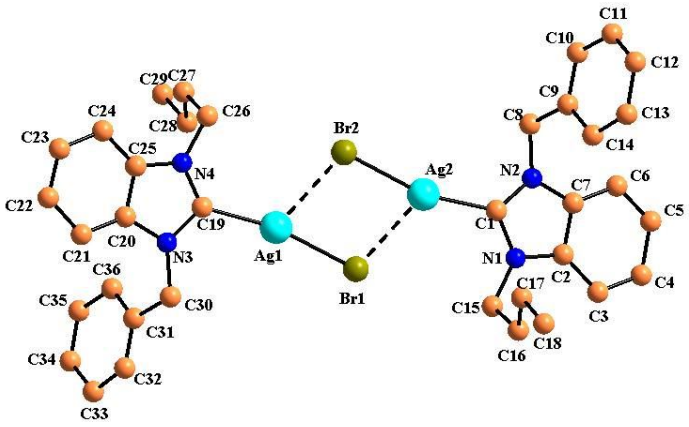


(b)

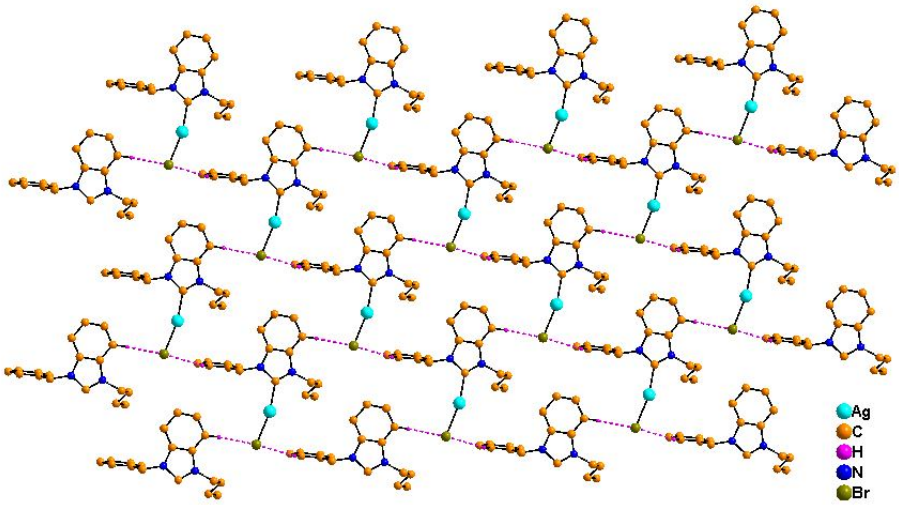


**Figure 5.3.** (a) Ball and stick presentation of the molecular structure of **2c (**two molecules interact by weak AgBr supramolecular interactions, shown by dotted line**)**, and (b) packing diagram in the crystal structure of **2c** (hydrogen atoms are omitted for clarity).

The distance between silver and bromine atoms in these complex units are 2.488 Å (Ag1–Br1), 2.484 Å (Ag2–Br2) respectively. The angle of carbene, silver through bromine *i.e.* <C19Ag1Br1 and <C1Ag2Br2 are 168.28°, 165.09° respectively indicating that C19–Ag1–Br1 and C1–Ag2–Br2 moieties have near linear structures. The linking region (supramolecular interactions) between silver and bromine that bring two complex units of the asymmetric unit together are Ag2····Br1 (3.067 Å) and Ag1····Br2 (3.083 Å). Four types of C–H···π interactions are present in the crystal structure of compound **2c**: two are between C28–H28B, C29–H29C and the centroid of the benzene ring (Cg = C31C32C33C34C35C36) with distances of 3.190 Å and 3.517 Å, respectively; rest two are between C18–H18A, C17–H17A and the centroid (Cg) of the benzene ring (C9C10C11C12C13C14) with distances of 3.209 Å, 3.338 Å respectively. A 2D network has been found to be formed via C–H···Br interactions (2.837–2.897 Å) as shown in Figure 5.3(b)).

*[{1-(10-bromo-9-anthracenylmethyl)-3-butylimy}AgBr]*: *[($C_{22}H_{21}N_2Br$)AgBr]* (**2h**)

The crystals of compound **2h** were crystallized in monoclinic system with *P*2(1)/*c* space group. The angle around silver, <C1AgBr3 (see Figure 5.4(a)) is 164.19° indicating near linear structure of C1–Ag–Br3 moiety. This value is comparatively smaller than that in related reported compounds.[63-65] The Ag–$C_{carbene}$ bond distance in this complex is 2.062 Å. The bromine atom, attached to the silver atom, is situated within a distance of 0.924 Å from the mean plane of imidazole moiety indicating that bromine atom is not in the plane of imdazole moiety. The π····π stacking interactions are observed between the two anthracene

(a)

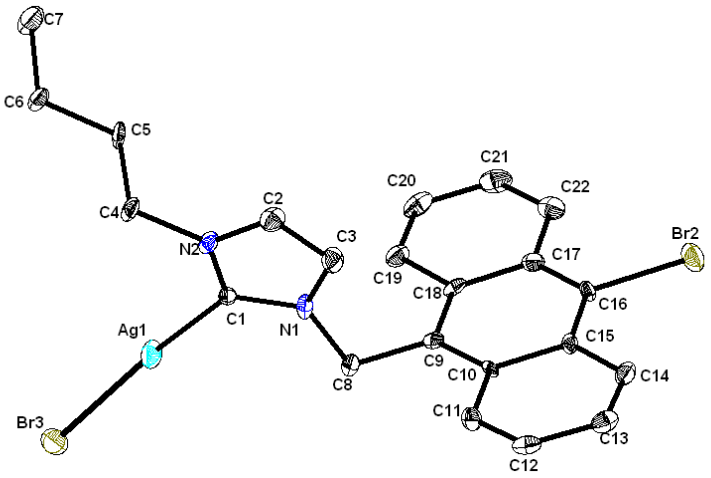

(b)

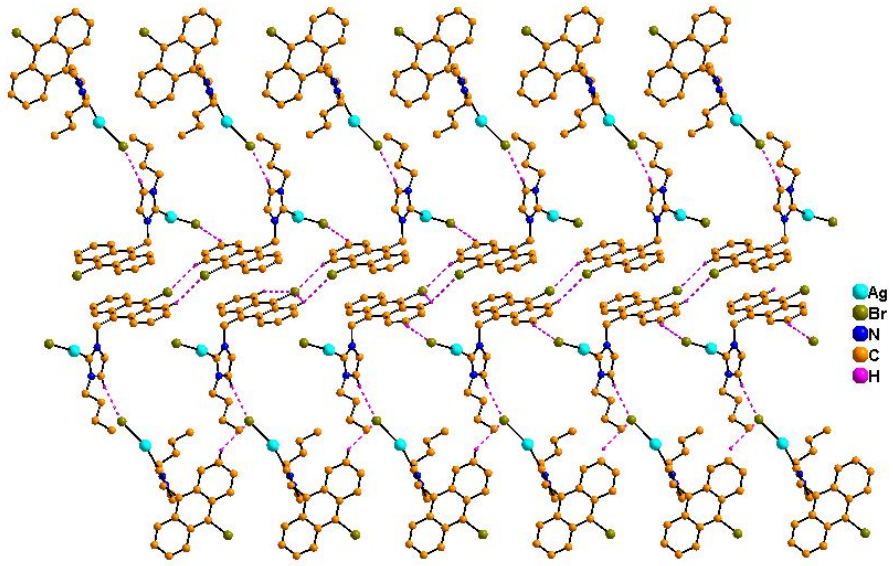


(c)

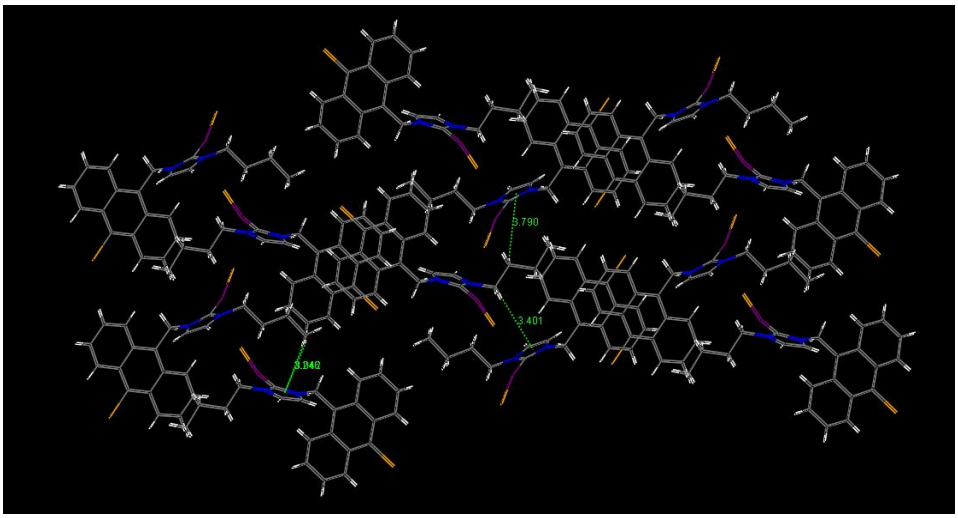


**Figure 5.4.** (a) Thermal ellipsoidal (40 %) plot of **2h**, (b) packing diagram in the crystal structure of compound **2h**, and (c) C–H···π interactions in the complex **2h** (Hydrogen atoms are omitted for clarity).

rings within a distance of 3.792 Å. As shown in the crystal packing diagram (Figure 5.4(b)), concerned molecules arrange in a zigzag manner; in this arrangement, several C–H···π interactions are found from C7–H7C, C7–H7A, C4–H4B and C5–H5A, to the centroid (Cg) of the imidazole ring (C1C2C3N1N2) with a distance of 3.042 Å, 3.246 Å, 3.401 Å and 3.790 Å, respectively (see Figure 5.4(c)). In anthracene moiety, the angle between the central ring

(C9C10C15C16C17C18) and one side ring (C10C11C12C13C14C15) is 2.21° and the angle between the central ring and the other side ring (C17C18C19C20C21C22) is 1.06°. This indicates that three aromatic rings in anthracene are not perfectly co-planar. Related anthracene carbene metal complexes from literature show both planar and non-planar anthracene moieties.[66-68,38-40,58] The bromine atom attached to the centre of benzene ring, is situated within a distance of 0.028 Å from the mean plane of the anthracene moiety.

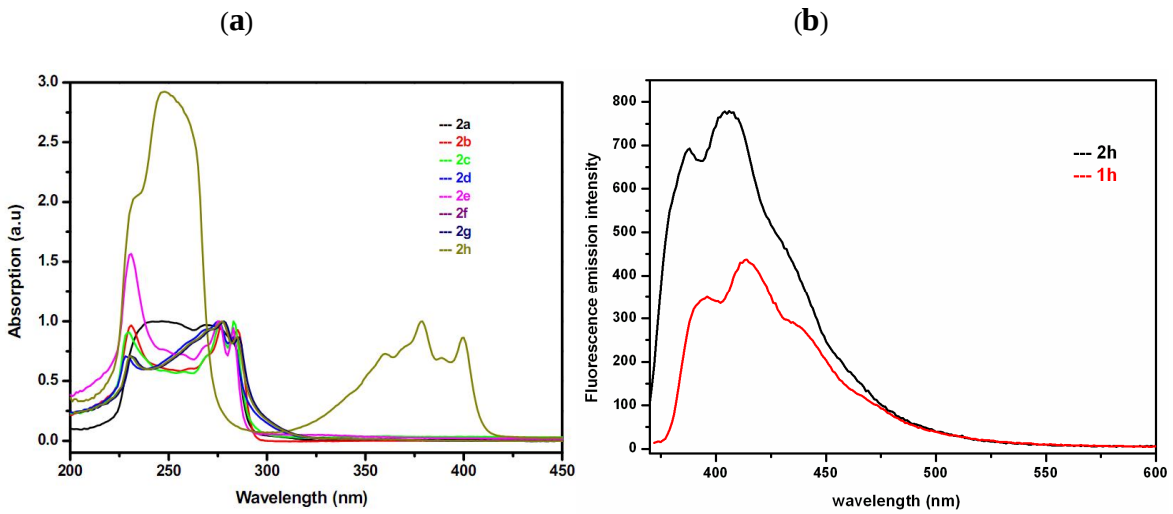


**Figure 5.5.** (a) Normalised electronic absorption spectra of the complexes **2a–2h** in dichloromethane solution, (b) Emission spectra of the complexes **1h** and **2h** at 298 K upon excitation at 370 nm in $CH_2Cl_2$ ($5.0X10^{-6}$ M).

## 5.4. Conclusion

The present article describes the synthesis and structural characterization of new *N*-heterocyclic carbene (NHC) Ag(I) complexes based on benzimidazolium/imidazolium salts. A comparison between the metal-carbene bond distances among all these complexes with related compounds, reported in literature, has been made. We have described the solution electronic absorption spectra of these complexes including emission studies. The supramolecular chemistry of four compounds **2a-2c** and **2h** is discussed in terms of weak interactions, present in their crystal structures.

**Table 5.1.** Crystallographic data and structural refinement for complexes **2a–2c** and **2h**.

| | **2a** | **2b** | **2c** | **2h** |
|---|---|---|---|---|
| Empirical formula | $C_{25}H_{26}AgClN_2$ | $C_{42}H_{35}AgBF_4N_4$ | $C_{36}H_{40}Ag_2Br_2N_4$ | $C_{22}H_{21}AgBr_2N_2$ |
| Formula weight | 497.80 | 790.42 | 904.28 | 581.10 |
| Temperature (K) | 298 | 298 | 100 | 298 |
| Crystal size [mm] | 0.24 x 0.22 x 0.16 | 0.22 x 0.18 x 0.16 | 0.22 x 0.20 x 0.16 | 0.20 x 0.16 x 0.14 |
| Space group | P-1 | P-1 | P2(1) | P2(1)/c |
| Wavelength (Å) | 0.71073 | 0.71073 | 0.71073 | 0.71073 |
| *a* [Å] | 8.955(5) | 11.037(2) | 8.716(9) | 8.058(16) |
| *b* [Å] | 10.877(6) | 12.798(3) | 9.339(10) | 28.650(6) |
| *c* [Å] | 12.538(7) | 13.550(3) | 21.049(2) | 8.931(18) |
| $\alpha$ [°] | 78.55 (10) | 105.78(3) | 90.00 | 90.00 |
| $\beta$ [°] | 72.530(10) | 94.27(3) | 97.403(2) | 90.83(3) |
| $\gamma$ [°] | 70.874(10) | 106.53(3) | 90.00 | 90.00 |
| $V$ [Å]$^3$ | 1093.99(11) | 1741.6(6) | 1699.1(3) | 2061.7(7) |
| *Z*, Calculated density [Mg/m$^{-3}$] | 2, 1.511 | 2, 1.507 | 2, 1.767 | 4, 1.872 |
| Reflections collected/ unique | 10223/3787 | 16522/6034 | 15836/5916 | 20939/4016 |
| R(int), F(000) | 0.0179, 508 | 0.0202, 806 | 0.0529, 896 | 0.0558, 1136 |
| Max. and min. transmission | 0.8164 and 0.5696 | 0.9048 and 0.8724 | 0.6016 and 0.5101 | 0.5492 and 0.4430 |
| θ range for data collection[°] | 1.71 to 24.90 | 1.74 to 24.92 | 1.95 to 24.99 | 1.42 to 25.97 |
| Refinement method | Full matrix least squares on $F^2$ | Full matrix least squares on $F^2$ | Full matrix least squares on $F^2$ | Full matrix least squares on $F^2$ |
| Data / restraints / parameters | 3787/0/266 | 6034/0/469 | 5916/1/399 | 4016/0/245 |
| Goodness-of-fit on $F^2$ | 1.190 | 1.141 | 1.077 | 1.248 |
| $R_1/wR_2$ [I>2sigma(I)] | 0.0248/0.0694 | 0.0380/0.1015 | 0.0466/0.1071 | 0.0626/0.1296 |
| $R_1/wR_2$ (all data) | 0.0251/0.0696 | 0.0385/0.1021 | 0.0606/0.1130 | 0.0712/0.1330 |
| Largest diff. peak and hole [e.Å$^{-3}$] | 0.369 and -0.761 | 1.632 and -1.210 | 1.963 and -1.187 | 1.921 and -1.393 |

**Table 5.2.** Selected bond lengths [Å] and angles [°] for complexes **2a–2c** and **2h**.

| | | | |
|---|---|---|---|
| | | Complex **2a** | |
| Ag(1)-C(1) | 2.082(2) | N(1)-C(19) | 1.462(3) |
| Ag(1)-Cl(1) | 2.3324(5) | N(2)-C(1) | 1.354(3) |
| N(1)-C(1) | 1.353(3) | N(2)-C(7) | 1.395(3) |
| N(1)-C(2) | 1.391(3) | N(2)-C(8) | 1.474(3) |
| C(1)-Ag(1)-Cl(1) | 175.02(6) | N(1)-C(1)-N(2) | 105.85(19) |
| C(1)-N(1)-C(2) | 111.21(19) | N(1)-C(1)-Ag(1) | 125.89(17) |
| N(1)-C(2)-C(3) | 132.3(2) | N(2)-C(1)-Ag(1) | 128.20(17) |
| N(1)-C(2)-C(7) | 106.02(19) | C(25)-C(20)-C(19) | 119.3(2) |
| | | Complex **2b** | |
| Ag(1)-C(22) | 2.089(3) | N(2)-C(29) | 1.460(4) |
| Ag(1)-C(1) | 2.089(3) | N(3)-C(1) | 1.351(4) |
| N(1)-C(22) | 1.356(4) | N(3)-C(15) | 1.471(3) |
| N(2)-C(28) | 1.389(4) | N(4)-C(8) | 1.464(3) |
| C(22)-Ag(1)-C(1) | 177.88(10) | N(1)-C(22)-Ag(1) | 127.1(2) |
| C(22)-N(2)-C(28) | 111.1(2) | N(3)-C(1)-N(4) | 105.7(2) |
| C(28)-N(2)-C(29) | 125.1(2) | N(3)-C(1)-Ag(1) | 128.5(2) |
| C(7)-N(4)-C(8) | 125.0(2) | N(4)-C(1)-Ag(1) | 125.6(2) |
| | | Complex **2c** | |
| Ag(1)-C(19) | 2.129(11) | C(12)-C(11) | 1.325(17) |
| Ag(1)-Br(1) | 2.4879(16) | Ag(2)-C(1) | 2.064(11) |
| Ag(1)-Br(2) | 3.0827(17) | Ag(2)-Br(2) | 2.4841(15) |
| C(35)-C(34) | 1.35(2) | Ag(2)-Br(1) | 3.0669(15) |
| Br(1)-Ag(1)-Br(2) | 86.89(4) | Br(2)-Ag(2)-Br(1) | 87.31(4) |
| C(31)-C(36)-C(35) | 120.0(14) | Ag(2)-Br(2)-Ag(1) | 92.75(5) |
| N(4)-C(19)-Ag(1) | 130.3(9) | Ag(1)-Br(1)-Ag(2) | 93.05(5) |
| N(3)-C(19)-Ag(1) | 122.8(9) | C(16)-C(17)-C(18) | 115.0(12) |
| C(1)-Ag(2)-Br(2) | 165.1(3) | C(27)-C(28)-C(29) | 111.1(14) |
| | | Complex 2**h** | |
| Ag(1)-C(1) | 2.062(7) | C(9)-C(18)-C(19) | 121.0(7) |
| Ag(1)-Br(1) | 2.4186(12) | C(17)-C(18)-C(19) | 118.6(6) |
| Br(2)-C(16) | 1.903(6) | C(7)-C(6)-C(5) | 112.3(6) |
| N(1)-C(1) | 1.352(9) | N(2)-C(1)-N(1) | 104.5(6) |
| N(1)-C(3) | 1.380(9) | N(2)-C(1)-Ag(1) | 126.3(5) |
| N(1)-C(8) | 1.470(9) | N(1)-C(1)-Ag(1) | 129.0(5) |
| C(18)-C(9)-C(10) | 120.5(6) | C(17)-C(16)-Br(2) | 118.5(5) |

**Table 5.3.** Hydrogen bonds for complexes **2a–2c** and **2h**.

| D–H···A | d(D···H) | d(H···A) | d(D···A) | <(DHA) |
|---|---|---|---|---|
| | | Complex **2a** | | |
| C(5)-H(5)...Cl(1)#1 | 0.93 | 2.78 | 3.578(2) | 144.4 |
| C(22)-H(22)...Cl(1)#2 | 0.93 | 2.81 | 3.739(3) | 174.3 |
| C(12)-H(12)...Cl(1)#3 | 0.93 | 2.86 | 3.748(2) | 159.2 |
| | | Complex **2b** | | |
| C(29)-H(29A)...F(1)#4 | 0.97 | 2.41 | 3.155(3) | 133.3 |
| C(11)-H(11)...F(3)#4 | 0.93 | 2.43 | 3.347(4) | 169.0 |
| C(36)-H(36B)...F(4)#5 | 0.97 | 2.48 | 3.190(4) | 130.1 |
| C(36)-H(36B)...F(1)#5 | 0.97 | 2.45 | 3.381(4) | 161.2 |
| C(8)-H(8A)...F(3)#6 | 0.97 | 2.41 | 3.177(3) | 135.6 |
| C(8)-H(8A)...F(2)#6 | 0.97 | 2.43 | 3.323(4) | 152.9 |
| | | Complex **2c** | | |
| C(10)-H(10)...Br(2)#7 | 0.95 | 2.86 | 3.635(11) | 139.9 |
| C(3)-H(3)...Br(2)#8 | 0.95 | 2.80 | 3.657(11) | 150.5 |
| C(32)-H(32)...Br(1)#2 | 0.95 | 2.90 | 3.659(13) | 138.0 |
| C(24)-H(24)...Br(1)#9 | 0.95 | 2.84 | 3.693(12) | 150.5 |
| | | Complex **2h** | | |
| C(2)-H(2)...Br(1)#10 | 0.93 | 2.73 | 3.540(7) | 146.6 |
| C(20)-H(20)...Br(1)#4 | 0.93 | 2.95 | 3.771(8) | 147.9 |
| C(22)-H(22)...Br(2)#11 | 0.93 | 2.95 | 3.607(7) | 129.3 |

Symmetry transformations used to generate equivalent atoms: #1 x-1,y+1,z; #2 x-1,y,z; #3 -x+3,-y,-z+1; #4 x,y,z-1; #5 -x,-y,-z+1; #6 -x+1, -y+1,-z+1; #7 x+1,y,z #8 x,y-1,z #9 x,y+1,z; #10 x+1,-y+3/2,z-1/2; #11 -x+1,-y+1,-z-1

## 5.5. References


[1] W. A. Herrmann, *Angew. Chem., Int. Ed*. **2002**, *41*, 1290

[2] A. J. Arduengo III, R. L. Harlow, M. Kline, *J. Am. Chem. Soc*. **1991**, *113*, 361.

[3] K. J. Ofele, *J. Organomet. Chem*. **1968**, *12*, 42

[4] H.-W. Wanzlick, H.-J. Schonherr, *Angew. Chem., Int. Ed*. **1968**, *7*, 141.

[5] T. Weskamp, F. J. Kohl, W. Hieringer, D. Gleich, W. A. Herrmann, *Angew. Chem., Int. Ed*. **1999**, *38*, 2416.

[6] J. C. Green, R. G. Scurr, P. L. Arnold, F. G. N. Cloke, *Chem. Commun*. **1997**, 1963.

[7] W. A. Herrmann, M. Elison, J. Fischer, C. Kocher, G. R. J. Artus, *Chem.-Eur. J.* **1996**, *2*, 772

[8] V. M. Baker, D. H. Brown, V. J. Hesler, B. W. Skelton, A. H. White, *Organometallics* **2007**, *26*, 250.

[9] S. Caddick, F. G. N. Cloke, P. B. Hitchcock, J. Leonard, A. K. de K. Lewis, D. McKerrecher, L. R. Titcomb, *Organometallics* **2002**, *21*, 4318.

[10] H. V. Huynh, T. C. Neo, G. K. Tan, *Organometallics* **2006**, *25*, 1298.

[11] A. J. Arduengo III, J. R. Goerlich, W. J. Marshall, *J. Am. Chem. Soc.* **1995**, *117*, 11027.

[12] D. S. McGuinness, M. J. Green, K. J. Caveli, B. W. Skelton, A. H. Whit, *J. Organomet. Chem*. **1998**, *565*, 165.

[13] A. Furstner, O. R. Thiel, L. Ackermann, H.-J. Schanz, S. P. Nolan, *J. Org. Chem.* **2000**, *65*, 2204.

[14] W. A. Herrmann, C.-P. Reisinger, M. Spiegler, *J. Organomet. Chem*. **1998**, *557*, 93.

[15] M. G. Gardiner, W. A. Herrmann, C.-P. Reisinger, J. Schwarz, M. Spiegler, *J. Organomet. Chem.* **1999**, *572*, 239.

[16] T. Weskamp, V. P. W. Bohm, W. A. Herrmann, *J. Organomet. Chem*. **1999**, *585*, 348.

[17] J. Ruiz, G. Garcia, M. E. G. Mosquera, B. F. Perandones, M. P. Gonzalo, M. Vivanco, *J. Am. Chem. Soc.* **2005**, *127*, 8584.

[18] L. H. Gade, S. B. Laponnaz, *Coord. Chem. Rev*. **2007**, *251*, 718.

[19] S. K. Schneider, C. F. Rentzsch, A. Kruger, H. G. Raubenheimer, W. A. Herrmann, *J. Mol. Cat. A: Chem*. **2007**, *265*, 50.

[20] J. J. Song, F. Gallou, J. T. Reeves, Z. Tan, N. K. Yee, C. H. Senanayake, *J. Org. Chem*. **2006**, *71*, 1273.

[21] O. Guerret, S. Sole, H. Gornitzka, M. Teichert, G. Trinquier, G. Bertrand, *J. Am. Chem. Soc*. 1997, *119*, 6668.

[22] C. K. Lee, J. C. C. Chen, K. M. Lee, C. W. Liu, I. J. B. Lin, *Chem. Mater*. **1999**, *11*, 1237.

[23] J. C. C. Chen, I. J. B. Lin, *J. Chem. Soc., Dalton Trans*. **2000**, 839.

[24] O. Guerret, S. Sole, H. Gornitzka, M. L. Teichert, G. Teingnier, G. Berte, *J. Am. Chem. Soc*. **1997**, *119*, 6668.

[25] R. Z. Ku, J. C. Huang, J. Y. Cho, F. M. Kiang, K. R. Reddy, Y. C. Chen, K. J. Lee, J. H. Lee, G. H. Lee, S. M. Peng, S. T. Liu, *Organometallics* 1999, *18*, 2145.

[26] I. J. B. Lin, C. S. Vasam, *Coord. Chem. Rev*. **2007**, *251*, 642.

[27] J. C. Garrisen, R. S. Simons, J. M. Talley, C. Wesdemiotis, C. A. Tessier, W. J. Youngs, *Organometallics* **2001**, *20*, 1276.

[28] U. Scheele, S. Dechert, F. Meyer, *Inorg. Chim. Acta* **2006**, *359*, 4891.

[29] M. K. Samantaray, V. Katiyar, K. Pang, H. Nanavati, P. Ghosh, *J. Organomet. Chem*. **2007**, *692*, 1672.

[30] M. V. Baker, D. H. Brown, R. A. Haque, B. W. Skelton, A. H. White, *Dalton Trans*. **2004**, 3756.

[31] H. M. F. Wang, I. J. B. Lin, *Organometallics* **1998**, *17*, 972.

[32] S.-T. Liu, T.-Y. Hsieh, G..-H Lee, S.-M Peng, *Organometallics* **1998**, *17*, 993.

[33] A. Melaiye, R. S. Simons, A. Milsted, F. Pingitore, C. Wesdemiotis, C. A. Tessier, W. J. Youngs, *J. Med. Chem*. **2004**, *47*, 973.

[34] A. Melaiye, Z. Sun, K. Hindi, A. Milsted, D. Ely, D. H. Reneker, C. A. Tessier, W. J. Youngs, *J. Am. Chem. Soc*. **2005**, *127*, 2285.

[35] S. Patil, J. Claffey, A. Deally, M. Hogan, B. Gleeson, L. M. M. Mendez, H. M.-Bunz, F. Paradisi, M. Tacke, *Eur. J. Inorg. Chem*. **2010**, 1020.

[36] Q. X. Liu, L. N. Yin, J. C. Feng, J. H. Guo, H. B. Song, *Acta. Crystallogr.,Sect. E* **2006**, *62*, o3604

[37] Q.-X. Liu, F.-B. Xu, Q.-S. Li, H.-B. Song, Z.-Z. Zhang, *Organometallics* **2004**, *23*,

610.

[38] Q. X. Liu, F. B. Xu, Q. S. Li, H. B. Song, Z. Z. Zhang, *J. Mol. Struct*. **2004**, *697*, 131.

[39] Q. X. Liu, H. B. Song, F. B. Xu, Q. S. Li, X. S. Zeng, X. B. Leng, Z. Z. Zhang, *Polyhedron* **2003**, *22*, 1515.

[40] Q.-X. Liu, L.-N. Yin, X.-M. Wu, J.-C. Feng, J.-H. Guo, H.-B. Song, *Polyhedron* **2008**, *27*, 87.

[41] Q.-X. Liu, A.-H, Chen, X.-J. Zhao, Y. Zang, X.-M. Wu, X.-G. Wang, J.-H. Guo, *CrystEngComm*. **2011**, *13*, 293.

[42] P. L. Arnold, I. J. Casely, *Chem. Rev*. **2009**, *109*, 3599.

[43] R. Hoffmann, R. Gleiter, *J. Am. Chem. Soc*. **1968**, *90*, 5457.

[44] R. Hoffmann, *J. Am. Chem. Soc*. **1968**, *90*, 1475.

[45] R. Hoffmann, G. D. Zeiss, G.W. Van Dine, *J. Am. Chem. Soc*. **1968**, *90*, 1485.

[46] W. A. Herrmann, J. Schutz, G. D. Frey, E. Herdtweck, *Organometallics* **2006**, *25*, 2437.

[47] A. T. Termaten, M. Schake, A. W. Ehlers, M. Lutz, A. L. Spek, K. Lammertsma, *Chem.-Eur. J.* **2003**, *9*, 3577.

[48] X. Hu, I. C.-Rodriguez, K. Olsen, K. Meyer, *Organometallics* **2004**, *23*, 755.

[49] W. A. Herrmann, C. Kocher, L. J. Goossen, G. R. J. Artus, *Chem.-Eur. J*. **1996**, *2*, 1627.

[50] D. A. Dixon, A. J. III. Arduengo, *J. Phys. Chem*. **1991**, *95*, 4180.

[51] C. Boehme, G. Frenking, *J. Am. Chem. Soc*. **1996**, *118*, 2039.

[52] A.J. III. Arduengo, R. H. V. Dias, J. C. Clabrese, F. Davidson, *Organometallics* **1993**, *12*, 3405

[53] D. Tapu, C. Owens, D. VanDerveer, K. Gwaltney, *Organometallics* **2009**, *28*, 270.

[54] A. Caballero, E. D.-Barra, F. A. Jalon, S. Merino, J. Tejeda, *J. Organomet. Chem*. **2001**, *617-618*, 395.

[55] C. K. Lee, K. M. Lee, I. J. B. Lin, *Organometallics* **2002**, *21*, 10.

[56] A. A. D. Tulloch, A. A. Danopoulos, S. Winston, S. Kleinhenz, G. Eastham, *J. Chem. Soc., Dalton Trans*. **2000**, 4499.

[57] A. M. Magill, D. S. Mcguinness, K. J. Cavell, G. J. P. Britovsek, V. C. Gibson, A. J. P. White, D. J. Williams, A. H. White, B. W. Skekton, *J. Organomet. Chem*. **2001**, *617- 618*, 546.

[58] Q. X. Liu, F. B. Xu, Q. S. Li, X. S. Zeng, X. B. Leng, Y. L. Chou, Z. Z. Zhang, *Organometallics* **2003**, *22*, 309.

[59] C. K. Lee, C. S. Vasam, T. W. Huang, H. M. J. Wang, R. Y. Yang, C. S. Lee, I. J. B. Lin, *Organometallics* 2006, 25, 3768.

[60] X. Wan, F. Xu, Z. Zhang, H. Song, *Z. Anorg, Allg, Chem.* **2011**, *637*, 34.

[61] J.-W. Wang, H.-B. Song, Q.-S. Li, F.-B. Xu, Z.-Z. Zhang, *Inorg. Chim. Acta* **2005**, *358*, 3653.

[62] Q.-X. Liu, L.-N. Yin, J.-C. Feng, *J. Organomet. Chem*. **2007**, *692*, 3655.

[63] Y. Han, Y.-T. Hong, H. V. Huynh, *J. Organomet. Chem*. 2008, 693, 3159.

[64] Y. Li, X. Chen, Y. Song, L. Fang, G. Zou, *Dalton Trans.* **2011**, *40*, 2046.

[65] D. V. Partyka, N. Deligonul, *Inorg. Chem*. **2009**, *48*, 9463.

[66] F. DeRosa, X. Bu, P. C. Ford, *Inorg. Chem*. **2003**, *42*, 4171.

[67] F. Sancenon, A. Benito, F. J. Hernandez, J. M. Lloris, R. M.-Manez, T. Pardo, J. Soto, *Eur. J. Inorg. Chem*. **2002**, 866.

[68] E. S. Meadows, S. L. DeWall, L. J. Barbour, F. R. Fronczek, M.-S. Kim,G. W. Gokel, *J. Am. Chem. Soc*. **2000**, *122*, 3325.

[69] J.-Y. Cheng, Y.-H. Chu, *Tetrahedron Letters* **2006**, *47*, 1575.

[70] M. Cichelswirth, M. Rakers, C. Schafer, J. Mattay, M. Neumann, U. Heinzmann, *J. Phys. Chem. B*. **2010**, *114*, 3482.

[71] Bruker. *SADABS*, *SMART*, *SAINT* and *SHELXTL*, **2000** (Bruker AXS Inc., Madison, Wisconsin, USA).

[72] G. M. Sheldrick, *Acta Crystallogr. Sect*. *A* **2008**, *64*, 112.

# Future Scope of the Present Thesis

## Near-IR dithiolene complexes

Metal dithiolene complexes have attracted considerable attention because; such solid-functional materials have potential to be used as gas storage, nonlinear optical, conducting, magnetic materials, near-IR dyes and DSSC (Dye Sensitized Solar Cells). In the first and second chapter of the present thesis, we have described the substituent effect on the counter cation in ion-pair dithiolene complexes, whereas in third chapter we have demonstrated the substituent role on dithiolene ligand of metal-bis(dithiolene) complexes. The HOMO and LUMO are delocalized over two dithiolate ligands, and electronic transition among these orbitals gives rise to a strong absorption in the near-IR region. In heteroleptic system of dithiolene based complexes, donor substituents in the parent dithiolate raise the energy level of HOMO more than that of LUMO, resulting in a shift of the near-IR absorbance to lower frequencies.

Dithiolene complexes are much influenced by the substituent groups which are present in dithioelene core moiety. The delocalization in chelate ring system is the key role to exhibit NIR electronic absorption. Metal complexes with sulfur-rich dithiolene ligands exhibit conductivity behavior because of intermolecular sulfur-sulfur interactions of the ligands. Boon-Chuan group prepared multi-sulfur dithiolene ligand metal complexes with different substituent groups on dithiolene core moiety. Based on this aspect, we wish to choose different type of ligands with donating and withdrawing nature of groups on phenyl ring as well as thiophene, furan and naphthalene rings to obtain eccective delocalization in dithiolene core moiety. Using these ligands, we would like to prepare Pt-based dithiolene complexes, as shown in Scheme 1. Generally, Pt-based dithiolene complexes, especially heteroleptic dithiolene complexes, have been used in the areas of near-IR dyes and DSSC because of their pull-push nature of ligands on both side of the Pt metal.

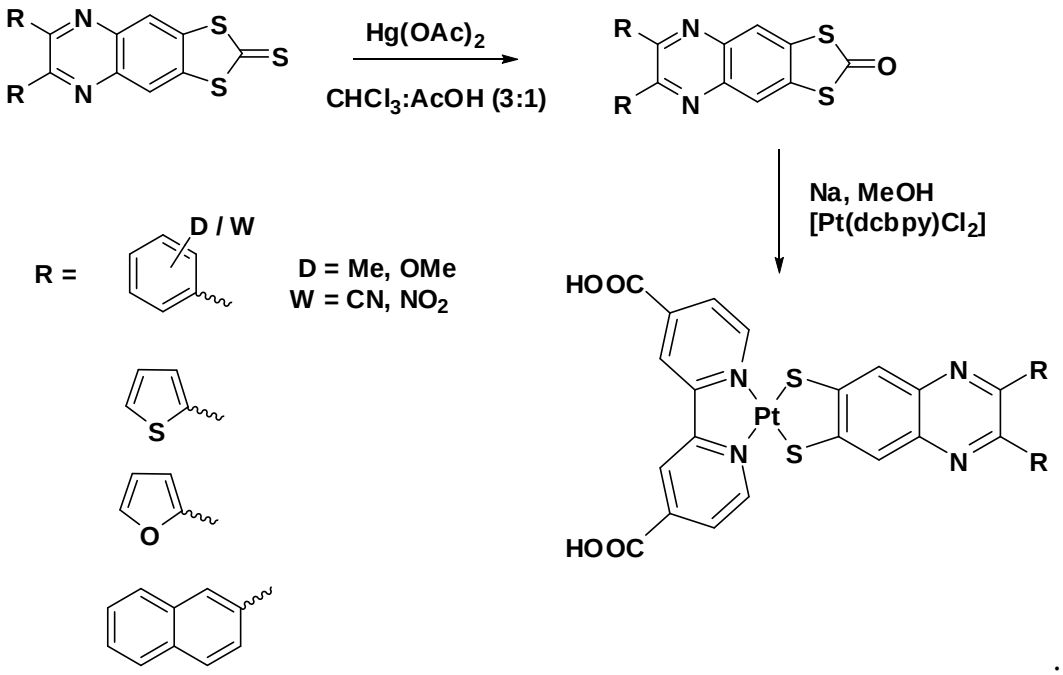


**Scheme 1.** Proposed synthetic procedure to prepare Pt-dithiolene complexes.

Apart from these dithiolene complexes, tetrathiofulvalene compounds are also important to exhibit molecular conductivity. Recently our group reported role of substituent on electronic delocalization of TTF core moiety and it exhibits solvotochromic effect in different solvents,. It also shows solvent dependent fluorescence (different colors in different solvents). In this regard, we would like to synthesize new type of hetero based tetrathiofulvalene derivatives. Some of the 1,2-diketo substituted hetero based compounds (indene, *N*-methyl indolene) are commercially available and few compounds, we have to prepare, which can be further treated (condensation step) with 1,2-di amino based compounds. Finally homo coupling reaction can be done in the presence of $P(OEt)_3$ to obtain TTF derivatives. New type of hetero based TTF molecules have been represented in Scheme 2. In addition to this, we wish to compare the role of electronic delocalization between phenyl, pyrene substituted groups of TTF molecules.

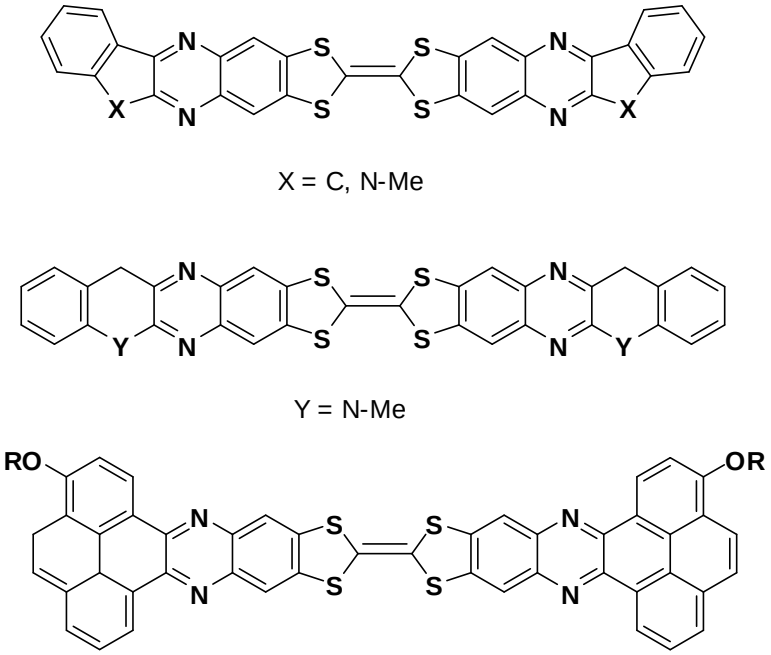


**Scheme 2.** Proposed molecular structures of tetrathiofulvalenes.

N-heterocyclic carbene complexes (NHCs) have several applications in the field of catalysis and transmetalation. Sivler carbene complexes are used as the starting materials to prepare Cu, Pd, Au etc. NHCs. recently W. Chen *et.al.* reported heteoarene based NHCs to exhibit catalytic activity. In this similar manner, we would like to prepare 2,3-dichloro based quinoxaline derivatives that can be treated with imidazolium moieties. The $PF_6^-$ / $BF_4^-$ salts can be treated with $Ag_2O$ to achieve Ag–NHCs, as shown in Scheme 3. This material can be used for the preparation of other NHCs (Pd, Au, Rh, etc) and these compounds have potential in exhibiting catalytic activity.

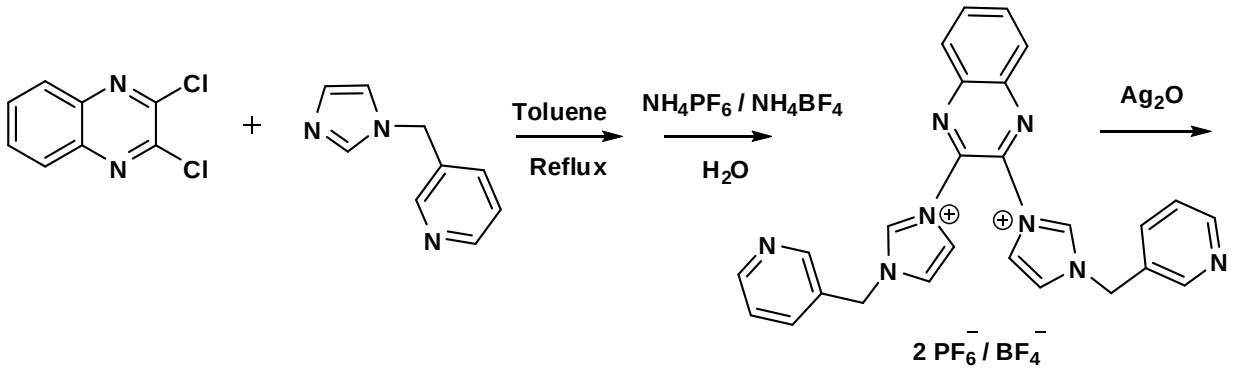


**Scheme 3.** Proposed schematic representation of the preparation of Ag–NHC complexes.

# List of Publications

**1.** Diversities of Coordination Geometry Around the $Cu^{2+}$ center in Bis(maleonitriledithiolato)metalate Complex Anions: Geometry Controlled by Varying the Alkyl Chain Length of Imidazolium Cations

**Ravada Kishore**, S. K. Das, *Cryst. Growth Des.* **2012**, 12, 3684-3699.

**2.** Thieno[3,2-*c*]pyran-4-one based novel small molecules: Their synthesis, crystal structure analysis and in vitro evaluation as potential anticancer agents

A. Nakhi, R. Adepu, D. Rambabu, **Ravada Kishore**, G. R. Vanaja, A. M. Kalle, M. Pal, *Bioorg. Med. Chem. Lett.* **2012**, 22, 4418-4427.

**3.** Pyrrole[2,3-*b*]quinoxalines as inhibitors of firefly luciferase: Their Cu-mediated synthesis and evaluation as false positive in a reporter Gene Assay

A. Nakhi, Md. S. Rahman, **Ravada Kishore**, C. L. T. Meda, G. S. Deora, K. V. L. Parsa, M. Pal, *Bioorg. Med. Chem. Lett.* **2012** (**Article in Press**)

**4.** Ion-pair charge transfer complex with near-IR absorption: Synthesis, crystal structure and properties of $[Hb]_2[Cu(mnt)_2]$ (Hb = 1-(4-((1H-imidazol-1-yl)methyl)benzyl)-1H-imidazol-3-ium)

**Ravada Kishore**, B. K Tripuramallu, G. Durgaprasad, Samar K. Das, *J. Mol. Str*., **2011**, *990*, 37.

**5.** A new route to indoles via in situ desilylation–Sonogashira strategy: identification of novel small molecules as potential anti-tuberculosis agents

A. Nakhi, B. Prasad, U. Reddy, R. M. Rao, S. Sandra, R. Kapavarpu, D. Rambabu, G. R. Krishna, C. M. Reddy, **Kishore Ravada**, P. Misra, Javed Iqbal and Manojit Pal, ***Med. Chem. Commun.*, 2011**, *2*, 1006-1010.

**6.** Understanding the formation of metal-oxide based inorganic solids: Assessing the influence of tetrazole molecule

B. K. Tripuramallu, **Ravada Kishore**, Samra K. Das, *Inorg. Chim. Acta*, **2011**, *362*, 132.

**7.** Acid-base behaviour of a simple metal-bis(dithiolate) system: Synthesis, crystal structure and spectroscopy of $[Bu_4N]_2[M^{II}(ppdt)_2]$ (M = Ni, Pt; ppdt = pyrido[2,3-b]pyrazine-2,3-dithiolate)

R. Bolligarla, **Ravada Kishore**, G. Durgaprasad, Samar K. Das, *Inorg. Chim. Acta*, **2010**, *363*, 3061-3069.

**8.** Synthesis, structural characterization and properties of one-dimensional coordination polymers of cobalt(II)-and nickel(II)-phosphonate complexes with 2,2'-bipyridine as a secondary ligand component: Observation of both *cis* and *trans* conformations of a diphosphonic acid

B. K. Tripuramallu, **Ravada Kishore**, Samar K. Das, *Polyhedron*, **2010**, *29*, 2985-2990.

**9.** 2-Aminoanilinium 2-chloroacetate

A. S. Rao, B. K. Tripuramallu, **Kishore Ravada**, Samar K. Das, *Acta Cryst.* E66, **2010**, o1945.

**10.** *N*-Heterocyclic based new nickel-bis(dithiolene) complexes: synthesis, characterization and properties

**Ravada Kishore**, Samar K. Das (Submitted)

**11.** Synthesis, structural characterization and properties of New *N*-heterocyclic Carbene Ag(I) Complexes

**Ravada Kishore**, Samar K. Das (Submitted)

## Poster and Oral Presentations

1. **R. Kishore** and S. K. Das*, Conformational Change of Organic Cation Receptors Through Supramolecular Interactions in Ion-Pair Complexes with Metal-Dithiolates, Poster presentation at "**Chemfest-2009 (*In-house*)**" which was held in School of Chemistry, *University of Hyderabad*, Hyderabad, India.

2. **R. Kishore** and S. K. Das*, Distortion in the Square Planar Metal Dithiolene complexes: Pivotal Role of Supramolecular Chemistry.

   (**i**) Poster presentation at "**Chemfest-2011** (***In-house***)" which was held in School of Chemistry, *University of Hyderabad*, Hyderabad, India on January, **2011**.

   (**ii**) Poster presentation at the "Chemical Research Society of India and Royal Society of Chemistry" (**13$^{th}$ CRSI & 5$^{th}$ RSC**) which was held in National Institute of Science Education and Research, Bhubaneswar, India on February, **2011**.

   (**iii**) Poster presentation at the "International Year of Chemistry (**IYC-2011**)'' which was held in *University of Hyderabad*, Hyderabad, India on December, **2011**.

3. **R. Kishore** and S. K. Das*, Heterocyclic tetrathiafulvalene derivatives and metal-bis(dithiolene) complexes.

   (**i**) Poster presentation at the "**MTIC-XIV-2011**" which was held in School of Chemistry, *University of Hyderabad*, Hyderabad, India on December **2011**.

   (**ii**) Poster and Oral presentation at "**Chemfest-2012**" which was held in School of Chemistry, *University of Hyderabad*, Hyderabad, India on March, **2012**.

# SYNOPSIS

The thesis work entitled with **"Synthesis and Characterization of Metal-Bis(dithiolene) Complexes and *N*-heterocyclic Silver-Carbene Complexes"**, consists of five chapters followed by future scopes: (**1**) Introduction and motivation of the present work: A broad outline of metal 1,2-dithiolene chemistry and *N*-heterocyclic carbene complexes, (**2**) Diversities of coordination geometry around $M^{2+}$ (M = Cu, Ni) center in the bis(maleonitiledithiolato)metalate complex anions: Geometry controlled by varying alkyl chain length of imidazolium cations, **(3)** Synthesis, crystal structure and properties ion-pair charge transfer complexes: conformational change in organic cation receptor through supramolecular interactions, **(4)** Synthesis and characterization of new *N*-heterocyclic 1,2-ene dithiolate based nickel(II) complexes and intramolecular A-D-A tetrathiafulvalene-fused charge transfer derivatives, **(5)** Synthesis, structural characterization and properties of new *N*-heterocyclic carbene Ag(I) Complexes.

Apart from the first chapter (introduction), each chapter is subdivided into three parts: (a) Introduction (literature survey), (b) Experimental Section and (c) Results and Discussion. The compounds obtained in the present study are generally characterized by $^{1}$H NMR, IR, EPR, and HRMS spectral techniques followed by elemental analyses and unambiguously characterized by X-ray crystallography.

## Chapter 1

## Introduction and Motivation of the Present Work: A Broad Outline of Metal 1,2-dithiolene Chemistry and *N*-heterocyclic Carbene Complexes

This chapter begins with more basic knowledge about dithiolene ligands and their metal complexes. It also reveals brief discussion emphasizing their syntheses, characterization and properties. Applications of metal dithiolene complexes are mainly divided into two categories: (1) near-IR dithiolene complexes: influence of cation and substituent effect on metal complexes, and (2) uses of metal dithiolene complexes in the area of catalysis and biology. Some of the important transition metal 1,2–dithiolene complexes are picked up to describe their solid state properties, such as, magnetic, conducting and optical properties (NLO, emission properties). The discussions on structural, spectroscopic, bonding, reactivity and electrochemistry of transition

metal 1,2–dithiolene complexes are also briefed. In addition to this, classification of *N*-heterocyclic carebene complexes has been described.

## Chapter 2

## Diversities of Coordination Geometry Around $M^{2+}$ (M = Cu, Ni) Center in the Bis(maleonitiledithiolato)metalate Complex Anions: Geometry Controlled by Varying Alkyl Chain Length of Imidazolium Cations

Chapter 2 describes twelve new ion-pair metal-bis(dithiolene) complexes with the formulae, $[C_9H_{14}N_4][Cu(mnt)_2]$ **(1a)**, $[C_{10}H_{16}N_4][Cu(mnt)_2]$ **(1b)**, $[C_{11}H_{18}N_4][Cu(mnt)_2]$ **(1c)**, $[C_{12}H_{20}N_4][Cu(mnt)_2]$ **(1d)**, $[C_{13}H_{22}N_4][Cu(mnt)_2]$ **(1e)**, $[C_{14}H_{24}N_4][Cu(mnt)_2]$ **(1f)** and corresponding nickel(II) analogues (**2a**–**2f**). Compounds **1a**–**1f** and **2a**–**2f** have been synthesized starting from M(II) salt (M = Cu, Ni), $Na_2mnt$ (disodium maleonitriledithiolate) and bromide salts of alkyl-bis(imidazolium) cations $[C_8H_{12}(CH_2)_nN_4Br_2]$ (n = 1–6, **a–f**). In this series of ion-pair compounds **1a**–**1f** and **2a**–**2f**, a common $[M(mnt)_2]^{2-}$ complex anion is associated with alkyl imidazolium cations of varied alkyl chain lengths. We have described a systematic study of deviation from square planar geometries (in terms of distortion) around the metal ion in customary square planar metal-dithiolene complexes. The distortion in the geometry around the metal ion (Figure 1) can be explained on the basis of centre of symmetry along C–H···M (M = Cu, Ni) supramolecular interaction and un-balanced supramolecular interactions, such as, S···H, N···H and M···S type weak contacts. Dianionic copper(II) complexes **1a**–**1f** show an electronic absorption in the near infrared (NIR) region, which has been attributed to the charge transfer transition from the HOMO level of copper dithiolate anion $[Cu(mnt)_2]^{2-}$ to the LUMO level of alkyl imidazolium cation $[C_8H_{12}(CH_2)_nN_4]^{2+}$. All these compounds are unambiguously characterized by single crystal X-ray crystallography, and further characterized by IR-, $^1$H NMR-, ESR-, LCMS-spectroscopic techniques, and electrochemical-studies.

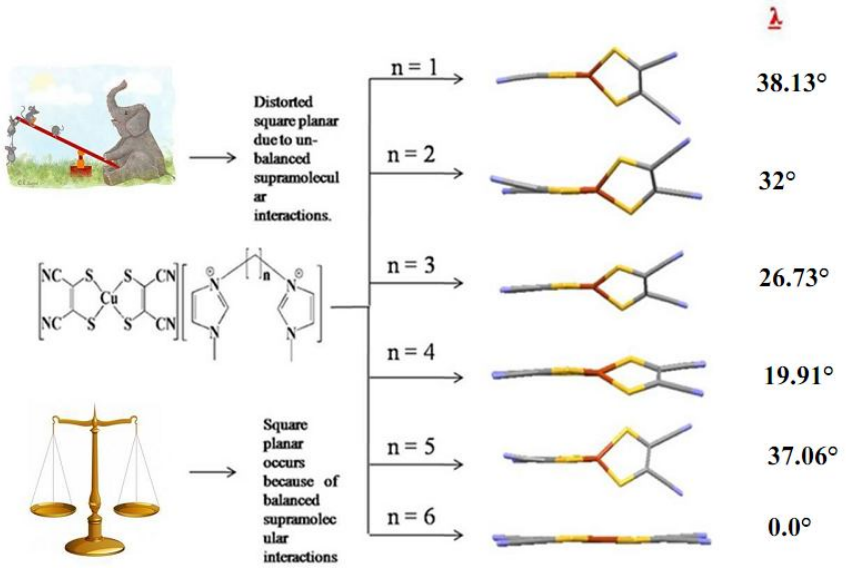


**Figure 1.** Schematic representation of the geometry around copper metal in $[Cu(mnt)_2]^{2-}$ anion.

## Chapter 3

## Synthesis, Crystal Structure and Properties of Ion-Pair Charge Transfer Complexes: Conformational Change in Organic Cation Receptor Through Supramolecular Interactions

Chapter **3** depicts the series of new ion-pair complexes $[Bz,R\text{-}BzBimy]_2[M(mnt)_2]$ {$[Bz,R\text{-}BzBimy]^+$ = 1-benzyl-3-(4-R-benzyl)benzimidazolium; M = Cu, R = H (**1a**), $NO_2$ (**1b**) and Br (**1c**); M = Ni, R = H (**2a**), $NO_2$ (**2b**) and Br (**2c**) and $mnt^{2-}$ = maleonitriledithiolate}. Due to flexible nature of aryl groups ($–CH_2–Ar$) in benzimidazolium salts (**a** and **b**), the orientation/conformational change of aryl groups have been changed in its corresponding metal based dithiolene ion-pair complexes **1a**, **1b**, **2a** and **2b** as shown in Figure 2.

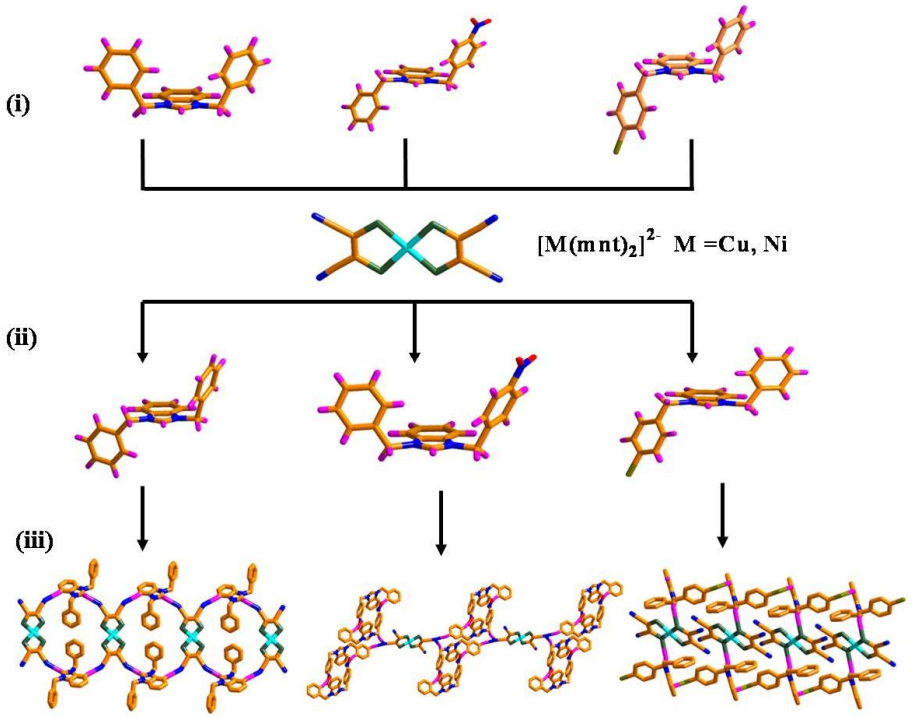


**Figure 2.** Schematic representation of the organic cation receptors' orientations (**i** and **ii**) and 2D supramolecular network formed through hydrogen bonding interactions (**iii**) in metal complexes **1a**–**1c**.

Any change in phenyl groups' orientation/conformation in metal complex **1c** and **2c** has not been observed, because in these complexes, C–H····π and π····π stacking interactions are reasonable to control the phenyl groups orientation, as shown in Figure 2. Supramolecular interactions (such as S···H, N···H, O···H, Br···Br and N···Br etc.) are responsible for the orientation of aryl groups in organic receptor compounds (benzimidazolium salts with tetrafluoroborate) as well as in ion-pair dithiolene complexes. The substituents (H, $NO_2$ and Br), which are present at the *p*-position of one of the phenyl rings in benzimidazolium moiety are accountable for the structural diversities in all the metal (copper and nickel) dithiolene complexes. The molecular structures of complexes **2a**, **2b** and **2c** are isostructural to the complexes of **1a**, **1b** and **1c**. Copper-dithiolene complexes exhibit a Z-shaped non-planar geometry with a different angles; this diversity is due to the change of substituent groups in the counter cation. All dianionic copper(II) complexes **1a-1c**, are evidenced by electron spin resonance spectroscopy. All these complexes exhibit an absorption in the near infrared (NIR) region at 1210 nm and 862 nm for the copper (**1a-1c**) and nickel (**2a-2c**) complexes respectively; these absorptions have been attributed to the charge transfer from the copper dithiolate anion $[Cu(mnt)_2]^{2-}$ to the benzimidazolium cation $[Bz,R\text{-}BzBimy]^{+}$.

The compound $[Hb]_2[Cu(mnt)_2]$ (**1**) [Hb = 1-(4-((1H-imidazol-1-yl)methyl)benzyl)-1H-imidazol-3-ium)] has been synthesized, starting from 1,4-bis((1H-imidazol-1-yl)methyl)benzene, cupric chloride, and $Na_2$mnt in methanol, as shown in Scheme 1. Compound **1** crystallizes in monoclinic system with *C2/c* space group. In the crystal structure, the interactions between cations and anions *via* bifurcated C–H···$(NC\text{-}mnt)_2$ hydrogen bonds give rise to a two dimensional supramolecular network. It has also been observed that two cation moieties (Hb) are attached by a very short C–H···N hydrogen bonding interaction with H···N distance of 1.74 Å, ∠CHN bond angle of 174.9°. Compound **1** is additionally characterized by cyclic voltammetry, UV-Vis, IR, $^1$H NMR and EPR spectroscopy. The ion-pair compound **1** shows an intense absorption in the near-IR region at ~1214 nm which has been described as a charge transfer band from HOMO of the copper dithiolate anion $[Cu(mnt)_2]^{2-}$, to LUMO of the $[Hb]^+$ cation. Compound **1** exhibits an oxidative response at +0.46 V *vs* Ag/AgCl and a reductive event at -0.67 V *vs* Ag/AgCl.

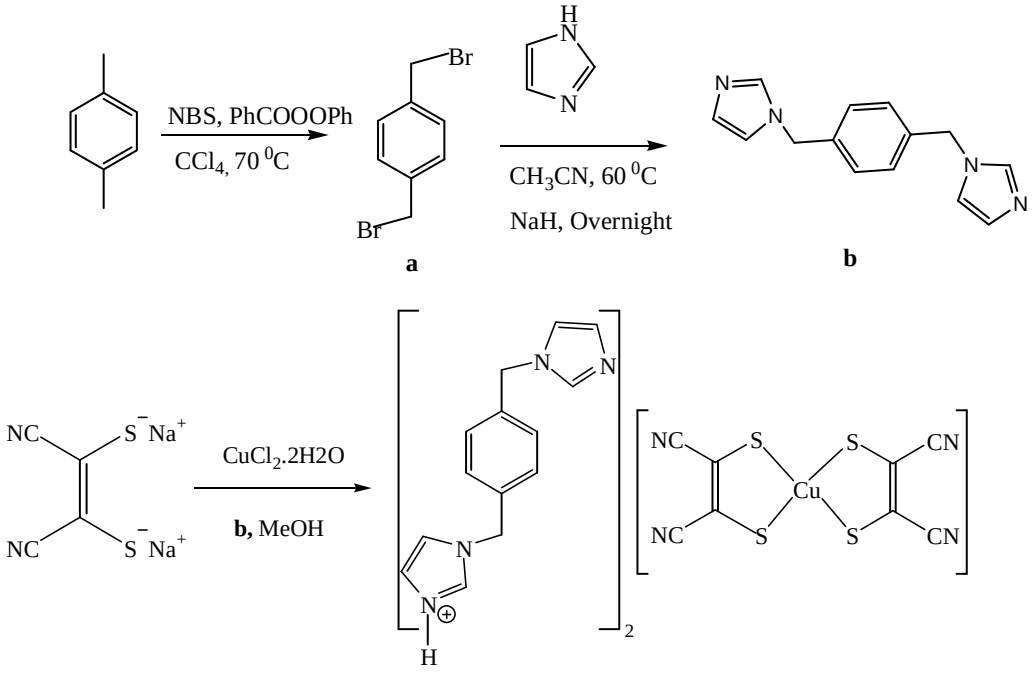


**Scheme 1.** Syntheses scheme for the ligand and complex **1.**

## Chapter 4

## Synthesis and characterization of new *N*-heterocyclic 1,2-ene dithiolate based nickel(II) complexes and intramolecular A-D-A tetrathiafulvalene-fused charge transfer derivatives

Chapter 4 deals with five new nickel-bis(dithiolene) complexes $(PPh_4)_2[Ni(C_8H_2N_2S_2R_2)_2]$ (R = Pyridin-2-yl (**1**), Pyridin-3-yl (**2**), Thiophen-2-yl (**3**), Furan-2-yl (**4**) and Naphthalen-2-yl (**5**)), that have been prepared by the treatment of *N*-heterocyclic based dithiolene ligands with sodium metal in dry methanol (Scheme 2). All these dithiolene ligands and metal complexes are characterized by LCMS-, $^1$H NMR- and HRMS-, IR-, UV-vis-NIR-spectroscopy, routine elemental analysis and cyclic voltammetry.

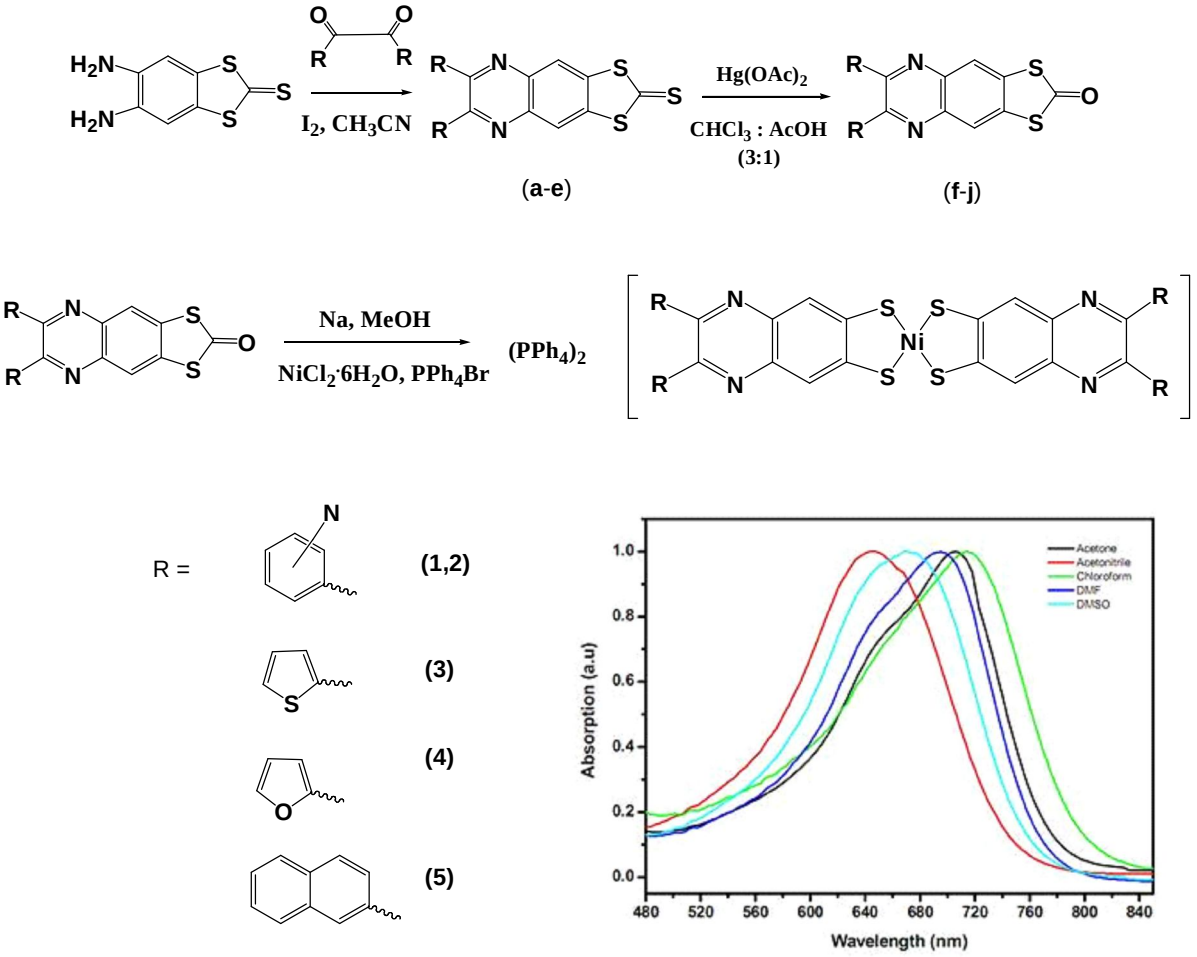


**Scheme 2.** Synthetic route for new nickel dithiolene complexes and solvatochromic effect of the complex **2.**

Compounds **2** and **3** are structurally characterized by single crystal X-ray crystallography. Complex **2** crystallizes in monoclinic space group *P*2(1)/*c*, whereas complex **3** crystallizes in triclinic space group *P*–1. Both these complexes (**2** and **3**) exhibit a two-dimensional network through C–H···N hydrogen bonding interactions in their crystal packing. Compound **2** undergoes a reversible oxidation ($\Delta E$= 83 mV) at $E_{1/2}$ = +0.21 V *vs* Ag/AgCl, whereas **5** shows quasi-reversible oxidation at $E_{1/2}$ = +0.09 V *vs* Ag/AgCl in dimethylsulfoxide solutions of electrochemical measurements. Interestingly, complex **5** is easily oxidized at very low oxidation potential compared to the other complexes **1**–**4**. These compounds exhibit absorption in the region of 630–1000 nm, in which complex **5** shows band towards longer wavelength side compared to the remaining complexes **1**–**4**. The positions of the absorption maxima in the electronic absorption spectra of the compounds **1** and **2** depend on the solvent polarity, whereas absorption bands of complexes **3**–**5** are not influenced by the solvent polarity.

The above mentioned compounds **f, g** and **i, j** (shown in Scheme 2), are further treated with triethyl phosphate at 130 °C to obtain tetrathiafulvalene derivatives (**6**–**9**), as shown in Scheme 3. The derivatives **6**–**9** are characterized by $^1$H NMR, HRMS and UV-Vis spectroscopy.

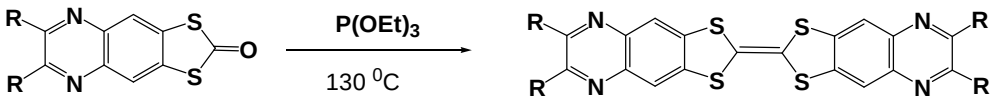


**Scheme 3**. Preparation of heterocyclic based tetrathiafulvalene derivatives (**6**–**9**).

## Chapter 5

## Synthesis, structural characterization and properties of new *N*-heterocyclic carbene Ag(I) Complexes

Chapter 5 describes syntheses, crystal structures and properties of new *N*-heterocyclic carbene complexes [{1-(2,3,5,6- tetra methyl benzyl)-3-benzylbimy}AgCl] (**2a**), [{1-(benzyl)-3-benzylbimy}$_2$Ag][$BF_4$] (**2b**), [{1-(benzyl)-3-butylbimy}AgBr]$_2$ (**2c**), [{1-(benzyl)-3-(4-nitro-benzyl)bimy}AgBr] (**2d**), [{1-(benzyl)-3-(4-bromo-benzyl)bimy}AgBr] (**2e**), [{1-(benzyl)-3-(4-nitro-benzyl)bimy}$_2$Ag][$BF_4$] (**2f**), [{1-(benzyl)-3-(4-bromo-benzyl)bimy}$_2$Ag][$BF_4$] (**2g**) (bimy = benzimidazol-2-ylidene), and [{1-(10-bromo-9-anthracenylmethyl)-3-butylimy}AgBr] (**2h**)

(imy = imidazol-2-ylidene). Compounds **2a**–**2h** have been characterized by IR-, $^{1}$H NMR-, UV-visible- LC/MS-spectral and electrochemical studies including elemental analysis. Compounds **2a**–**2c** and **2h** are unambiguously characterized by single crystal X-ray crystallography.

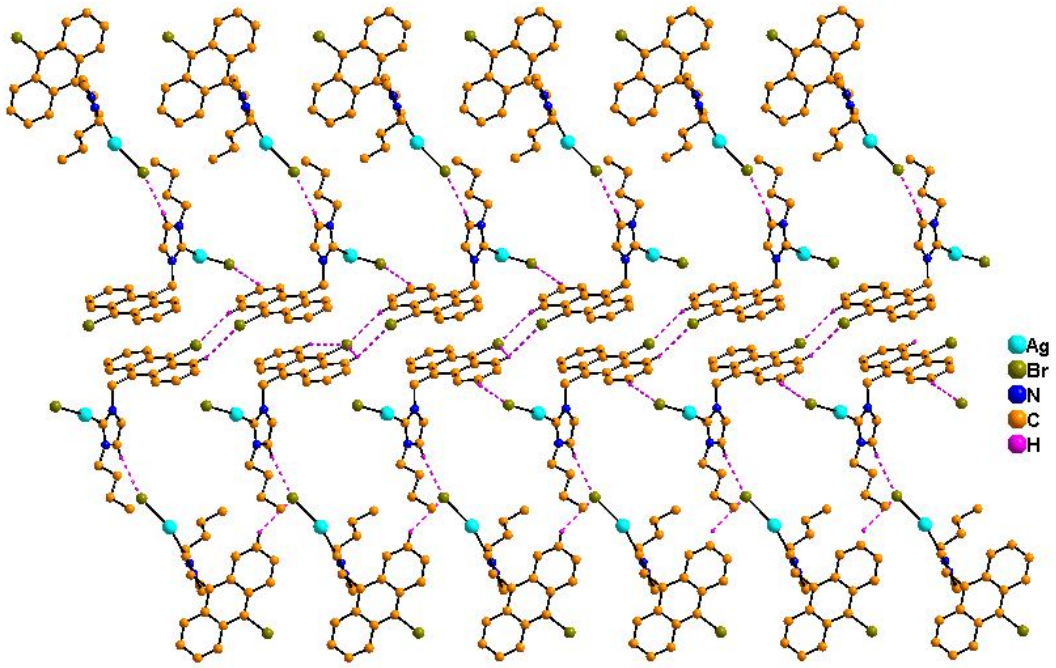


**Figure 3.** 2D supramolecular network in silver carbene complex **2h**.